THE UNIVERSITY
of EDINBURGH

Quest for early hematopoietic stem cell precursors

Kateryna Bilotkach

Thesis submitted in satisfaction of the requirements
for the degree of

Doctor of Philosophy

Scottish Centre for Regenerative Medicine, School of Biological Sciences,
University of Edinburgh

2018

I hereby declare that:

(a) this thesis has been composed by myself;

(b) presented here research data is my own except where it is stated otherwise;

(c) this work has not been submitted for any other degree or professional qualification.

Kateryna Bilotkach

В пам‘ять про тих, що живуть в моєму серці і про тих, що надихнули мене на цей шлях. З любов‘ю і вдячністю моїй родині: Володі, Ярославі, Руслану, які прокрокували зі мною цю дорогу від самого її початку до кінця. Для мого маленького дива, Зоряна, який прийшов розставити всі крапки над "і". З подякою всім щедрим душею людям, що зустрілися мені на цьому шлясі і подали руку помочі у часи випробувань.

Acknowledgements

First, I would like to thank my PhD adviser Professor Alexander Medvisnky who gave me the wonderful opportunity to engage in the captivating world of developmental biology and stem cell research. I am thankful for him to trust in me to establish the new direction for our group research studies of chick embryo haematopoiesis; and being patient in waiting for the results. I am also grateful for the inspiring and stimulating discussions we had about the research results and his suggestions.

I would like to thank my "comrade" Dr Stanislav Rybtsov who was always next to me in the laboratory "trenches" in the days and nights we spent at SCRM. I am obliged to Stanislav for his invaluable advice on my research and technical suggestions and for his compassion during desperate times.

I am indebted for Professor Helen Sang and Dr Adam Balik for advising and technical help on chicken haematopoiesis project and Debiao Zhao for teaching to work with chicken embryos. I am beholden for Dr Katie Long for helping with establishment of chick embryo culture in SCRM. Special thanks to Dr Manli Chuai for advising on early chick embryos culture protocol.

I am grateful to Dr Valerie Wilson for advice on early embryo development and technical support in work with early mouse embryos. I also would like to thank Dr Wilson's lab members Dr Ronald Wilkie, Dr Filip Wymeersch and Dr Yali Huang for technical help with histology and early mouse embryo work. I am thankful for my PhD committee members Dr Lesley Forrester and Dr Sally Lowell for advising on the results and next steps of my research project.

I would like to thank all my fantastic former and current lab members, who not only assisted on multiple technical and theoretical issues, but most importantly spent their spare time with me to support me through the challenges of a PhD student: Anahi, Andrey, Anna, Antoniana, Boni, Ceine, Dasha, David, Edie, Fiona, Heather, Javi, Jenny, Jordi, Niamh, Sabrina, Sara, Stas, Suling, Vincent, Yiding and a special thanks to my friend Natalia who also gave me shelter when I performed my night experiments.

I thank supporting staff: Dr Bertrand Vernay and Dr Valeria Berno for assisting with imaging; Dr Fiona Rossi, Dr Claire Cryer, Dr Olivia Rodrigues - for helping with flow cytometry; John Verth and Carol Manson for chick eggs supply.

Many thanks for Kelly Duglas – our postgraduate secretary, - for the unstopping help in managing my progression as a PhD student.

Finally, I would like to thank the University of Edinburgh for providing a rich personal and academic development environment that allowed me to broaden my perspectives on higher education and to realize my role as a student, researcher and a teacher for my younger student fellows. I am thankful, Institute of Academic Development for enrolling me in Postgraduate Certificate of Academic Practice programme and so making me a part of the vibrant academic community of the University of Edinburgh.

ABSTRACT

The first transplantable hematopoietic stem cells (HSC) arise in the aorta-gonad mesonephros region (AGM) during early stages of embryo development. Specifically, ventral aspect of embryonic dorsal aorta (DA) contains HSC that upon transplantation into irradiated recipients can reconstitute all lineages of the haematopoietic system [Medvinsky et al. 1993; Muller and Medvinsky, 1994; Medvinsky and Dzierzak, 1996; Cumano et al., 1996; Tavian et al., 1996; Peault and Tavian, 2003; Taoudi and Medvinsky, 2007; Ivanovs et al., 2011, 2014]. The ventral aspect of DA bears so-called intra-aortic cell clusters (IAC), the appearance of which coincides with the emergence of HSC [Babovic and Eaves, 2014; Bhatia, 2007; Boisset et al., 2010, 2011; Bollerot et al., 2005; de Bruijin et al., 2002; Bertrand et al., 2010]. According to recent reports, HSC are a heterogeneous population of cells [Dykstra et al., 2007; Seita and Weissman, 2010; Muller-Sieburg et al., 2012]. It is unclear whether all HSC precursors originate from the same location, for example, DA lining, IAC or sub-aortic tissues; or HSC precursors migrate into DA lining from other parts of the embryo [Tavian et al., 1999; Yoder et al., 1997; Oberlin et al., 2002; Peault and Tavian, 2003; Dzierzak, 2003; Samokhvalov et al., 2007; Medvinsky et al., 2011].

To elucidate ontogeny of early HSC precursors (pro-HSC), two approaches were applied in this PhD project. First, we mapped potential pro-HSC in pre-circulation mouse embryos (embryonic day 6-8.5, E6-E8.5). We defined potential pro-HSC as cells co-expressing the transcription factor Runx1, endothelial markers (VE-Cad or CD31) and/or haematopoietic markers (CD45, CD41) [Oberlin et al., 2002; de Bruijn and Dzierzak, 2012; Liakhovitskaia et al., 2009, 2014]. In E6-E8 mouse embryo, prospective pro-HSC were found to be located in chorionic plate, yolk sac and in allantoic core domain. In early somitic mouse embryo (E8-8.5) cells with pro-HSC phenotype (Runx1+CD31+CD41+) were found to be in cell clusters in forming vessel of confluence and in nascent dorsal aortae lining.

Pro-HSC are not directly transplantable [Cumano et al., 1996., 2001; Godin et al., 1993; 1995; Batta et al., 2016; Matsuoka et al., 2001; Nishikawa et al., 1998]. Therefore, cells and tissues containing prospective pro-HSC were initially matured using several *in-vitro* culture systems. According to our results, E8 mouse embryo pro-HSC are only preserved in explant cultures, but not in co-aggregate cultures with stroma cells. After culture, cells were transplanted into sub-lethally irradiated recipients. Six weeks after transplantation 19 out of 82 transplanted recipients had donor derived blood cells' chimerism at the level of 0.1-0.3%. Forty six percent of these grafts were derived from rostral part of the embryo tissues (head, heart, upper somites). Only one out of 82 recipients had donor cells contribution above 1% (1.2 %). This recipient was engrafted with cells derived from the E8 mouse embryo head and heart region.

Recipients having blood chimerism at the range of 0.1-0.3% had mainly lymphoid donor derived cells in their peripheral blood. The only recipient showing the high donor cells contribution (1.2%) had contribution mainly to myeloid lineage. Recorded low levels of blood chimersims are in line with those reported by Rybtsov et al. (2014) for early E9 mouse embryos. Donor derived cells formed clearly distinguishable populations on cytometry plots. This population of cells were absent from control engraftment experiments with carrier cells only. Previously, lymphoid potential was detected in paraaortic spnanchnopleura (P-Sp) of E8.5-9 mouse embryos, but not in E8 mouse embryos (0-5 somites, pre-circulation) and later in yolk sac [Cumano et al., 1996; Nishikawa et al., 1998; Fraser et al., 2002; Yokota et al., 2006]. However, prior works used different criteria to establish recipient reconstitution. Therefore, it is possible that recipients repopulated with E8 derived cells at the level of 0.1% were not considered as repopulated and hence, presence of lymphoid lineage precursors was overlooked in early somitic mouse embryos. The only recipient showing substantial myeloid cells contribution (73% Mac1+Gr1+ cells of donor derived cells) received engrafted cells from an

older (6-13 sp) embryo and therefore potentially has yolk sac derived myeloid cells. Yolk sac cell contribution to myeloid lineage, specifically to the brain microglia was reported in prior works [Samokhvalov et al., 2007].

Our data show that early E8 AGM cells do not expand in *in vitro* conditions. While in AGM, cells from E9 mouse embryo expand in culture [Rybtsov et al., 2014]. We have analysed Runx1 expression pattern and dorsal aorta morphology at the time when E9 HSC precursors acquire ability to expand in *in vitro* culture. Runx1 expression becomes clearly polarised at the time point (22-26 sp), when paired dorsal aortae fusion is initiated. We envision that intimate connection between DA fusion events and induction of pro-HSC maturation exists. According to prior reports, Bmp, Shh and VEGF signalling regulate DA fusion [Garriock et al., 2010]. Thereofore, to enhance *in vitro* HSC maturation system, DA fusion triggers (for example, Bmp4) might be added to culture.

Since, pro-HSC maturation methods established to date are not efficient to expand and differentiate E8 pro-HSC into potent HSC, another approach had to be implemented to study HSC ontogeny. The second approach we utilized was to trace the origin of HSC in chicken embryo, starting from the very beginning of cell fate specification, i.e. from gastrulation stages. Chick embryo haematopoiesis is similar in both human and mouse: precursors of HSC arise in the embryo proper in AGM, and IAC are formed in DA ventral aspect [Dieterlen-Lièvre, 1975; Dieterlen-Lièvre and Martin, 1981; Dieterlen-Lièvre and Jaffredo, 2009; Jaffredo et al., 2000; Le Douarin and Dieterlen-Lièvre, 2013]. In contrast to mammals, chick embryo develops *ex vivo*, making direct labelling and cell tracing possible. We aimed to identify cells giving rise to regions of DA that produce IAC. Therefore, segments of primitive streak (PS) were labelled with lipophilic dyes or by substituting segments of host PS with PS sections derived from transgenic (GFP+) stage matched chicken embryos.

Our results show that in an 18-25h chicken embryo (Hamburger and Hamilton developmental stage 4-6, HH4-6) cells giving rise to DA ingress through the wide region of PS (35-60% of its length) [Hamburger and Hamilton, 1951]. We identified that the section of DA producing HSC is formed by cells ingressing through PS in region of 40-55% of its length at 18-25h of chick embryo development. Regardless of the embryo development stage (HH4-6), in chimeras grafted at 40-55% of PS length, GFP+ cells contributed to DA and to the IAC. Within GFP+ labelled areas, we observed clusters consisting entirely of GFP+ and clusters having a mixture of GFP+ and GFP- cells. Entirely GFP+ clusters were found in the stretch of DA that had the entire aortic endothelial lining labelled. Clusters formed on the mosaic (GFP+/GFP-) aortic endothelium also had mosaic nature. According to our data, multiple descendants of PS contribute to the same stretch of dorsal aorta. This explains mosaicity of dorsal aorta lining and IAC labelling. Since we encountered clusters with mixture of GFP+ and GFP- cells, we conclude that IAC are not clonal formations. Mosaicity of IAC also does not exclude a scenario when cells migrate in and out of a cluster. Further tracing experiments are required to establish HSC nature of cells within a cluster.

LAY SUMMARY

Haematopoietic stem cells (HSC) are the cells that can produce all blood cells (red and white blood cells and platelets) throughout one's lifetime [Urso and Congdo, 1957; Till and McCulloch, 1961; Becker et al., 1963; Seita and Weissman, 2010]. Nowadays transplantation of HSC is widely used in treatments of blood and bone marrow cancers (for example, leukaemia, lymphoma, multiple myeloma etc.) [Schwaber et al., 2016]. Recently, HSC transplantation was also successfully used in treatment of multiple sclerosis and has shown promise in clearing a patient's blood from human immunodeficiency virus (HIV) [Hardy and Ikpeazu, 1989; Eaves et al., 2015; Schwaber et al., 2016].

For transplantations, HSC are obtained from bone marrow, peripheral blood, or umbilical cord blood [Turpen et al., 1981; Querol et al., 1998; Ramsfjell et al., 1999; Batta et al., 2016]. The immune system can recognise molecules on the surface of foreign cells that distinguish them from one's own cells. Therefore, for transplantations, clinicians will try to find a donor with the best possible "match" to the patient [Scott F. Gilbert, 2003]. This requirement significantly reduces the number of suitable HSC donors for certain patient groups. Therefore, there is a shortage of HSC donors [Heike and Nakahata, 2002; Sauvageau et al., 2004; Celebi et al., 2011]. To overcome this shortage, researchers are exploring methods of HSC maturation from various potential sources, for example from embryonic stem cells or induced pluripotent stem cells, which can make any cell type in the body [Qiu et al., 1999; Bhatia, 2007; Pick et al., 2007; Doulatov et al., 2013; Batta et al., 2016]. The main obstacle in producing HSC in the laboratory, however, is the lack of knowledge of where HSC mature (HSC niche) and what growth factors control this process. The best way to address this gap in knowledge is to look at how HSC first emerge *in vivo*. It may then be possible to recreate HSC maturation in the laboratory.

During embryo development, HSC first appear in the largest embryonic vessel, the dorsal aorta [Bertrand et al., 2010; Pardanaud et al., 1996; Zovein et al., 2008; Jaffredo et al., 1998]. They later migrate to the fetal liver and finally to the bone marrow [Hardy and Ikpeazu, 1989; Medvisnky et al., 2011; Rybtsov et al., 2011; Schwaber et al., 2016]. It is still unclear where HSC arise from before they appear in the dorsal aorta. This PhD project is aimed to identify where the very first HSC come from. We used several approaches: (1) various parts of early mouse embryos were transplanted into recipient mice to check which parts contain HSC or their precursors. To detect precursors of HSC, cells were cultured before transplantation. We found that current culture methods were not efficient at maturing these early precursors and therefore (2) we tried a second approach to trace the origin of HSC: we used chicken embryos to identify cells that contribute to the embryonic aorta. Chicken development can be easily tracked since they develop in eggs rather than inside the body. By grafting labelled cells into recipient embryos, we were to show that in chicks, the dorsal aorta is built from descendants of an earlier tissue called the primitive streak (PS) [Downs et al., 1993; Garcia-Martinez and Schoenwolf, 1992; Lawson et al., 1991]. Not all sections of dorsal aorta produce HSC. We identified the specific part of the PS that contributes to the region of the DA that is implicated in production of HSC. This work lays a foundation that will allow the establishment of the origin of HSC so that in future we could identify what factors influence HSC maturation.

ABBREVIATIONS

7-AAD	7 -amino-actinomycin;
Ac-LDL	Acetylated low-density lipoprotein;
ACD	Allantoic core domain;
AGM	Aorta-gonad-mesonephros region;
AlP	Alkaline phosphatase;
AO	Area opaca;
AP	Area pellucida;
A-P	Anterior-Posterior
BFU-E	Burst-forming unit erythroid;
CD	Cluster of differentiation (or classification determinant) is the nomenclature used for identification of cell surface markers;
CD41	Integrin alpha-IIb. Membrane bound molecule. Receptor for fibronectin, fibrinogen, plasminogen, prothrombin, thrombospondin and vitronectin. Also known as CD41;
CFU-C	Colony-forming unit-culture;
CFU-GM	Colony forming unit - granulocyte-macrophage;
CFU-M	Colony forming unit -macrophage;
CFU-S	Colony forming unit - spleen;
C-R	Caudal-Rostral;
DA	Dorsal aorta;
DAPI	4',6-diamidino-2-phenylindole, dihydrochloride;
HSC	Definitive hematopoietic cells;
DPBS	Dulbecco's phosphate buffer saline;
D-V	Dorsal-Ventral;
E or ED	Embryonic day of development (E for mouse, ED for chick);
EDTA	Ethylene-diamine-tetra acetic acid;
FACS	Fluorescence-activated cell sorting;
FCS	Fetal calf serum;
GEMM	Granulocyte, erythroid, macrophage, megakaryocyte CFU;
GFP	Green fluorescent protein;
HH	Hamburger and Hamilton stage of chick embryo development;

HN	Hensen's node;
HSC	Hematopoietic Stem Cells;
Ht	Heart;
IAC	Intra aortic clusters;
KO	Knockout. A mouse animal model with a disrupted gene;
LacZ	Beta-galactosidase;
Lin-	Population of cells lacking committed hematopoietic progenitors' markers: Ter119, Mac-1, Gr-1, B220, CD3ε, CD4 and CD8;
LPM	Lateral plate mesoderm;
LSK	Population of cells that are lineage negative (Lin−), Sca-1^+, c-kit^+
LTR	Long term repopulation;
Nc	Notochord;
NT	Neural tube;
PBS	Phosphate buffer saline;
PECAM-1	Platelet endothelial cell adhesion molecule – 1 (synonym – CD31);
PFA	Paraformaldehyde;
PS	Primitive streak;
Som	Somite;
STR	Short term repopulation;
Tris-HCL	Tris(hydroxymethyl) aminomethametane- hydrochloric acid;
UGR	Urogenital ridges;
VE-Cad	Vascular endothelial cadherin, cadherin 5;
VOC	Vessel of confluence;
VV	Vitelline vessels;
WT	Wild type;
X-gal	5-Bromo-4-chloro-3-indolyl beta-D-galactopyranoside;
YS	Yolk sac.

LIST OF FIGURES

CHAPTER 1.

CHAPTER 3.

LIST OF TABLES

CHAPTER 1

CHAPTER 2

CHAPTER 3

TABLE OF CONTENTS

CHAPTER 1. INTRODUCTION

1.1. Glossary of the key terms and definitions

Hematopoietic stem cell (HSC) – a cell that self-renews and can give rise to all elements of a hematopoietic system;

Self-renewal – is a process of stem cell division with maintenance of stem cell undifferentiated state;

Precursor of hematopoietic stem cells (pre-HSC and pro-HSC) – immature embryonic cell that eventually will become a HSC. ***Pre-HSC*** – HSC precursors apprearing in embryos with established blood circulation, but before appearance of HSC in fetal liver. ***Pro-HSC*** – HSC precursors appearing in embryo tissues before establishment of blood circulation.

Aorta-gonad mesonephros region – consists of the dorsal and embryonic rudiments of kidney and mesonephros (urogenital ridges);

Intra-aortic clusters – clusters of cells appearing on the internal endothelial lining of the dorsal aorta;

Primitive haematopoiesis – process of generation of immature (fetal type) hematopoietic stem cells in the yolk sac;

Extra-embryonic tissues - yolk sac and its vessels, allantois, chorion, placenta;

Hematopoeitc system reconstitution (or repopulation) – a process when donor cells injected into a lethally irradiated recipient give rise to hematopoietic cells that compliment the recipient's hematopoietc system;

Blood chimerism - percentage of donor-derived blood cells appearing in recipient's peripheral blood after transplantation.

1.2. On hematopoietic stem cell

In the 1950s, it was discovered that bone marrow injections into lethally irradiated recipients allow complete reconstitution of the recipient's hematopoietic system [Urso and Congdon, 1957; Lorenz et al., 1952; Hardy and Ikpeazu, 1989; Seita and Weissman, 2010]. McCulloch and Till, experimenting with bone marrow injections in mice, observed that in 8-14 days cell colonies appear within mice spleens. These colonies later were termed – "colony forming unit-spleen" (or CFU-S) [Till and McCulloch, 1961; Becker et al., 1963; Siminovitch et al., 1963]. When these colonies were analysed it was concluded that each colony was derived from one transplanted bone marrow cell [Becker et al., 1963; 2014]. Moreover, when cells isolated from CFU-S were injected into secondary irradiated recipients, the complete reconstitution of the host hematopoietic system was also observed. Therefore, it was concluded that cells in one CFU-S colony are descendants of one bone marrow cell that gives rise to all lineages of committed hematopoietic progenitors and are also able to self-renew [McCulloch and Till, 2005]. Later, McCulloch and Till proposed to term cells giving rise to CFU-S **- "stem cells"** [Becker et al., 1963, 2014; Wolf and Trentin, 1968].

According to the given above stem cell definition, adult hematopoietic stem cells are the cells that can provide lifelong reconstitution of all lineages of the hematopoietic system in an irradiated recipient. Under normal conditions these cells reside in the bone marrow of adults [Hopman and DiPersio, 2014; Schwaber et al., 2016]. HSC are responsible for keeping the hematopoietic system of an adult in homeostasis, e.g., maintaining numbers of terminally differentiated blood cells constant, the timely rise to multipotent hematopoietic progenitors (for example, during injury) and keeping the pool of hematopoietic stem cells under control [Babovic and Eaves, 2014; Mendelson and Frenette, 2014; Seita and Weissman, 2010]. The latter is of a special interest to modern cancer biology. E.g., at present, it is hypothesised that

some blood malignancies can result from proliferation of a hematopoietic stem cell that has a genetic lesion dysregulating stem cell's control of self-renewal [Carlesso and Cardoso, 2010; Babovic and Eaves, 2014].

Initially bone marrow transplants in humans were challenging, but after blood cell allotypes were discovered, bone marrow transplantation became one of the methods of choice in treatment of blood malignancies (leukaemia, lymphoma, multiple myeloma) and some immunodeficient conditions [Thomas et al., 1970; 1971; Hardy and Ikpeazu, 1989; Schwaber et al., 2016]. For today, HSC are isolated from bone marrow, new-born umbilical cord blood and adult peripheral blood [Hopman and DiPersio, 2014]. Due to the need to match blood allotypes of the donor to the recipient, there are still shortages in bone marrow donors [Hardy and Ikpeazu, 1989; Hopman and DiPersio, 2014; Schwaber et al., 2016]. Therefore, delineation of the ontogeny and the process of hematopoietic stem cells maturation is of great interest in the field of regenerative medicine [Rowe et al., 2016].

1.3. Hierarchical organization of the adult hematopoietic system in mammals

A hematopoietic stem cell (HSC) is positioned at the top of the hematopoietic system hierarchy [Babovic and Eaves, 2014; Seita and Weissman, 2010]. HSC represent a very small pool of bone marrow cells. According to Szilvassy et al. in the whole mouse bone marrow there is just 1 in 10 000 cells with the ability to engraft and completely reconstitute the hematopoietic system [Szilvassy et al., 1990]. HSC mainly remain in the G0 phase (quiesce) of the cell cycle [Passegué et al., 2005; Wilson et al., 2008; Pietras et al., 2011]. HSC slowly cycle, which slows down the cell's metabolic rate, reduces oxidative stress and prevents HSC from accumulation of genetic mutations [Pietras et al., 2011].

From the very beginning of stem cell discovery McCulloch and Till recognized that the pool of HSC is not homogeneous. The authors observed that propensity of CFU-S to support further colonies' expansions broadly varies between them [Siminovitch et al., 1963; McCulloch and Till, 2005]. Over the last decade, new insights were obtained for the heterogeneity of HSC pool in mice [Copley et al., 2012; Muller-Sieburg et al., 2012; Crisan and Dzierzak, 2016; Weissman, 2015; Bush et al., 2015]. Dykstra et al., proposed to distinguish 4 types of HSC: α, β, γ and δ [Dykstra et al., 2007]. According to the authors, α and β HSC both support self-renewal, but provide quite a different spectrum of hematopoietic progenitors. For example, α-HSC mainly produce myeloid lineage progenitors, while β-HSC produce both myeloid and lymphoid progenitors. Upon secondary transplantations α-HSC can give rise to β-HSC, indicating that α-HSC are not devoid of the ability to give rise to both myeloid and lymphoid lineages, but require special conditions to trigger this process. The abundancy of α and β-HSC is approximately 30% of all bone marrow HSC. Both α and β HSC provide so-called "long term" or "life-long" engraftment [Seita and Weissman, 2010]. In animal models, long term engraftment is accepted when HSC support hematopoietic system reconstitution for 4 months. This kind of HSC are also called long-term repopulating HSC or LTR-HSC [Seita and Weissman, 2010; Liu et al., 2012].

There are also short-term repopulating cells, the cells that provide complete hematopoietic system reconstitution for a period shorter than 4 months (short-term repopulating cells or STR-HSC) [Liu et al., 2012; Fibbe et al., 1997]. As self-renewal property is lost by these cells, they cannot be seen as "true" HSC, even though they give rise to both myeloid and lymphoid lineages. As McCulloch and Till noticed, the initial stem cell goes through a pivotal point when a decision is made to differentiate or to self-renew [McCulloch and Till, 2005]. If the differentiation pathway is selected, the self-renewal ability is lost and

there is no way to distinguish this stem cell from a hematopoietic progenitor. Therefore, establishing if a cell is a HSC or a progenitor remains a controversial issue.

Other components of bone marrow HSC pool are γ and δ cells. These cells support multilineage life-long engraftment but are not able to repopulate secondary recipients, which indicates limits of their self-renewal ability [Seita and Weissman, 2010]. Moreover, while the level of blood chimerism (percentage of donor derived cells) in mice transplanted with α and β HSC stays at a high level, percentage of donor derived cells in mice engrafted with γ and δ HSC drops (though remains above 1%) [Dykstra et al., 2007]. γ and δ HSC provide low levels of myeloid engraftment with a particularly diminishing number of donor derived myeloid cells (derived from δ HSC). In mice, γ and δ types represent 12 and 22% of all HSC accordingly. γ and δ HSC can be derived from α and β HSC *in vivo* and *in vitro*. Interestingly, *in vitro* culture of bone marrow cells reduces numbers of α and β HCS and expands γ and δ types. Longer culture (10 days) eliminates α and β HSC, but expands δ HSC % [Dykstra et al., 2007].

HSC gives rise to multi-potent hematopoietic progenitors (MPP), which are different from HSC in that they have lost their self-renewal property [Babovic and Eaves, 2014; Seita and Weissman, 2010]. MPP can generate all types of more differentiated oligopotent progenitors [Kawamoto et al., 2010; Eaves, 2015; Snoeck, 2013; Muller-Sieburg et al., 2012]. In particular, common myeloid, common lymphoid and common megakaryocyte-erythrocyte progenitors (Figure 1.). Even though the lifespan of committed hematopoietic progenitors is much shorter than that of HSC, they are available at higher quantities, have fast proliferation rates and are widely used in clinic for reconstitution of the lymphoid compartment in some immunodeficient patients [Hardy and Ikpeazu, 1989; Hopman and DiPersio, 2014; Schwaber et al., 2016]. Common myeloid progenitors give rise to restricted megakaryocyte-erythrocyte progenitors and granulocyte-macrophage progenitors. Common lymphoid progenitors give rise

to pre-B; -T and -normal killer cells [Babovic and Eaves, 2014; Kawamoto et al., 2010; Eaves, 2015]. Dendritic cells represent a separate group of hematopoietic cells and can be derived from both lymphoid and myeloid progenitors [Watowich and Liu, 2010; Merad et al., 2013]. Committed progenitors can be identified with specific surface markers (Table 1.).

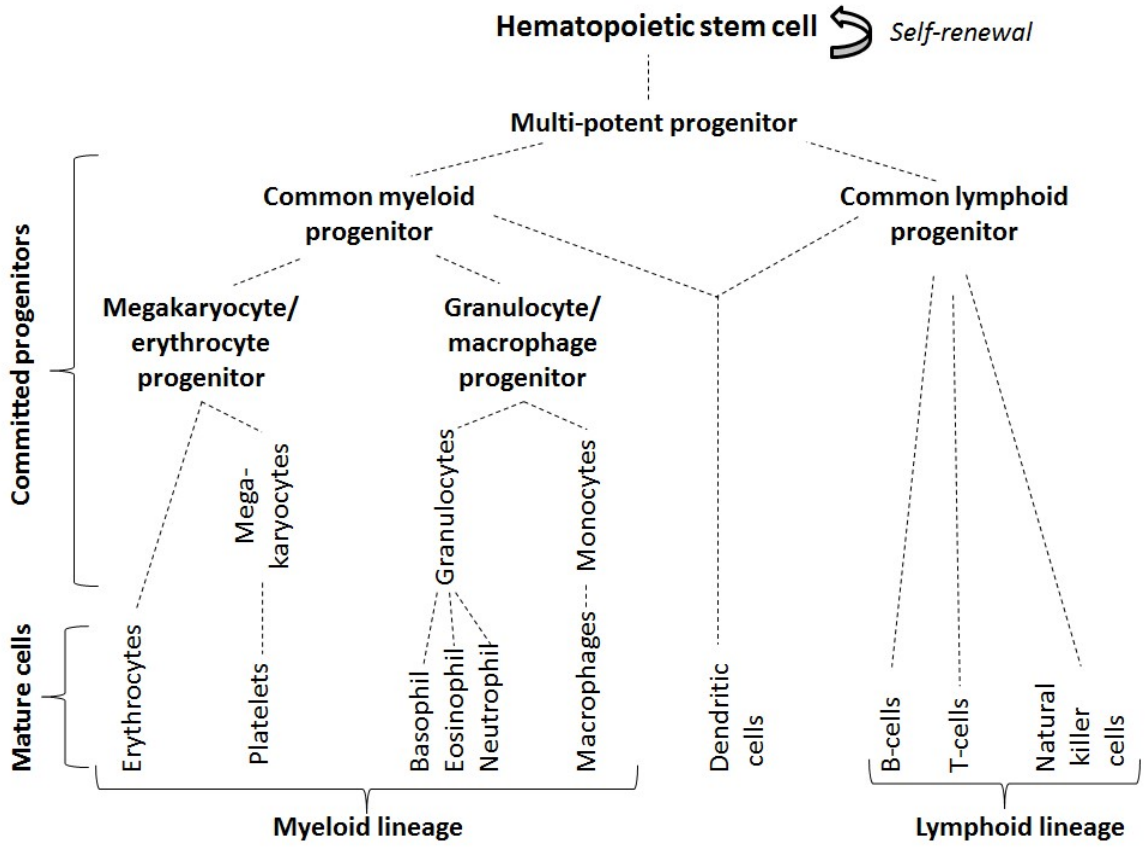

Figure 1. Adult hematopoietic system hierarchy.

Table 1. Markers most frequently used to quantify myeloid and lymphoid cell lineages

Hematopoietic lineage	Marker	Function	Reference
Leucocytes	CD45/Ly-5	Cellular differentiation/ activation, tyrosine phosphatase pan-leukocyte marker	Komuro et al., 1974; Scheid, M.P. and Triglia, 1979
Erythroid lineage			
Late stage erythroid cells	Ter119	TER-119 antigen is a molecule associated with cell-surface glycophorin A but not with glycophorin A itself	Kina et al., 2000
Erythroid precursors	CD71	Transferring receptor-1	Dong et al., 2011; Marsee et al., 2010
Lymphoid lineage			
T cells	CD4ε	TCR coreceptor, MHC class II receptor, signal transduction. Single chain transmembrane glycoprotein	Lai et al., 1998; Dialynas et., al, 1993
	CD8α	TCR coreceptor, MHC class I receptor, signal transduction. Surface glycoprotein	Lai et al., 1998; Ledbetter and Herzenberg; 1979
B-cell	B220	pan-B-cell-specific isoform of CD45. Protein Tyrosine Phosphatase, Receptor Type C	Blessing et al., 2003; Lai et al., 1998
	CD19	BCR co-receptor, signal transduction, pan-B-marker	Rolink et al., 1996
Natural killer cells	NK1.1	Killer cell lectin-like receptor subfamily B, member 1	Vicari AP and Zlotnik A, 1996
Myeloid lineage			
Macrophages	CD11b/Mac-1α	Integrin alpha M	Stewart et al., 1995
Granulocytes	Gr-1	Myeloid differentiation antigen	Fleming et al., 1993

1.4. Fetal haematopoiesis in mammals

1.4.1. Definitive hematopoietic potential

While in adults, hematopoietic stem cells (HSC) reside in the bone marrow. In an embryo, hematopoietic stem cells (HSC) and their precursors (pro- and pre-HSC) migrate from one tissue niche to another until they reach their final destination – the bone marrow. HSC, pro- and pre-HSC migrate from the tissue of their origin (which is still under investigation) to the aortic floor, fetal liver, spleen and thymus (or para-aortic foci and bursa in avians). In mouse and human, HSC expand and further differentiate in the fetal liver. In avian embryo para-aortic foci might play the role of fetal liver. Timeline of HSC migration between niches is different for each particular specie [Müller at al.,1994; Medvinsky et al. 1996; Babovic and Eaves 2014; Eaves, 2015; Rybtsov et al., 2016]. The comparison of HSC migration between human, chick and mouse is given on Figure 2.

In this work, to describe hematopoietic stem cells of embryonic origin we use the term “definitive hematopoietic stem cells” (dHSC) [Medvinsky et al., 2011]. dHSC are embryonic cells that can provide complete and lifelong reconstitution of all hematopoietic cell lineages in an adult irradiated recipient.

1.4.2. Timeline of hematopoietic stem cells and their precursors appearance in a mouse embryo

In a mouse embryo, cells with hematopoietic potential reside in various locations (yolk sac, allantois, placenta, dorsal aorta, fetal liver, main hematopoietic organs) starting from embryonic (E) day 7 [Melchers, 1979; Godin et al., 1995; Yoder et al., 1997; Palis et al., 1999; Kumaravelu et al., 2003; Alvarez-Silva et al., 2003; Gekas et al., 2005; Ottersbach and

Dzierzak, 2005; McGrath and Palis, 2005; Zeigler et al., 2006; Corbel et al., 2007; Rhodes et al., 2008; Lux et al., 2008; Dieterlen-Lièvre et al., 2010; Yoshimoto et al., 2012; Arora and Papaioannou, 2012]. This hematopoietic potential was elucidated either in *vivo* assay by transplantations or *in vitro* in hematopoietic colony-forming cell assays* (*- glossary of terms and definitions).

First hematopoietic cells (primitive erythroblasts and some macrophages) appear in the yolk sac around embryonic day (E) 7-8 in so-called blood islands (Figure 2) [Moore and Metcalf, 1970; Cumano et al., 1996; Yoder et al., 1997; Lichanska and Hume, 2000; Cumano et al., 2001; Lux et al., 2008]. These cells in contrast to mature erythrocytes are nucleated and express an embryonic type of haemoglobin [McGrath and Palis, 2005]. Cells with lymphoid and myeloid potential were identified in E8.5 mouse embryos in the placenta labyrinth and allantois [Zeigler et al., 2006; Alvarez-Silva et al., 2003; Ottersbach and Dzierzak, 2005; Melchers, 1979]. In mouse embryos blood circulation starts around E8.5 when embryo develops 5-8 somite pairs (sp) [McGrath et al., 2003]. Released with blood flow primitive hematopoietic cells migrate from yolk sac into the embryo proper. These primitive blood cells are not able to reconstitute the hematopoietic system of myeoablated recipients and therefore are not dHSC [Medvisnky et al., 1996; 2011; Seita and Weissman 2010; McGrath and Palis, 2005].

The first cells supporting lifelong multilineage engraftment can be detected in mouse embryo at late embryonic day 11.5 (E11.5) in the so-called aorta-gonad mesonephros region (AGM) [Medvinsky et al. 1993; Muller et al., 1994; Medvinsky and Dzierzak, 1996; de Bruijn et al., 2000; Taoudi and Medvinsky, 2007]. By series of works of *in vitro* culture of E9-E10 AGM derived cells it was demonstrated that dHSC originate in AGM autonomously [Taudi and Medvinsky, 2007; Rybtsov et al. 2011, 2014; Ivanovs et al., 2014]. dHSC and their precursors were found to be localized to the ventral aspect of dorsal aorta in E10-E11 mouse embryos [de

Bruijn et al., 2002; Taudi and Medvinsky, 2007; Rybtsov et al., 2011] and in human [Péault et al., 2002; Ivanovs et al., 2011]. Emergence of dHSC and their precursors in AGM coincides with appearance in the ventral aspect of dorsal aorta (DA) so-called intra-aortic cell clusters (IAC) [Yokomizo and Dzierzak, 2010; Yokomizo et al., 2011; Mizuochi et al., 2012; Boisset et al., 2011]. Today, it is broadly accepted that dHSC mature in hemogenic endothelium and give rise to intra-aortic clusters (IAC) [Jaffredo et al., 1998, 2005; Zovein et al., 2008; Boisset et al., 2010; Bertrand et al., 2010; Kissa and Herbomel, 2010; Swiers et al., 2010]. After dHSC potential is detected in AGM, other vascularized organs (placenta, allantois, yolk sac vasculature, embryonic head) acquire dHSC potential [Ottersbach and Dzierzak, 2005; Rhodes et al., 2008; Alvarez-Silva et al. 2003; Dieterlen-Lièvre et al., 2010; Gordon-Keylock et al., 2013; Kumaravelu et al., 2002; Gekas et al., 2005]. At embryonic day 12 (E12) dHSC and their precursors (pre-HSC) migrate into the fetal liver, where they expand and mature [Kumaravelu et al., 2002; Zovein et al., 2008; Rybtsov et al., 2011; 2014; 2016].

Even though today it is known that maturation of dHSC precursors takes place in the ventral aspect of dorsal aorta, it is still not known where early dHSC precursors come from in the E8 mouse embryo. Since blood flow effectively disseminates cells from one embryonic compartment to another, after E8.5 (initiation of blood circulation) it is difficult to unequivocally determine where precursors of dHSC come from. Therefore, the best strategies to answer this question would be the lineage tracing of descendants of selectively labelled regions (or cells) in pre-blood circulation embryo tissues.

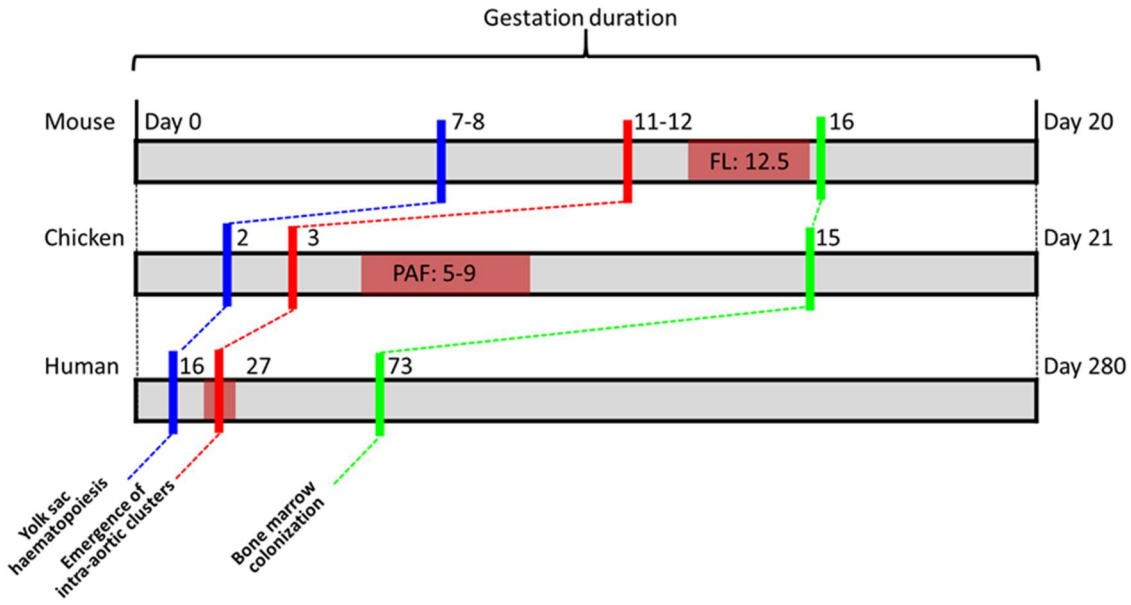

Figure 2. Timeline of hematopoietic stem cells and their precursors migration during gestation. Chronology of hematopoietic stem cells and their precursors migration between tissues is shown. Numbers indicate day of embryonic development. Coloured rectangles represent colonization of fetal liver (FL) in humans and mouse or para-aortic foci – in chicken embryo.

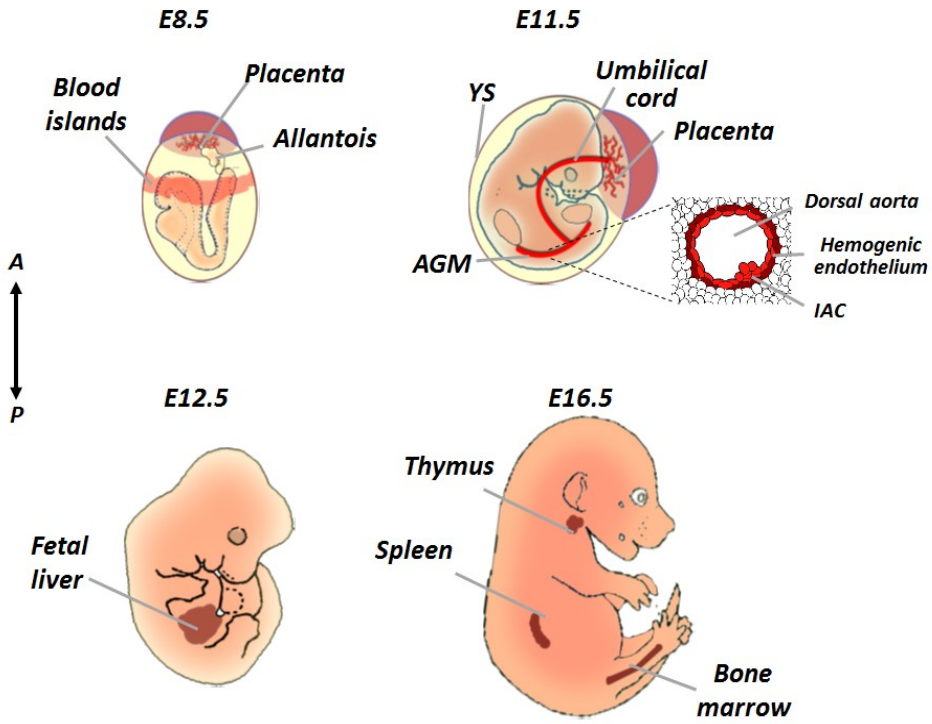

Figure 3. Timeline of hematopoietic stem cells and their precursors appearance in mouse embryo. First primitive hematopoietic cells appear in mouse embryo at E7-8 in yolk sac blood islands. At around E8-8.5, hematopoietic cells autonomously appear in placenta and allantois [Alvarez-Silva et al., 2003; Ottersbach and Dzierzak, 2005; Corbel et al., 2007; Dieterlen-Lièvre et al., 2010]. First transplantable dHSC appear in E11.5 mouse embryo. They first appear in aorta-gonad mesonephros region (AGM). Simultaneously inta-aortic clusters (IAC) appear in the lumen of the dorsal aorta. Shortly after that dHSC can be identified in the yolk sac (YS), future umbilical cord and placenta. At E12.5 dHSC migrate into the fetal liver and at E16.5 colonise the fetal thymus, spleen and bone marrow. A – anterior, P- posterior end of the embryo.

1.4.3. Early mouse embryo tissues definitive hematopoietic potential

Prior reports demonstrate that several tissues in early mouse embryos (placenta, allantois, yolk sac vasculature, head, heart) possess hematopoietic potential [Godin et al., 1995; Yoder et al., 1997; Palis et al., 1999; Gekas et al., 2005; Ottersbach and Dzierzak, 2005; Lux et al., 2008; Dieterlen-Lièvre et al., 2010; Yoshimoto et al., 2012]. Hematopoietic cells isolated from these tissues cannot directly engraft irradiated recipients and hence are not mature dHSC. According to Cumano et al., these immature dHSC lack expression of MHC1, and after injection into immunocompetent recipients are eradicated by normal killer cells (NK) [Cumano et al., 1996, 2001; Kieusseian et al., 2012; Rybtsov et al., 2011, 2014]. To prove early mouse embryo tissues have definitive hematopoietic potential, cells must be pre-cultured *iv vitro* in the presence of stromal cells and/or growth factors (thrombopoietin, stem cell factor, Flt3 ligands, some interleukins). Kieusseian et al., (2012) demonstrated that dHSC precursors upregulate MHC1 expression during culture. Before recent, cells isolated from mouse embryos younger than E10 after *in vitro* culture step could engraft only NK deficient mice (Ragγc-/- recipients), but not adult or Rag2$^{-/-}$ mutant mouse recipients (Rag2$^{-/-}$ has no mature T or B lymphocytes). However, in Rybtsov at al. (2014) work, we demonstrated that E9 pro-HSC could mature into transplantable cells if co-cultured in 3D co-aggregates with OP9 stromal cells and in the presence of stem cell factor (SCF).

Majority of published works to date indicate the presence of pro-HSC in early mouse embryos (starting from E8). In these works, definitive hematopoietic potential was shown in immuno-deficient animal models or with utilization of not existing for today components (some stromal cell lines). Also, the level of blood chimersim (% of donor derived blood cells) was not clearly reported [Cumano et al., 2001; Godin et al., 1993; 1995; Fraser et al., 2002; Cumano et al., 1996]. Therefore, there is no clear proof that reported hematopoietic potential

was the definitive one: providing high level and complete lifelong reconstitution of the hematopoietic system with the ability to engraft secondary recipients [Custer et al., 1995; Mombaerts et al., 1992]. Below we will review details of works reporting definitive hematopoietic potential in E8 mouse embryos.

Cumano et al. (2001) reported that mice lacking normal killer cells (Ragγc$^{-/-}$) were repopulated after injection of 10-12 ee (embryo equivalents) of cells derived from the caudal parts of 0-10 sp mouse embryos (E8-E8.5) after 4 days of the explant culture. Although, the extent of repopulation is not mentioned, it is much lower than that of control experiments in which a suspension from 3 pooled AGMs was injected. The authors show that only splanchnopleura-explants (P-Sp) provided multilineage engraftment. Authors also showed dose-dependent engraftment, e.g., 8 ee did not provide long term repopulation while 10-12 ee did. Although it is difficult to judge what was the percentage of recipient blood chimerism, authors reported that there were no lower than 0.5% of donor derived cells in the bone marrow. Long term repopulation was not achieved. Yolk sac (YS) tissues provided only transient myeloid repopulation [Cumano et al., 2001].

With utilization of the co-culture with S17 stromal cell line, Godin et al. (1995) showed that multipotent hematopoietic progenitors appear around 10 sp simultaneously in YS and splanchnopleura (P-Sp) [Godin et al., 1995]. Godin et al. (1993) grafted P-Sp cells from early mouse embryos under the kidney's capsule of the recipient mice and found that only P-Sp (but not YS) from embryos older than 5 sp could reconstitute recipients [Godin et al., 1995]. Most generated cells were B1a cells. B1a cells are the cells mainly functioning in infants. There are several points of view on B cell development, according to one of them B1 and B2 cells appear from different progenitors, therefore it is not clear whether hematopoietic potential reported was a definitive one [Kantor and Herzenberg, 1993; Tung et al., 2006].

Fraser et al., were studying hematopoietic potential of Flk1+VE-Cad+ cells. E9 derived Vec_cad+Cd45+ cell from YS and caudal parts (CP) were injected intrahepatically into newborn SCID (Severe Combined Immunodeficiency) recipients. Donor cells contributed to the lymphoid compartment and had a weak contribution to the myeloid compartment. This repopulating activity was limited to E9 cells or older. E8.5 cells were unable to repopulate SCID recipients even when increased doses of cells were used (13 ee for YS and 22 ee for CP) [Fraser et al., 2002]. However, level of blood chimerism was not described and hence, it is difficult to judge whether that was definitive HSC engraftment or not.

Matsuoka et al., co-cultured cells derived from E8 embryos with AGM-S3 stromal cell line. Preconditioned cells were injected into recipients and reconstitution for all hematopoietic system components was achieved. However, levels of blood chimersim were not reported [Matsuoka et al., 2001].

When P-Sp and YS tissues derived from 0-15 sp mouse embryos were pre-cultured with S17 stromal cells line, both P-Sp and YS cells could generate myeloid cells. Lymphoid cells could be only generated by P-Sp tissues [Cumano et al., 1996]. Nishikawa et al. (1998) showed that Flk1+VE-Cad+ fraction, but not CD45-Ter119+ fraction of cells from E8.5 mouse embryos after co-culture with OP9 stromal cell line exhibited myeloid potential. Both myeloid and lymphoid potentials could only be detected in embryonic tissues starting from E9.

To summarise, in mouse embryos, early dHSC precursors are most probably localized to splanchnopleuric mesoderm, in particular, to the caudal portion of the embryo. This zone is situated in close proximity to the allantoic core domain, which was earlier proposed to be a stem cell zone [Downs et al., 2009]. Yet, proving that cells expressing markers of maturing HSC are true dHSC precursors remains challenging as direct methods of grafting do not allow repopulation of recipients' hematopoietic system. *In vitro* methods of early embryonic tissues co-culture with stromal cell allow detecting multilineage hematopoietic potential when cells

are injected in immunodeficient recipients. Yet, in the majority of cases this kind of donor cell engraftment was a short term one and published reports are not detailed in levels of donor cells engraftment. Therefore, the presence of committed dHSC precursors in early mouse embryo tissues remains a controversial issue.

1.4.4. Localization of early HSC precursors in mouse embryo

Localization of the very early (pro-HSC) precursors is currently under debate. Even though, hematopoietic activity is detected in early somitic mouse embryo (E8) in allantois, chorion, and in the yolk sac, definitive hematopoietic potential cannot be established directly. Immuno-fluorescent and histochemical studies of early mouse embryo tissues revealed multiple sites of vascularised tissues containing clusters of Runx1+ cells, resembling cell clusters found in the dorsal aorta. These clusters of cells were detected in extraembryonic arteries, allantois, placenta and head – all sites of definitive haematopoiesis identified in E11 embryos [Palis et al., 1999; Sugiyama et al., 2007; Yoshimoto et al., 2012; Zovein et al., 2010; Mizuochi et al., 2012; Vodyanik et al., 2005; de Bruijn et al., 2000; Gordon-Keylock et al.,2012; Zovein et al., 2010; Gekas et al., 2005; Inman et al., 2007; Zeigler et al., 2006].

For instance, Zovein et al., (2010) observed Runx1+ cell clusters during ventral vascular beds remodelling. At embryonic day 9 (E9) at the vitelline artery (VA), the dorsal aorta and umbilical artery are connected by the vessel of confluence (VOC) [Zeigler et al., 2006; Daane et al., 2011]. VA and VOC connection is gradually lost, and VA moves by "walking" on temporary vascular beds towards the fetal liver and the umbilical artery (UA). Together with VA, clusters of Runx1+ cells travel along the vasculature in the direction of the fetal liver – the future site of intra-embryonic dHSC expansion. Zovein et al. proposed that observed Runx1+ cell clusters contain precursors of definitive hematopoietic stem cells. On the contrary, Rybtsov

et al., did not detect dHSC potential in the ventral vasculature of E9 mouse embryos, but only in the caudal part of future AGM [Zovein et al., 2006; Rybtsov et al., 2013].

Rhodes et al., (2008) reported presence of Runx1+ clusters in the early placenta [Rhodes et al., 2008]. According to Gekas et al., (2005) definitive hematopoietic potential will only be detected starting from E11.5. Identified in the placenta, definitive hematopoietic cells behaved in the same way as dHSC from AGM, e.g. they disappeared from placenta vasculature at E12 – when dHSC migrate to the fetal liver to expand [Gekas et al., 2005].

As blood circulation is established in mouse embryos from early somitic stages (5 sp), it is difficult to delineate innate dHSC activity from activity brought by the blood flow. For example, Kulkeaw et al. demonstrated that cells from yolk sac migrate to the embryonic caudal parts at E10.5. Yet, these cells did not possess dHSC potential [Kulkeaw et al., 2009]. An interesting approach was demonstrated by Rhodes et al. (2008) with application of the heartbeat lacking the Ncx-/- mutant. In this experiment, the placenta was demonstrated to develop multilineage hematopoietic potential in the absence of blood circulation [Rhodes et l., 2008].

One of the solutions would be to conduct experiments with pre-circulation mouse embryo tissues cultured in an HSC maturation system. In mouse embryos, younger than embryonic day 11 (E 11) dHSC are not mature, and hence they cannot be directly detected in a transplantation assay [Kieusseian et al., 2012; Rybtsov et al., 2011; 2016]. However, if cells isolated from AGMs of E9-E10 mouse conceptus are cultured in the right conditions, pre-HSC are able to mature into functional dHSC [Rybtsov et al., 2014, 2016; Sheridan et al., 2009]. In our group, an air-liquid interface 3D co-aggregate method of pro-HSC was developed. The details of this procedure are given in Materials and Methods.

1.4.5. Molecular phenotypes of maturing mouse HSC precursors

Hierarchy of maturing HSC precursors is partially elucidated. After the culture step, HSC precursors were detected in cell suspensions derived from caudal parts of mouse embryos, starting from embryonic (E) day 9 [Taudi and Medvinsky, 2007; Rybtsov et al., 2011; 2014; 2016]. All early dHSC precursors express endothelial markers: vascular endothelial cadherin (CD144 or VE-Cad); endothelial marker CD31 (platelet endothelial cell adhesion molecule), and vascular endothelial cell growth factor receptor 2 VEGFR2 (or kinase insert domain receptor, fetal liver kinase-1, Flk1, CD309) [Garcia-Porrero et al., 1998; Fraser et al., 2002; Rybtsov et al., 2011; 2016]. Early dHSC precursors express low levels of integrin alpha IIb (or platelet fibrinogen receptor, CD41) and are negative for protein tyrosine phosphatase, receptor type C (CD45) and major sialoglycoprotein (CD43) [Ferkowicz et al., 2003]. In general, molecular phenotype of dHSC precursors found in E9.5 (pro-HSC) mouse embryos can be described as: VE-Cad+ CD41$^{low/+}$CD45−CD43− [Rybtsov et al., 2011; 2014; 2016].

dHSC gradually upregulate their expression of CD41 and CD43 markers when becoming pre-HSC type I with molecular phenotype of VE-Cad+ CD41+ CD45−CD43+ at E10.5 [Rybtsov et al., 2014; 2016; Mikkola et al., 2003; Hashimoto et al., 2007]. According to Kieusseian et al., (2012), the MHC1 antigen starts to be expressed at E10.5, just before upregulation of CD45 antigen expression. Finally, the CD45 marker starts to be expressed at E11.5 and dHSC transit to pro-HSC type 2 cells with phenotype VE-Cad+ CD41+ CD45+CD43+. After culture step with OP9 stromal cell line, pre-HSC type II become transplantable into adult irradiated recipients [Rybtsov et al., 2011; 2014; 2016]. Upregulation of CD41, CD43 and CD45 markers during pro-HSC maturation closely correlates with the expression of these markers in intra-aortic clusters and in the dorsal aorta endothelium [Taudi and Medvinsky, 2007; Yokomizo and Dzierzak, 2010; Yokomizo et al., 2011; Boisset et al., 2011; Rybtsov et al., 2011 Mizuochi et al., 2012].

Other markers that have been found to distinguish intra-aortic clusters in the dorsal aorta are: VEGFR2 (Flk1); mast/stem cell growth factor receptor (or tyrosine-protein kinase Kit, CD 117 or c-kit); adhesion molecule CD34; and stem cell antigen-1 (phosphatidylinositol-anchored protein that is a member of the lymphocyte antigen 6 (Ly-6) family or Sca-1) [Spangrude et al., 1989; Wood et al., 1997; Mikkola et al., 2003; Lux eta l., 2008; Hashimoto et al., 2007; Ding et al., 2012].

One of the most promising markers for early HSC precursors identification is transcription factor Runx1 [Yokomizo and Dzierzak, 2010; Lam et al., 2010; Liakhovitskaia et al., 2014].

1.4.6. Regulation of HSC emergence in dorsal aorta

Based on recent works done on signalling pathways regulating HSC maturation, today it is recognised that HSC specification starts before intraembryonic vasculogenesis takes place [Kobayashi at al., 2014; Ciau-Uitz et al., 2010]. HSC specification is initiated in the unspecified lateral plate mesoderm cells that migrate towards the embryonic midline to contribute to the forming dorsal aorta [Butko et al., 2016; Leung et al., 2013]. Mesoderm "lateralization", that results in a generation of DA precursors, is regulated by Bone Morphogenic Protein (BMP, expressed in ventral embryonic part) and Wnt (Wingless-related integration site or WNT protein, expressed in dorsal part) signalling [Gilbert, 2003; Hohan, 1996]. Hedgehog (Hh) is expressed in the neural floor plate and the notochord and specifies dorsal cell fate [Wilkinson et al., 2009].

HSC potential is not detectable before paired dorsal aortae are fused (in mouse, chick and human) or a single luminised DA is formed. BMP antagonists Chordin and Noggin prevent premature dorsal aortae fusion [Resse et al., 2004; Garriock et al., 2010]. Garriock et al., (2010) showed that Chordin downregulation and the presence of vascular endothelial growth factor

(VEGF) and Sonic hedgehog (Shh) are necessary for DA fusion [Garriock et al., 2010; Nagase et al., 2006]. Notably, VEGF and Shh also regulate the Notch signalling cascade that leads to vessel arterialization and HSC specification [Leung et al., 2013; Lawson et al., 2002].

Several signalling pathways (BMP, Wnt, Shh, RA and Notch) were found to be involved in the regulation of angioblasts migration, vessels arterialization and formation of hematogenic endothelium in dorsal aorta [Lee at al., 2014; Clements and Traver, 2013]. Regulation of HSC specification is orchestrated by molecular queues that are either secreted from surrounding dorsal aorta tissues (somites, notochord, neural tube floor plate, or by urogenital ridges) or presented to HSC on ventral side of somites or dorsal aorta endothelium. [Lawson et al., 2002; Lee at al., 2014; Clements and Traver, 2013]. Below we will briefly review regulation of HSC specification by Runx1, Gata2 and BMP, Shh and Notch signalling cascades.

1.4.6.1. Runx1 role in HSC maturation

Runx1 (Runt Related Transcription Factor 1, also known as acute myeloid leukaemia 1 protein, AML1) is an alpha DNA binding subunit of core binding factor (CBF). CBF binds to multiple enhancers and promoters of the genes implicated in haematopoiesis development [Bee et al., 2009; Swiers et al., 2010(b); Cai et al., 2011; Chen et al., 2011]. In adults, Runx1 is mainly expressed in differentiated myeloid and lymphoid cells [North et al., 1999; Richard et al., 2013]. With application of recent high throughout sequencing techniques, Runx1 expression in adults was also identified in the lung, gastrointestinal tract, kidney and urinary bladder, the ovaries and in multiple tumour tissues [http://www.proteinatlas.org/ENSG00000159216-RUNX1/tissue]. Runx1 gene disruption in adults has been associated with the development of several types of leukaemia [Look, 1997; Speck and Gilliland, 2002; Kurokwa, 2006; Ichikawa et al., 2013; Dowdy et al., 2013].

Embryonic Runx1 knock-out is lethal [Okuda et al., 1996; Wang et al., 1996]. Mouse embryos die prematurely around embryonic day (E) E11-E12 due to anaemia and widespread haemorrhaging. Runx1$^{-/-}$ embryos have normal primitive haematopoiesis, but do not develop any dHSC precursors and present signs of an anaemic fetal liver [Samokhvalov et al., 2006; 2014; Tanaka et al., 2012; Liakhovitskaia et al., 2014]. Runx1 null embryos lack cell populations identified to give engraftment in myeloablated recipients (CD41+Vec+CD45+) and pre-HSC precursors (CD41$^{+/low}$Vec+CD45-) [Okuda et al., 1996; Liakhovitskaia et al., 2014]. Runx1 KO embryos also lack specific intra-aortic clusters (IAC) that are believed to contain developing dHSC [Samokhvalov et al., 2006; 2014].

Intra-aortic clusters are CD31+Runx1+c-kit+ and were observed to bud into the blood vessel during dHSC maturation [Mizuochi et al., 2012; Jaffredo et al., 2000]. In wild type embryos, these clusters of cells were detected in the dorsal aorta of E10 mouse embryos and in the vitelline vessel of E9 embryos. These clusters were found to be absent in Runx1 knockouts [North et al., 1999; Okuda et al., 1996; Samokhvalov et al., 2006; Tanaka et al., 2012]. Strikingly, for all other tissues except AGM, for which dHSC potential was reported at E11.5 (placenta, allantois, yolk sac arteries) Runx1+ clusters of cells were identified at E8-10 [Godin et al., 1995; Palis et al., 1999; Kumaravelu et al., 2003; Gekas et al., 2005; Ottersbach and Dzierzak, 2005; McGrath and Palis, 2005; Yoshimoto et al., 2012].

Runx1 gene dosage affects spatial and temporal distribution of dHSC in mouse embryos. For instance, dHSC are released earlier and are already detectable in AGM and YS of E10.5 Runx1 haploinsufficient embryos [Cai et al., 2002; Lacaud et al., 2003]. According to Sun and Downing (2004), loss of one Runx1 allele leads to a 50% reduction in the number of LT-HSC. Yet, Runx1+/- HSC acquire accelerated propensity to generate multilineage progenitors which keep hematopoietic system in homeostasis [Sun and Downing, 2004].

During embryogenesis, Runx1 is widely expressed in all sites of haematopoiesis (yolk sac, placenta, allantois, dorsal aorta), in hematopoietic cells, and (in particular) in hemogenic endothelium of the dorsal aorta floor and intra-aortic clusters [Lam et al., 2010; Swiers et al., 2010; Chen et al., 2011; Samokhvalov et al., 2014]. After endothelium-hematopoietic transition is initiated (E9-E11), Runx1 expression becomes detectable in the embryonic nervous system, sternum and hair follicle, but for the hematopoietic system development, Runx1 becomes dispensable [Zagami and Stifani, 2010; Kimuraet al., 2010; Liakhovitskaia et al., 2010; 2014; Osorio et al., 2011 Cai et al., 2011; Kobayashi et al., 2012].

Runx1 gene has two alternative promoters (distal P1 and proximal P2 promoters). In mice, Runx1 pre-mRNA can be spliced in several different ways resulting in at least three different Runx1 isoforms: Runx1a, Runx1b and Runx1c [Pozner et al., 2007; Bee et al., 2009; Sroczynska et al., 2009]. The Runx1c isoform is expressed from distal promoter P1and is the longest one. The other 2 isoforms (Runx1a and Runx1b) are expressed from the proximal P2 promoter and are shorter versions of the Runx1 protein. All three isoforms contain DNA binding Runt homology domain (exons 3-5). Isoforms b and c contain transcription regulatory domain while isoform c misses it. Runx1b is the most abundant isoform found in sites of embryonic haematopoiesis at midgestation. Runx1c is the rarest isoform [Challen and Goodell, 2010; Bee et al., 2009].

In Runx1 gene 531-bp enhancer is located at position +23.5 in the first Runx1 intron - in between promoters P1 and P2 [Nottingham et la., 2007; Bee at al., 2009]. In the central part of the +23 enhancer, there are at least four conservative DNA sequences – binding sites for families of transcription factors previously shown to be implicated in dHSC maturation: Myb, Gata, Ets Runx. SCL also binds to this region, most probably via mediation of the Gata2 protein [Nottingham et la., 2007; Bee at al., 2009]. Binding of Gata2, Ets, and SCL to the +23 enhancer

region is critical for Runx1 function. Mutations in Runx or Gata binding motifs abolishes all Runx1 *in vitro* activity [Nottingham et la., 2007; Bee at al., 2009].

Histochemical staining of embryos expressing the Runx1 gene mutated in one of the sites binding transcription factors (Runx1, Gata2 or Ets1) showed that spatial distribution and density of Runx1+ expression is different from that in wild type (WT) embryo. Runx1+ cells were found in WT embryos in YS's blood islands and nascent DA; absence of Runx1 binding motif leads to expansion of Runx1 expression in YS up to embryo proper. Absence of Gata2 motif almost exterminated Runx1 expression in YS, indicating that Gata2 is upstream of Runx1 and positively regulates Runx1 expression. Absence of Ets1 narrowed down Runx1 expression in YS. Interestingly, in all mutants (disrupted Runx1, Gata2 or Ets1 binding sites in +23 enhancer region), intra-aortic clusters were still formed, but they lacked Runx1 expression [Nottingham et la., 2007; Bee at al., 2009; Pozner et al., 2007; Sroczynska et al., 2009]. Hence, the function of master regulator of HSC maturation, Runx1, is critically dependent on expression of Gata2 and Ets. Runx1 expression by itself regulates spatial distribution of Runx1+ cells in the early mouse embryo.

Multiple works were devoted to the identification of differences in Runx1 isoforms' expression and their functional effect on dHSC development, yet, all isoforms were found to be expressed simultaneously in the same hematopoietic sites with no specific functional effect on maturing dHSC. All adult hematopoietic cells were found to be descendants of cells expressed +23 Runx1 region [Sroczynska et al., 2009; Bee et al., 2009; 2010; Challen et al., 2010].

1.4.6.2. Gata2 role in dHSC maturation

Gata2 is a member of zinc-finger transcription factors that are named for the consensus nucleotide sequence that they bind. Gata2 transcription factors family determine cell fate in

multiple tissues. Gata1, 2 and 3 are mainly expressed in hematopoietic cells. Gata1 and 3 are lineage specific effectors responsible for hematopoietic cells differentiation and expansion [Shivdasani et al., 1997; Pandolfi et al., 1995]. In contrast to Gata1 and 3, Gata2 is predominantly expressed in hematopoietic stem cells in adult and in embryo [Tsai and Orkin, 1994; Tsai et al., 1997; Rodrigues et al., 1995]. Gata2 knock out (KO) is embryonic lethal, embryos die around E10-11. Gata2 KO exhibit severe anaemia with loss of all hematopoietic lineages. Anaemia becomes apparent early in embryonic development, at E9.5. Primitive haematopoiesis (erythroid cells maturation) is not affected in Gata2 KO, but the number of cells in the yolk sac is sufficiently lower than in wild type embryos [Tsai et al., 1997]. This implies Gata2's central role in embryonic haematopoietic cells proliferation and in HSC maintenance and expansion in particular.

Gata2 gene dosage has biological effect on HSC numbers and localization. For instance, in heterozygous Gata2+/- mice, number of phenotypically defined HSC in DA decreases while HSC expand and are maintained in the E11-12 yolk sac (YS). Therefore, YS in Gata2 haploinsufficient animals plays a role of a compensatory HSC generator [Ling et al., 2004]. According to Yoder et al., the YS has the ability to generate HSC autonomously, however, in a normal situation, major embryonic arteries are the main source of HSC [Yoder et al., 1997; de Bruijn et al., 2004].

Gao et al., (2013) showed that Gata2 +9.5 cys regulatory element (which contains enhancer, spacer and GATA motif) controls Runx1 expression in hemogenic endothelium and it is specifically required for emergence of c-kit+ IAC and HSC generation. In YS, + 9.5 cys regulatory element affects vascular integrity, but not haematopoiesis. [Gao et al., 2013]. Gata2 deletion in endothelium (VE-Cad+ cells) leads to haemorrhages and loss of functional HSC [de Pater et a., 2013]. Gata2 is activated by Notch1 receptor and its transcriptional factor RBKjk. In zebrafish, Notch1a and Notch1b are required for gata2a and gata2b expression in hemogenic

endothelium. In Gata2b KO, Runx1 expression is reduced in the dorsal aorta [Bee et al., 2009; Nottingham et al., 2007; Butko et al., 2016]. Therefore, Gata2 is an indispensable regulator of Runx1 expression and is critically required for vasculogenesis and HSC specification.

1.4.6.3. Role of BMP and Hh signalling in dHSC emergence in the dorsal aorta

Bone morphogenic protein 4 (BMP4) is a member of transforming growth factor beta (TGF-β) superfamily of proteins. Secreted TGF-β ligands form homo- or heterodimers with similar TGF-β proteins (e.g. BMP7) and bind to TGFR-β receptors. Activation of TGFR-β leads to activation of SMAD family transcription factors [Kawabata et al., 1998; Nohe et al., 2004; Dunn et al., 1997].

Hedgehog (Hh) signalling plays a critical role in embryo patterning and regulates morphogenesis of the number of embryonic tissues and organs. Hh acts as a ventralizing morphogen during neural tube patterning and limb bid. In mammals, there are three ligands Hh homologs: Sonic hedgehog (Shh), Indian hedgehog (Ihh) and Desert hedgehog (Dhh). Hh signalling is activated by Hh ligands binding to canonical Hh receptor Patched 1 (PTCH1) leading to de-repression of membrane-associated protein Smothered (SMO). SMO gets phosphorylated on its intracellular tails and transmit the transduction signal downstream via several intracellular Hh pathway effectors (GLI, Kif7, SUFU). Hh targets genes regulating expression of the components of Hh signalling pathway and the genes responsible for cell proliferation and definition [Pepinsky et al., 2000; Rohatgi et al., 2007; Beachy et al., 2010].

During early embryo development BMP4 (which is expressed in the neural tube roof plate) and Shh (expressed in the notochord and neural tube floor plate) establish the neural tube dorsal-ventral axis [Gilbert, 2003; Hohan, 1996]. Clearly demonstrated in chicken embryos, BMP4 and Shh are also expressed in tissues giving rise to DA precursors, and then surrounding

forming DA [Yoshino et al., 2016]. Before paired DA appear, BMP4 is expressed in an entire lateral plate mesoderm. When DA precursors start to form primordial DA, BMP4 expression becomes restricted to splanchnopleuric mesoderm. At the same time, Shh expression is upregulated in the endoderm. When primordial dorsal aorta lumen is first visible, BMP4+ mesoderm underlines that part of the DA endothelium where Runx1+ cells will appear. Similarly, Shh+ endoderm is situated strictly underneath the position of future Runx1+ endothelium [Yoshino et al., 2016].

Marshall et al., showed that in human embryos that developed to the stage of intra-aortic cluster appearances, Bmp4 expression is polarised. BMP4 is expressed in ventral mesoderm and not expressed above the dorsal aorta and under the neural tube [Marchall et al., 2000]. Similarly, Durand et al. (2007) show that BMP4 is expressed in a polarized fashion around mouse dorsal aorta at E11 [Durand et al., 2007]. Therefore, Bmp4 and Shh expressing cells are strategically localized within tissues predispositioned to give rise to hemogenic endothelium and HSC, implying their essential function in HSC specification.

In zebrafish embryos, Wilkinson et al. (2009) demonstrated that BMP signalling is required for the initiation and maintenance of Runx1 expression in the ventral wall of the DA. With use of zebrafish temperature sensitive mutants expressing truncated Bmp receptor (inhibits BMP signalling), Wilkinson et al. demonstrated that BMP signalling initiates and maintains Runx1 expression in hemogenic endothelium. When these zebrafish mutants were heat shocked before hemogenic endothelium appearance, Runx1 expression was not upregulated in the DA. After Runx1 has already been expressed in the DA, inhibition of BMP signalling leads to reduction Runx1 expression. Notably, Bmp4 morphants lost Runx1 expression completely within the DA while neural Runx1 expression was not affected, indicating specific action of BMP4 on hemogenic endothelium [Wilkinson et al., 2009].

Gering and Patient (2005) demonstrated that Hedgehog signalling (Hh) is required for Flk1+angioblasts migration and for aortic specification in zebrafish embryos. Ihh KO (Ihh is expressed in visceral endoderm) causes defective YS vasculature. One of Ihh mesodermal targets is Foxf1. Bmp4 was shown to be downstream of Foxf1. Therefore, Hh signalling might act via Foxf1 mediator on Bmp4. If Bmp4 is added to $Foxf1^{-/-}$ explants, normal vasculogenesis is observed (Byrd et al., 2002). In early somitic embryos Hh signalling induces the expression of arterial marker ephrinb2a and hematopoietic markers Vegf, Notch and Runx1 [Gering and Patient, 2005].

Mouse embryonic stem cells treatment with exogeneous BMP4 leads to mesoderm induction and appearance of cells with myeloid markers [Johansson and Wiles, 1995]. AGM explants culture with exogeneous BMP4 results in HSC expansion revealed via increase in numbers of myeloablated recipients repopulated with donor AGM cells. AGM explants treatment with Bmp4 decreases pool of CD45-CD34+Flk1+ cells, but expand numbers of $CD45+CD34^{low}$c-kit+ cells. Hence, Bmp4 might accelerate endothelium to hematopoietic transition which is reflected in decrease of cells with endothelial phenotype (Flk1+) and expansion of population of cells with preHSC phenotype ($CD45+CD34^{low}$c-kit+). BMP4 action is specific, as treatment with gremlin (Bmp4 antagonist) abolishes HSC expansion in AGM explants [Johansson and Wiles, 1995].

In mouse, notochord, neural tube and gut tissues express Shh. Co-culture of AGM explants with Shh expressing tissues or addition of exogeneous Shh or Indian hedgehog (Ihh) expands pool of HSC (evaluated by CFU-S or by transplantations). This HSC expansion can be abolished with addition of Hedgehof signalling pathway inhibitors [Dyer et al., 2001; Peeters et al., 2009]. Using reporter mouse for Gli1 (one of Hh signalling target) Gli1 expression was found to be around E9 mouse aorta, indicating activation of Hh signalling [Peeters et al., 2009].

AGM explants with addition of SHH or BMP4 (in serum free medium) led to expansion of HSC detected by high level of donor blood chimerism in myeloablated recipients (2/6). Yet, treatment of AGM explants with both BMP4 and SHH revealed synergistic action of these proteins (increase in number of repopulated mice to 5/6) [Crisan et al., 2016].

Crisan et al., (2016) found that AGM contains two populations of cells: BMP- activated and non-BMP-activated HSC. Using the mouse model with GFP reporter for BMP signalling, authors showed that both E11 GFP+ and GFP- populations of cells are true HSC, which support a high level of engraftment in primary and secondary transplantations. When AGM explants were treated with cyclopamine (Hh pathway inhibitor) it had no effect on GFP+ (HSC with active BMP signalling) but eliminated HSC in the GFP- fraction of cells. Treatment of GFP- cells with exogeneous VEGF allowed rescue of HSC maturation and the obtainment of engraftable cells. The observed level of engraftment was lower than in transplantations carried out within cells not treated with cyclopamine. Hence, Crisan et al., proposed HSC heterogeneity is already initiated at this stage of development. E11 AGM contains at least 2 different HSC populations: Hh signalling dependent and Hh independent, but with active BMP signalling [Crisan et al., 2016].

There are other mechanisms that might induce BMP signalling in the dorsal aorta. For example, blood circulation causes shear stress on dorsal aorta endothelium cells. Kim et al. (2015) demonstrated that VE-Cad+ cells in response to shear stress secrete BMP ligands, inducing HSC maturation in autocrine-paracrine mode. One of the BMP targets is shear-stress response pathway mediated by protein kinase A (PKA)-cAMP response element binding protein (PKA-CREB) [Kim et al., 2015].

BMP and Shh signalling is responsible for HSC maturation during a narrow window of time. At the time when the DA is forming or is still paired, anti-BMP signalling molecules (chordin, noggin2, and type II collagen) surround the dorsal aorta and prevent aortae fusion.

Shortly before HSC emergence, genes supporting BMP signalling (Bmpr2, Smad5, Tolloid (cleaves chordin) start to be expressed and the dorsal aorta is able to fuse [Huber et al., 1999; Wilkinson et al., 2009]. Fusion of the DA requires presence of Shh [Garriock et al., 2010]. Simultaneously, Bmp and Hh signalling initiate HSC specification.

1.4.6.4. Notch signalling in HSC specification

Series of works done in zebrafish and Xenopus embryos allowed light to be shed on the complex process of HSC specification. Notch signalling was identified to take place in multiple steps of HSC specification: controlling pre-HSC migration, dorsal aorta assembly, emergence of hemogenic endothelium and HSC maturation. Different Notch receptors and ligands dynamically regulate HSC specification. The united picture of the whole mechanism of HSC maturation by Notch signalling is yet to be constructed, however some steps are already described.

Notch signalling. Notch pathway ligands and receptors

Higley evolutionary conserved Notch signalling pathway serves for cell-to-cell communication during cell fate determination. During development, Notch was found to be implicated in maintenance and differentiation of multiple types of stem cells (epithelia hematopoietic system specification, neurogenesis and myogenesis, and other) [Liu et al., 2010]. In particular, Notch is known for the regulation of cell-fate decision of neighbouring cells with the same differentiation potential (also known as lateral inhibition or lateral specification) [Chen and Streit, 2013]. Cells expressing mainly the Notch ligand differentiate according to

"default program" and cells expressing predominantly Notch receptors, will differentiate by "an alternative route" [Chen and Streit, 2013; Bray, 1998]

Notch receptors and their ligands (in case of canonical Notch signalling) are single pass transmembrane proteins with extracellular domains composed of a different number of tandem epidermal growth factor (EGF)-like repeats. In vertebrates, there are four Notch receptors (Notch1-Notch4) and five Notch ligands Delta-like1, Delta-like3, Delta-like4 and Jagged1, Jagged 2) [Kopan and Ilagan, 2009; Hori et al., 2013]. Before the Notch receptor is presented on the surface of a cell, it undergoes enzymatic cleavage inside cell's Golgi apparatus (so called S1 furine-dependent cleavage). On the surface of the cell upon binding to one of the Notch ligands (Delta-like: DLL1, DLL3, DLL4 or the Jagged: JAG1, JAG2), second (S2) and third (S3) cleavage of the Notch receptor takes place [Hori et al., 2013]. S1 is mediated by A disintegrin and metalloproteinase domain (ADAM) and S3 takes place inside the membrane of a Notch receptor bearing cell by multimeric gamma-secretase. After these series of cleavages, a Notch receptor is released from the membrane, undergoes endocytosis and triggers activation of Notch target genes [Hori et al., 2013]. Activated intracellular Notch receptor domain localize to the nucleus where it binds to stem cell leukaemia (SCL, also known as T-Cell Acute Lymphocytic Leukaemia, TAL1) transcription factor. CSL is implicated in haematopoietic malignancies and hemopoietic differentiation. SCL binds to specific DNA sequences on promoters of Notch target genes (Hairy and Enhancer of Split, HES-1) [Tun et al., 1994]; and genes implicated in haematopoiesis: Hes1, Hes5, Hey2 and Gata2 [Iso et al., 2003; Guiu et al., 2012; Davis and Turner, 2002].

Notch signalling is regulated on multiple levels. Notch receptor extracellular domain is glycosylated in multiple ways, which affects its recognition [Xu et al., 2007]. Notch receptor endocytosis could result not only in Notch signalling activation, but also in receptor recycling or receptor degradation [Yamamoto et al., 2010; Mukherjee et al., 2005]. Notch signalling

depends on the type of ligand that binds to its receptor and also on ligand endocytosis-recycling by signal-sending cells [Shergill et al., 2012]. The Notch receptor can be also activated by soluble ligands in non-canonical way or in the absence of a ligand. In modern day, the latter process is not entirely understood [Kopan and Ilagan, 2009].

Notch role in adult haematopoiesis

In human CD34+, hematopoietic precursors expression of Notch1 and Notch2 was identified - on bone marrow derived myeloid cells, but not on erythroid cells (Ter119+ cells). Notch ligand expression was also identified on the surface of bone marrow stromal cells. When Sca-1+c-kit+lin− bone marrow cells were transduced with viral construct to overexpress Notch1, HSC become immortalized and were able to generate lymphoid and myeloid progeny when treated with IL-7 or GM-CSF, correspondingly [Varnum-Finney et al., 2000; Stier et al., 2002]. Stier et al., noted that transplantation of Notch1 transduced murine bone marrow Sca1+lin- cells into Rag-/- recipients shifted balance in donor-derived cells progeny towards more primitive phenotype. Yet, cell differentiation was not blocked and a leukemic population did not appear. The authors proposed that Notch1 triggers HSC differentiation towards lymphoid lineage in dispense of myeloid one (the default choice) [Stier et al., 2002]. Radtke et al., showed that transplantation of lethally irradiated wild type recipients with cells derived from Notch deficient animals reconstitute all hematopoietic lineages except T-cell one. [Radtke et al., 1999]. Therefore, in adults Notch specifically promotes T-cell differentiation and the absence of Notch signalling leads to early B-cell commitment [Radtke et al., 1999; Pui et al., 1999].

Activation of the Notch pathway with a Delta-1 ligand by its overexpression in feeder layer or Delta-1 absorption on a plastic surface, induces dramatic expansion of Sca1+c-kit+lin- murine bone marrow cells treated with SCF, FLT3L, IL-6 and IL-11. Transplantation of these

cells in culture revealed a multilineage engraftment, but loss of self-renewal potential, suggesting that in adults Notch is responsible for differentiation and expansion of HSC, but not for maintaining the stem cell phenotype [Varnum-Finney et al., 2000].

Notch signalling role in HSC specification

Early wave of primitive haematopoiesis is independent on Notch signalling, as Notch deficient embryos maintain normal haematopoiesis in the yolk sac [Lawson et al., 2001; Robert-Moreno et al., 2008]. Further on, during the definitive wave of embryonic haematopoiesis, Notch1 signalling is indispensable for all processes related to HSC specification [Hadland et al., 2004]. Utilizing mouse embryo chimeras composed of wild type and Noth1-/- cells, Hadland et al., showed that Notch1-/- do not to contribute to adult hematopoietic lineage [Hadland et al., 2004].

Master regulator of HSC maturation, Runx1, is downstream under Notch1 signalling [Burns et al., 2005; Nakagawa et al., 2006; Richard et al., 2013]. At the time of HSC specification, disruption of Notch1 signalling abolishes Runx1 expression in para-aortic splanchnopleura (P-Sp). Runx1 enforced expression rescues Notch1 deficient cells isolated from E9 mouse embryo P-Sp. Rescued cells in the OP9 co-culture system are able to differentiate towards hematopoietic lineage (CD45+ cells) [Nakagawa et al., 2006]. There is an indication that Notch1 does not directly regulate Runx1 expression as Runx1 +23 enhancer region (which marks all definitive hematopoietic and clonogenic progenitors of the dorsal aorta, fetal liver, umbilical artery and IAC) does not have sequences binding Notch1. Activity of Runx1 +23 enhancer depends on intact Gata2, Ets and SCL binding sequences. Hence, these transcription factors are upstream of the signalling cascade that induce HSC maturation [Nottingham et al., 2007].

Notch2 does not exhibit obvious hematopoietic defects while Notch3 is required for sclerotome development and acts on HSC specification indirectly [Kumano et al., 2003; Kim et al., 2014]. Notch4 is dispensable for embryonic haematopoiesis but has overlaps with Notch1 roles [Krebs et al., 2000]. For instance, Notch4 is responsible for initiation of Gata2 expression while Notch1 is required for Gata2 expression maintenance [Leung et al., 2013].

Similar to the adult bone marrow, E12-E17 mouse fetal liver cells express Notch receptors and ligands Jagged1 and Delta1 [Walker et al., 2001]. While the role of Notch signalling is clear for HSC specification, at the time when pre-HSC I and II appear in the dorsal aorta, dependence on Notch signalling decreases [Tang et al., 2013; Lizama et al., 2015; Souilhol et al., 2016]. Today it is not clear whether Notch signalling regulates maintenance and expansion of HSC in the fetal liver and later in embryonic bone marrow [Souilhol et al., 2016(a) and 2016(b)].

Regulation of HSC specification by the Notch pathway is proved to be complex, and the entire mechanism is yet to be elucidated [Gering M, Patient, 2010; Hori et al., 2013]. Notch signalling can take place on multiple levels: it can be triggered by Sonic Hedgehog (Shh), Etv6 or Wnt16 and be mediated via diffusible VEGF, FGF or directly by cell to cell contacts, by Notch ligands or other factors [Lawson et al., 2002; Ohishi et al., 2003; Kobayashi et al., 2004; Kopan and Ilagan, 2009]. Initially, it was difficult to unlink the Notch signalling role in angioblasts migration, arterialization and HSC emergence [Robert-Moreno et al., 2008]. For instance, Notch ligand Jagged1 deficiency results in vascular defects, but still allows arterial markers (EphrinB2, CD44 and SMA) to be expressed. In E10.5-11 mouse Jagged1 KO, number of Gata2+Runx1+ cells are decreased and hemogenic endothelium fails to produce HSC [Robert-Moreno et al; 2008]. Delta4 deficiency leads to arterial defects and early lethality [Duarte et al., 2004; Krebs et.al., 2004]. Therefore, Notch signalling is required for both arterial specification and maturation of HSC.

Several mechanisms of HSC specification by Notch signalling regulation have been described.

In zebrafish embryos, Sonic Hedgehog (Shh), which is expressed in floor plate of neural tube and notochord, induces production of vascular endothelial growth factor (VEGF) in somitic tissues [Lawson et al., 2002; Ciau-Uitz et al., 2010]. VEGF acts on its receptor VEGFR2 (also known as Flk1 or Kdr – kinase insert domain receptor, a type III receptor tyrosine kinase), expressed on migrating towards embryonic midline angioblasts and later on the dorsal aorta endothelium cells [Cleaver and Krieg, 1998; Hogan and Bautch, 2004]. Notch signalling activated by VEGFR2 regulates cell migration and their arterial identity. With Notch1 signalling activation in the DA endothelium, arterial markers EphrinB2 and/or hematopoietic transcription factors Gata2 and Runx1 start to be expressed [Lengerke et al., 2008, Lawson et al., 2002].

In *Xenopus leavis,* somitic expression of VEGFA is regulated by transcription factor Etv6 (also known as TEL1 or ETS Variant 6) [Ciau-Uitz et al., 2010]. In frogs (before DA assembly) vascular endothelium growth factor A (VEGFA) directs migration of Flk1+ DA precursors towards embryonic midline [Cleaver and Kreig, 1998]. If Flk1 or Notch1 are mutated, HSC fail to specify the DA endothelium. Injection of VEFGA morpholino that blocks all VEGFA isoforms led to abrogation of the DA precursors migration and absence of DA. Reduction of morpholino concentration allows the DA to assemble, but did not allow the hemogenic endothelium to form (detected as absence of Runx1, Gata2 and Notch1 expression). Expression of arterial markers (Dll4, Cx37) was present, but weak in comparison to WT [Ciau-Uitz et al., 2010; Leung et al., 2013].

VEGFA is expressed in somites and notochord and its effect is dosage dependent: haploinsufficient embryos have defective vasculogenesis [Carmeliet et al., 1996; Ferrara et al.,

1996]. Three different VEGFA isoforms are expressed: short diffusible, medium and long membrane-bound forms. The diffusible short isoform is the most abundant in Xenopus somitic tissues. Cleaver and Krieg (1998) proposed that short diffusible isoform of VEGFA expressed in notochord regulates migration and assembly of the DA [Cleaver and Kreig, 1998]. Leung at al., (2013) has suggested that the short VEGFA isoform also controls lumenization and arterialization of DA cord [Leung et al., 2013]. Low concentration of VEGFA long and medium isoforms disrupt arterial specification, but not endothelial. Chen et al., (2010) proposed that soluble and membrane bound VEGFA isoforms activate different signalling cascades with different outcomes: vascularization, arterialization and HSC specification [Chen et al., 2010].

VEGFA long and medium isoforms specific KO phenocopies Eto2 knockout. Eto2 (also known as CBFA2/RUNX1 Translocation Partner 3) is a transcriptional co-repressor participating in regulation of hematopoietic gene expression such as GATA-1, SCL/TAL1 and LMO2 [Fujiwara et al., 2013]. In *Xenopus,* Eto2 morphants have normal primitive erythroid lineage development. In Eto2 morphants, the aorta is formed and luminized; arterial markers (EphrinB2, Delta like 4, Notch4, Cx37) and vascular markers (VE-Cad, CD31, Tie2, Fli1) expression is normal. Yet, Runx1, SpiB (Pu.1 homolog), Gli1, Scl and Notch1 expression is absent in endothelial lining of the DA, indicating failure of hemogenic endothelium maturation. Interestingly, that expression of the Fli1 marker is downregulated by Notch1 by stage 39 (frogs), yet in ETO2 morphants Fli1 expression persists [Leung et al., 2013]. In Eto2 morphants, level of long and medium VEGFA isoforms were decreased in comparison to untreated embryos. In contrast, short VEFGA isoform concentration was largely not affected. Restoration of levels of long isoform could rescue hematopoietic marker expression (Runx1 and Gfi1). Therefore, this Notch signalling pathway responsible for HSC specification can be described as: ETO2->VEGFRA->Notch1. This pathway is Hedgehog (HH) independent as Eto2 morpholino does not affect Patched 1 (Ptc1, receptor for HH) expression and cyclopamine

(specific HH inhibitor) treatment also does not affect Eto2 expression (but affect Ptch1) indicating that this HSC specification pathway is not Hh dependent.

Leung et al., (2013) proposed that expressed in somites, medium and/or long VEGFA isoforms induce Notch1 expression in the DA. In contrast, high levels of short VEGFA isoform in somites and dorsal lateral plate trigger arterial specification and Notch4 activation. Notch4 upregulates Gata2 expression in the DA, while Notch1 is required for Gata2 maintenance [Leung et al., 2013].

Another Notch activating mechanism was described by Kobayashi at al., (2014). Ventral sides of somites transmit signal to lateral plate mesoderm (LPM) cells that migrate to form the dorsa aorta endothelium. Ventral sides of somites express junctional adhesion molecules Jam2a and Jam1a - on LPM cells. Disruption of any of the Jam-s leads to failure to specify HSC while arterial specification still takes place. Enforced Notch ligands expression rescue the generation of hemogenic endothelium, but with different efficiency while abrogation of Jam1a expression abolishes expression of Notch1 in the dorsal aorta endothelium [Kobayashi at al., 2014].

Ectopic activation of Notch1 in veins induces expression of Runx1 and c-myb and causes ectopic haematopoiesis [Burns et al., 2005]. This does not transform veins in arteries and it is not known whether the ectopic haematopoiesis produces HSC. Hence, it is not possible to conclude that HSC specification takes place only in arteries.

Fibroblast growth factor (FGF) was found to be another molecule able to activate Notch signalling during HSC specification. Somitic tissues, but not LPM cells express FGF receptors (FGFR1 and FGFR4). FGF acts in concert with Wnt and Notch signalling. Wnt16 (non-canonical Wnt signalling) was shown to regulate expression of Notch ligands (DeltaC and DeltaD) in somites. Abrogation of Wnt16 expression in somites reduces the level of FGFR4.

Wnt16 acts via FGFR4 to regulate levels of Notch ligand DeltaC, but not DeltaD within somites [Lee at al., 2014].

Lee at al., (2014) used transgenic zebrafish embryos in which FGF signalling can be blocked by keeping the embryo at an elevated temperature. The authors utilized time-specific FGF pathway inhibition to target HSC specification only (14-17 hours post fertilization, hpf). When the FGF pathway was knocked out during early stages of development, this reduced some of the Notch pathway ligands expression: DeltaC, but not DeltaD and blocked HSC specification. In this model, ectopic activation of Notch signalling leads to rescue of HSC specification. Overexpression of DeltaC also rescued HSC specification. In this FGF KO, the hemogenic endothelium was not affected. At later stages of development, FGF inhibits HSC emergence, for instance by contracting BMP signals [Pouget et al., 2015]. Analysis showed that this FGF signalling does not interact with signalling pathways described above (Hh independent Eto2 or Etv6 -> VEGFA -> Notch1 and Shh -> VEFG -> VEGFR2 -> Notch), which are required for DA assembly, arterialization and HSC specification [Lee at al., 2014]. FGFR4 KO also leads to loss of HSC and does not affect vascular or arterial gene expression. Instead, FGFR4 KO leads to loss of sclerotome tissue [Lee at al., 2014]. Hence, Notch signalling within somites indirectly regulates HSC specification and does not affect vasculogenesis or arterialization.

Sclerotome cells might contact migrating LPM cells before they contribute to the primordial dorsal aorta cord. Alternatively, smooth vascular muscle cells, precursors of which reside in somites, might migrate to envelop the DA and possibly induce final steps of HSC specification [Pouget et al., 2008; Kobayashi et al., 2014]. Nguyen et al., (2014) demonstrated the contribution of endotome cells (another somitic part) to endothelium of the DA. In chicken embryos, Pouget et al. (2006) showed that after intra-aortic hematopoietic clusters disappear from the dorsal aorta, hemogenic endothelium is substituted by somatically derived cells

[Wasteson et al., 2008; Pouget et al., 2006; Nguyen et al., 2014]. Hence, somites directly or indirectly regulate hematogenic endothelium maturation and HSC specification: by secreting factors regulating Notch signalling within lateral plate mesoderm or via direct contact with somatic cells or their derivatives. Different branches of the Notch pathways network are dynamically involved in HSC specification, possibly enabling different steps of HSC specification maturation. Yet, the complete mechanism of HSC regulation by Notch signalling remains to be clarified.

1.5. Maturation and expansion of HSC and their precursors *ex vivo*

Today there is a shortage of HSC available for transplantations in clinics [Sauvageau et al., 2004, 2010; Batta et al., 2016]. One of the solutions for this problem is to expand the pool of HSC in donated chord blood or to derive functional HSC from human embryonic or pluripotent stem cells or somatic cells [Wang et al., 2005; Bhatia, 2007; Oubari et al., 2015]. Both methods include a HSC culture step. Culture conditions attempt to recapitulate the microenvironment in which HSC reside *in vivo* [Zhang and Lodish, 2008]. The aim of HSC culture is to direct HSC to divide with preservation of their self-renewal potential; mature into functional HSC from an HSC precursor or to differentiate. To date, the recreation of HSC microenvironment is carried out with utilization of feeder layers (mesenchymal stem cells); co-culture with stroma cell lines; culture of HSC in various 3D scaffolds and by addition of cytokine cocktails to the culture medium [Oubari et al., 2015; Celebi et al., 2011; Heike and Nakahata, 2002]. In the HSC niche (AGM, fetal liver, adult bone marrow) cytokines are secreted by stromal cells, modulating HSC maintenance in this way [Nishikawa et al., 2001]. Cytokines were shown to induce upregulation of critical for HSC self-renewal and maturation genes: Gata2, Runx1, Tal-1, Gata1, Pu.1, Bmi-1, Lmo2 [Noda et al., 2008; Stanley, 2009 Zhu and Emerson, 2002].

An additional approach often utilized to generate hematopoietic cells is human embryonic stem cells (hESC) differentiation or somatic cells reprogramming into HSC by recreation of HSC niche microenvironment and enforced overexpression of transcription factors like Runx1, Gata2, Scl, Hoxb4, Pu.1 [Bhatia, 2007; Wang et al., 2005; Batta et al., 2016]. This approach shows promising results. Some works reported short term cell engraftment and generation of cells of several hematopoietic lineages [Pick et al., 2007; Suzuki et al., 2013; Vereide et al., 2014]. In particular, Doulatov et al. demonstrated that enforced expression of Hoxa9, Erg, Rora, Sox4, and Myb in differentiated hESC generated short term engrafting lymphoid progenitors [Doulatov et al., 2013]. Overexpressing of Runx1a isoform in hESC allowed to derive short term engrafting multilineage potential HSC cells. [Ran et al., 2013]. Gori et al., reconstructed the endothelial niche of maturing dHSC by culturing differentiating hESC in presence of endothelial cells expressing Notch ligands Jagged-1 and Delta-like ligand-4. This allowed the generation of HSC with high levels of long term engraftment [Gori et al., 2015]. Yet, methods using forced gene expression require further development to attenuate potential teratogenic outcome. Detailed discussion of the methods of HSC derivation from embryonic stem cells or induced pluripotent cells is reviewed in Batta et al., 2016. Below we will discuss the method of HSC expansion that recreates the HSC microenvironment with addition of exogenous cytokines and/or in the presence of cells that secrete these cytokines.

The method of HSC (or their precursors) culture in presence of cocktails of growth factors is widely used in experimental procedures that are aimed to recapitulate mechanisms of HSC development [Heike and Nakahata, 2002]. Phenotypical HSC (in humans - CD34+ cells) or their precursors (in mice - VE-Cad+CD41$^{+/low}$c-kit+CD34$^{-/+}$ cells) might be cultured on air-liquid interface or as submerged culture in suspension, on a feeder layer of mesenchymal stem

cell or in presence of stromal cell lines (for example with OP9) [Celebi et al., 2011; Oubari et al., 2015] One of these methods, co-aggregation of pro-HSC cells with OP9 stromal cell line in presence of selected cytokines was utilized in this work (technical details are described in Materials and Methods). For instance, Rybtsov et al. showed that cells derived from caudal parts of E9 mouse embryos contain the very early CD34- HSC precursors (pro-HSC) that are able to mature into functional dHSC in the presence of SCF and OP9 stromal cell lines when cultured at air-liquid interface for prolonged period of time [Rybtsov et a., 2014]. For clinical applications, serum-free culture media has to be used. Serum is a known source of undefined growth factors, and the utilization of a serum-free medium might lead to reduction of HSC expansion method success [Solar et al., 1998; Alexander et al., 1996; Sauvageau et al., 2004]. There is no ideal cytokine formulation developed yet, but some working components have been identified. The most frequently used set of cytokines for HSC expansion or maturation is: SCF, Il3, Flt3-ligand, IL-6; IL-11, TPO and VEGF. More rarely used components are: Insulin-like growth factor 2 (IGF-2), fibroblast-growth factor 1 (FGF-1) and angiopoietin like 2 and 3 [Heike and Nakahata, 2002; Zhang and Lodish, 2008; Batta et al., 2016].

Examples of combination of growth factors allowing significant expansion of HSC pool of cells are: SCF/TPO/Flt3-L and SCF/TPO/Flt3-L/IL-formulations. At these conditions the fraction of human CD34+ cells increased up to 1200-fold [Arrighi et al., 1999]. SCF/TPO/Flt3-L/IL-3 and SCF/Flt3-L/IL-11 increased CD34+ fraction of cells in 6300-fold [Bryder and Jacobsen, 2000]. Culture with addition of SCF/TPO/Flt3-L and SCF/TPO/Flt3-L/IL-3 or SCF/Flt3-L/IL-11 allowed the preservation of long-term engraftment ability [Ramsfjell et al., 1999]. In contrast, addition of SCF/TPO/Flt3-L/VEGF and SCF/Flt3-L/IL-3/IL-6 induces HSC differentiation into committed progenitors, but not HSC [Fu et al., 2005; McKinney-Freeman et al., 2008]. Regrettably, *ex vivo* methods of HSC expansion lead to decrease in self-renewal property of CD34+ cells. Expanded cells were tried in clinic and were proved to be safe, but

application of *ex vivo* CD34+ cells expansion currently might not be economically reasonable [Müller et al., 2016; Sauvageau and Humphries, 2010]

Below we will discuss in detail role of three cytokines used in this work and the ones used the most frequently HSC *ex vivo* expansion protocols. Those are: SCF, IL-3, Flt-3.

1.5.1. Role of stem cell Factor in *ex vivo* HSC expansion

Stem cell factor (or c-kit ligand) is a ligand for the receptor-type protein-tyrosine kinase KIT (c-kit) [Anderson et al., 1990; Matsui et al., 1990; Broudy, 1997]. SCF is a pleiotropic factor found to be important for neural and hematopoietic cell development, hematopoietic cell survival, proliferation and migration [Keshet et al., 1991; Lev et al., 1994; Matsui et al., 1990]. SCF exists in 2 splice forms, one of which is secreted protein and another one is a membrane-bound one [Anderson et al., 1990]. Both forms are identical in sequence except for a short (20 AA) site for metalloproteinase cleavage on soluble form of SCF [Anderson et al., 1991]. Both splice forms of SCF are initially generated as membrane-bound proteins, the soluble form gets cleaved and acts as a long-range signalling molecule. Recently, it was reported that “soluble” SCF can be also generated by premature splicing termination [Saravanaperumal et al., 2012].

One of the roles of SCF is to guide HCS migration towards their niche. Hematopoietic cells migrate towards a higher concentration gradient of SCF emanating from the niche (fetal liver, spleen, bone marrow) [Meininger et al., 1992; Blume-Jensen et al., 1993]. Seeding of embryonic hematopoietic organs takes place over the days. During this time, dHSC circulate at low quantities in the embryo blood and gradually seed hematopoietic organs in response to SCF signalling [Driessen et al., 1993; Hoffman et al., 1993; Wang et al., 2016]. Therefore, SCF is a chemoattractant allowing HSC to migrate towards their niche.

SCF binding to c-kit leads to c-kit autophosphorylation and activation of signal transduction regulating genes implied in haematopoiesis [Rönnstrand, 2004; choice [Nishikawa et al., 2001; Zhang and Lodish, 2008]. c-kit is expressed on all hematopoietic stem cells progenitors and HSC. After differentiation, c-kit expression is lost in all but dendritic and mast hematopoietic cells [Broudy, 1997; Okada et al., 1991]. During embryonic development, SCF/c-kit acts synergistically with other cytokines, promote HSC maintenance in the absence of cell division [Keller et al., 1995; Hoffman et al., 1993]. SCF/c-kit promotes activation of AKT1, RAS, RAF1 and the MAP kinases; promote activation of signal transducer and activator of transcription (STAT) protein family [Yu et al., 2009; Lennartsson et al., 1999; Rönnstrand, 2004].

1.5.2. Role of interleukin 3 in *ex vivo* HSC expansion

Interleukin-3 (IL-3), previously known as "haemopoietin growth factor" [Whetton et al., 1985] or "multi-colony stimulating factor (multi-CSF)" [Evans et al., 1999] belongs to the same family of cytokines as granulocyte-macrophage colony-stimulating factor (GM-CSF) and IL-5. These cytokines are involved in immune response and induce leukopoiesis. Il-3 is secreted by T cells, macrophages and stoma cell in bone marrow [Mangi and Newland, 1999; Kim et al., 2010]

Signalling cascade activated by IL-3 is triggered via a heterodimeric receptor assembly. One of the receptor subunits is major signalling subunit (beta common, βc). βc subunit is not specific and binds any of the IL-3 cytokines family. The second receptor - major binding subunit (alpha, α) is specific for IL-3, GM-CSF or IL-5 [Broughton et al., 2012; 2015]. GM–CSF/IL-3/IL-5 receptors are expressed at relatively low level on committed hematopoietic cells while specific IL-3Rα (interleukin - 3 receptor subunit alpha, CD123) is highly expressed on stem and leukemic cells [Gomes et al., 2001; Testa et al., 2002]. βc is also expressed on

endothelial cells. IL-3 stimulation of endothelial cells increases these cell motility and vasculogenesis. [Dentelli et al., 1999]. Activation of GM–CSF/IL-3/IL-5 receptor initiates signalling cascade leading to activation of STAT (signal transducer and activator of transcription), MAPK (Ras-mitogen-associated protein kinase) or PI3K (phosphoinositol 3-kinase).

IL-3 activates a wide range of bone marrow cells (mast cells, basophils, neutrophils, eosinophils, macrophages, erythrocytes, megakaryocytes) and recruits basophils and mast cells to the lymph nodes [Mangi and Newland, 1999; Kim et al., 2010]. IL 3 is responsible for multi-lineage hematopoietic progenitors and committed myeloid, erythroid and megakaryocytic lineages survival, maintenance or proliferation and/or differentiation [Guthridge et al., 1998]. Mice deficient for IL-3 have no apparent defect in haematopoiesis but show defect in immune response to parasites due to impaired recruitment of effector hematopoietic cells [Lantz et al., 1998].

IL3 applicability for *ex vivo* HSC expansion is a controversial issue. [Bryder and Jacobsen, 2000; Yonemura et al.,1996]. According to published reports, IL3 can not only promote self-renewal of cultured HSC, but also can trigger their differentiation with decrease in long-engrafting property [Itoh et al., 1992; Yanai et al., 1995; Peters et al., 1996; Yonemura et al., 1996]. Effect of IL-3 on cells self-renewal or differentiation *in vitro* is concentration dependent and is synergistic with other cytokines. Presence of fetal calf serum in HSC culture strongly affects IL-3 action on cultured cells. Serum is well known undefined component of culture media that contains various growth factors and hormones. Hypoxic conditions can also alter extent of IL-3 action on cell culture [Bryder and Jacobsen, 2000].

Culture of human bone marrow HSC derived from IL-3 receptor mutants (α and βc receptors) and wild type HSC with addition of IL-3 abrogated B-lymphoid potential and negatively affected reconstructing ability of HSC [Matsunaga et al., 1998; Zandstra et al.,

1997]. Yonemura showed that culture of adult mouse bone marrow c-kit+ cells reduces numbers of repopulating cells. Donor cells contribution to hematopoietic system was ~70% when freshly isolated c-kit+ cells were injected in lethally irradiated recipients. On the contrary, donor contribution dropped to ~60% when c-kit+ cells were cultured with exogeneous SCF, IL-6, IL-11 for 7 days and to ~2% when culture was extended to 14 days. When IL-3 was added the culture, after 7 days culture, donor contribution was just 20% and after 14 days - ~1%. Decrease in number of injected cells also reduced donor contribution to recipients' hematopoietic system [Yonemura et al.,1996]. Rybtsov et al. (2014) showed that IL-3 does not negatively influence maturation of very early dHSC precursors in mice, but can be omitted in cytokine cocktails for pro-HSC expansion [Rybtsov et al., 2014].

On the contrary [Bryder et al., 2000] found that addition of IL-3 to HSC cultures supports HSC self-renewal; increased the cycling of LSK HSC and it did not affect myeloid or lymphoid reconstitution. Possible explanation for this discrepancy is presence of FCS in cultures. FCS contains various undefined factors and as IL-3 acts synergistically, presence of FCS unpredictably affects HSC development. In serum free cultures, IL-3 was found to accelerate expansion of primitive and mature hematopoietic cells and heterogenic population of HSC.

For today IL3 is widely utilized component of many cytokine cocktails for HSC *ex-vivo* expansion. Due to heterogeneity of HSC, usability of IL-3 has to be tested separately for each set of target cells, with clearly defined concentration of other cytokines and utilization of calf serum of defined origin and concentration [Qui et al., 1999; Querol et al., 1998; Capmany et al., 1998].

1.5.3. Role of Fms related tyrosine kinase 3 ligand in *ex vivo* HSC expansion

Flt3-ligand (FLTL) is the ligand for Fms-like tyrosine kinase 3 type receptor (FLT3 or CD135) [Gilliland and Griffin, 2002]. FLT3 in mice is known as fetal-liver kinase-2 (FLK-2) or in humans - stem cell kinase-1 (STK-1) [Matthews et al., 1991(a), 1991(b); Rosnet et al., 1991; Jaye et al., 1992]. FLT3 shares structural homology with other tyrosine kinase type cytokine receptors, for example, stem cell factor receptor (c-kit) or platelet-derived growth factor receptor (PDGFR). FLT3 has extracellular (immuno-globulin like domains) and intracellular tyrosine kinase domain. Similar to SCF, FLT3L exists is soluble and membrane-bound forms and is secreted by bone marrow cells [Lyman et al.,1993; Lyman et al.,1994]. Soluble form of FLT3L is produced by alternative splicing by premature termination condone [Lyman et al., 1995; Saravanaperumal et al., 2012]. To activate signalling through FLT3, receptor subunits dimerization is required. FLT3 activation leads to induction of signalling cascades via STAT, ERK and PI3K.

FLT3 signalling regulates differentiation, proliferation and survival of hematopoietic progenitor cells. FLT3 is expressed on myeloid and lymphoid progenitors. Injection of FLTL induces HSC migration of HSC into peripheral blood and trigger maturation of multipotent progenitors into myeloid and lymphoid lineages in dispense of megakaryocyte-erythroid lineages. Transgenic mice overexpressing FLT3L develop splenomegaly, blood leucocytosis and anaemia resulted from reduction of erythroid progenitors [Tsapoggas et al., 2014]. Mice deficient for FLT3 or FLT3L have impaired myelo- and lymphopoiesis and have deficit in B cells, natural killer cells and dendritic cells. Yet, neither Flt3-/- nor Flt3l-/- mice' hematopoietic system development is not affected [McKenna et al., 2000; Sitnicka et al., 2002].

Previously it was supposed that FLT3 induces exclusively committed hematopoietic progenitors to differentiation and that treatment of HSC with FLT3 expands their pool, but with a significant lost in self-renewal potential. Yet, according to recent reports, pool of HSC is

heterogeneous and contains HSC with various propensity to contribute to myeloid or lymphoid lineage (or both) and with long or short repopulation abilities. In humans Kikushige and others reported that human bone marrow and cord blood contain FLT3+CD34+ fraction of cells that support lifelong multilineage recipient reconstitution. Therefore, role of FLT3L stimulation might have several functionalities: HSC pool expansion and differentiation [Gabbianelli et al., 1995; Shah et al., 1996; Kikushige et al., 2008]. This scenario is even more feasible having in mind that FlT3L acts synergistically with other haematopoietic growth factors and interleukins [Buza-Vidas et al., 2009; Diehl et al., 2007; Gilliland and Griffin, 2002]. In ex vivo HSC expansion protocols FLT3 ligand is often used in combination with SCF and IL3 or IL6 though the exact mechanism of these cytokines synergistic action is not yet clarified.

1.6. Conclusions

McCulloch and Till introduced the term hematopoietic stem cell (HSC) to define the cell that is able to provide lifelong and complete hematopoietic system reconstitution of a lethally irradiated recipient [Becker et al., 1963, 2014; Wolf and Trentin, 1968]. E.g. HSC will provide precursors of all hematopoietic lineage (myeloid, lymphoid and erythroid) and is able to self-renew. To date it is hypothesised that some blood malignancies can result from uncontrolled proliferation of a hematopoietic stem cell that acquired a genetic lesion affecting it's control of self-renewal [Carlesso and Cardoso, 2010; Babovic and Eaves, 2014]. Therefore, HSC studies are important for fundamental and for translational sciences.

In adults, HSC are rare cells found in bone marrow, they slowly cycle and mainly remain in G0 phase [Copley et al., 2012; Muller-Sieburg et al., 2012; Crisan and Dzierzak, 2016]. This slowly cycling of HSC preserves them for the host lifetime. HSC is positioned at the top of the hematopoietic system hierarchy [Babovic and Eaves, 2014; Seita and Weissman,

2010]. HSC gives rise to multi-potent hematopoietic progenitors (MPP), which are different from HSC in that that they lost their self-renewal property [Babovic and Eaves, 2014; Seita and Weissman, 2010]. Recently it was discovered that HSC pool is heterogenic. There are 4 types of HSC: α, β, γ and δ cells [Weissman, 2015; Bush et al., 2015]. α-HSC mainly produce myeloid lineage progenitors, while β-HSC produce both myeloid and lymphoid progenitors; γ and δ cells support multilineage life-long engraftment, but are not able to repopulate secondary recipients [Seita and Weissman, 2010; Dykstra et al., 2007].

HSC transplantation is the method of choice in blood malignancies treatment and some immunodeficiencies [Sauvageau et al., 2004, 2010; Batta et al., 2016]. For clinical applications, HSC are isolated from bone marrow, new-borns umbilical cord blood or adults peripheral blood [Hopman and DiPersio, 2014]. Due to the need to match blood allotypes of the donor and the recipient, there are still shortages in bone marrow donors [Hardy and Ikpeazu, 1989; Hopman and DiPersio, 2014; Schwaber et al., 2016]. Hence, development of *in vitro* methods of HSC expansion and derivation are of the great interest for regenerative medicine.

In vitro culture conditions attempt to recapitulate the microenvironment in which HSC reside *in vivo* [Zhang and Lodish, 2008]. The culture systems utilize cocktails of cytokines to stimulate HSC maturation and proliferation. There is yet no ideal cytokine formulation developed, but some working components have been identified. The most frequently used set of cytokines for HSC expansion or maturation is: SCF, Il3, Flt3-ligand, IL-6; IL-11, TPO and VEGF. More rarely used components are: Insulin-like growth factor 2 (IGF-2), fibroblast-growth factor 1 (FGF-1) and angiopoietin like 2 and 3 [Heike and Nakahata, 2002; Zhang and Lodish, 2008; Batta et al., 2016]. Yet, to date attempts to expand the pool of donor HSC were mainly fruitless as HSC culture leads to HSC differentiation and loss of the cells self-renewal capacity [Solar et al., 1998; Alexander et al., 1996; Sauvageau et al., 2004]. Application of *in*

vitro methods of HSC maturation was more successful for embryonic HSC [Rybtsov et al., 2011; 2014].

Additional approach that can be utilized in future to generate hematopoietic cells is human embryonic stem cells (hESC) differentiation or somatic cells reprogramming into HSC. This is achieved by recreation of HSC niche microenvironment and enforced overexpression of transcription factors like Runx1, Gata2, Scl, Hoxb4, Pu.1 [Bhatia, 2007; Wang et al., 2005; Batta et al., 2016; Pick et al., 2007; Suzuki et al., 2013; Vereide et al., 2014; Doulatov et al., 2013; Ran et al., 2013; Gori et al., 2015]. Yet, methods using forced genes expression require further development to attenuate potential teratogenic outcome.

Delineation of the ontogeny and the process of hematopoietic stem cells maturation *in vivo* is of a great interest in the field of regenerative medicine and would allow to recreate HSC maturation *in vitro* [Rowe et al., 2016].

In early mouse embryo (embryonic day 7-9), cells with hematopoietic potential reside in various locations (yolk sac, allantois, placenta, dorsal aorta, fetal liver) [Melchers, 1979; Godin et al., 1995; Yoder et al., 1997; Palis et al., 1999; Kumaravelu et al., 2003; Alvarez-Silva et al., 2003; Gekas et al., 2005; Ottersbach and Dzierzak, 2005; McGrath and Palis, 2005; Zeigler et al., 2006; Corbel et al., 2007; Rhodes et al., 2008; Lux et al., 2008; Dieterlen-Lièvre et al., 2010; Yoshimoto et al., 2012; Arora and Papaioannou, 2012]. However, first transplantable HSC (or definitive HSC, dHSC) are identified in midgestation embryo, in the aorta-gonad mesonephros region (AGM) [Medvinsky et al. 1993; Muller et al., 1994; Medvinsky and Dzierzak, 1996; de Bruijn et al., 2000; Taoudi and Medvinsky, 2007]. In particular, in ventral aspect of dorsal aorta (DA) in E10-E11 mouse embryos [de Bruijn et al., 2002; Taudi and Medvinsky, 2007; Rybtsov et al., 2011] and in human [Péault et al., 2002; Ivanovs et al., 2011]. Today, it is broadly accepted that dHSC mature in DA hemogenic

endothelium that gives rise to Runx1+ intra-aortic clusters (IAC) [Jaffredo et al., 1998, 2005; Zovein et al., 2008; Boisset et al., 2010; Bertrand et al., 2010; Kissa and Herbomel, 2010; Swiers et al., 2010]. Embryonic Runx1 knock-out is lethal [Okuda et al., 1996; Wang et al., 1996]. Mouse embryos die prematurely around embryonic day (E) E11-E12 due to anaemia and widespread haemorrhaging. Runx1-/- embryos have normal primitive haematopoiesis, but do not develop any dHSC precursors and present signs of anaemic fetal liver [Samokhvalov et al., 2006; 2014; Tanaka et al., 2012; Liakhovitskaia et al., 2014]. Runx1 null embryos lack cells populations identified to give engraftment in myeloablated recipients (CD41+Vec+CD45+) and pre-HSC precursors (CD41+/lowVec+CD45-) [Okuda et al., 1996; Liakhovitskaia et al., 2014]. Runx1 KO embryos also lack specific intra-aortic clusters (IAC) that are believed to contain developing dHSC [Samokhvalov et al., 2006; 2014]. Therefore, Runx1 is the critical mediator of HSC maturation and can be used as a marker of maturing HSC in early mouse embryos.

Immuno-fluorescent and histochemical studies of early mouse embryo tissues revealed multiple sites of vascularised tissues containing clusters of Runx1+ cells, resembling cell clusters found in dorsal aorta [Yokomizo and Dzierzak, 2010; Yokomizo et al., 2011]. During embryogenesis, Runx1 is widely expressed in all sites of haematopoiesis (yolk sac, placenta, allantois, dorsal aorta), in hematopoietic cells, and in particular in hemogenic endothelium of dorsal aorta floor and intra-aortic clusters [Lam et al., 2010; Swiers et al., 2010; Chen et al., 2011; Samokhvalov et al., 2014]. Runx1+ clusters of cells were detected in extraembryonic arteries, allantois, placenta and head – all sites of definitive haematopoiesis identified in E11 embryos [Palis et al., 1999; Sugiyama et al., 2007; Yoshimoto et al., 2012; Zovein et al., 2010; Mizuochi et al., 2012; Vodyanik et al., 2005; de Bruijn et al., 2000; Gordon-Keylock et al.,2012; Zovein et al., 2010; Gekas et al., 2005; Inman et al., 2007; Zeigler et al., 2006]. Rybtsov et al., did not detect dHSC potential in ventral vasculature of E9 mouse embryos, but

only in caudal part of future AGM [Zovein et al., 2006; Rybtsov et al., 2014]. Thus, while looking for a niche where dHSC specification takes place, special attention has to be paid to mouse embryo caudal part. In younger mouse embryos (E8) dHSC precursors are most probably localized to splanchnopleuric mesoderm – situated in the caudal portion of the embryo. The golden standard to prove dHSC potential of the cells is to try them in a transplantation assay. However, cells derived from early mouse embryos are immature, for example do not express MHC1 and therefore eliminated by NK cells in recipients. To overcome this difficulty early mouse embryo tissues/cells have to be cultured in a potent HCS maturation system cell tracing experiments have to be tried out.

All early dHSC precursors express endothelial markers: vascular endothelial markers: vascular cadherin (CD144), endothelial marker CD31, VEGFR2 [Garcia-Porrero et al., 1998; Fraser et al., 2002; Rybtsov et al., 2011; 2016]. Early dHSC precursors express low levels of CD41 and are negative CD45, CD43 [Ferkowicz et al., 2003]. In general, molecular phenotype of dHSC precursors found in E9.5 (pro-HSC) mouse embryos can be described as: VE-Cad+ CD41low/+CD45−CD43− [Rybtsov et al., 2011; 2014; 2016]. dHSC gradually upregulate expression of CD41 and CD43 markers becoming pre-HSC type I with molecular phenotype of VE-Cad+ CD41+ CD45−CD43+ at E10.5 [Rybtsov et al., 2014; 2016; Mikkola et al., 2003; Hashimoto et al., 2007;]. Finally, CD45 marker starts to be expressed at E11.5 and dHSC transit to pro-HSC type 2 cells with phenotype VE-Cad+ CD41+ CD45+CD43+. After culture step with OP9 stromal cell line, pre-HSC type II become transplantable into adult irradiated recipients [Rybtsov et al., 2011; 2014; 2016]. Utilization of these markers allows to evaluate process of maturation of dHSC in the culture system.

Regulation of HSC specification is orchestrated by molecular ques that are either secreted from surrounding dorsal aorta tissues (somites, notochord, neural tube floor plate, or by urogenital ridges) or presented on the cells HSC precursors come in contact with (ventral

side of somites or dorsal aorta endothelium cells) [Lawson et al., 2002; Lee at al., 2014; Clements and Traver, 2013]. Some of these markers are Bone Morphogenic Protein (BMP, expressed in ventral embryonic part) and Wnt (Wingless-related integration site or WNT protein, expressed in dorsal part) [Gilbert, 2003; Hohan, 1996]. Hh (hedgehog) is expressed in neural floor plate and notochord and specifies dorsal cell fates [Wilkinson et al., 2009]. BMP signalling antagonists Chordin and Noggin prevent premature dorsal aortae fusion [Resse et al., 2004; Garriock et al., 2010]. Garriock et al., (2010) showed that Chordin downregulation and presence of Vascular endothelial growth factor (VEGF) and Sonic hedgehog (Shh) are necessary for DA fusion [Garriock et al., 2010; Nagase et al., 2006]. Comparing patterns and timeline of morphogens and growth factors expression and appearance of dHSC potential in early mouse embryo allows to propose that dHSC appear after DA fusion events takes place. Therefore, those two events could be linked and application of BMP or Shh in *in vitro* cultures might improve HSC maturation protocols.

1.7. Early stages of avian embryo development

After fertilization, chick embryo zygote appears as a disc (termed blastodisc) that floats on the top of yolk (Figure 4., A). Series of cleavages take place in the blastodisc gradually transforming it into a 5-6 cells thick layer of cells (Figure 4 C, *i*). Cells situated at the central lower part of blatodisc shed and die out leaving a monolayer of cells called epiblast. Epiblast cells absorb overlaying them albumin (egg white) and secrete it on the opposite side creating in this way a cavity between the yolk and epiblast (subgerminal space), (Figure 4, C,*ii*). At this stage, epiblast looks like a transparent discoidal formation surrounded by opaque ring of tissue (Figure 4., B) [Eyal-Giladi and Kochav, 1976]. The transparent epiblast area is termed area pellucida and opaque zone – area opaca. There are multiple layers of cells underneath area opaca, also called marginal zone. Then, some epiblast cells delaminate and migrate into subgerminal space forming primary hypoblast. Other cells, also contribute to hypoblast. For example, deep layer of cells from marginal zone of prospective posterior end of the embryo migrate towards primary hypoblast. Delaminated epiblast cells and deep layer cells from marginal zone together from secondary hypoblast. Epiblast, blastocoel and hypoblast all together represent blastoderm (Figure 4, C,*iv*) [Bellairs and Osmond, 2005; Gilbert, 2003].

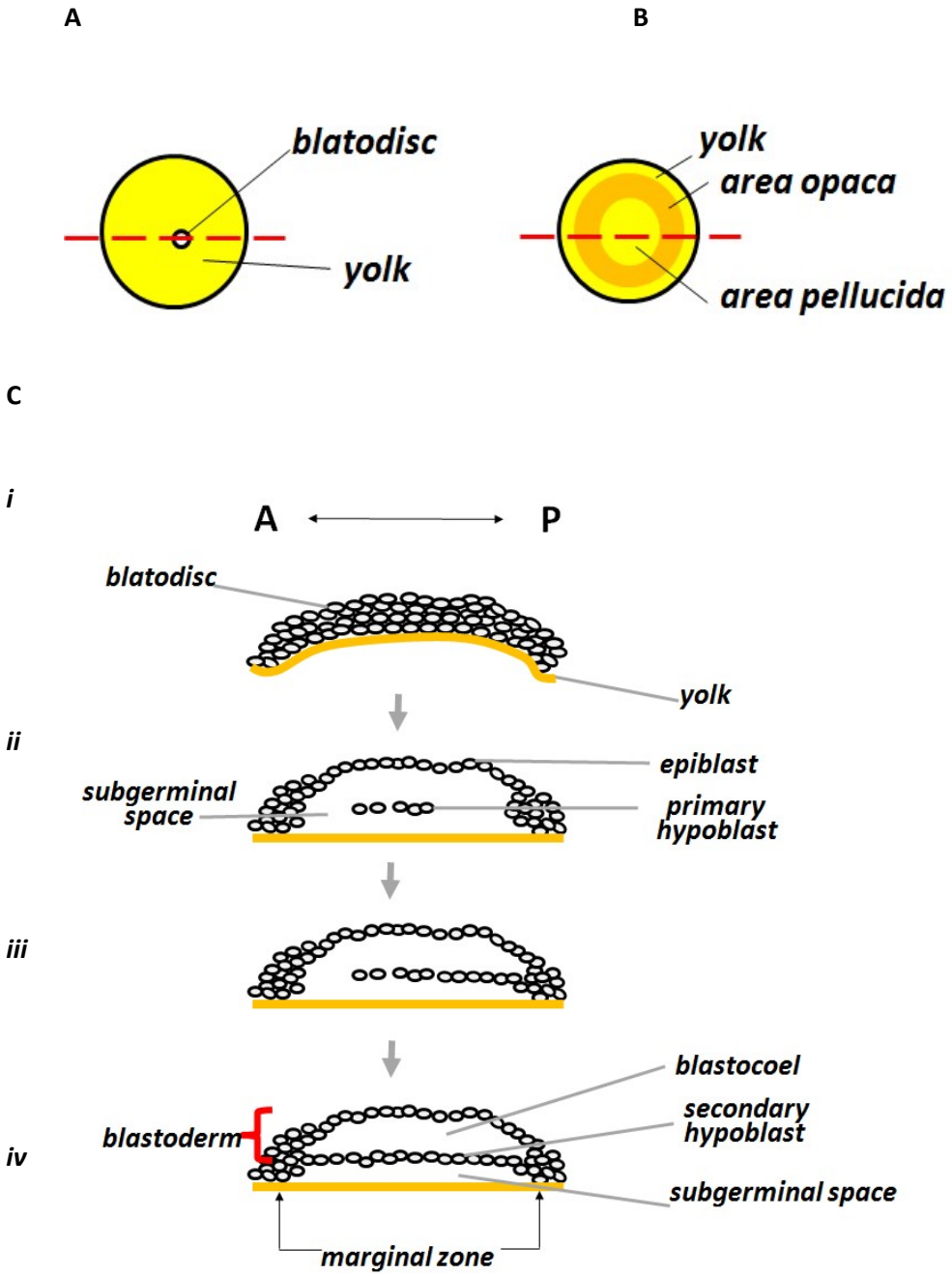

Figure 4. Pre-gastrulation chick embryo development. Chick embryo zygote appearance (before egg is laid) (A). Red line shows cross-section through the embryo and yolk. Schematic representation of this section Is given in (C,*i)*. Appearance of chick embryo shortly before gastrulation (B). Red line represents crossection schematically represented in (C, *iv*). Delamination of epiblast cells and formation of subgerminal cavity (C,*ii*). Migration of deep layer of cells from prospective posterior part of marginal zone (C, *iii*). Formation of secondary hypoblast and blastoderm (C, *iv*). Not to scale. A – anterior; B – posterior.

1.7.2. Chicken embryo gastrulation

Gastrulation is the process of tissues specification. In chicken embryo, gastrulation starts around 6 h of egg incubation (by Hamburger and Hamilton classification, HH, stage 2) [Hamburger and Hamilton, 1951]. First, a special structure, primitive streak, starts to form at the prospective posterior part of the embryo (Figure 5.). PS is formed by epiblast cells migrating towards the prospective embryo midline. Starting from 12h of egg incubation (HH3) cells in PS undergo epithelial- mesenchymal transition and migrate (ingress) into blatocoel. Cells ingressing through PS form a depression (primitive groove) along primitive streak. In about 18 h of egg incubation (HH4), at the anterior end of the primitive streak a thickening is formed - the Hensen's node. There is a funnel-shaped deepening inside HN, which is another entry site for epiblast cells into blastocoel [Bellairs and Osmond, 2005; Gilbert, 2003].

As cells migrate thought primitive streak, it continues to extend. When primitive streak reaches approximately 75% of the area pellucida length, avian embryo is considered to be at the stage of full primitive streak extension (or at HH stage 4). From this moment, primitive streak starts to regress (shortens). Epiblast cells continue their ingression through PS till the very end of gastrulation. Cells ingressing gradually slows down starting from 2.5 days of egg incubation (HH 16) and completely ceases at HH24 (4 days of incubation) [Garcia-Martinez and Schoenwolf, 1992; Stern, 2004].

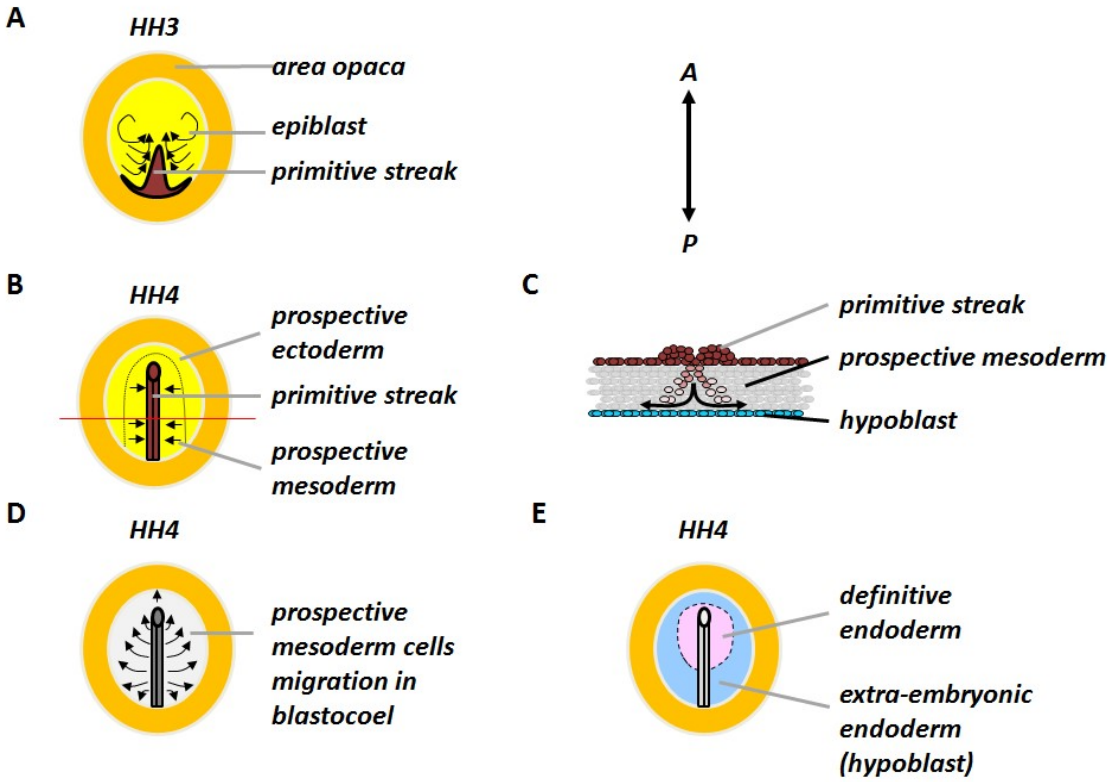

Figure 5. Initial stages of gastrulation. Primitive streak appearance at HH3. Black arrows show epiblast cells migration towards forming primitive streak (A). Primitive streak at full length. Black arrows show epiblast cells migration towards primitive streak. Dotted line shows approximate border prospective mesoderm/ectoderm. Red line shows position of cross-section shown in C (B). Cross-section through middle primitive streak at stage HH4. Black arrows show migration of ingressed epiblast cells (C). Trajectories of prospective mesoderm cells migration (D). Lower layer of blastoderm showing hypoblast cells, future yolk sac endoderm (blue) with and already ingressed prospective endoderm of gut (pink) (E).

1.7.3. Primitive streak and epiblast fate maps

umber of works were devoted to the primitive streak and epiblast fate mapping. According to published fate maps, the first cells which migrate (ingress) into blastocoel will form definitive endodermal tissue (gut) [Psychoyos and Stern, 1996; Sweetman et al., 2008]. These cells migrate anteriorly and deep – they insert themselves in-between of hypoblast cells, pushing the latter anteriorly. Cardiac progenitors ingress after endoderm progenitors (HH3-4) [Selleck and Stern, 1991; Sawada and Aoyama, 1999]. Mid-primitive streak gives rise to paraxial, intermediate and lateral plate mesoderm. Caudal primitive streak also contributes to the lateral plate mesoderm, but for extra-embryonic tissues (yolk sac) [Ooi et al., 1986; Lopez-Sanchez, et al., 2001; Withington et al., 2001]. The regions of PS and epiblast giving rise to different progenitors partially overlap, so there are no exact borders between PS regions giving rise to one or another particular tissue, nor exact borders dividing primitive mesoderm into embryonic- or extra-embryonic mesoderm [Schoenwolf et al., 1992; Hatada and Stern, 1994].

The part of the lateral plate mesoderm that overlies the endoderm will form the splanchnic mesoderm, which gives rise to mesentery, endothelium, vessels and hematopoietic cells [Downs et al., 2004, 2009]. Lateral plate mesoderm that lies underneath ectoderm will form somatic mesoderm that gives rise to vessels and connective tissues of body wall and limbs. Neural and surface ectoderm will be formed by epiblast cells that do not ingress through the primitive streak during gastrulation. Hypoblast cells do not contribute to the embryo proper tissues [Psychoyos and Stern, 1996; Sweetman et al., 2008]. Hypoblast contribute to extra-embryonic membranes, e.g. to the yolk sac endoderm (Figure 4.).

The fate of ingressed epiblast cells depends on their position in PS indirectly. E.g. the cells will be fated only when they reach their destination in endoderm or mesoderm and fate

will be determined by the microenvironment cues [Bellairs and Osmond, 2005; Gilbert, 2003; Lopez-Sanchez, et al., 2001]. As the migratory routes of epiblast cells depend on their position in PS, cells position in PS determines destination of the epiblast cells in the embryo. Therefore, cells in PS are considered to be specified, but not having a determined fate.

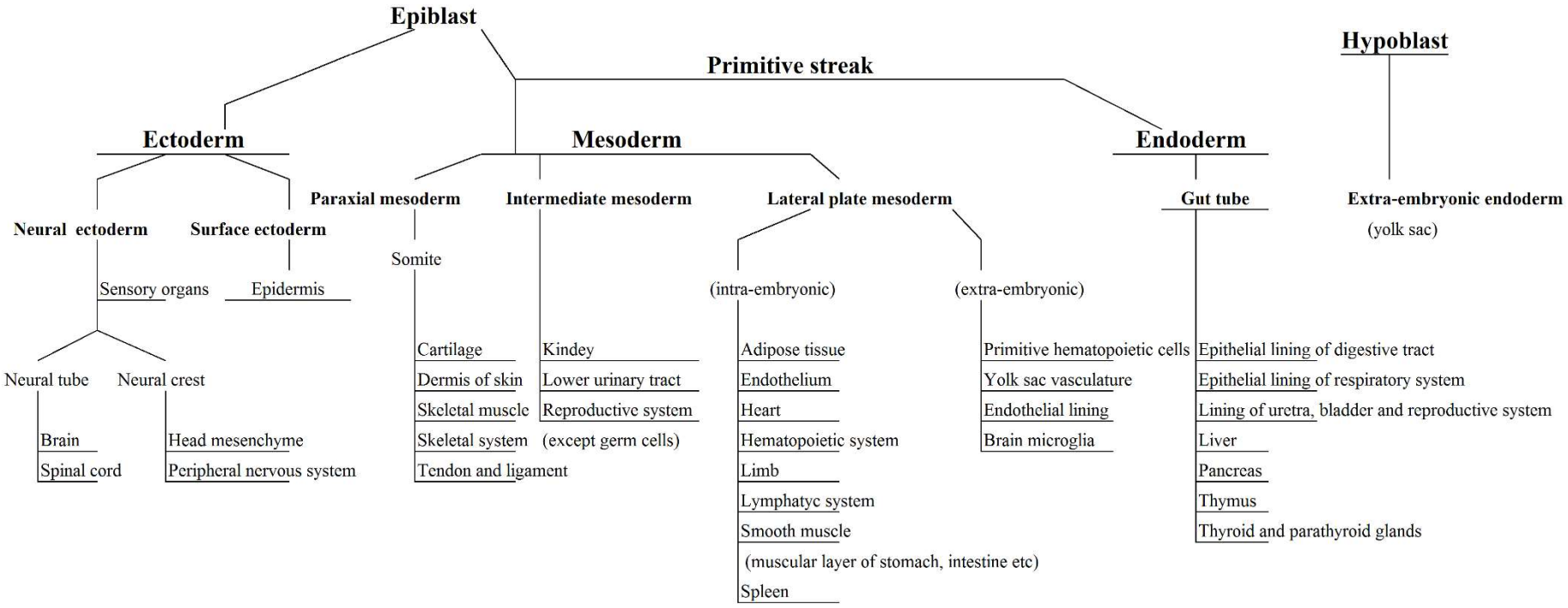

Figure 6. Three germ layers formed during gastrulation and their derivatives.

1.8. Ontogeny of hematopoietic stem cells in chicken embryo

1.8.1. Haematopoietic stem cells and their precursors originate in embryo proper

One of the key questions in the field of haematopoiesis, the origin of the hematopoietic stem cells, was first answered with help of a chicken embryo. Observing chick embryo development, it was noticed that the newly forming erythroblasts and endothelial cells appeared in the yolk sac in close proximity inside the so-called blood islands. Based on this observation, Sabin proposed that there is a common progenitor that gives rise to endothelial and hematopoietic cells [Sabin, 1917]. In 1932 to describe this common progenitor, Murray coined the term “hemangioblast” [Murray, 1932]. However, at that time not all hematopoietic cells were considered to originate from the common mesodermal progenitor. For instance, the lymphocytes were suggested to appear from an endodermal-epithelial precursor [Le Douarin and Dieterlen-Lièvre., 2013]. Moore and Owen were the first to question this hypothesis about a common mesodermal progenitor [Moore and Owen., 1965]. The authors carried out vascular anastomosis (operation to connect two vessels carrying blood) between two early chick embryos. They have demonstrated that if such anastomosis took place before embryonic day 7 (E7), the thymus of each of the embryos would be populated by the T cells specific for both embryos. Hence, they proposed that thymus is colonized by the lymphocyte progenitors derived from the blood flow before E7. To verify their findings, Moor and Owen used yolk sac suspension of E7 chick embryos to restore the hematopoietic system of the irradiated E14 chick embryo. As the engraftment of the yolk sac cells was successful, Moore and Owen extended their conclusions proposing that the common precursor of HSC resides in the YS. Yet, Owen and Moore did not consider that the blood circulation was already established and so, the cells they collected from the yolk sac tissues could come from the embryo proper. In addition, primitive and definitive waves of embryonic haematopoiesis were not described at that time.

As we discuss in the next chapter, later on Dieterlen-Lièvre overturned Moor's and Owen's hypothesis and demonstrated that definitive hematopoietic stem cells arise in the embryo proper [Dieterlen-Lièvre., 1975; Lassila et al., 1979; 1982].

In 1969, Dourain and colleagues developed the new advanced microsurgery method that allowed to graft quail embryos onto the yolk sac of the chick embryo [Le Douarin, 1969; Le Douarin and Dieterlen-Lièvre., 2013]. In 1975, Dieterlen-Lièvre and his colleagues used this technique in lymphopoiesis studies [Dieterlen-Lièvre, 1975]. Surprisingly for the authors, they discovered that the major hematopoietic organs (thymus, and spleen) in quail-chick chimeras were populated by the quail (donor) hematopoietic cells. This contradicted Owen' and Moore's hypothesis about the yolk sac as the place of origin of hematopoietic stem cells [Dieterlen-Lievre F., 1975].

As chick and quail phases of embryonic development might be different, cell-cell interactions could have been affected in Dieterlen-Lièvre experiments. To solve this issue, Lassila et al., in 1978 created chick-chick chimeras in which host and graft tissues differed from one another by sex [Lassila et al., 1978]. To exclude the possibility that cells from embryo proper enter yolk sac, Lassila and colleagues used pre-circulation chick embryos in this experiment. According to the design of the experiment, when embryos were grafted randomly, there would be 50% of grafts whose sex is different from the host tissues. In a report by Lassila and colleagues' results, authors did not discover embryo sex hematopoietic cells in the spleen, thymus or bursa opposite to the host. However, the rare cells of opposite to the host sex were detected in the bone marrow – the final niche of hematopoietic stem cell. This meant that all hematopoietic cells were derived from the host embryo proper, but rare primitive erythrocytes temporarily home to bone marrow flow.

1.8.2. Hematopoietic stem cells and their precursors migrate into yolk sac from embryo proper

To establish the possibility of intraembryonic HSC migration into YS tissues, Lassila and colleagues designed the following experiment. The authors used allogeneic chick-chick chimeras (derived from genetically different zygotes). For this, they grafted the whole central area of blastoderm of the chick line B2B2 (donor) on the area opaca of chick line B15B15 (host). Therefore, graft and host derived cells were of different chicken allotypes which allowed easy identification of the cells origin by the cells surface antigens expression. Five days after grafting, yolk sacs were removed, and the cell suspension was prepared. This cell suspension was transplanted into irradiated E14 recipient chick embryos. After recipient embryos hatched, engraftment of yolk sac cells and input of cells derived from embryo proper were evaluated. According to the authors, the majority of blood cells were derived from the embryo proper [Toivanen et al., 1982; Lassila et al., 1982]. Only low numbers of recipient's peripheral blood erythrocytes came from donor's yolk sac. Hence, the authors proposed that the YS provides significant numbers of primitive erythrocytes progenitors during embryogenesis. Yet the number of YS derived erythrocytes turned out to be below the limit of detection after embryo hatching. Simultaneously, erythrocyte progenitors coming from embryo proper produce definitive erythrocytes in increased numbers during embryonic life and apparently are the only source of erythropoiesis after embryo hatching [Lassila et al., 1982].

To demonstrate that the detected intraembryonic HSC precursors give rise to the functional HSC, Martin et al., created chick-chick embryo-yolk sac chimeras before the onset of circulation [Martin et al., 1979]. Eighteen chimeras survived after transplantation, hatched and were analysed at age of 5-20 weeks. Analysis of chimeras revealed that their embryo proper derived hematopoietic system was completely normal, e.g. B and T lymphocytes produced

normal levels of IgM and IgG upon stimulation. From this, Martin and colleagues verified that adult-type HSC originate from the embryo proper, but not from the YS.

Therefore, the hematopoietic stem cells and their precursors do not originate in the yolk sac but migrate there from the embryo proper with blood circulation. Yolk sac produces primitive erythroblasts, which in limited quantities persist till embryo hatching and disappear shortly after that. In addition, colonization of hematopoietic organs was not demonstrated for the YS derived cells. Soon after establishment of the blood circulation, the second definitive hematopoietic wave takes place in the embryo proper. During this time, hematopoietic precursors [and/or HSC] colonize the hematopoietic organs (bursa, thymus, bone marrow, spleen). Intra-embryonic HSC precursors mature during the second wave of definitive haematopoiesis and give rise to the stem cells that maintain adult haematopoiesis [Toivanen et al., 1982; Lassila et al., 1982].

1.8.3. Location of hematopoietic stem cells and their precursors in the embryo proper

In 1996 Medvinsky et al reported that in the mouse embryo, definitive hematopoietic stem cells reside in the so-called aorta-gonad-mesonephros region (AGM) [Medvinsky and Dizerzak, 1996]. Later it was also revealed that the hematopoietic activity in mouse AGM is localized to the ventral part of the main AGM vessel, the dorsal aorta. [Taoudi S, Medvinsky A., 2007]. In the DA, in contrary to the YS hematopoiesis, endothelium appears first before the generation of the hematopoietic cells (while in yolk sac they appear simultaneously). Perhaps because of this, the paradigm of ontogeny of hematopoietic stem cells has shifted from the "hemangioblast" to the "hemogenic endothelium". Currently, hemogenic endothelium is recognized to be the tissue that gives rise to HSC and/or their precursors. According to fate mapping studies, aortic endothelium is mesoderm derivative [Psychoyos and Stern, 1996]. In

particular, the spnanchnopleura derivative: splanchnic mesoderm overlaying endoderm [Cumanp et al., 2001]. In search of definitive hematopoietic cell precursors, Pouget and colleagues performed grafting of the quail somatopleural derivative in place of the last two formed somites in the chicken embryo. The authors observed formation of vascular networks formed from quail angioblasts (reviled with quail specific QH1 antibody that specifically recognizes quail endothelium) [Pouget et al., 2006]. The descendants of the quail somatopleural mesoderm were detected in all somatopleural derivatives (e.g. kidney, limbs, body wall). Quail angioblasts were also found to be integrated into the roof and sides of the dorsal aorta. In contrast, quail angioblasts were never found in the floor of the dorsal aorta or any other visceral organs. From this, Pouget and colleagues concluded that somatopleura serve as the source of angioblasts for vasculatization of the dorsal aspect of the embryo, including the roof and sides of the dorsal aorta and thus excluding hemogenic endothelium [Pardanaudt et al., 1996; 1999; Pouget et al., 2006].

Grafting of quail spnanchnopleura into the place of last 1-2 somites in chicken embryos provided the opposite results. Here, quail angioblasts emigrated into the visceral part of the embryo, formed the floor of the dorsal aorta, and gave rise to hematopoietic cells. From here it was concluded that the dorsal aorta is the chimerical vessel, which is formed by two distinct endothelial lineages, derivatives of somatopleura and spnanchnopleura, respectively. Only one of their derivatives, namely spnanchnopleura, is endowed with hematopoietic potential [Pardanaudt et al., 1996; 1999; Pouget et al., 2006].

It is still unclear how endothelial to hematopoietic transition occurs. Recently, some insights were obtained with experiments of Pardanaud and Dieterlen-Lièvre where the mesoderm was pre-treated under various conditions before its grafting. The mesoderm was conditioned in presence of germ layers that normally surround it in the embryo (endoderm or ectoderm) or in presence of ectoderm/endoderm derived growth factors. Authors reported that

the conditioning with endoderm as well as conditioning with endoderm derived growth factors (VEGF, bGFG and TGFbeta1) gives rise to progenitors with endothelial and hematopoietic potential, while conditioning with ectoderm and ectoderm derived growth factors (EGF/TGF) completely abolishes hematopoietic potential of spnanchnopleura [Pardanaud L, Dieterlen-Lièvre F., 1999].

Another critical mediator involved in endothelium to hematopoietic transition is transcription factor Runx1. Jaffredo and colleagues studied Runx1 expression in avian embryos by means of *in situ* hybridization. They have discovered that Runx1 starts to be expressed in dorsal aorta 1 day before the intraembryonic hematopoiesis takes place. The pattern of expression is different from that observed in the mouse. In chick embryos, Runx1 is expressed in paired dorsal aortae bi-laterally. It is only after DA fusion, Runx1 expression was observed in the ventral aspect of the dorsal aorta. During intra-embryonic hematopoiesis, Runx1 is expressed in the whole dorsal aorta floor and in intra-aortic clusters (IAC). In contrast, in mouse embryos, sub-aortic cells express Runx1 at a high level (in chick, the adjacent sub-aortic mesenchyme remains Runx1 negative). Therefore, Jaffredo and colleagues proposed that the sub-aortic mesenchyme is not the source of HSC precursors in chick embryos but serves as an inductive tissue to promote endothelial to hematopoietic transition [Jaffredo et al., 2000; Dieterlen-Lièvre and Jaffredo, 2009].

To conclude, to initiate hematopoietic stem cell maturation from mesoderm precursors, the lateral plate mesoderm needs to be in contact with the endoderm. Lateral plate mesoderm that is in contact with the endoderm is called spnanchnopleura and experimentally it was demonstrated that this tissue forms the dorsal aorta floor. The initiation of HSC maturation in the mesoderm is mediated by endoderm secreted growth factors (VEGF, bGFG and TGFbeta1). Successful initiation of HSC maturation will be highlighted by upregulation of Runx1 expression. In chick embryos, Runx1 is expressed in the dorsal aorta endothelium from where

later intra-aortic clusters appear. The exact role of Runx1 in HSC maturation is still to be clarified.

1.8.4. Lateral plate mesoderm is the reservoir of cells forming intra-aortic clusters in the chick embryo

To determine the origin of intra-aortic clusters, Jaffredo and colleagues performed an elegant experiment where they mechanically separated lateral plate mesoderm from the newly formed dorsal aorta. Runx1 expression and hematopoietic clusters formation was absent on the operated sides of the embryo while IAC appeared at normal frequency and size in non-operated sites [Jaffredo et al., 1998; 2005; Bollerot 2005]. This might mean that LPM induces Runx1 expression and IAC appearance. On the other hand, it could be a consequence of disruption of cell migration from the mesoderm to the DA. To exclude the second possibility, in a separate experiment, Jaffredo et al. labelled the lateral plate mesoderm with permanent lipophilic dye and observed LPM cells migration into the DA. On examination, labelled cells were absent in the endothelial lining of the dorsal aorta or in IAC. From this, Jaffredo and colleagues concluded that the sub-aortic mesenchyme is not the source of HSC precursors. Yet, it induces Runx1 expression and in the DA endothelium and so triggers HSC maturation. These conclusions however shall be clarified: at the stage when the DA is already formed, LPM might induce HSC maturation in endothelial and do not contribute new cells to the DA, yet LPM shall give rise to the DA at the earlier stages [Richand C. et al., 2013].

1.8.5. Tracing fate of intra-aortic clusters

To delineate the fate of IAC, IAC were labelled with a retroviral vector engineered to carry the lacZ reporter [Jaffredo et al., 2000]. When the DA was infected with retrovirus at E2,

the labelling of the hemogenic endothelium took place. At E3 IAC were labelled. By tracing progeny of labelled cells in the DA, Jaffredo et al. were able to distinguish 2 groups of cells. The first was shed into the bloodstream and the second migrated into the dorsal mesentery and formed their so-called para-aortic foci [Jaffredo et al., 2000].

Para-aortic foci appear around E6-7 after intra-aortic hematopoietic events, but before the colonization of main hematopoietic organs. By the series of works, Dieterlen-Lièvre proved that hematopoietic cells which were derived from foci colonize hematopoietic organs [Dieterlen-Lièvre F, Martin C., 1981]. Lassila and colleagues also showed that hematopoietic foci contain definitive hematopoietic cells. For this, they performed transplantation of the E14 irradiated chick embryos with cell suspensions derived from dorsal mesentery [Lassila et al., 1979]. Dorsal mesentery provided hematopoietic reconstitution in parallel to functional restoration of the lymphoid cell compartment [Lassila et al., 1979; Dieterlen-Lièvre F, Martin C., 1981]. These findings show that mesenchymal para-aortic foci could be a transitory niche for maturing hematopoietic stem cells on their way to main hematopoietic organs: thymus, spleen, bursa and bone marrow.

To conclude, the hematogenic endothelium seems to be the origin for HSC and para-aortic foci to be a temporary niche for maturing HSC. Intra-aortic clusters migrate in the area where para-aortic foci are formed and hence IAC might contain precursors of HSC. Yet, there are no reports showing a direct link between hemogenic endothelium-IAC-para-aortic foci-HSC. For example, experiments described above could not reject the possibility that HSC appear in the para-aortic foci from another source, e.g. from the blood flow. To clarify this question, the DA endothelium would need to be permanently labelled and its derivatives traced in adult chicks. There are technical challenges to do this. For example, there are no known unique markers expressed exclusively in hemogenic endothelium. To perform a grafting

experiment labelling lateral plate mesoderm that contributes to dorsal aorta endothelium, first fate mapping of dorsal aorta shall be completed.

Even though we know that vasculature and the DA in particular is the mesoderm derivative, we do not know the exact region of the LPM will contributes to IAC. For example, the heart is formed by LPM regions closely adjacent to each other. Munstenberg et al., show that two closely adjacent regions of HH3-3+ anterior primitive streak give rise to two separate regions of the heart. Namely, to a) anterior heart field and b) combined primary, secondary and anterior heart fields [Yue et al., 2008; Münsterberg and Yue, 2008; Sweetman et al., 2008; Camp and Munsterberg, 2011]. The primary heart field forms the heart tube, while anterior heart field forms the outflow myocardium. Hence, cells from anterior heart field reside in splanchnic mesoderm awaiting the signal to contribute the outflow of myocardium. Therefore, it could be that a similar scenario is applied to dorsal aorta formation. For example, different regions of PS might contribute to the dorsal aorta floor or intra-aortic clusters. Mapping of the DA will allow the eludication of this question.

1.8.6. Dorsal aorta formation

Regardless of the fact that a number of works were devoted to fate map the primitive streak, no works were done to construct a fate map of the dorsal aorta. We generally know that LPM will contribute to the dorsal aorta and that splanchnopleura grafts will contribute to the hemogenic endothelium [to Jaffredo et al., 2000]. Psychoyos and Stern and others developed detailed fate maps of the primitive streak [Psychoyos and Stern, 1996; Downs, 2003; Sato, 2013]. According to these maps, intra-embryonic LPM is generated by the middle portion of the PS.

Other works which were devoted to dynamics of the DA assembly show that the assembly of the DA follows these steps. First, primitive mesoderm cells randomly transform into angioblasts which initially are scattered between the mesoderm cells [Sato et al., 2010;

Hiruma 1981, 1983, 1995; LaRue et al., 2003]. Starting at HH9 (6 sp), angioblasts migrate and align bi-laterally at some distance from the embryonic midline. These angioblasts coalesce forming short, tubular vascular plexi. According to recent studies, these primary vascular plexi have a dynamic nature [Sato et al., 2010]. E.g. cells of these plexi still possess motility and the direction of these cells movement is not necessarily coordinated. With time, these initial vascular plexi move towards each other and merge forming one single aorta. With the use of two photon-laser scanning microscopy and a tie1-eYFP transgenic quail embryo, Sato et. al observed DA formation and concluded that the dorsal aorta walls get contribution from mainly intra-embryonic endothelial cells. In contrast, caudal regions of the DA are built from extra-embryonically derived endothelial cells (Sato et al., 2010). This result requires further clarification as it will be critical to label the intra-aortic part of the DA exclusively.

An additional insight in DA formation from the earliest stages of embryo development could be done with *in situ* hybridization screens done for angioblast or cells expressing endothelial markers. For example, endoglin is a good marker for endothelial cell identification. The Geisha project provides a detailed endoglin expression screen (GEISHA Id ENG.UApcr) for chick embryos at stages HH 4-25 [Bell et al., 2004; Darnell et al., 2007]. From the in-situ endoglin screen, it follows that the first angioblasts are scattered in extraembryonic spaces. At HH9, angioblasts already assemble into primordial DA simultaneously with formation of the area pellucida vasculature. At HH10 the anterior part of DA (paired) is already formed, together with the heart tube. The area pellucida vasculature is almost assembled. By HH12, which is when blood circulation starts, the anterior DA is completed and joined to the area pellucida and the yolk sac vasculature. Area pellucida is densely vascularized starting from HH10. Therefore, lateral plate mesoderm grafting shall not be done later than the beginning of stage HH9, e.g. when the DA lumen is formed. Operation of luminised DA will destroy the fragile DA lumen and might not heal before the initiation of fluid circulation – just in a couple of hours at HH10.

Clusters bearing endothelium is a long stretch of mesoderm which at HH9 extends from heart loop to the Hensen's node. It will be difficult to label this long stretch of mesoderm surgically. A much easier alternative would be to label a lateral plate mesoderm that contributes to intraembryonic part of the DA. Though, as was mentioned above, to fulfil this goal one would need to fate map the DA first.

1.8.7. Conclusions

In her pioneering works with quail-chick chimeras, Dieterlen-Lievre (1975) established that major hematopoietic organs in chicken (thymus, and spleen) were populated by the quail (donor of intraembryonic tissues) derived hematopoietic cells. This meant that, similar to mammals, all hematopoietic cells are derived from the host embryo proper in chickens. Later, Lassila showed that only rare primitive erythrocytes temporarily home to the bone marrow [Toivanen et al., 1982; Lassila et al., 1982; Martin et al., 1979]. This might be compared to Cumano et al (2011) reports where some yolk sac derivatives home to the mouse fetal liver where they might contribute to some obscure pool of HSC.

Similar to mice, in chicken embryos after establishment of the blood circulation that carry primitive YS derived erythrocytes, the second definitive hematopoietic wave takes place in the embryo proper. During this time, hematopoietic precursors [and/or HSC] colonize the hematopoietic organs (bursa, thymus, bone marrow, spleen – in contrast to mouse where pro-HSC and HSC colonise the fetal liver).

Currently, the hemogenic endothelium is recognized to be the tissue that gives rise to HSC and/or their precursors. According to fate mapping studies, the aortic endothelium is a mesoderm derivative [Psychoyos and Stern, 1996]. Pouget and colleagues demonstrated that

the dorsal aorta is the chimerical vessel, which is formed by two distinct endothelial lineages, derivatives of somatopleura and splanchnopleura. Somatopleura serves as the source of angioblasts for vascularisation of the dorsal aspect of the embryo, including roof and sides of the dorsal. Only spnanchnopleura derivatives contribute to the DA floor and are endowed with hematopoietic potential [Pardanaudt et al., 1996; 1999; Pouget et al., 2006]. Chick mesoderms show some plasticity in cells fates: mesoderm conditioning with endoderm as well as conditioning with endoderm derived growth factors (VEGF, bGFG and TGFbeta1) gives rise to progenitors with endothelial and hematopoietic potential. Mesoderm conditioning with ectoderm and ectoderm derived growth factors (EGF/TGF) completely abolishes hematopoietic potential of spnanchnopleura [Pardanaud L, Dieterlen-Lièvre F., 1999; Jaffredo et al., 1998; 2005; Bollerot 2005]. Therefore, in chicken embryo development of hematopoietic cells (and HSC in particular) it is position dependent.

In chicken embryos, during intra-embryonic phase of haematopoiesis Runx1 is expressed in the whole dorsal aorta floor and in intra-aortic clusters (IAC). In contrast, in mouse embryos, Runx1 is also expressed in subluminal tissues. Jaffredo and colleagues proposed that the sub-aortic mesenchyme in chicken embryos is not the source of HSC precursors, but serves as an inductive tissue to promote endothelial to hematopoietic transition [Jaffredo, 2000; Dieterlen-Lièvre F, Jaffredo, 2009]

By tracing progeny labelled in DA cells, Jaffredo et al. were able to distinguish 2 groups of cells. The first was shed into the blood stream and the second migrated into the dorsal mesentery and formed their so-called para-aortic foci [Jaffredo et al., 2000]. Dorsal mesentery provided hematopoietic reconstitution in parallel to functional restoration of the lymphoid cell compartment [Lassila et al., 1979; Dieterlen-Lièvre F, Martin C., 1981]. Hence, mesenchymal para-aortic foci could be a transitory niche for maturing hematopoietic stem cells on their way to main hematopoietic organs: thymus, spleen, bursa and bone marrow. Yet, there are no

reports showing a direct link between hemogenic endothelium-IAC-para-aortic foci-HSC. It could be also possible, that HSC appear in para-aortic foci from another source, e.g. with the blood flow. To clarify this question, cell tracing experiments of the DA endothelium would need to be done.

No DA mapping experiments were conducted to date. For instance, it is not known what region of the LPM will contribute to IAC bearing portion of the DA. For example, the heart is formed by LPM regions closely adjacent to each other [Yue et al., 2008; Münsterberg and Yue, 2008; Sweetman et al., 2008; Camp and Munsterberg, 2011]. Therefore, it could be that adjacent LPM regions contribute to hemogenic and not hemogenic portions of the DA. Mapping of the DA will allow the eludication of this question.

1.9. Project aims

Tp define the area containing prospective early HSC precursors in mouse and in chicken embryo. For this:

I. By means of immunofluorescence:

- map Runx1+ cells in wild type E7-8 mouse embryo;

- describe dynamics of Runx1+ cells appearance in early mouse embryo (E7-8).

II. Isolate tissues containing prospective pro-HSC (Runx1+CD31+CD41+ cells) from precirculation mouse embryos (E7-E8) and determine these tissues definitive hematopoietic potential in transplantation assays;

- cells isolated from early mouse embryos are not directly transplantable. Therefore, implement a culture step to mature prospective pro-HSC:

    - with utilization of the protocol of 3D co-aggregation with stromal cells;

    - whole tissues explants.

III. Map the dorsal aorta from the primitive streak (PS) stages of chick embryo development. For this:

- establish chick embryo culture and the method of PS labelling that allows easy visual recording;
- determine the area of the primitive streak that contributes exclusively to intra-aortic clusters bearing portion of the dorsal aorta;
- study primitive streak grafts contribution to dorsal aorta endothelium and intra-aortic clusters.

CHAPTER 2. MATERIALS AND METHODS

2.1. Materials

Mouse cell and tissue culture medium. IMDM (Sigma-Aldrich, I3390), HyClone™ Fetal Bovine Serum (GE healthcare Life Sciences, SH30071.03) – 20%; Penicillin/streptomycin solution (Sigma-Aldrich, P4333) 1:100; L-glutamine solution (Sigma-Aldrich, 59202C) – 1:50; Sodium pyruvate solution (Sigma-Aldrich, S8636) - 1:100. For co-aggregation and embryo explant cultures, this media was supplemented with IL-3 (100ng/ml); SCF (100ng/ml) and Flt3 (100ng/ml).

Nitrocellulose filter membranes (0.65 μm) for air-liquid interface co-aggregate cultures were purchased from Sigma-Aldrich (N9022). Membranes were washed in autoclaved milliQ water 3 times for 15 minutes each time. Then, membranes were dyed in a laminar hood. Before loading cell co-aggregates, membranes were carefully deposited on the surface of culture media (2 mL) in 6-well plates (Nunc, ThermoFisher Scientific, 140675). All procedures were carried out in aseptic conditions.

Beta-galactosidase staining buffers – recipes are given in Appendix A9.

DiI and DiO stains. DiI and DiO were purchased from Thermo Fisher Scientific (1,1'-Dioctadecyl-3,3,3',3'-Tetramethylindocarbocyanine Perchlorate, D282; 3,3'-Dioctadecyloxacarbocyanine Perchlorate, correspondingly, D275).

Dye stock preparation: Dye in the tube was dissolved in 10 uL of 100% ethanol. DiI stock solution was kept at -20 ºC.

Working solution preparation. On the day of injection, 10 uL of dye stock was dissolved 1:10 with preheated to 40-45 ºC 0.3M sucrose.

Collagenase/dispase (Roche, 11097113001), 1 mg/mL on PBS (Ca++/Mg++).

Pannett and Compton saline for early chick culture was prepared according to [Pannett and Compton, 1924; New, 1966; Stern, 1993]. Recipes are given in Appendix A10.

Plates preparion for early chick culture. Plates were prepared minimum 2 hours in advance before the experiment. Egg albumine was collected from 6 fresh eggs. 50 mL of warmed up to 49 ºC albumin was mixed with 50 mL of 0.6% of agarose (Difco Agar, RF214530) dissolved on Pannett-Compton saline. Immediately, liquid agarose/albumin mix was dispensed in plates (~ 5mL/plate) and left to set at room temperature.

Paper rings (frames) for chick embryo culture were cut from Whatman Chromatography Paper (3mm Chr, Cat. # 3030 017, GE Healthcare UK Limited). The opening in a paper ring was not of cloverleaf shape, but of an oval. Paper rings size: outer diameter – 24 mm; internal ellipse diameters: 13mm and 11 mm.

2.2. Animal husbandry

Bl6 and AML1LacZ/+ animals were housed within the University of Edinburgh according to Animals Scientific Procedures Act, UK, 1986. All procedures were carried out according to the animal license issued by the Home Office. Animals were kept on 14 hours

light/10 hours dark cycle in a pathogen free environment. Mice were provided a sufficient supply of food and water.

Fresh (laid on the day of the experiment) fertile chicken' eggs were sourced by a Transgenic Chicken Facility from Roslin Institute (Edinburgh, Scotland). Embryos from the brown leghorn line were used as wild type embryos. Fertile eggs containing transgenic embryos ubiquitously expressing membrane bound form of GFP were also sourced by the Transgenic Chicken Facility with the permission of Helen Sang who derived this transgenic chick line (Roslin Institute) [McGrew at al., 2004].

2.3. Mouse embryos collection and dissection

For embryonic tissue collection, timed matings were set overnight. In morning, upon discovery of a vaginal plug in female mice, embryonic day was assumed to be E0.5.

Mouse tissues were dissected in 7-10% FCS/PBS (Ca++/Mg++) solution. Embryo stage, number of somites were recorded and embryos were pooled according to their stage: 0-5sp; 6-15 sp.

For the transplantation experiments, Bl6 recipients were irradiated with full body doze of ionizing radiation (3.5 Gy at 0.75 Gy/min). After irradiation, animals were kept on 10% Baytril solution (Bayer) for 4 weeks. Blood chimerism was assessed starting from the 6th week after transplantation by tail vein veno-puncture.

2.4. Mouse tissues preparation for hematopoietic potential assessment

Cell suspension preparation. To prepare cell suspension from fresh embryonic tissues, cultured explants or co-aggregates, tissues/membranes with cells were carefully transferred into a 5 mL cytometry tubes prefilled with 1 mL of 7% FCS-PBS (+/+). Then, the tube was

topped up with 1 mg/mL collagenase/dispase solution (Roche) in 7% FCS-PBS (+/+). Prepared tubes were incubated in set to 37 ºC shaking water bath for 35 min. After incubation, the tube was topped up with one mL of 7% FCS-PBS(Ca-/Mg-), penicillin/streptomycin solution (1:100). Tubes were centrifuged for 5 min (400G, Beckman Coulter Allegra X-15R Centrifuge with SX4750A Rotor). 1 mL of the solution was discarded while the rest of the solution was used to disaggregate tissues by pipetting up and down. Used nitrocellulose membranes were discarded and tubes were spinned down again for 5 min (1500 rpm).

Co-aggregate cultures. To prepare co-aggregates, 20 uL of cells suspension (for example, mixture of cells isolated from E8 embryo and 100 000 stroma cells) were loaded in sealed 20-200 uL pipette tips. The tips were spun down at 400G for 12 min in Beckman Coulter Allegra X-15R Centrifuge with SX4750A Rotor. Obtained cell pellets are denoted in this work as co-aggregates. The seals on pipette tips were opened and the co-aggregates were deposited, floating on the medium membranes. 3-5 co-aggregates were cultured on one membrane.

Explant cultures. Dissected embryonic tissues were placed on: (a) floating on complete medium nitrocellulose membranes or (b) on the bottom of 6 wells plate and spinned down at 400G for 5 minuts in Beckman Coulter Allegra X-15R.

Plates with explants or co-aggregate cultures were incubated in humidified conditions at 37 ºC, 5% CO2 for 3-7 days. In 24h after culture initition, the medium was exchanged for a fresh one.

Stroma cells preparation. AGM cell suspensions in 7% FCS/PBS (no Ca/Mg ions) were stained with 1:200 anti-CD16/32 (clone 93, Abcam); 1:100 anti-CD45-biotin (clone 30-F11, BD Pharmingen), 1:100 anti-CD43-biotin (clone eBioR2/60, eBioscience), 1:100 anti-CD41-biotin (clone MWReg30, BD eBioscience); 1:100 anti-Ter119-biotin, (clone TER-119, BD Pharmingen) for 30 minutes on ice. After staining, cells were washed with 7% FCS/PBS (no Ca/Mg ions) and cell suspension (450 uL) was mixed with 50 uL of prewashed in 0.5%

BSA/PBS (no Ca, Mg ions) Streptavidin Particles Plus-DM (BD Biosciences). Cells were incubated with the beads for 20 min. Bead separation from CD41-CD43-CD45-Ter119- cell suspension was carried out with the BD IMagnet™. Separation was carried out twice.

2.5. Blood chimerism assessment

Blood samples (about 50 uL) were collected into a plate (round bottom wells) prefilled with 200 uL of 5 mM EDTA in 2% FCS – PBS(Ca-/Mg-). Samples were mixed, and the plate was centrifuged at 13000 rpm (250-400G) rpm for 5 min at 4 ºC. Plasma was removed, and 200 uL of lysis buffer was added (BD Pharm Lyse buffer diluted with water 1:10). Red blood cells lysis continued up to 15 min.

Cells were stained in 30-50 uL/well in diluted up to 1:200 Fc block and antibodies set A or set B (Appendix A26). Antibodies were diluted in 2% FCS-PBS for 30 min at 4 ºC. Cells were spun down and then stained with vital dye 7AAD (BD, 1:30) in 20 uL of 2% FCS-PBS. In this buffer, cells were transferred into FACS tubes and analysed on BD FACS Calibur for antibodies set A and FACS Fortessa for antibodies set B (Appendix A26).

Since early pre-HCS (E9 pre-HSC) showed only low levels of blood chimerism (Appendix A11), E8 pro-HSC would produce either similar or even lower levels of blood cihemrism. Therefore, a cut-off level of donor cells contribution below in which a recipient is considered to be not repopulated had to be established. This level was chosen on the basis of flow cytometric analysis of blood samples drawn from mice injected with either carrier cells alone (10^5 Ly5.1 cells) or a mix of OP9 cell suspension and carrier cells. We injected 300 000 OP9 cells per a recipient (an equivalent of three OP9 co-aggregates). In total there were five mice injected with control cell suspensions at different time points. For determining percentage of blood chimerism, we utilized two different sets of antibodies. Background level of false positive staining for set #1 (Ly5.1/2 het) was 0.04±0.03% (m±SD). For the second set of

antibodies, level of false positive staining was in the range of 0.027 – 0.1%. 0.1% of background staining level is the highest observed here and therefiore, 0.1% cut-out level shall be suitable to discriminate genuine hematopoietic system repopulation from antibodies unspecific binding. Hence, we have set the cut-out level to be 0.1% of blood chimerism.

Table 3.2.2. Background anibody staining assessment

Donor	Recipient	Mice injected with 10^5 Ly5.1 carrier cells only			Mice injected with 10^5 Ly5.1 carrier cells and $3*10^5$ OP9 cells		
		# of mice	% of cells showing donor phenotype, STR	% of cells showing donor phenotype, LTR	# of mice	% of cells showing donor phenotype, STR	% of cells showing donor phenotype, LTR
Ly5.2 homo	Ly5.1/2het	1	0.004([A])	0.018([B])	0	N/A	N/A
Ly5.1/2 het	Ly5.1 homo	2	0.006([A]) 0.046([A])	0.106([B]) 0.063([A])	2	0.094([A]) 0.024([A])	0.055([A]) 0.027([B])
Background staining for Ly5.1/2+ cells in blood drown from Ly5.1 recipients with antibodies set #1, mean±SD				0.04±0.03			

[A] – antibodies set A; [B] - antibodies set B (Appendix A26)

2.6. Beta-galactosidase staining on mouse embryos

Embryos were dissected from the uterus (leaving aside yolk sac) in Buffer A. Then we fixed embryos in Buffer B. Embryos E6.5 and E7.5E were fixed for 10 minutes (on ice); embryos E8.5 were fixed for 15 minutes (on ice).

After fixation, embryos were washed in Buffer C using the following procedure. First, embryos were briefly rinsed. Then, they were washed three times for 15 minutes each in a cold room, making sure they remain protected from light. Embryos were stained for 2h in Buffer D

at 37ºC. For this, embryos were incubated in a thermostat without a CO_2 supply. Afterwards, we fixed embryos in 4% PBA-PBS for 1h or overnight.

2.7. Early chick embryo culture

Chick embryo extraction. Embryo extraction was carried aseptically in a hood. All equipment for this procedure (forceps, paper rings, wipes) was sterilized. The following procedure was employed. An egg was first opened into a 15 cm plastic dish. The thick albumen above the embryo was removed with sterile tissues. A sterile paper ring was placed around the embryo. The vitelline membrane was partially cut around the embryo at "9-3 hours". The released edge of the paper ring (from the site of cut vitelline membrane) was picked up using forceps. Then, two simultaneous movements followed: 1) the rest of vitelline membrane was cut; 2) the paper ring was tangentially removed from the yolk (direction – towards the first cut of vitelline membrane).

Embryos collected on the paper rings were carefully cleaned from the yolk with the help of the forceps and were washed with Pannet-Compton saline. Cleaned embryos were placed ventral side up on the surface of agar plate taking care so that no air bubbles were trapped between the embryo and the agar surface. The lid was placed on the 30mm agar plate and the plate was transferred into a140 mm plate containing wet tissues and a 30mm plate with water. Six embryos were cultured in one 190 mm plate. Until six embryos had been collected, extracted embryos were kept in a closed 190mm plate in the hood. After six embryos had been collected, they were taken into a dissection room where they were either injected with a lipophilic dye or grafted with tissues from GFP+ embryos.

Extracted embryos were incubated in humidified plates in Brinsea incubator set to 37.8 C, 45% humidity. Embryos were incubated for 75 h.

2.8. Chick embryo grafting

Grafting was carried out with conventional methods under Nikon AZ100 stereomicroscope. In short, sections of primitive groove were excised from GFP+ donor and transplanted (complete tissue substitution) into stage-matched wild-type chick embryo donors in iso- or heterotopic position within the recipient primitive groove. Graft position and embryo development were recorded with the Nikon stereomicroscope using NIS Elements software. Images were processed with open source software ImageJ. Where labels were required, they were overlaid in with Photoshop software.

2.9. DiI DiO chick embryo labelling

Chick embryos were injected under PBS solutions with a mouth pipette with a pulled glass capillary loaded with working solutions of DiI or DiO. After injection, embryos were washed twice, checking under epifluorescent microscope for dye residues.

2.10. Gelatin cryostat sections

Tissues (mouse and chick embryos) were collected in PBS, washed and then transferred into 4% PFA for 2h. Tissues were then transferred into 15% sucrose/PBS(Ca-/Mg-) buffer and left for 2h at 4 ºC to equilibrate. After the tissues sank to the bottom of the tube, they were further transferred into 15% sucrose/7% gelatine in PBS(Ca-/Mg-) buffer. Tissues in 15% sucrose/7% gelatine PBS (Ca-/Mg-) were incubated at 37 ºC for 2h or till they sank to the bottom of the tube.

Prepared for freezing tissues, were transferred into moulds with help of glass wide mouth pipette and set into 37ºC incubator for equilibration. In 30 minutes, moulds were frozen in liquid nitrogen and transferred into a -80 freezer for storage.

Before cryoectioning, tissues were equilibrated at -28 ºC in cryostat and cut for 7um thick sections.

2.11. Immunohistochemistry with alkaline phosphotase on sections

Gelatine from sections was removed by submerged slides in PBS slides and treatment in microwave owen (10-20 s). Sections were twice washed with fresh PBS and dried at room temperature for 10 minutes in the dark. Tissue sections were encircled with “Liquid blocker” PAP pen (Sigma-Aldrich, Z672548) and left to dry for another 5 minutes. Tissue sections were blocked for unspecific protein binding in the block solution (0.1% Tween 20, 10% FCS, 10% normal goat serum) for 30 min at 21 ºC. Incubation with primary antibodies was carried out either for 18h at 4 ºC or for 2 h at 21ºC. Sections were incubated in block solution with 1:1000 diluted a-GFP rabbit serum (Invitrogen) for 1 h at 21ºC or for overnight at 4ºC. After incubation, sections were washed with PBS 3 times for 5 min. Sections were incubated in secondary antibody (1:1000 goat-anti-AP, Vector) for 1h at 21 ºC.

For alkaline phosphotase (AP) detection, vector Blue kit was used according to the manufacturer instructions (Vector, SK-5300). Sections were counterstained with nuclear fast red dye (Vector, H-3403) for 1 minute and washed for 10 minutes under running water. Then the slides were dehydrated in ethanol (2 minutes 90% ethanol/H2O; 2 minutes 100% ethanol) and cleared in Histo-clear (Agar) for 5 minutes twice. Tissue sections were mounted in VectaMount permanent mounting medium (Vector, H-5000) according to manufacturer instructions.

2.12. Immunofluorescence on cryostat sections

Initially slides were prepared the same at in section 2.11.

After blocking, sections were incubated with primary antibodies (1:250 anti-CD45, Ab Serotech) or 1:100 anti-Runx1 (Abcam) in 0.1% Tween-20, 5% FCS/PBS for 18h at 4 ºC. On the next day, sections were washed for 2 h at 4 ºC first in fresh PBS and then in 0.1% Tween 20, 10% FCS, 10% normal goat serum in PBS.

Secondary antibodies (anti-rabbit-A647, Invitrogen; anti-mouse-A546, Invitrogen) were added and diluted to 1:250 in 0.1% Tween-20, 5% FCS, PBS. Incubation with secondary antibodies was carried out for 18h at 4 ºC.

Anti-GFP antibody was applied on the 3d day, after wash and 2h sections block in 10% FCS, 0.1% Tween-20, PBS. Rabit-anti-GFP antibody was from Invitrogen, applied diluted to 1:250 in block solution for 2h at 21 ºC.

After immunostaining, sections were thoroughly washed with PBS (2h at 21ºC) and conterstained with 1:500 DAPI in PBS. Rinsed in PBS sections were mounted in Vectashield Antifade Mounting Medium (Vector, H-1000) according to manufacturer instructions. Sections were analysed under a confocal microscope Leica SP8.

Obtained images were collated in Fiji and labelled in Photoshop.

3.1. Mapping early hematopoietic precursors based on Runx1 expression

3.1.1. Introduction

To date the mechanism of HSC development is not clear. To elucidate this mechanism of HSCs maturation, it is necessary to study HSC development from the very first steps of HSC specification. Previously published works cite multiple sites of early HSCs appearance: dorsal aorta; yolk sac, placenta, head, heart. Today, there is still a disagreement as for the origin of pro-HSC [Medvinsky et al., 2011; Cumano et al., 2001; Rybtsov et al., 2014; Dzierzak and Speck, 2008; Gordon-Keylock et al., 2013; Samokhvalov et al., 2013; Gekas et al., 2010; Li et al., 2012; Nakano et al., 2013].

Runt related transcription factor 1 (Runx1, also known as Acute Myeloid Leukaemia protein 1, AML1) was identified to be the critical mediator of HSCs maturation [Okuda et al., 1996; Tanaka et al., 2012]. Generally, mouse embryos lacking functional Runx1 gene ($AML1^{-/-}$) appear to be normal till embryonic day 11 (E11). Around E11.5, AML1 knockouts (KOs) exhibit pale livers and at E12 $AML1^{-/-}$ mutants develop haemorrhages in the central nervous system (CNS) and die. Microscopic examinations of fetal livers, yolk sac sections and blood samples derived from AML1 KOs revealed that these mutants completely lack definitive haematopoiesis in both the yolk sac and the fetal liver. Only primitive nucleated erythrocytes generated in the yolk sac were detected in $AML1^{-/-}$ embryos. All other blood elements (erythroid, myeloid, megakaryocytes or platelets) were absent [Okuda et al., 1996]. Most importantly, in transplantation assays, no tissues derived from Runx1 KOs embryos contained

repopulating HSC [Mikkola et al., 2003; Liakhovitskaia et al., 2009 and 2014]. None of the other animal knock out models that affect haematopoiesis (*tal/SCL, PU.1, GATA1, GATA2, GATA3, c-myb* null mutations) has this widespread abrogation of all hematopoietic lineages development [Shivdasani et l., 1995; Polli et al., 2005; Gao et al., 2013; Fujiwara et al., 1996; Pandolfi at al., 1995; Hahl et al., 2009].

Rescue of definitive haematopoiesis was demonstrated to be possible in the conditional Runx1 ($AML1^{+/SACRE}$) model [Samokhvalov et al., 2013; Liakhovitskaia et al., 2009 and 2014]. In $AML1^{+/SACRE}$ mouse model, upon tamoxifen injection, one copy of the Runx1 gene is reactivated, leading to normal haematopoiesis and embryo survival. On the basis of the results obtained in timed rescue experiments, Samokhvalov et al. (2013) suggested that dHSC specification takes place early during embryo development - around E7.5±1 day.

To summarise, Runx 1 is the earliest regulator involved in hematopoietic stem cell maturation and/or a factor that controls development of HSC niche. In either way, expression of Runx1 shall mark a niche where pro-HSCs reside in early mouse embryos. According to several previous reports, Runx1 haploinsufficiency might lead into spatio-temporal alteration of Runx1 expression pattern [Cai et al., 2000]. Therefore, while useful insights have been obtained with utilization of $Runx1^{+/LacZ}$ transgenics [Daane and Downs, 2011], here we concentrated on Runx1+ cell mapping in wild type mouse embryos by means of immunofluorescence. This approach also allowed obtainmentm of better 3D representation of the expression map, and to combine identification of multiple markers simultaneously.

3.1.2. Experimental approach

To detect prospective pro-HSCs in early mouse embryos (from neural plate to early somites stages of development, embryonic day 7-8), we mapped cells expressing Runx1 transcription factor by means of immunofluorescence. Specificity of the Runx1 antibody was tested on AML1 $^{LacZ/LacZ}$ KO embryos (Appendix A1). To verify our findings for early somitic mouse embryos we also carried out beta-galactosidase staining on AML1$^{+/LacZ}$ heterozygotes. No differences in Runx1 expression in haploinsufficient AML1 and wild type early mouse embryos were found (Appendix A2 and A3). To get an insight into the phenotype of Runx1+ cells, some embryos were co-stained with endothelial (CD31 or VE-Cad), hematopoietic (CD41), or stem cell (c-kit) markers. Embryo staining was performed according to the morphological landmarks of gastrulating mouse embryo described by Downs and Davies (1993).

3.1.3. Mapping Runx1+ cells in early mouse embryo

3.1.3.1. Runx1+ cells location in the neural plate stage mouse embryo

In the neural plate stage, gastrulation is not completed yet and the primitive streak (PS) cells continue to contribute to the embryonic and extraembryonic tissues. One of the latest extraembryonic tissues posterior PS contributes to is the allantois [Stern, 2004; Psychoyos and Stern, 1996; Sweetman et al., 2008]. Allantois is responsible for establishing a fetal-maternal interface by fusion with chorionic plate and later on transforming into an umbilical artery. Currently two alternative hypotheses exist for the allantois formation. According to the "classical" hypothesis, allantois is generated by the mesoderm displaced from the embryonic area [Tam and Beddignton, 1987; Parameswaran and Tam, 1995]. An alternative hypothesis developed by Downs states that allantois is generated by the posterior primitive streak only [Downs et al., 2004, 2009]. In the latter case, the posterior PS physically spans the embryonic-extraembryonic boundary and remains there to give rise to allantois and to coordinate alignment of the umbilical artery and the dorsal aorta. Extraembryonic part of the posterior PS forms so called "allantoic core domain" (ACD)– reservoir of cells responsible for allantois elongation. ACD was also implicated in maintenance of Primordial Germ Cells during gastrulation. Recently, several reports have been published claiming allantois, umbilical cord and placenta are a niche for dHSC [Zeigler et al., 2006; Dieterlen-Lievre et al., 2010]. Therefore, in our mapping we have paid special attention to Runx1+ cells observed in the base of allantois or in its body.

According to our results, in neural plate stage (no bud, early bud or late bud stages) there is no Runx1+cells present in embryo proper (Table 3, Figure 7.). In small number of cases (one and two out of 19, respectively), we found Runx1+ localized to the base of the allantois

and in the middle of the allantois (Table 3, and Figure 7.). In relation to the ACD, Runx1+ cells were found at the edge of the ACD, in the ACD or in more distal position from the ACD. Our results mainly agree with Runx1 expression reported by Downs et al. (2011) for haploinsufficient Runx1 mutants. One exception is we did not identify Runx1 staining in the distal allantois and the endoderm of the visceral yolk sac. When we carried out beta-galactosidase staining on haploinsufficent $AML1^{+/LacZ}$, we also did not find these cells. We could explain this by the LacZ staining modification (enhancement) performed by the authors. However, our main conclusions about the presence of Runx1+ cells in the ACD and later on in umbilical artery (UA) and omphalomesenteric artery (OMA), agree.

Single Runx1+ cells were also found at the edge of the ACD, adjacent to the extraembryonic visceral endoderm, Figure 7., E. We would speculate that these cells were marking prospective vessel of confluence (VOC). VOC is poorly defined in the literature vessel that connects embryonic (dorsal aorta) and extra-embryonic (omphalomesenteric and umbilical arteries) vasculature [Inman and Downs, 2006; Daane and Downs, 2011]. When we examined older embryos, we found clusters of Runx1+ cells in the same position in forming VOC (Figure 8, B and F).

In all examined neural plate embryos, the yolk sac contained bright Runx1+ in large quantities. In three out of 19 embryos, Runx1+ cells were also found in chorionic plate lining (Figure 7, C, D). In four out of 19 cases, Runx1+ cells were found in clumps of cells protruding from the chorionic plate (Figure 7, D). We also found these cell clusters in the chorionic plates of older embryos. Strikingly, similar clusters of Runx1+ cells were previously reported for placenta lining in E10-11 mouse embryos and were found to be associated with definitive hematopoietic potential [Rhodes et al., 2008; Gekas et al., 2008].

No staining except in the yolk sac was found for hematopoietic CD41 (four samples) and endothelial CD31 (three samples) markers in neural plate mouse embryos. We could not identify c-kit+ cells in any of the examined neural plate (NP) embryos (three samples, Appendix A4). Similar observations with immunofluorescent CD31 and CD41 antigens detection were reported by other authors, indicating weak, if any expression of these genes in other parts of the NP mouse embryo [Rhee and Iannaccone, 2012].

Table 3. Runx1+ cells location in early mouse embryo

Location*	**Embryo development stage**		
	NP	**HF**	**1-13 sp**
	Embryos # with given localization/ Total embryos # examined, (%)		
Base of allantois, separate Runx1+ cells	1/19 (5%)	3/10 (30%)	19/24 (79%)
Clusters of Runx1+ cells at the base of allantois	0/19 (0%)	0/10 (0%)	10/24 (42%)
Runx1+ cells in the middle of allantois, separate cells	2/19 (11%)	5/10 (50%)	16/21 (76%)
Runx1+ clusters of cells in the middle of allantois	0/19 (0%)	0/10 (0%)	3/21 (14%)
Single Runx1+ cells in caudal part	0/19 (0%)	1/10 (10%)	15/19 (79%)
Spindle-shaped Runx1+ cells in dorsal aorta lining	0/19 (0%)	0/10 (0%)	8/18 (44%)
Runx1+ cells in chorionic plate lining	3/19 (16%)	7/10 (60%)	15/16 (94%)
Runx1+ cells clusters in chorionic plate	4/19 (21%)	0/10 (0%)	1/16 (6%)

* - in all examined embryos yolk sac contained Runx1+ cells. Neural plate stage comprises: NB – no bud, EB – early bud and LB – late bud stages. Headfold stage comprises: EHF – early head fold and HF – headfold stage; sp – number of somite pairs. Embryos staging was done according to Downs and Davies, 1993.

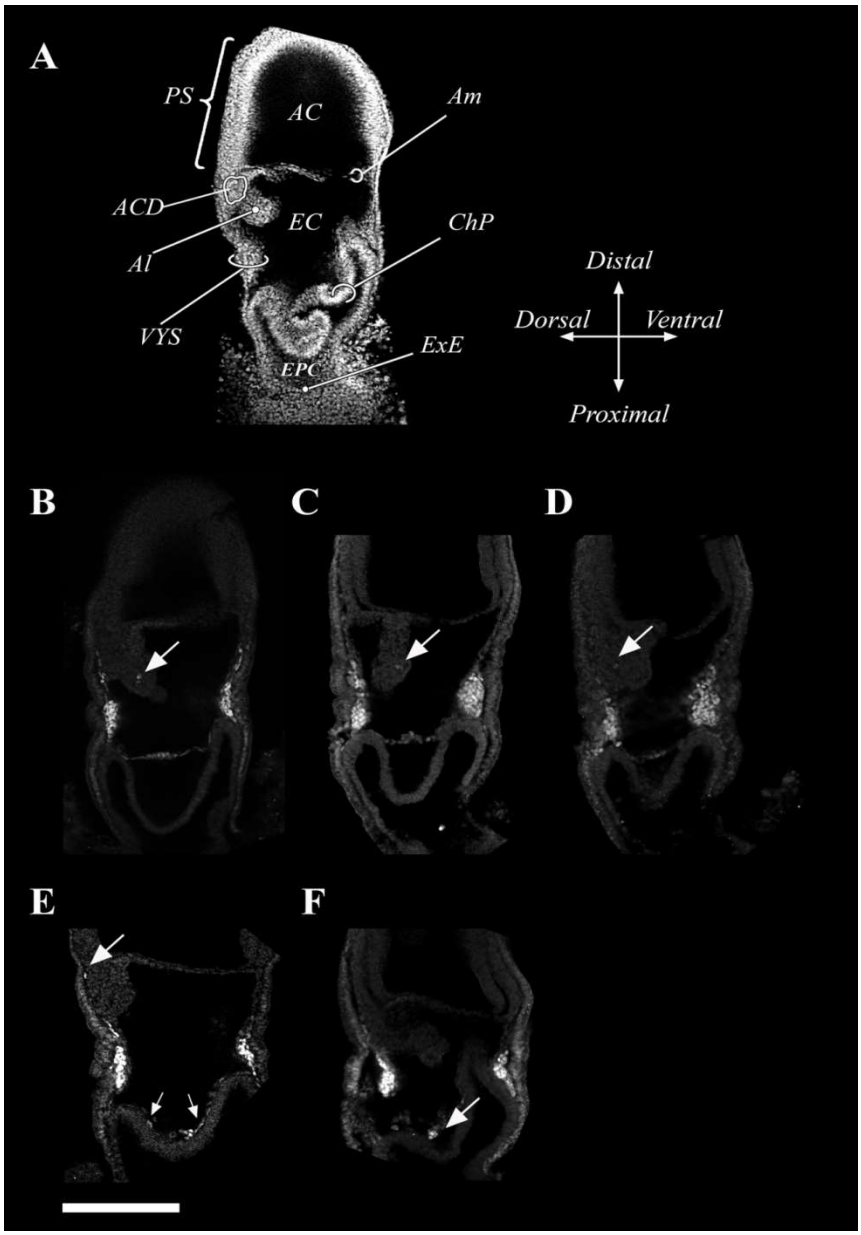

Figure 7. Runx1+ cells location in the neural plate mouse embryos. Scheme of mouse embryo in neural plate stage of development. The image of DAPI stained mouse embryo in late bud stage is shown (A). Runx1 is expressed in all NP embryos in the yolk sac (B-F). In some embryos Runx1+ cells were also found in allantoic bud (B-D); in ACD (D), in chorionic plate (E,F) and in cells clusters in ChP (F). Scale bar is 500 μm. Allantoic bud (Al), allantoic core domain (ACD), amniotic cavity (AC), amniotic membrane (Am), Chorionic plate (ChP), ectoplacental cavity (EPC), exocoelomic cavity (EC), extraembryonic ectoderm (ExE), primitive streak (PS), visceral yolk sac (VYS).

3.1.3.2. Runx1+ cells in headfold stage mouse embryo

With progression of mouse embryo development from neural plate (NP) to late head fold (HF) stage, number of embryos in which Runx1+ cells were found in allantoic core domain (ACD) or in the middle of the allantois increased (from 5 to 30% and from 11 to 50% of embryos, correspondingly), Table 3. During HF stage, the yolk sac vasculature expands, allantois and vessel of confluence (VOC) vasculogenesis begins. In contrast to the neural fold stage, at HF stage, endothelial cells (CD31+) were found not only in the blood belt, but also at the border of the embryo proper (Figure 8., C). On 3D reconstruction of the embryo surface, it is visible that endothelial cells are not dispersed homogeneously on the surface of the yolk sac but are aligned along the prospective vessels. Between these CD31+ cells (reaching almost to the embryo proper) rare cells express Runx1 transcription factor (Figure 8., C). Simultaneously, rare endothelial cells start to appear in the embryo proper - presumably along the future dorsal aorta (DA), (Figure 8., D). Initiation of the DA at HF stage was previously documented with staining for CD34, Flk1, CD31 and other endothelial markers [Wood et al., 1997; Strilic et al., 2009; Drake and Flemming 2000].

Vascularisation of the allantois takes place at a more rapid pace than that for the embryo proper. At the end of the HF stage, main allantoic vessel is already formed and it is marked by CD31+ and CD41+ cells, Figure 8., D-F. Rare separate Runx1+ cells were detected in the middle of the allantois, Figure 8., D. At the base of allantois, Runx1+ cells were found in the nascent vessel of confluence, VOC (Figure 8, B, and Appendix A5). VOC is initiated at the edge of the allantois adjacent to the yolk sac as a one-cell size opening at the allantois border [Inman and Downs, 2006; Daane and Downs, 2011]. This opening gradually increases in size, and VOC spouts towards the DA, the allantoic vessel and yolk sac vasculature. In observed embryos, this one-cell size opening was surrounded by CD31+Runx1+ cells (Figure 8., B). CD41+ cells were also found to localize to nascent VOC, however we did not find

CD41+Runx1+ cells in examined embryos (three samples), see Appendix A5. c-kit+ cells were dispersed in allantoic core domain (ACD) but did not particularly localize to VOC (Appendix A5). It is worth noting that primordial germ cells (PGC) migrate through the ACD at E8 are c-kit positive. Hence, relating c-kit+ cells to pro-HSC at E8 could be misleading [Manova and Bachvarova, 1991].

To summarize, similarly to the NP stage, the majority of Runx1+ cells in the HF stage are localized to the blood islands belt. Rare Runx1+ cells appear in forming yolk sac vasculature, VOC and allantoic vessel. We did not observe Runx1+ cells in embryo proper in pre-somitic embryos.

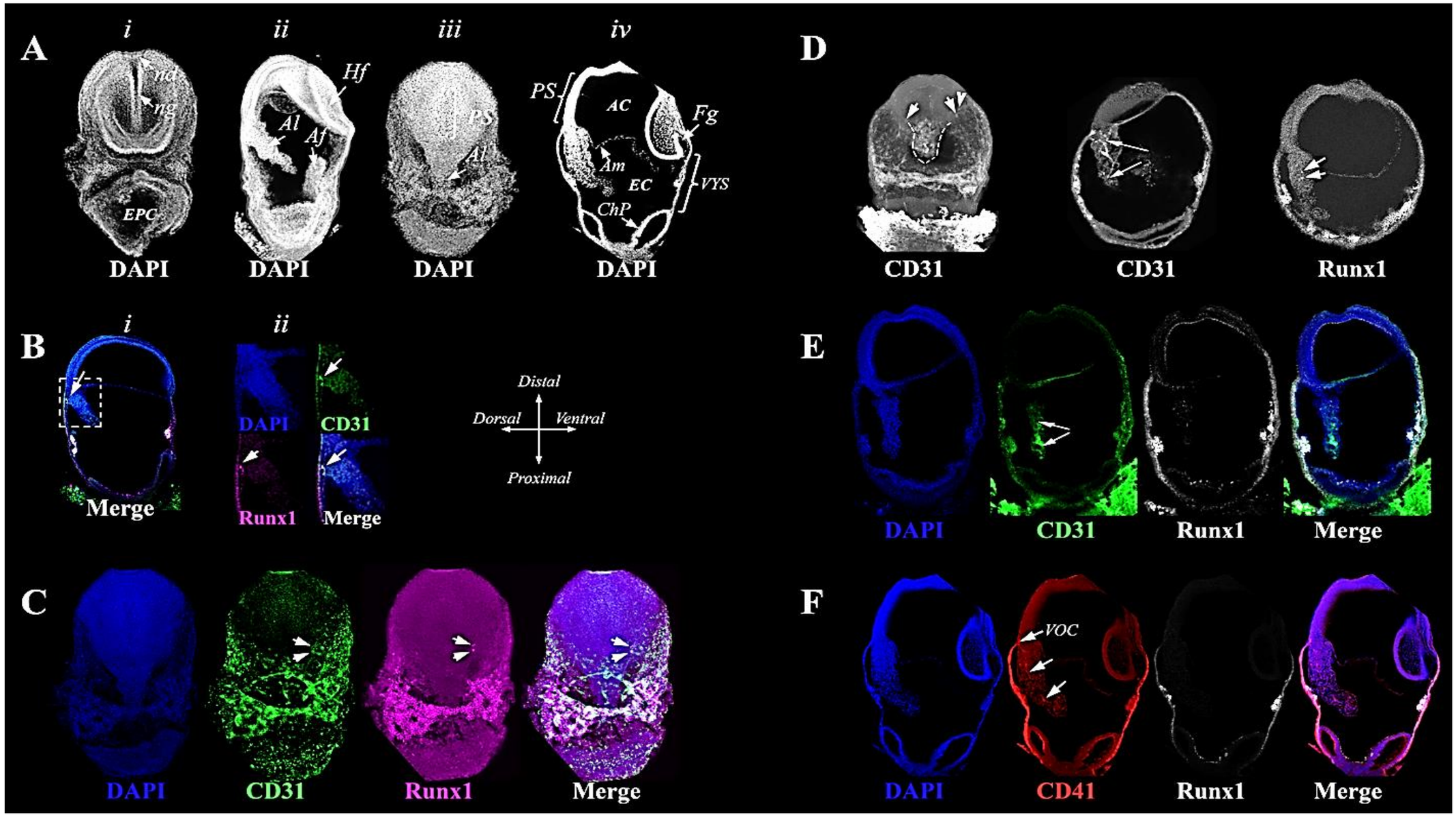

Figure 8. Rare Runx1+ cells localize to non yolk sac extraembryonic space in HF mouse embryo. Morphological features of headfold stage mouse embryo. 3D reconstruction. Anterior view showing the headfold (i); lateral view (ii); Posterior view showing posterior primitive streak and allantois (iii); Optical cross-section of headfold embryo (iv) (A); Runx1 expression in the point of initiation of the vessel of confluence (B); Spreading of CD31+ yolk sac vasculature and Runx1+ cells identified at the border of the embryo proper (C); Initiation of allantoic vessel formation: at early HF stage, CD31+ cells dispersed in allantois body; at late HF stage, they assemble into a branched. Rare Runx1+ cells localize to the body of the allantois (D); CD31_ allantoic vessel with no visible Runx1 cells inside it (E); Similar to F, CD41+ allantoic vessel (F). Af – amniotic fold; EPC – ectoplacental cone; ng – neural groove; nd – node; Hf – head fold; Al – allantois; PS – primitive streak; AC – amniotic space; EX – exocoelomic cavity; ChP – chorionic plate; VYS – visceral yolk sac; Am – amnion; fg - foregut diverticulum.

3.1.3.3. Runx1+ cells in the early somites mouse embryo

One of the signifying features of the early somites mouse embryos is the rampant development of intra-embryonic vasculature [Wood et al., 1997; Strilic et al., 2009; Drake and Flemming 2000]. Blood circulation starts gradually at 5 sp, but it is already completely established in the eight somite pairs mouse embryo [Jones, 2011; McGrath et al., 2003].

At the beginning of early somatic stage, Runx1+ cells were appearing in yolk sac vasculature bordering the vessel of confluence (VOC). Simultaneously Runx1+ cells were bordering VOC from the side of allantois (Fig 3.1.3.., D-F). Inside the allantois, Runx1+ were expressed along the nascent allantoic vessel so that its backbone now could be distinguished not only by CD31 or CD41 staining, but also by Runx1 staining (Figure 9., G).

Extra-embryonic and intra-embryonic vasculature could now be completely visualized by endothelial cell markers (CD31, VE-Cad) staining (Figure 10., E). We found that at the beginning of the somitic stage, nascent vessels were formed by the cords of endothelial cells consisting not only of spindle-like cells (representing endothelial cells), but also by round cells which are usually characteristic of migrating cells (Figure 11., A, E). These cords were formed almost entirely from Runx1 negative cells. In the cords that would become a straight portion of the vessel, only spindle-like cells express Runx1 transcription factor (Figure 11., E). However, we found clusters of round Runx1+CD31+ cells at the junction between allantois and VOC (Figure 8., C). At the time of blood circulation initiation (5-8 sp), these clusters of cells transformed in

formations, strikingly resembling blood islands usually found in the yolk sac blood belt (Figure 10., D, F). These Runx+ cell clusters were expressing CD41 and CD31 markers. Clusters of Runx1+ cells were also found in the chorionic plate and inside the allantois (Figure 10. B).

When we examined processed beta-galactosidase staining sections of haploinsuficient (AML1 $^{+/LacZ}$) early somitic mouse embryos, we found Runx1+ cells in clusters in the VOC, allantois and chorionic plate. Therefore, at least at the early stages of mouse embryo development, the spatio-temporal pattern of Runx1 expression is not affected in AML1 haploinsufficient embryos [Cai et al., 2000].

Earlier, it was reported that in E9-E10 mouse embryos, clusters endowed with hematopoietic potential were found in the placenta, omphalomesenteric and umbilical arteries [Wood et al., 1997; Zeigler et al., 2006; Rybtsov et al., 2014]. We envision that these reported clusters are the descendants of the Runx1+ cell clusters we identified here in VOC, allantoic mesoderm and chorionic plate.

At around the 13 sp embryo, when embryo turning has been initiated, we found polarized Runx1 expression in the lining of the dorsal aorta (Figure 15, F). Interestingly, this Runx1 expression was oriented towards the omphalomesenteric artery (or according to Downs, VOC that becomes a part of OMA). In contrast, the forming of an umbilical artery (allantoic vessel, future umbilical artery, UA) was not represented by one vessel at this time point, but by a branching tree of vessels and cords. Some cells in nascent UA, expressed Runx1, Figure 11., G, H.

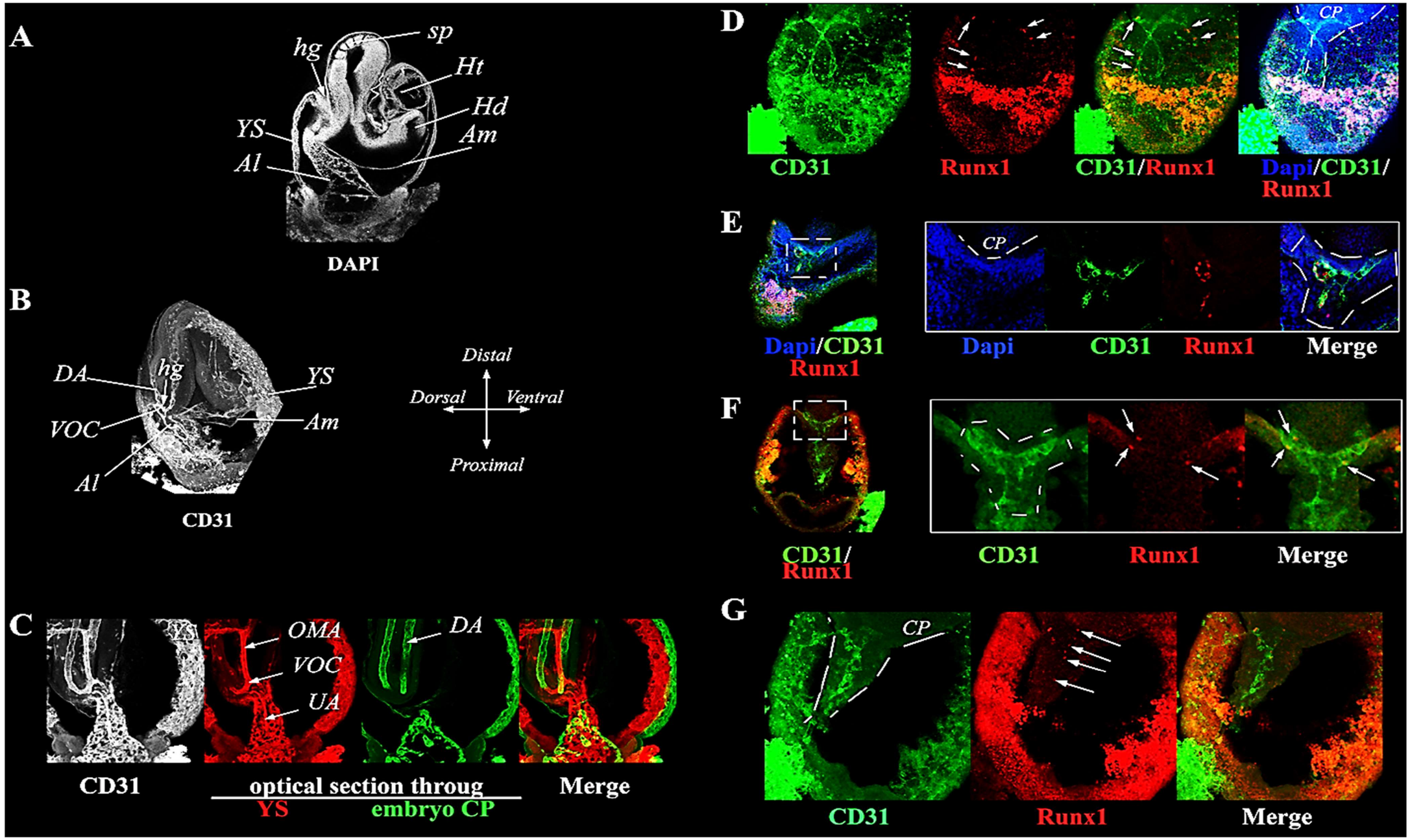

Figure 9. In early somitic mouse embryo, Runx1+ localize to nascent extraembryonic vasculature of allantois and VOC. Scheme of early somitic embryo (A); Vascular structure of pre-circulation embryos (B); Vascular structure of embryo with formed DA and initiated blood flow. Note elongated VOC (C); Spread of extraembryonic vascular network on the surface of the yolk sac in early somitic embryo. Arrows point to Runx1+ cells localized to endothelial cells aligned along nascent YS vessels. Some of the Runx1+ cells reached YS-embryo proper border. Black outline – caudal part, connected to allantois (D); Runx1+ cells form a branch of VOC (E); Runx1+ cells symmetrically outline VOC – YS vasculature junction (F); Runx1 is expressed in backbone of CD31+ allantoic vessel (G). Al- allantois; YS – yolk sac; hg – hindgut; sp – somites; Ht – heart; Hd – head; Am – amnion; DA – dorsal aorta, VOC – vessel of confluence.

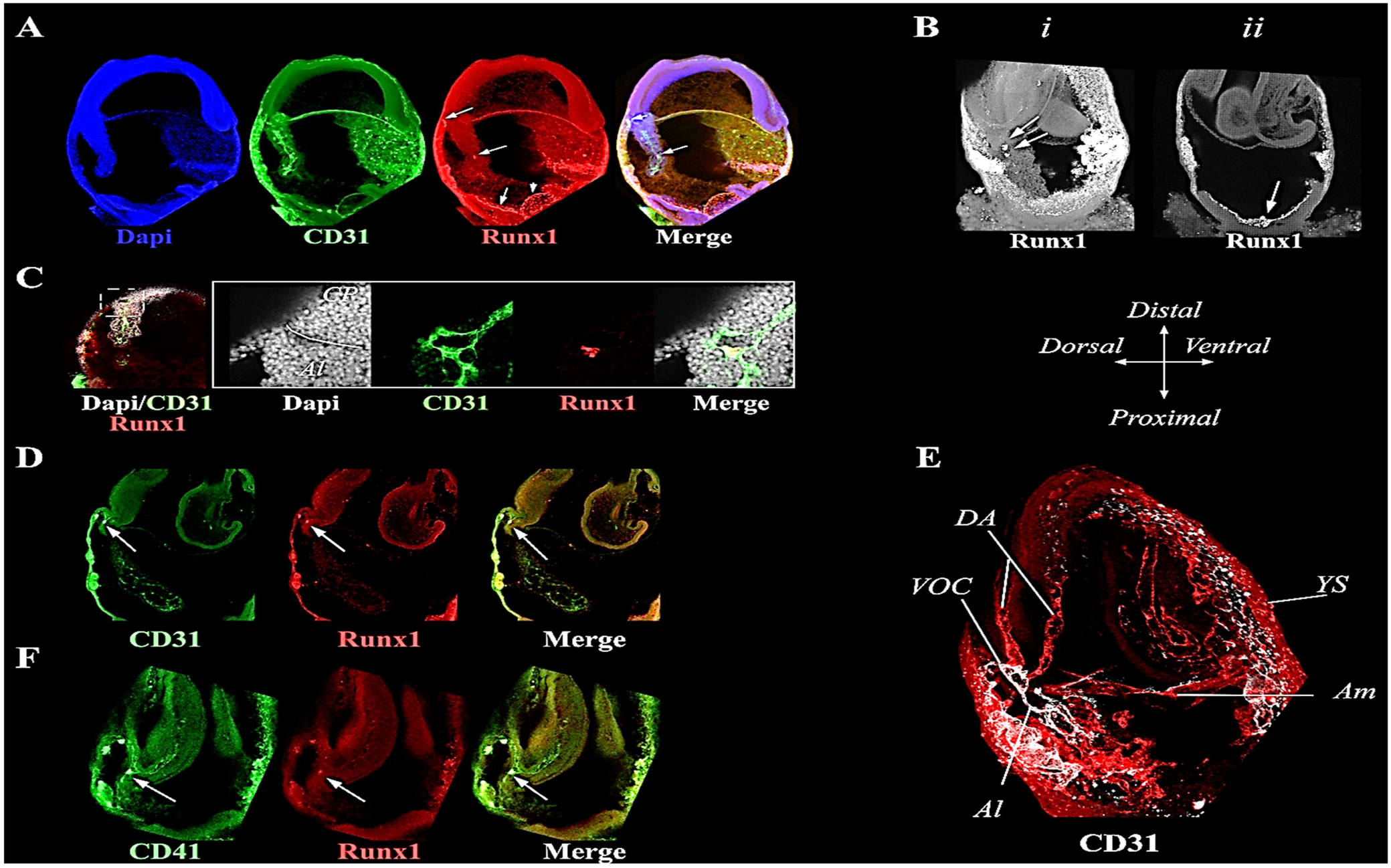

Figure 10. Runx1+ cells clusters in early somitic embryos localize to VOC, allantois and chorionic plate. Runx1+ clusters in the middle and the base of CD31+ allantoic vessel (A); 3D reconstruction of early somitic embryo. Pair of Runx1+ cell clusters in the base of allantois (i); Runx1+ cells cluster in chorionic plate (ii) (B); CD31+Runx1+ cluster of cells at the junction allantois – VOC (C); Optical cross-section of 5 sp embryo showing CD31+ extraembryonic vasculature with Runx1+CD31+ cluster in VOC (D); Optical cross-section of mouse embryo with established blood circulation showing CD41+ extra- and intraembryonic vasculature connected by VOC. CD41+Runx1+ cells cluster in at the base of VOC (F); 3D reconstruction of the stack of optical sections showing extra- and intra-embryonic vasculature (red) connected by VOC (white) (E). Al- allantois; CP – caudal part; YS – yolk sac; hg – hindgut; sp – somites; Ht – heart; Hd – head; Am – amnion; DA – dorsal aorta, VOC – vessel of confluence.

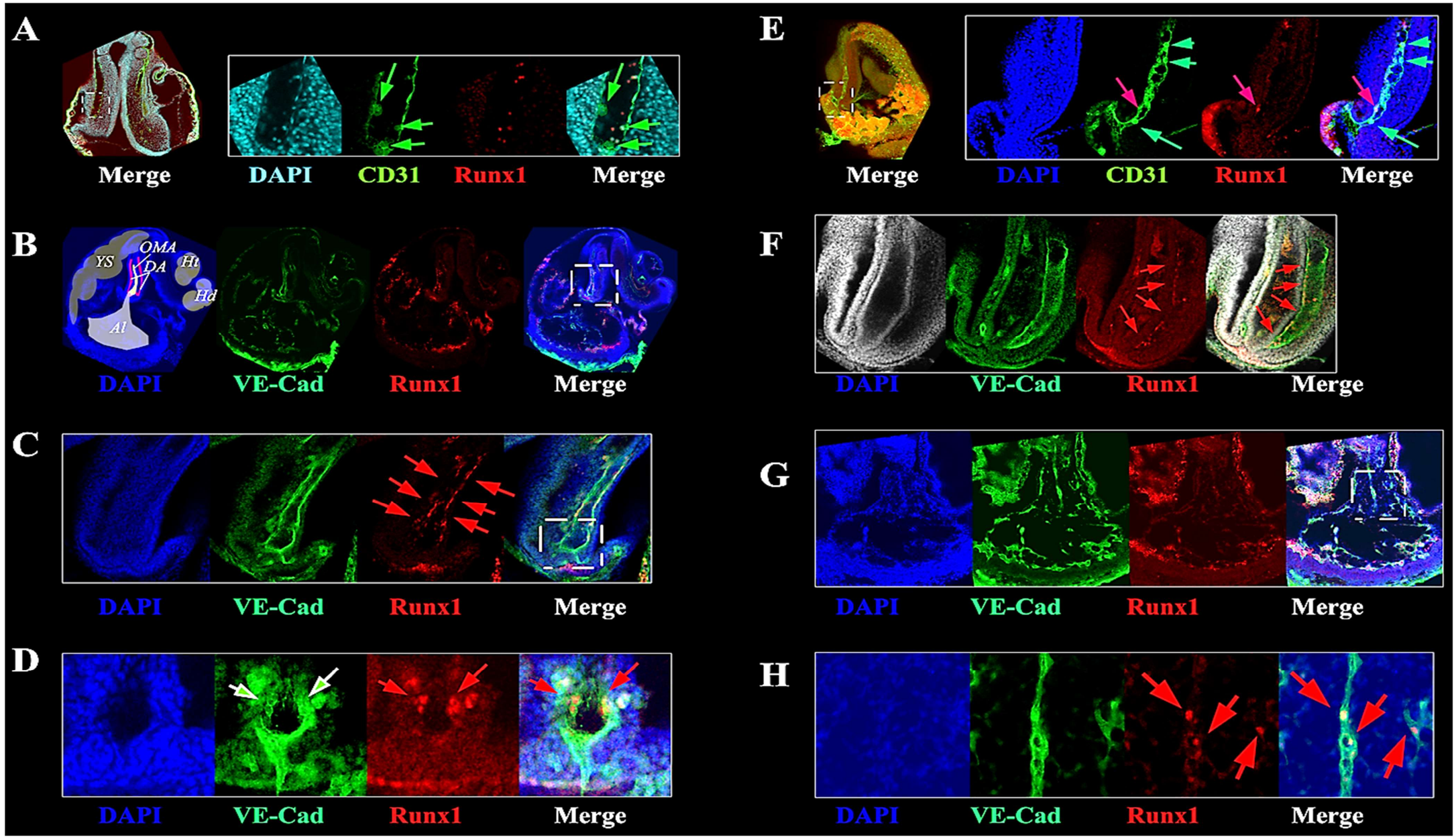

Figure 11. Forming in early somites vasculature gradually acquire spatially-defined Runx1 expression. Five sp mouse embryo DA optical cross-section showing Runx1+ primitive erythroblasts in DA lumen and large CD31+ cells with philopodia. DA lining is Runx1 negative (A); General view of mouse embryo with established blood circulation (B); Inset from B. Optical section showing caudal part focusing on OMA lumen. OMA lining expresses Runx1(C). Inset from C. CD31+ Runx1+ cells clusters symmetrically surround base of OMA (D); DA in pre-circulation embryo is formed from endothelial cell cords. Some cells exhibit round morphology characteristic for migrating cells. Only rare spindle-like cells express Runx1 (E). Inset from B. Optical section showing caudal part focusing on DA lumen. DA lining exhibits polarized Runx1 expression (F); Allantois from embryo show on B. Early stage of UA formation. Highly branched structure of CD31+ endothelial cords is visible with some CD31+ cells expressing Runx1 (G); Inset from G. A subset of CD31+ endothelial cells nascent UA show Runx1 expression (H). Al- allantois; CP – caudal part; YS – yolk sac; OMA – omphalomesenteric artery; Ht – heart; Hd – head; Am – amnion; DA – dorsal aorta, VOC – vessel of confluence.

3.1.4. Conclusions

In agreement with prior reports, our mapping of Runx1+ cells show that in pre-somitic mouse embryos the majority of Runx1+ cells are localized to the yolk sac blood islands and the chorionic plate [Lacaud et al., 2004; Samokhvalov et al., 2006; 2009; 2014; Challen and Goodell, 2010; Yokomizo and Dzierzak, 2010; Yokomizo et al., 2011]. Rare single Runx1+ cells were found in the allantois. Runx1+ cells were identified in the base of the allantois, where they were marking the site of initiation of the vessel of confluence (VOC). These observations are in agreement with those obtained with haploinsufficient $AML^{+/LacZ}$ embryo mutants [Zeigler et al., 2006; Downs et al., 2009; Daane et al., 2011]. With embryo development beyond the headfold stage, Runx1+ cells were also found in clusters situated in the VOC. We envision that found Runx1+ cell clusters are the predecessors of hematopoietic clusters found in later stages of embryo development in the placenta and the umbilical artery [Zovein et al., 2010; Wood et al., 1997; Zeigler et al., 2006]. To elucidate whether these Runx1+ cell clusters have HSC potential, one would need to mature and expand these cells in *in vitro* culture [Cumano et al., 1996; 2001]. In this work we attempted E8 pro-HSC maturation in co-aggregate and explant culture. These results are described in the next chapter.

According to our observations, initially intro-embryonic and intro-alantoic vasculature is built from cords of endothelial cells. These cords are built from two types of cells: CD31+ flat, elongated (spindle-shaped) cells and round CD31+ cells. Runx1 expression is rare in these cords and if present, restricted to spindle-like endothelial cells. Spindle-like cells have the same morphology as the endothelium lining cells found in the dorsal aorta. Elucidation of the function of round CD31+ cells will require further investigation. For

example, formation of the dorsal aorta in an embryo might be followed *in vitro* by means of light sheet fluorescence microscopy.

In embryos with established blood circulation (e.g., starting from 5-8 somite pairs, sp) Runx1+ cells are found in caudal parts in the lining of the dorsal aorta (DA). Runx1 in the DA is expressed in a polarized fashion. Specifically, according to our data, in E8-E9 mouse embryos are the only cells of the dorsal aorta wall that are the closest to the omphalomesenteric artery (OMA) expresses Runx1+. To note, in older mouse embryos, Runx1 is expressed in endothelia cells of the ventral and dorsal aorta walls and in sub-aortic spaces as well [Boisset et al., 2010; Yokomizo and Dzierzak, 2010; Yokomizo et al., 2011].

Our results show that in the E8 mouse embryo, the vessel of confluence (VOC) is marked with intensive Runx1 staining. This pattern of Runx1 expression is preserved till E9, when the DA fusion takes place. Site where the first DA fusion events take place co-insides with the site where Runx1 expression is upregulated in the early E9 mouse embryo. According to Rybstov et al. (2014) fist transplantable HSC in the E9 mouse embryo also originate from that portion of the DA. Therefore, the DA fusion might be a signal necessary to initiate maturation of Runx1+ HSC precursors. The DA fusion depends on bone morphogenic protein (BMP), vascular endothelial growth factor (VEGF) and Sonic hedgehog (Shh) signalling [Garriock et al., 2010; Nagase et al., 2006]. Therefore, OP9 stromal cells transduced to express *Bmp4, Shh,* and *Vegf* might be a good substitute to the currently use OP9 cell line.

3.2. Early hematopoietic precursors engraftment potential

3.2.1. Experimental approach

According to the preceding reports, cells isolated from early mouse embryos (embryonic day 7-8, E7-E8) do not reconstitute the hematopoietic system of irradiated recipients directly [Medvinsky and Dzierzak, 1996; Cumano et al., 2001; Godin et al., 1993; Fraser et al., 2002]. In this work, hematopoietic stem cell precursors contained in the E7-8 mouse embryo are denoted as pro-HSC and HSC precursors contained in the E9-E10 mouse embryo – as pre-HSC. To reveal pro-HSC hematopoietic potential, early embryo tissues must be cultured *in vitro*: as explants or co-cultured with stromal cell lines [Cumano et al., 2001; Fraser et al., 2002]. Successful engraftment with pre-cultured pro-HSC was demonstrated in transplantations into severe combined immunodeficient (SCID) or in natural killer-deficient Rag2γc-/- mice [Godin et al., 1993; Cumano et al., 2001]. Pro-HSC are unable to engraft immunocompetent recipients due to the lack of sufficient expression of major histocompatibility complex (MHC) class I molecules [Cumano et al., 2001; Kieusseian et al., 2012]. Cells missing MHC-I molecules become targets of recipients' natural killer cells [Cumano et al., 2001; Kieusseian et al., 2012]. Mature dHSC in contrast to pro-HSC express sufficient levels of MHC-I. It was demonstrated that during *in vitro* maturation, HSC precursors upregulate MHC-I expression and become transplantable [Kieusseian et al., 2012].

In our group, an efficient method of early (E9 derived) pre-HSC maturation and expansion was developed and successfully implemented in practice [Rybtsov et al., 2014]. This

approach consists of pre-HSC co-aggregation with the OP9 stromal cell line [Sheridan et al., 2009; Gordon-Keylock et al., 2013; Rybtsov et al., 2014; Rybtsov et al., 2016]. The OP9 stromal cell line has been shown to stimulate maturation and expansion of hematopoietic progenitors and embryonic stem cells [Vodyanik et al., 2005; Ji et al., 2008; Rybtsov et al., 2014; Gordon-Keylock et al., 2013; Souilhol et al., 2016). HSC precursors and stroma cells are mixed together and brought together by centrifugation. Formed co-aggregates are cultured on the top of floating nitrocellulose membranes for 4-7 days. An air-liquid interface culture method increases gas exchange within a co-aggregate, which might facilitate HSC maturation. Although the process of pre-HSC maturation in co-aggregate in not entirely understood, we hypothesize that this method will allow us to reconstruct a HSC niche microenvironment by promoting cell-to-cell contacts between pre-HSC and stroma cells. Therefore, in this work we utilized the co-aggregation technique to induce maturation of the E8 mouse pro-HSC.

Prior data suggests that stromal cell lines derived from the AGM possess capacity to induce HSC maturation [Weisel et al., 2006; Oostendorp et al., 2002; Krassowska et al., 2006]. Assuming that the AGM stoma cells have similar properties to fresh AGM stroma, we tested co-aggregation of freshly isolated stroma cells with E8 tissues. For stroma cells, we used E9 or E10 CD45, CD41, CD43, Ter119 negative cells isolated from the mouse embryos AGM region. E8 cells were co-cultured with AGM stroma in two steps. First, E8 cells were co-cultured with E9 AGM stroma cells. Then, co-aggregates were dissociated and obtained cells were co-aggregated with E10 AGM stoma cells. In this way, E8 cells are gradually positioned in the environment in which HSC mature. We were particularly interested to see if cells from the base of allantois (to which Runx1+CD31+CD41+ cell clusters were mapped) would repopulate the recipient's haematopoietic system.

To compare efficiency of HSC maturation induced by fresh stoma to that induced by OP9 cells, in a separate experiment we substituted co-aggregation with fresh stroma by co-aggregation with OP9 cells.

As an alternative method of pro-HSC maturation, we carried out a previously described explants culture method (at air-liquid interface or as a submerged culture) [Cumano et al., 2001; Kieusseian et al., 2012]. In a separate experiment, cells isolated from explants were further co-aggregated with OP9 cells. The summary of culture methods used for E8 pro-HSC maturation is given in Table 4. and Figure 12.

Table 4. Pro-HSC maturation culture methods used for E8 tissues

<table>
<tr><th colspan="2">Culture Step 1</th><th>Culture Step 2</th></tr>
<tr><td rowspan="3">Culture at air-liquid interface</td><td rowspan="2">E8 cells co-aggregated with fresh E9 stroma</td><td>Cells from Step 1 co-aggregated with fresh E10 stroma</td></tr>
<tr><td>Cells from Step 1 co-aggregated with OP9 cells</td></tr>
<tr><td rowspan="2">E8 explants culture</td><td>Cells from Step 1 co-aggregated with OP9 cells</td></tr>
<tr><td>N/A</td></tr>
<tr><td>Submerged culture</td><td>E8 explants culture</td><td>N/A</td></tr>
</table>

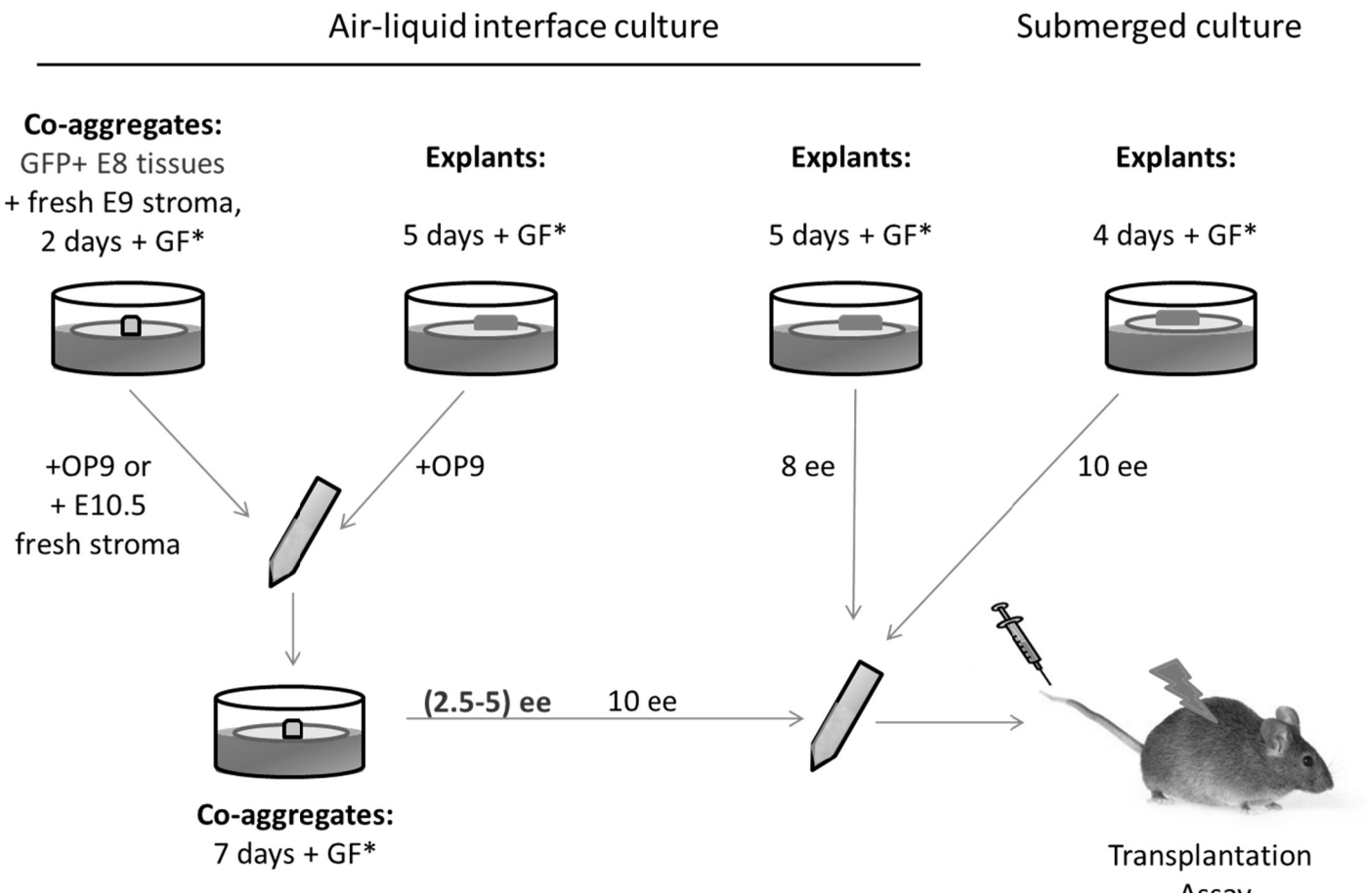

Figure 12. E8 pro-HSC maturation culture methods used in this work. ee – embryo equivalents.

3.2.2. Pro-HSC maturation at air-liquid interface by co-culture with stromal cells

Stromal cell lines and fresh stoma cells derived from the AGM possess a capacity to induce HSC maturation and expansion [Weisel et al., 2006; Oostendorp et al., 2002; Krassowska et al., 2006; Nishikawa et al., 2001; Souilhol et al., 2013A and 2016B]. Therefore, a co-culture of E8 mouse embryo derived cells with E9 stoma cells might also induce pro-HSC maturation. In our experiments, E8/E9_stroma co-aggregates were cultured for two days at air-liquid interface. Then, these co-aggregates were dissociated and re-aggregated with E10 stoma cells (producing E8/E9_stroma/E10_stroma co-aggregates) Figure 12. In this way, E8 pro-HSC would be subsequently placed in microenvironments in which E9 and then E10 pre-HSC reside.

Appearance of GFP+VE-Cad+CD45+ cells in co-aggregates would indicate E8 pro-HSC maturation into transplantable pre-HSC [Rybtsov et al., 2011 and 2014]. When E8/E9/E10 co-aggregates were analysed by flow cytometry, we found that the GFP+ fraction of cells essentially disappeared from co-aggregates (Appendix A7 and A8). No GFP+ cells with a transplantable pre-HSC phenotype (VE-Cad+CD45+) were detected. Remarkably, in all cultures, GFP negative (GFP-) VE-Cad+CD45+cells appeared, indicating that some HSC precursors are negative for CD41, CD45 and CD43 markers were contained in E9 and E10 AGM fraction of stroma cells. There could be several explanations for this: (1) non-complete stroma cells depletion from $CD41^{low}$ pre-HSC, or (2) maturation of negative for hematopoietic markers, but positive for endothelial marker VE-Cad+ cells into pre-HSC. If $CD41^{low}$ cells were retained in the stroma cells population, they could mature into CD45+VE-Cad+ pre-HSC. For instance, in a separate set of experiments we showed that E9.5 pre-HSC are VE-Cad+CD45-$CD41^{low}$CD43- cells dispersed between stroma cells underlying the dorsal aorta. In addition, E9 pro-HSC maturation depends on the presence of stem cell factor (SCF) – one of the growth factors we used in our culture medium [Rybtsov et al., 2014].

As no GFP+ cells with a pre-HSC phenotype were found after the co-aggregate culture, we substituted the co-culture step with E10 AGM stroma by a co-culture step with OP9 stroma cells. When the content of these co-aggregates was analysed, we only observed the increase in GFP+ cells number in yolk sac cultures (Figure 13. and Appendix A7 and Appendix A8). Similar to E8 tissues co-aggregated with E9/E10 stroma, no GFP+ cells having a transplantable pre-HSC phenotype (CD45+VE-Cad+) were found in E8/E9_stroma/OP9 co-aggregates. The same as in the previous experiment, a small number of CD45+VE-Cad+ cells were detected in the GFP negative fraction. We propose that the GFP-CD45+VE-Cad+ cells were derived from the E9 VE-Cad+CD41^{low} cells. Therefore, the E9 mouse embryo aorta and subaortic space already contain hematopoietic stem cell precursors, which express endothelial marker VE-Cad, but do not express sufficient levels of hematopoietic markers (CD45, CD41, Ter119 or CD43). These cells can be matured into HSC in a prolonged co-aggregate culture (7 days). Yet, E8 pro-HSC do not mature or expand in such a co-aggregate culture.

To test whether the rare GFP+ cells after co-aggregate culture can proliferate in favourable conditions (for example, in a semi-solid medium supplemented with growth factors) we seeded cell suspensions obtained from dissociated co-aggregates in a MethoCult methylcellulose medium. GFP+ cells formed colonies in none of the cultures seeded with E8 embryo proper tissues. It is only in YS co-cultures that multiple GFP+ cells were identified. These GFP+ cells did not proliferate more than forming clumps of 3-6 GFP+ cells and did not form any hematopoietic colonies. To note, cells derived from E9 stoma cells formed multiple hematopoietic colonies (Appendix A10). Therefore, pro-HSC contained in the E8 mouse embryo tissues cannot be matured in the co-aggregate culture described here.

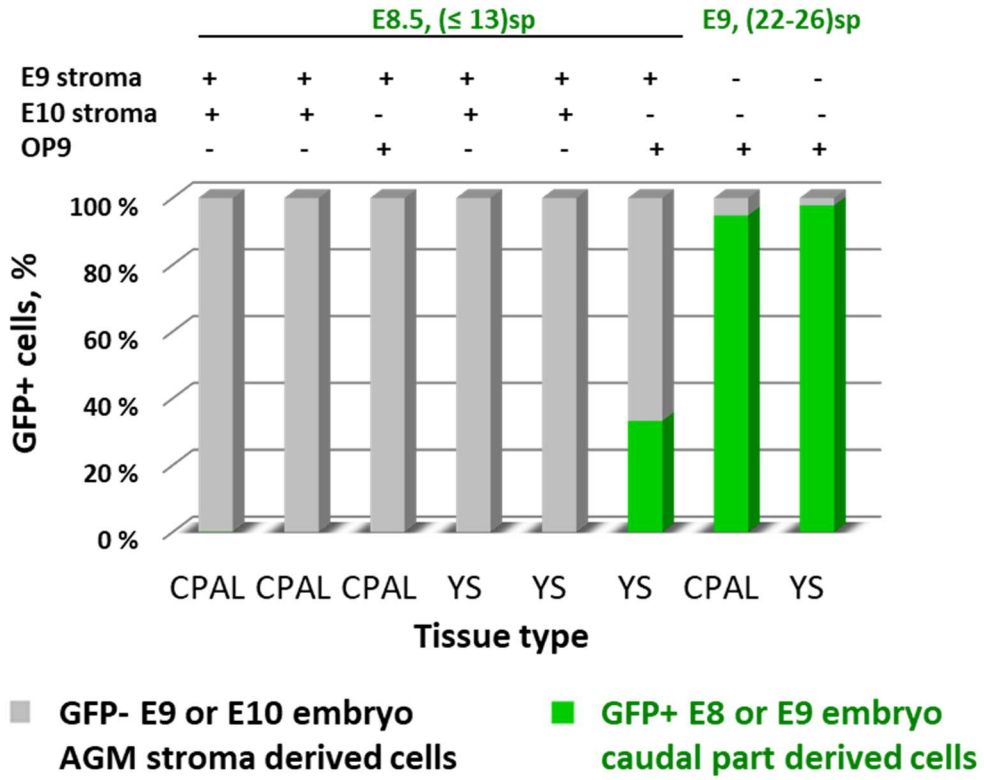

Figure 13. Cellular composition of co-aggregates after culture. Co-aggregates were prepared with cells isolated from E8 or E9 mouse GFP+ embryos and with E10 or OP9 (GFP-) cells. Caudal part (CP), allantois (AL), the region of the vessel of confluence (CPAL), yolk sac (YS). GFP+ cells – are E8 or E9 CP derived cells. GFP- cells – are CD41-CD45-CD43-Ter119- cells (stroma) isolated from AGMs of E9, E10 mouse embryos or OP9 cells.

One small scale transplantation experiment was carried out with cell suspensions derived from cultured co-aggregates. All the recipient mice were injected with 2.5 embryo equivalents (ee) of an initial E8 isolated cell suspension. Recipients blood chimerism analysis showed that no E8 embryos derived GFP+ cells that were able to engraft the recipients, Figure 14. and Appendix A11. Yet, the recipients' haematopoietic system was repopulated with GFP- cells (up to 30% of blood chiemrsims) derived from the AGM region of E9 or E10 mouse embryos. These GFP- HSC shall be derived from the AGM cells population - e.g. from CD41-CD43-CD45-Ter119- population assumed to be stroma cells. Notably, in accordance to prior reports, only E9 and E10 cells derived from caudal parts, but none from the yolk sac were able to engraft the recipients [Müller and Medvinsky et al., 1994; Godin et al., 1995; Medvinsky and Dzierzak, 1996; Cumano et al., 1996 and 2001]. Therefore, the utilized HSC maturation co-aggregate culture method is a powerful one and allows the revelance of hematopoietic potential of E9 and E10 pre-HSC, but not efficient enough to induce maturation of E8 pro-HSC.

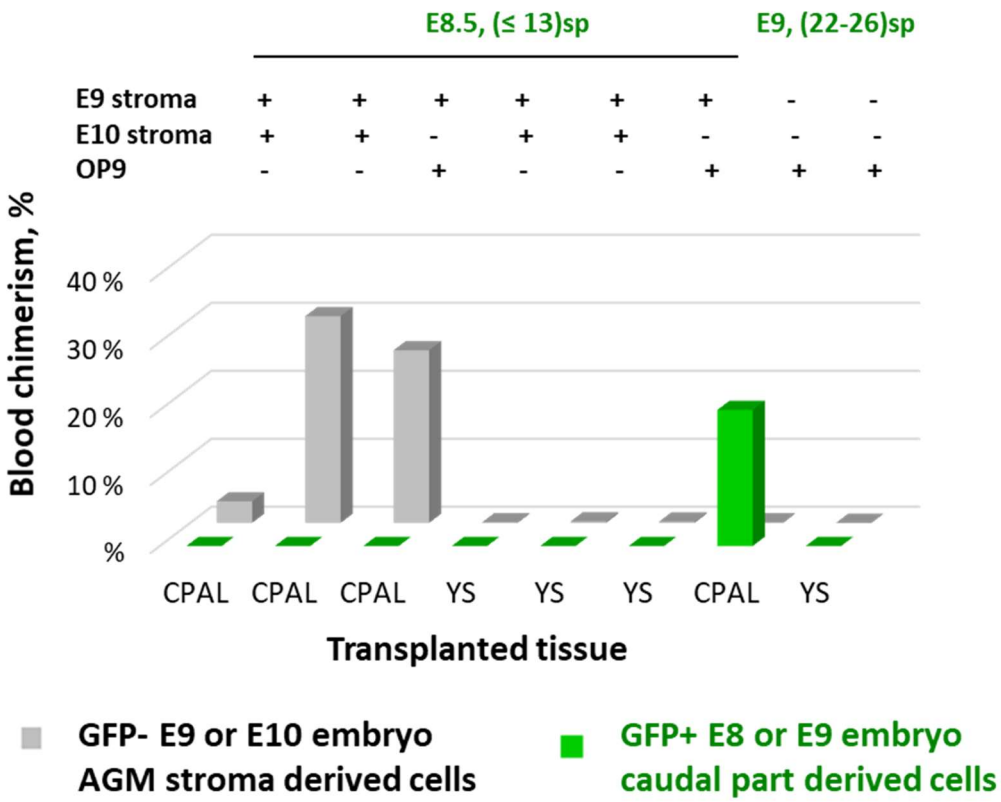

Figure 14. Engraftment of E8 and E9 embryo derived cells. Blood chimerism 6 weeks after transplantation with cells obtained from dissociated co-aggregates. Co-aggregates were prepares from cells isolated from E8 mouse embryo caudal parts and CD41-CD45-CD43-Ter119- cells (stroma) isolated from AGMs of E9 or E10 mouse embryos or OP9 cell line. Caudal part (CP), allantois (AL), the region of the vessel of confluence (CPAL); yolk sac (YS).

3.2.3. Dorsal aortae fusion in E9 mouse embryos and its potential role in pro-HSC maturation

According to our data, cells isolated from the E9 mouse embryo caudal parts proliferate and survive better in culture than those from the E8 embryo (Figures 13). Cells derived from 22-26 somite pairs (sp) of the E9 mouse embryo possess low definitive hematopoietic potential, which is comparable to that of the younger E8 embryo (Appendix A11). In contrast, cells derived from mouse embryos having more than 26 sp are able to mature into potent highly engrafting dHSC. Number of transplantable pre-HSC rise sharply after embryo develops beyond 26 sp [Rybtsov et al., 2014].

We investigated what changes take place in the mouse embryo AGM when the embryo acquires 26 somites pairs. For this, we extended our Runx1 mapping to E9 mouse embryos. We specifically were looking at the 6-23sp area which was reported to possess the highest definitive hematopoietic potential. Three E9 mouse embryos were examined by immunofluorescence for a Runx1 expression pattern.

According to our observations, the pattern of Runx1 expression in the caudal portion of the E9 mouse embryo remained the same as in early somitic E8 embryos: intensive staining in the omphalomesenteric artery (OMA) and polarised Runx1 expression in the dorsal aorta (Appendix A13). Clusters of Runx1+ cells are still observable in the OMA, Figure 15. According to prior data, the OMA carries multiple clusters of cells [Wood et al., 1997; Zovein et al., 2010]. Yet, as it was shown in Rybtsov et al., (2013) the area containing these clusters does not possess definitive hematopoietic potential.

Polarisation of Runx1 expression in the dorsal aorta (DA) was different only in how Runx1+ cells were localized in the floor of the DA. Specifically, in E8 mouse embryo, Runx1+

cells were localized to the medium DA wall, while in E9 mouse embryo Runx1+ cells were situated in the floor of the DA.

3D reconstruction of the stack of optical sections done for three E9 caudal parts revealed that Runx1 expression is the strongest and specific to the ventral aspect of the DA around the level of the hind limb buds (Figure 15 and Appendix 6). At the same position we detected initiation of DA fusion, Figure 16. Similar to Udan et al. (2014) results, we found that DA fusion is initiated at several sites simultaneously. Remarkably at the same portion of the DA, the dHSC providing the highest level of engraftment was identified. Therefore, we can propose that maturation of pro-HSCs is initiated by events associated with DA fusion. Whether pro-HSCs maturation spreads to other parts of the DA, following aortae fusion is the question that shall be answered in the consequent experiments.

If DA fusion is the necessary step that precludes pro-HSC maturation, what would be the trigger that causes this maturation? Runx1 is already expressed in this portion of the DA and therefore, Runx1 by itself should not serve as this trigger. Runx1 then shall be a permissive factor allowing initiation of pro-HSC maturation. Could it be that factors that stimulate dorsal aorta fusion also trigger pro-HSCs maturation?

Garriock et al., (2010) in studies on chicken dorsal aorta fusion showed that Chordin (*Chrd*, a BMP antagonist) downregulation is necessary to allow DA fusion to occur. Authors demonstrated that *Chrd* expression is spatially and timely downregulated over the regions of the DA before aortae fusion. It is unclear how *Chrd* is downregulated in the notochord. Having in mind widespread BMP expression in early embryos, authors proposed that BMP signalling only primes endothelial cells to receive further positive vasculogenesis signals: vascular endothelial growth factor (VEGF) and Sonic hedgehog (Shh). They found that VEGF and Shh are necessary for DA fusion but could not trigger DA fusion by themselves [Garriock et al.,

2010]. Inhibition of Shh delays DA fusion in chicken and mouse [Garriock et al., 2010; Nagase et al., 2006].

According to prior works, factors listed above also play a role in HSC maturation. Pardanaud and Dieterlen-Lièvre (1999) have shown that VEGF, fibroblast growth factor (bFGF) and transforming growth factor b (TGF-beta1) were able to induce hemangiopoietic (endothelial and hematopoietic) potential in the mesoderm. Bmp4, another positive vasculogenesis factor, was identified to be expressed in the mesenchyme underlying the DA in E10.5-E11 mouse embryos – in the site where pro-HSCs were found to reside [Le Douarin and Dieterlen-Lièvre, 2013; Pimanda et al., 2007; Rybtsov et al., 2011]. Inhibition of *Bmp4* in the AGM explants abolishes development of [Souilhol et al., 2016A and 2016B]. Strikingly, miss-expression of *Bmp4* in midline of DA pre-fusion chick embryos causes precocious aortae fusion [Garriock et al., 2010)].

To summarise, the site of appearance of first detectable pre-HSC in E9 DA coincides with the site where the DA fusion starts. BMP signalling was demonstrated to be implicated in both: DA fusion and in modulation of pre-HSCs maturation. Therefore, in future works on the development of the systems for early HSC maturation, it is necessary to explore effects of BMP signalling on E8 cells maturation. For example, by E8 cells co-culture with stoma lines differentially expressing Bmp4, Shh, and VEGF.

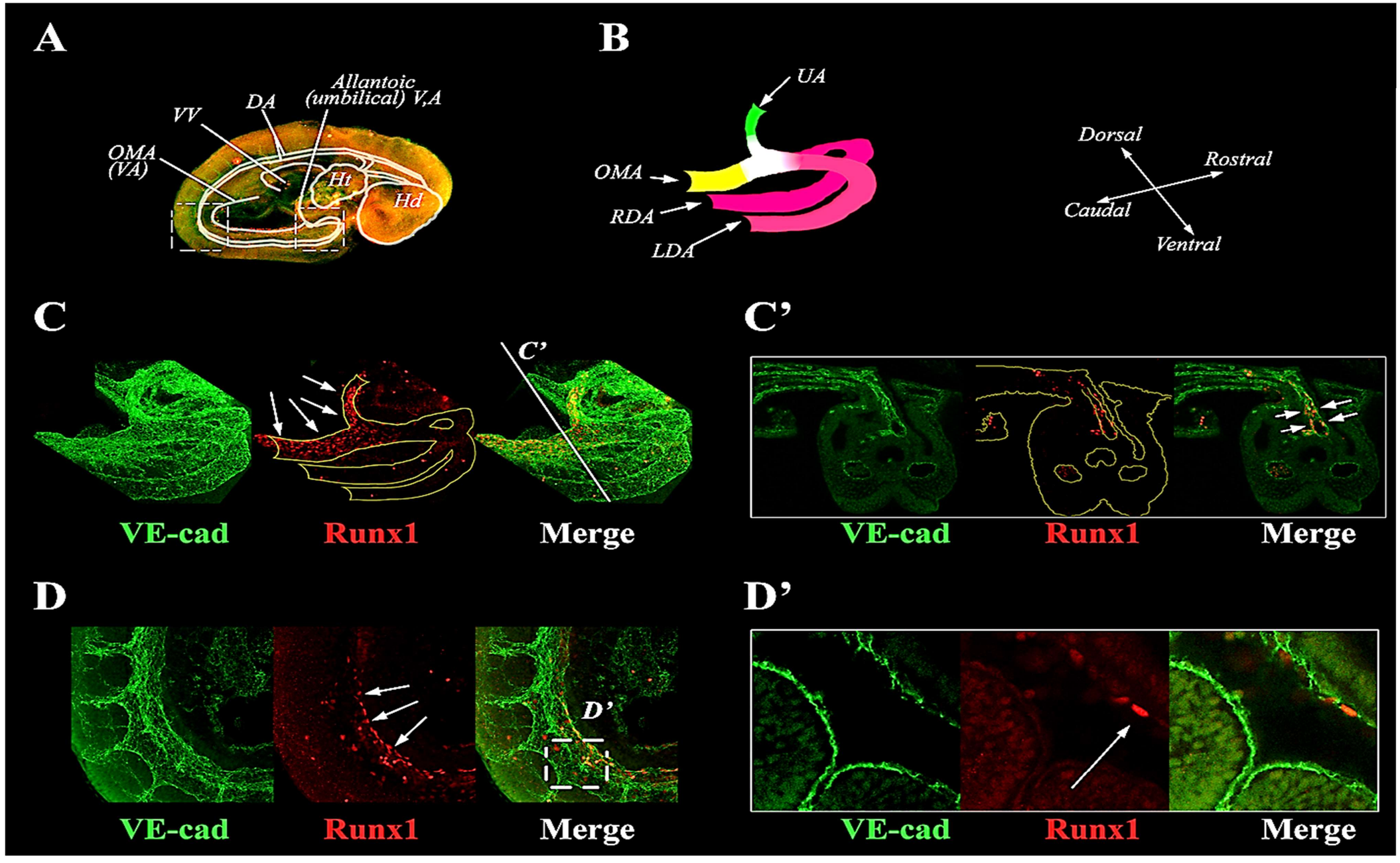

Figure 15. Runx1 is expressed in polarized fashion in E9 caudal vascular network. General view of E9 embryo (A); Structure vascular connection between extra- (OMA, UA) and intro- (DA) vessels (B); Strong Runx1 expression in OMA and UA. C' Inset – crossection of vascular network shown in C (C); Polarized Runx1 expression in E9 DA. D' inset – single optical section of region shown in D (D).

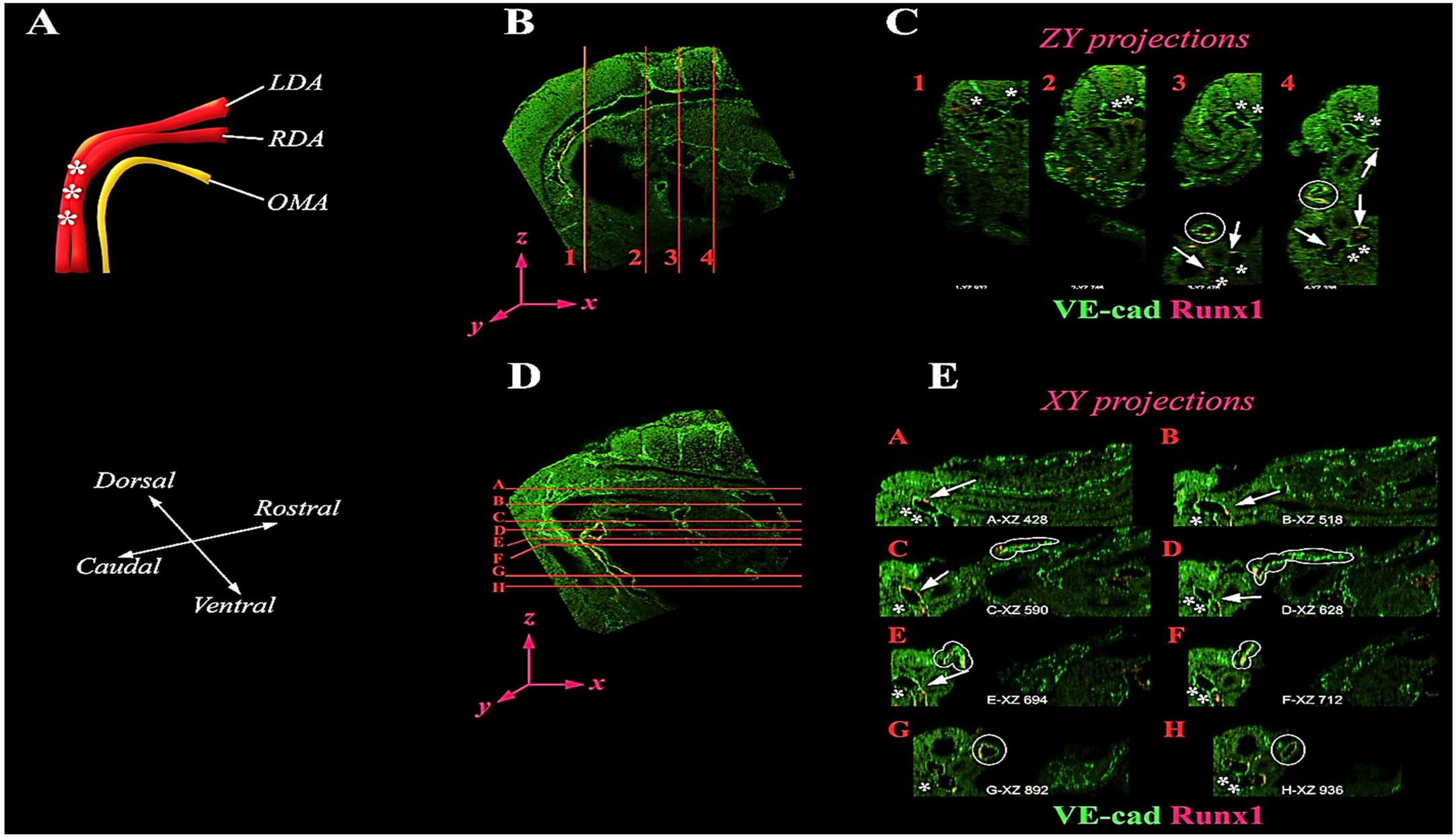

Figure 16. DA region carrying the highest number of pre-HSCs undergoes paired aortae fusion shortly before HSC potential is detected. Superposition of dorsal aortae and OMA in E9 mouse embryo (A); 3D reconstruction of a stack of optical sections done on E9 DA region expressing Runx1 in polarized fashion (B, D); ZY and XY projections of the region of DA shown in B and D (C, E).

3.2.4. Pro-HSC maturation in explants with subsequent co-aggregation with OP9 cells

According to our results, early mouse embryo pro-HSC do not survive in utilised co-aggregate culture. There could be several explanations for that. For example, E8 tissues collagenisation might destroy the niche in which early pro-HSC reside [De La Garza et al., 2016]. The niche disaggregation separates pro-HSC from their cellular environment leaving pro-HSC devoid of stimuli which are necessary for their survival and maturation. A good candidate to be the pro-HSC niche is in the vicinity of the vessel of confluence where we identified clusters of Runx1+ cells (VOC) [Zeigler et al., 2006; Daane et al., 2011]. Therefore, the next pro-HSC maturation method we applied was E8 mouse embryo tissues explant culture.

In the explant culture, small sections of E8 the caudal part (CP) or allantois (AL), yolk sac (YS), head, heart and somites (Ht, Ht or HH and Som) or the region of the vessel of confluence (VOC or CPAL) were cultured as an intact section of tissue. Tissues were cultured as explants on the floating nitrocellulose membranes for five days. After the explants culture, tissues were dissociated and either co-aggregated with OP9 cells or directly injected into mice recipients (Appendix A4 and Appendix A7). To compensate for E8 cells loss, we increased the dose of injected E8 cells to 6-10 ee per recipient.

Analysis of blood chimerism in mice injected with cells after explant culture showed that 6 out of 15 mice (40%) had donor derived cells 6 weeks after transplantation (short term repopulation , STR). 5 out of 15 mice (33%) had donor derived cells in blood flow 3.5 months after transplantation (long term repopulation, LTR). Levels of blood chimerism were low (up to 0.3% of donor derived cells for STR and up to 0.2% in LTR) but above the cut-off level (0.1%). On the cytometry plots, donor cell population was clearly distinguishable from

recipient and carrier cell populations (Appendix A13). Therefore, explants culture is preferable for E8 pro-HSC preservation. Though, this explant culture does not allow to mature E8 pro-HSC –to the state when they fully repopulate the recipient's hematopoietic system.

In 3.5 months after injection, 33% of mice still contained donor derived cells in their blood flow. Not all of these mice had a level of blood chimerism above 0.1% at six weeks after transplantation (STR). In some mice that had blood chimerism above 0.1% in STR, further on number of donor derived cells dropped below 0.1% (the background level).

Recipients peripheral blood was analysed for multilineage cell engraftment (3 recipients transplanted with cells derived from 3-8sp embryos and having blood chimerism above 0.1%). According to our results, the majority of donor derived cells were of T-lymphoid lineage (Appendix A13). In contrast to our observations, Nishikawa et al. (1998) showed that after co-culture with OP9 stromal, cells from E8.5 mouse embryos exhibited myeloid potential. Previously, Fraser et al. (2002) reported that the E8.5 mouse embryo caudal part or yolk sac does not contain myeloid or lymphoid progenitors. It is only E9 embryos or older which contain these progenitors. Prior reports lack consistency as for the E8 cells contribution, yet all reports agree that lymphoid contribution is only observed for intraembryonically (caudal part) derived cells. Since we were able to identify lymphoid progenitors in immunocompetent recipients one day earlier that it was reported before, our explants method (prolonged culture at air-liquid interface in presence of growth factors) is superior to that reported before [Fraser et al., 2002; Matsuoka et al., 2001; Cumano et al., 1996; Nishikawa et al., 1998].

Therefore, E8 pro-HSC for their survival and maintenance require a microenvironment in which they reside. However, this niche does not contain maturation signals required for E8 pro-HSC development. Perhaps these maturation signals are triggered

by blood circulation, heartbeat or DA fusion. OP9 stromal cell line do not provide E8 pro-HSC maturation signals and hence co-aggregation with OP9 does not mature of E8 into pre-HSC.

3.2.5. Pro-HSC maturation in explants at an air-liquid interface

According to our conclusions in the previous part, co-aggregation with OP9 cells does not mature E8 pro-HSC. Instead, low levels of engraftment (0.1-0.3%) are observed in mice injected with cells derived from explant cultures of E8 mouse embryo tissues. Therefore, here in a small-scale experiment we tested whether co-aggregation with OP9 has any effect on donor cell engraftment. For this, we cultured a caudal part with allantois and yolk sac as explants for five days. Resulted explants were collagenized and injected into recipients directly after the culture.

Our results show that co-aggregation with OP9 neither positively nor negatively affects pro-HSC fraction. Pro-HSC are still able to engraft recipients at the threshold level (above 0.1%). However, the donor population is reduced below the level of detection 3.5 months after engraftment. Judging by our flow cytometric analysis of recipients 'peripheral blood, even though the donor cell fraction is very small, it is distinguishable from the recipient and carrier cells fraction, and the number of donor cells is larger than the number of false-positively stained cells (Appendix A15).

We analysed the multilineage composition of donor derived cell population and found out that the majority of donor cells are of T-lymphoid lineage, the same as in a previous E8 culture experiment conducted with OP9 step co-culture. Low numbers of B-lymphoid cells and myeloid cells were detected as well (Appendix A15; Appendix A21)

3.2.6. Pro-HSC maturation in submerged culture

Since pre-cultured at an air-liquid interface, E8 mouse embryo cells did not seem to provide significant levels of recipient mice engraftment, next we used a culture method described in Cumano et al. (2001). In short, we cultured explants in submerged conditions for four days. Cumano et al. (2001) reported that the four days explant culture is the optimal period of time that allows us to maximize the yield of multipotent HSC. The difference between this method and methods of culture that we used before is that the cells inside submerged explants shall be under hypoxic conditions. For example, in prior publications it was shown that in 3D tissue cultures, the concentration of oxygenation is limited in tissue structures thicker than 100-200 [Muschler et al., 2004; Malda et al., 2007; Volkmer et al., 2008]. Hence, all cells localized inside explants deeper than 200 μm will be under hypoxic conditions. We hypothesized that these hypoxic conditions could imitate the microenvironment in which pro-HSC exist before the onset of blood circulation.

All E8 tissue explants (caudal part and allantois - CPAL, yolk sac - YS, Heart – Ht and head - Hd) showed efficient cell proliferation in culture. Extensive outgrowth (adherent cells) were observed around explants except for in the yolk sac (YS) cultures.

Yolk sac explants description. In YS cultures, tissues were increasing in size, but they were rarely attached to the floor of the plate. Usually, tissues formed sphere-like structures, which floated at the top of the culture medium. Inside these structures, patches of red blood cells were appearing in the space of 2-4 days. According to our observations, the YS tissues floating was caused by YS tissues "healing" (re-connecting cut YS tissue) and forming sphere-like structures resembling a YS of reduced size. According to our observations, YS tissues secrete a liquid compound, the density of which is less than that of the culture medium. This is

what makes YS cultures float on the top of culture medium. Therefore, Yolk sac explants were not at hypoxic conditions during culture.

Description of explants of caudal part and allantois. Head and heart explants. In these explant cultures, extensive cells outgrowth was observed around the tissues laying on the bottom of the well. Acidification of the culture medium was also evident from the phenol red colour change. In the caudal part and allantois (CPAL) explants, allantois produced vessel-like structures around which round hematopoietic-like cells appeared in 2-4 days. Previously, similar observations were reported by Matsuoka et al. (2001). Heart explants in two days developed rhythmic contractions.

In total we carried out three transplantation experiments with cells obtained from submerged explants. Mice were transplanted with an increased dose of cells, e.g. each mouse obtained an injection equivalent to ten E8.5 embryo equivalents, Appendix A22. Two later experiments (Appendix A16 and A17) were designed to distinguish maternal (Ly5.2 homo cells) contribution from that of donor embryonic cells (Ly5.1/2 het cells). No maternal contribution was found.

7 out of 54 (13%) of recipients had donor cell contribution above the threshold level (0.1%) in a short term (6 weeks) donor cells engraftment assessment. Two recipients had the highest observed level of contributionin this study: 1.2 and 0.3% of donor cells. These two mice were transplanted with cells obtained from head and heart (HdHt) explants from 6-13sp (established blood circulation) mouse embryos. In 3.5 months after transplantation, the level of blood chimerism in these two mice dropped to 0.3% and 0.13%, correspondingly. When we looked at the components of the donor cell population in these recipients, we found that the mouse with the highest blood chimersim observed in this study (STR blood chimerism - 1.2%) had myeloid and B-cells contribution but did not generate T-cell lineage. Therefore, donor

derived cells were most probably myeloid and lymphoid progenitors, but not genuine HSC. On the other hand, the detailed development of HSC is still not elucidating. Thus, it is possible, that the earliest pro-HSC have restricted hematopoietic potentials and will generate multipotent HSC later in embryonic life. For example, mature HSC are not a uniform population of cells and have different myeloid and lymphoid potentials [Dykstra et al., 2007]. For today, it is unknown where and when this heterogeneity originates in the embryo.

The other recipient (STR blood chimerism - 0.3%) similar to other recipients which showed donor cells blood chimerism 0.1-0.2% had mainly contribution to T cell lineage (88.5%). Therefore, we could propose that the early mouse embryo contains lymphoid progenitors or pro-HSC prone to generate lymphoid cells only. In this work we detected this lymphoid potential one day earlier than it was previously reported and in all studied compartments (yolk sac and embryo proper) [Fraser et al., 2002; Matsuoka et al., 2001; Cumano et al., 1996; Nishikawa et al., 1998]. In contrast to this, when myeloid donor derived cells were detected, the level of recipient engraftment was much higher than in other cases. Nishikawa et al., (1998) reported that contribution to myeloid lineage takes place earlier than to lymphoid lineage, yet detectable at E8.5 embryos. The levels of blood chimersim in peripheral blood using CD45.1 and CD45.2 markers are not reported in prior works [Fraser et al., 2002; Matsuoka et al., 2001; Cumano et al., 1996; Nishikawa et al., 1998]. Therefore, it might be that the recipients with the level of blood chimerism about 0.1% were not considered as having been repopulated and therefore were not studied in detail. If only recipients with higher levels of blood chimerism were studied, E8.5 mouse embryo tissues contribution to lymphoid lineage was missed.

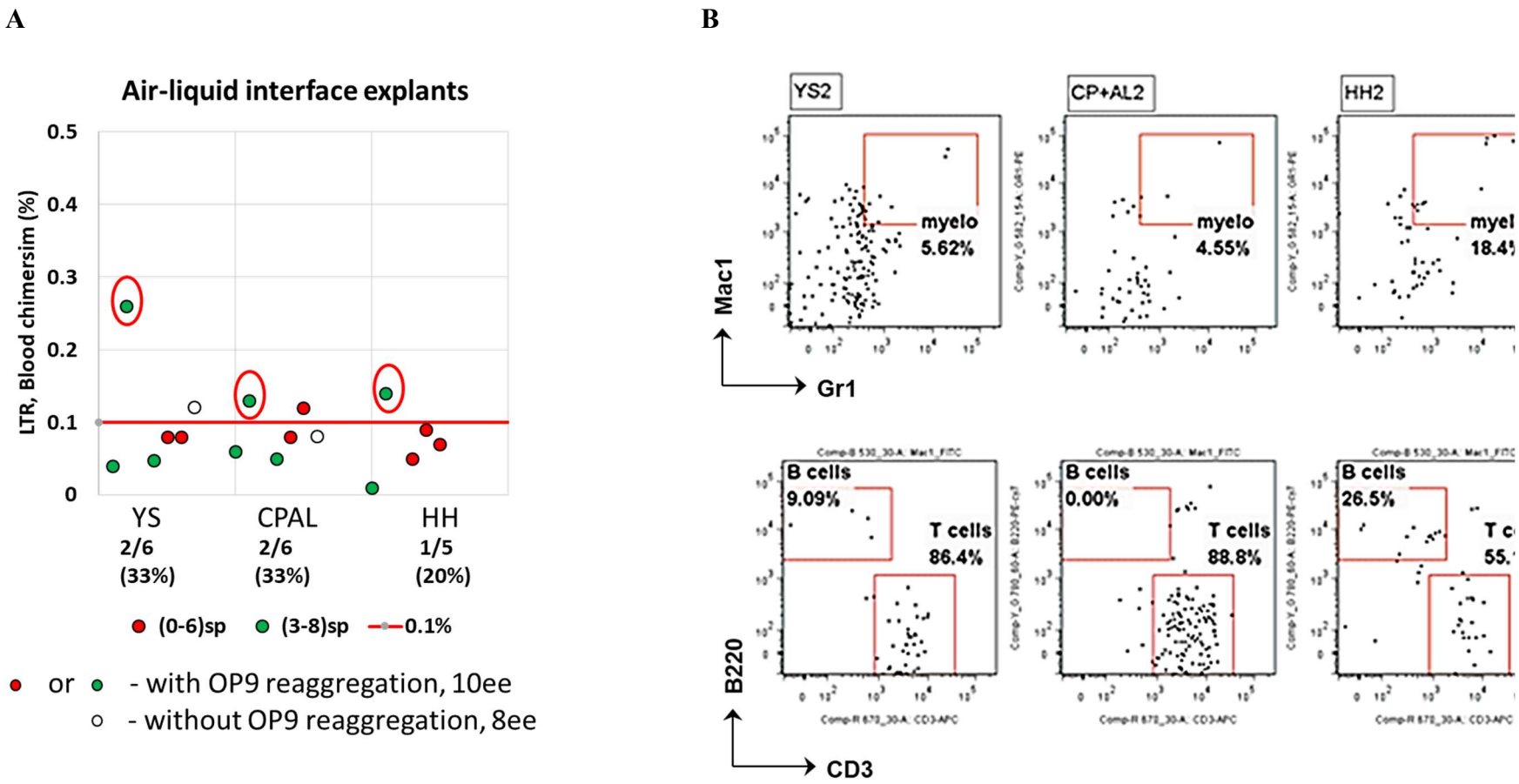

Figure 17. Recipients engraftment with cells derived from early mouse embryo tissues (embryonic day 8) after tissues culture as explants at air-liquid interface. Levels of donor cells blood chimerism (A); Multilineage engraftment (B). In circles – recipients whose blood was analysed for lymphoid and myeloid cells contribution. YS- yolk ac; CPAL – caudal part and allantois; HH – head and heart; sp – somite pairs; LTR – long term repopulation.

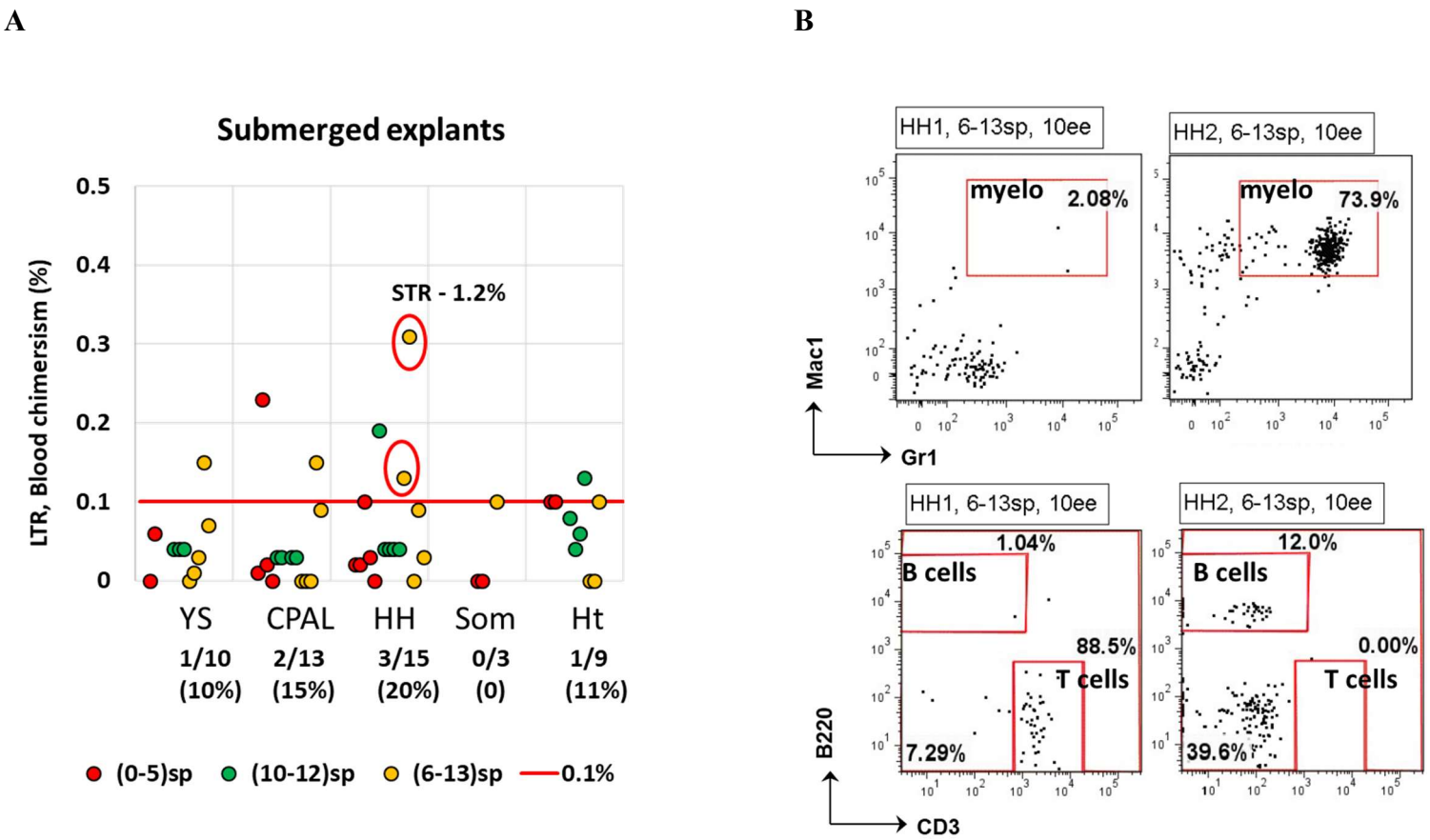

Figure 18. Recipients engraftement with cells derived from early mouse embryo tissues (embryonic day 8) after tissues culture as submerged explants. Levels of donor cells blood chimerism (A); Multilineage engraftment (B). In circles – recipients whose blood was analysed for lymphoid and myeloid cells contribution. YS- yolk ac; CPAL – caudal part and allantois; HH – head and heart; sp – somite pairs; LTR – long term repopulation.

3.2.7. Conclusions

Runx1 mapping described in Chapter 3.1. shows that early somitic embryos (E8) contain Runx1+ cell clusters in the nascent omphalomesenteric artery (OMA) and allantois. Similar clusters of cells were found in E9-E10 embryos and were proposed to possess hematopoietic potential [Wood et al., 1997; Zovein et al., 2010]. Around E8 upregulation of Runx1 expression takes place in the dorsal aorta (DA) endothelium, which indicates the beginning of pro-HSC maturation [Lam et al., 2010; Swiers et al., 2010; Chen et al., 2011; Samokhvalov et al., 2014]. Having in our hands the new powerful method of pre-HSC maturation in co-aggregates, we endeavoured to attempt to reveal the potential of early pro-HSC contained in E8 mouse embryo tissues.

In this chapter, we discussed results of transplantation experiments carried out with cells derived from early mouse embryo tissues (embryonic day 8-9, E8-9, 0-26 somite pairs). Mouse tissues were preconditioned in a set of culture systems ranging from co-aggregation with OP9 or E9-10 AGM stroma cells to tissue explants.

The most efficient culture condition to detect hematopoietic potential of E8 embryo tissues was proved to be the explants submerged culture (Table 5). The percentage of donor derived cells in recipients' blood flow was low (0.1%-1.2%), but donor derived cells formed a clearly distinguishable population on flow cytometry plots. Here using mice engrafted with carrier cells and/or stromal cells only we established the cut-out level of blood chimerism above which the recipient reconstitution can be considered to be the valid one. This allowed us to study engraftment of donor cells at the very low level (above 0.1% of blood chimerism).

According to our data, after culture, cells derived from explants demonstrate limited lymphoid and myeloid potentials. In all but one reconstituted recipient, engrafted cells produced mainly T-cells and limited numbers of B- and myeloid cells. Interestingly, in the only case when donor cells produced substantial number of myeloid cells, the overall level of repopulation was an average tenfold higher than the observed level of blood chimerism (1.2% versus 0.1-0.3%). In this case, in contrast to all other reconstituted recipients, T-cells were absent in the recipient's peripheral blood. Some previous works reported the appearance of myeloid cells prior to lymphoid ones. At E8.5 lymphoid potential was found to be restricted to the embryo proper tissues [Fraser et al., 2002; Matsuoka et al., 2001; Cumano et al., 1996; Nishikawa et al., 1998]. Yet, from the prior reports it is unclear what percentage of donor derived CD45+ leukocytes were the reconstitution threshold level. Therefore, it is possible that recipients showing low levels of reconstitution (around 0.1% of blood chimerism) were previously not studied in detail and therefore the hematopoietic potential of cells derived from early E8 mouse embryos was missed. Using our criteria of recipient reconstitution allowed us to detect engraftable hematopoietic cells one day earlier than it was demonstrated before. Yet, this hematopoietic potential was limited – low levels of donor derived cells contributing mainly to the T-lymphoid lineage. According to the hematopoietic stem cell definition – HSC is a cell able to fully reconstitute recipient's hematopoietic system to the high level [Urso and Congdo, 1957; Till and McCulloch, 1961; Becker et al., 1963; Seita and Weissman, 2010]. Our culture conditions failed to mature E8 pro-HSC into mature HSC. Whether this is because we detected early hematopoietic progenitors or HSC, requires further investigation. For example, to prove HSC nature of identified hematopoietic progenitors, it might be necessary to conduct secondary transplantation experiments (e.g., donor cells isolated from primary hosts re-transplanted into secondary recipients).

Table 5. Efficiency of pro-HSC maturation culture methods used for E8 tissues

	Culture Step 1	Culture Step 2	STR (>0.1%)	LTR (>0.1%)
Culture at air-liquid interface	E8 cells co-aggregated with E9 stroma	Cells from Step 1 co-aggregated with E10 stroma	0/3	N/A
	E8 cells co-aggregated with E9 stroma	Cells from Step 1 co-aggregated with OP9 cells	0/3	N/A
	E8 explants culture	Cells from Step 1 co-aggregated with OP9 cells	6/15	5/15
	E8 explants culture	N/A	1/1	0/1
Submerged culture	E8 explants culture	N/A	6*/34	6/34

None of the applied methods were efficient enough to trigger complete E8 pro-HSC maturation. Cells, assumed to be AGM stoma cells (CD45-CD43-CD41-Ter119-), derived from caudal parts of E9 and E10 mouse embryos did not stimulate E8 pro-HSC maturation. Yet, these cells in co-culture with E10 stroma cells produced low level repopulating HSC and co-culture with OP9 induced derivation of potent HSC. Hence, (1) the E9 mouse embryo

already contains almost mature pre-HSC; (2) E9 and E10 tissues do not contain factors that induce pro- and pre-HSC maturation; (3) OP9 stroma cell line induce HSC maturation and expansion of pre-HSC contained in E9 mouse embryos.

Subaortic tissues of E9 and E10 mouse embryos contain pre-HSC precursors. For instance, cells isolated from the AGM region of E9 and E10 mouse embryos and depleted from CD41, CD45, CD43 and Ter119 positive cells after a culture step were able to engraft onto irradiate recipients. This could be explained by retaining in this cell suspension VE-Cad positive $CD41^{low}$ (endothelial) cells. Rybtsov et al. (2014) have demonstrated that pre-HSC are primed by low expression of CD41. In agreement with Rybtsov et al. (2014), pro-HSC in 22-26 sp (E9) embryos have only low repopulating potential, which is comparable to E8 repopulating potential. It is still unclear why earlier E8 pro-HSC cannot be matured in culture systems. In our experiments, we show that a fraction of E8 cells when co-cultured with other cells rapidly disappear. In contrast, E9 cells have superior proliferation and survival potential to E8 cells. Therefore, one of the possibilities could be that the E8 cells have blocked proliferation and in culture are outcompeted by faster proliferating E9 cells. To elucidate what could be the trigger inducting E8 pro-HSC proliferation, we investigated the events that take place in AGM of 21-29 sp mouse embryos.

In early E9 mouse embryos, intensive vessels remodelling in caudal parts takes place [Walls at al., 2008; Garcia-Porrero et al., 1998; Zovein et al., 2010]. For instance, the midline of the DA extends from mid-trunk caudally into the proximal part of the tail region. With the application of optical projection tomography, Walls et al. (2008) have demonstrated that by 26 sp diameter of ompalomesenteric artery (also called vitelline artery, VA) becomes much smaller than that of the umbilical artery. The authors suggested the blood flow shifts towards the feto-maternal interface at this time point.

At the beginning of E9, the vitelline artery is initially connected to the umbilical arteries. By 22 sp the vitelline artery (VA) establishes a new connection with the DA [Garcia-Porrero et al., 1998]. Soon after the VA disconnects from the umbilical artery, large clusters of CD31+VE-Cad+ cells appear in the ompalomesenteric artery (OMA) [Zovein et al., 2010]. These events coincide with the appearance of dHSC precursors in the E9 embryo [Rybtsov et al., 2014]. We envision that the clusters we identified in early somitic embryos (E8) are the predecessors of those described by others in E9 and E10 embryos [Wood et al., 1997; Zovein et al., 2010].

When we examined early E9 embryos, we found that the Runx1 expression pattern is not essentially changing when embryo develops from E8 to early E9 embryos. Intensive Runx1 expression is observed around the vessel of confluence (VOC). VOC is the point of amalgamation of the omphalomesenteric artery (OMA), umbilical artery and dorsal aorta [Zeigler et al., 2006; Daane et al., 2011]. Runx1 expression in the dorsal aorta (DA) is polarized. Runx1 is specifically expressed in the section of DA adjacent to the VOC. We also found that the area reported by Rybtsov et al. (2014) to bear the pre-HSC in fact is the site where paired aortae first fuse. According to our data, the aortae fusion takes place immediately before transplantable HSC cells appear in the embryo.

Garriock et al. (2010) reported that BMP antagonist (chordin) downregulation is required for DA fusion. Overexpression of Bmp4 triggers precocious DA fusion, while Shh and VEGF inhibition delays the fusion. Therefore, we envision an intimate connection between DA fusion events and induction of pro-HSC maturation. Hence, future studies in the direction of development of pro-HSC maturation systems shall also involve cultures treatment with BMP signalling mediators. For instance, Bmp4-expressing stromal cell lines could be utilized. Most probably, such pro-HSC maturation would require a fine tuning of multiple mediators, which could be achieved by intermixing various stromal cell lines expressing different mediators.

3.3. Tracing DA progenitors in early chick embryo

3.3.1. Experimental approach

Since existing to date methods of pre-HSC maturation are not applicable to mature the earliest precursors of HSC (pro-HSC), another approach had to be developed to clarify the ontogeny of embryonic HSC.

Today it is broadly accepted that first HSC arise in the aorta-gonad mesonephros region (AGM) [Medvinsky et al. 1993; Muller et al., 1994; Medvinsky and Dzierzak, 1996; de Bruijn et al., 2000]. Specifically, appearance of transplantable HSC coincides with the appearance of so-called inta-aortic clusters (IAC) [Babovic and Eaves, 2014; Bhatia 2007; Boisset et al., 2010, 2011; Bollerot et al., 2005; de Bruijin et al., 2002; Bertrand et al., 2010]. These clusters can be found in the floor of the mouse embryo's dorsal aorta starting from embryonic day 10.5 (E10.5) [Taoudi and Medvinsky, 2007; Rybtsov et al., 2011]. Similarly, in chick embryos, clusters of Runx1+ cells appear in the dorsal aorta (DA) floor around embryonic day 3 (ED3) [Jaffredo et al., 1998, 2005; Zovein et al., 2008; Boisset et al., 2010; Bertrand et al., 2010; Kissa and Herbomel, 2010; Swiers et al., 2010]. Therefore, one of the methods to trace ontogeny of HSC would be to label the DA and IAC and to trace their progeny in adult animals. Since transgenic mouse models that allow exclusive DA labelling are not developed yet, a method of surgical labelling of the DA, for example by grafting, would suffice this aim. The chick embryo is a robust animal model allowing various surgical manipulations and capable of surviving into adulthood afterwards [Stern, 2004]. Therefore, we have selected chicken embryo as a model for labelling the DA. Our first task was to identify an area that gives rise to DA progenitors.

Prior data suggest that the DA is formed by lateral plate mesoderm descendants. According to Stern, lateral plate mesoderm (LPM) arises from the middle-primitive streak (mid-PS) [Stern and Psychoyos, 1996]. Yet, as for today no studies were conducted to identify the exact primitive streak (PS) position and stage at which the LPM generates DA precursors. Therefore, our task here became to identify a PS area generating DA portion that bears IAC. To fulfil our goal, we labelled PS with lipophilic dyes and by grafting labelled PS regions (sections of GFP+ PS extracted from stage-matched GFP+ chick embryo donors). We also established a chick embryo culture facility at Scottish Centre for Regenerative Medicine (SCRM) and worked out conditions allowing us to culture generated chimeras in vitro for 3 days.

All chimeras and donors were photographed at several time points: at the time of grafting and at least once a day for the next 3 days. For the timed observations, chimeras were photographed every 3 hours. First, chimeras were scored for DA contribution under stereomicroscope in culture on day two (so-called “early chick embryo culture”, EC day 2). This method of scoring was verified with the whole mount anti-GFP stained chimera under confocal microscope. Chimeras were collected and preserved at EC day 2-3 (chimeras showing signs of deterioration were terminated at EC day 2). Some chimeras were examined as whole mounts under confocal microscope. Other chimeras were cryosectioned and processed to reveal GFP staining with anti-GFP alkaline phosphatase or combined immuno-fluorescent method to examine GFP, Runx1 and CD45 expression in chimera’s tissues. Generalized conclusions as for DA contribution presented below were drawn on pooled data for stereomicroscopic chimeras observation at EC day 2. Conclusions as for contribution to other tissues and contribution to DA lining and intra-aortic clusters (IAC) were made on the data obtained with immuno-staining on cryosections.

3.3.2. Defining early aortae landmarks for scoring contribution to the dorsal aorta

To enable scoring grafts contribution to the dorsal aorta (DA) we had to decide on a set of landmarks that would enable DA identification in transparent pre-circulation chick embryos. For this we initially looked at *in ovo* cultured chick embryos with initiated blood circulation (48-50h embryos). Embryos were extracted and prepared as they would be observed in early chick culture (EC), i.e. oriented ventral side up (Figure 19., A). In a 48h old chick embryo the dorsal aorta is situated directly above the somites. It is represented by two transparent aortae (Figure 19. B and C). When the DA is filled with blood cells, its identification does not present difficulties. However, when the DA is devoid of blood, it might be difficult to spot an aorta. In this case, we found it helpful to identify the DA wall that faces the embryo midline (Figure 20., C). This wall appears to be built from a single layer of spindle-like angioblasts. Due to these cells' elongated shape and refraction properties, they form a distinct feature that allows the DA identification from the very beginning of its formation (happens at Hamburger and Hamilton stage of chick embryo development 9, or HH9) [Hamburger and Hamilton, 1992].

To guide us on the margins of the DA, we injected a blue fluorescent dye (extracted from a common highlighter, according to Takase et al., 2013) into the vascular system of 50h old chick embryos. Embryo examination showed that caudally to the vitelline vessels (VV), the DA is not formed yet. It is represented by the interrupted line of spindle-like cells (angioblasts) rostrally to the VV. Laterally, the DA wall is not continuous. It is merged with area pellucida vessels in multiple sites. Similarly, in younger embryos, forming DA also can be identified by its facing embryo midline wall (lateral DA wall virtually does not exist). The DA is intimately merged with the area pellucida (AP) vasculature and so, to the yolk sac. As the embryo develops beyond E3 (70h), the aortae fuse and get gradually surrounded by lateral

body folds becoming totally encircled by the embryo body around HH20 (72h). From this point it is impossible to tell the contribution to DA without sectioning off the embryo (Figure 21.). As our final goal is to culture chimers till hatching, non-invasive methods of validation contribution to DA are preferable. We have selected EC day 2 to be the time point when initial scoring of grafts contribution to DA is carried out.

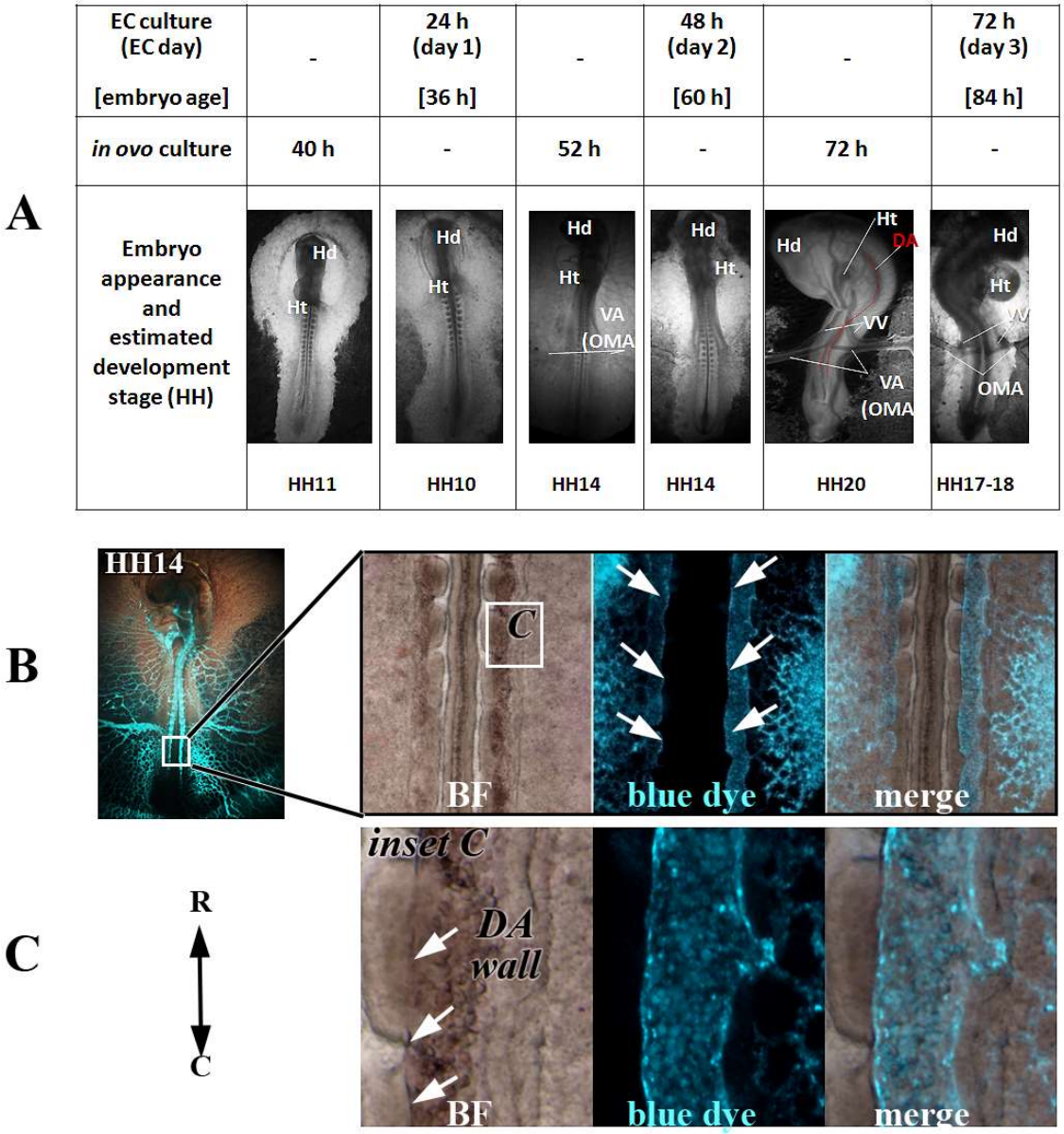

Figure 19. Distinguishing dorsal aorta in chick embryos and embryo development in culture. Chick embryo appearance in *in ovo* and in EC culture (A). 50h in ovo cultured chick embryo injected with a blue fluorescent dye (according to Takase et al., 2013). Dorsal aorta identification is possible when focusing on the cord of angioblasts next to the embryo midline (white arrows) (B-C).

3.3.3. Embryo survival and development in early chick embryo culture

EC chick embryo development is similar to that observed for *in ovo* cultured embryos (Table 6.).

At EC day 1 the embryo reaches HH stage 10-11. The number of somites increases totalling on average 10 sp. At the end of EC day 2, heartbeat starts. Heartbeat initiation correlates with embryo survival in the culture at day 1 (93.8±13%), Table 6. No lag in development of cultured embryos is apparent at EC day 1.

At EC day 2, the number of somites continue to increase reaching at the end of EC day two twenty-five somites on average. In the *in ovo* cultured embryos, the number of somites would reach 30; therefore, at EC day 2 embryos start to show signs of lagging development. Visually EC cultured embryos are smaller, but otherwise they are comparable to those cultured *in ovo* (Figure 19., A). At EC day 2, area pellucida vasculature expands and connects intra- and extra-embryonic circulation loops; the DA matures, and blood circulation is initiated. Visually, blood circulation rate is slower in EC embryos; however, it is hard to address this question as upon examination of EC embryos, they are exposed to a lowered temperature (which drops from 38 to 22 ^{o}C during embryo examination). Temperature drop slows down blood circulation. Blood circulation is re-established when the embryo is returned to the incubator. EC embryos look paler than *in ovo* cultured ones; yet, blood cells are present in their circulation. Visually the amount of blood cells in EC cultured embryos is lower than that in *in ovo* cultured ones.

We have established that the absence of blood circulation is a sure sign of embryo deterioration at day 3. Embryo decomposition happens on a rapid scale in EC culture, leading in some instances to the complete loss of the embryo within 24 hours. Therefore, all embryos

exhibiting poor development at EC day 2 were terminated and preserved for further examination.

Contribution to the DA becomes evident at EC day 2. Further on, the DA is encircled by the embryo body, and non-invasive examination of the DA becomes impossible. Therefore, initial scoring of the contribution to DA was done at EC day 2. Further below we show that this scoring corresponds well to GFP+ cells contribution to the DA, which was revealed on sections or with whole mount confocal microscopy (Figure 25.). The only discrepancy between scoring at EC day 2 and at EC day 3 on sections was observed for grafts that contributed to the caudal portion of the DA. In these embryos, contribution to the DA is not yet evident. Contribution to the caudal DA takes place at the end of EC day 3. Here, we need to notice that the contribution to caudal DA is not of main interest in this work, as caudal DA does not bear IAC.

EC day 3 was the last day of an embryo in EC culture. Less than 10% of embryos survived into day 4 in *in vitro* conditions. For our purposes, embryo culture beyond day 3 was not required. First, we were looking at the contribution to DA anterior to omphalomesenteric artery (OMA). This kind of contribution is evident at EC day 2. Second, we were looking for IAC production by cultured embryos. *In ovo*, IAC are formed starting from HH19 and peak at HH21 (84h). At EC day 3, the total embryo age in hours is 84, which corresponds to the age when the maximum number of IAC could be observed. Therefore, at the end of EC day 3 embryos were collected and preserved for further examination.

Lagging of embryo development in EC culture becomes evident at EC day 3. The embryo head is underdeveloped, the heart is extended, blood circulation is slowed or interrupted, and the embryos are pale. Yet, the number of somites increases, reaching 35-40, showing about two stages lag in development in comparison to *in ovo* cultured embryos (Figure

19.). We have identified that the critical factor in embryo survival in EC culture is the freshness of the used eggs. E.g., eggs used for EC culture started at HH3-4 shall be laid at the day of the experiment. Otherwise, the embryos deterioration becomes evident starting from EC day 2 and embryos survival till day 3 becomes impossible.

Table 6. Grafted chick embryo survival and development in early chick embryo culture (EC) versus *in ovo* intact embryo culture

EC day	% embryo survival ± SD (4 experiments, 49 chimeras)	Embryo stage at grafting		
		HH4	HH5	HH6
		Observed in EC (expected *in ovo*) stage of embryo development, HH		
1	93.8 ± 12.5	HH9-10 (HH10)	HH9-10 (HH10)	HH10 (HH11)
2	82.8 ± 19.8	HH12-16 (HH17)	HH15-16 (HH17)	HH16 (HH18-19)
3	61.8 ± 15.1	HH18-19 (HH23)	HH 18-19 (HH23)	n/a (HH23)

3.3.4. Labelling by injection with lipophilic dyes is not efficient method to trace mesodermal progenitors of dorsal aorta

Initially, we attempted to trace mesodermal progenitors of the dorsal aorta (DA) with primitive streak (PS) labelling done with lipophilic dyes (DiI and DiO) by injection. This method was widely utilized before for mapping the chick embryo primitive streak [Psychoyos and Stern, 1996; Sweetman et al., 2008; Limura et al. 2007; Sawada and Aoyama et al., 1999]. For this, HH4-10 embryos were injected with dyes in the groove of PS, trying to label only a limited number of cells.

With lipophilic dyes injections, we found that it was hard to achieve visual DA labelling. For example, from 27 labelled embryos, only 3 exhibited limited labelling of the DA wall: one, labelled at HH5 at 62% of PS length, and two embryos labelled at HH6 in PS positions 57 and 61% (Figure 20.). In these embryos, contribution to the DA was presented only by a short stretch of cells in the DA wall. Even though we were able to see extensive dyes contribution to lateral plate mesoderm, contribution to the DA was not evident. This finding contradicted our expectations built on previously published results for PS mapping [Psychoyos and Stern, 1996]. For instance, the lateral plate mesoderm that gives rise to the DA is derived from the middle region of HH3-6 PS, and therefore DA labelling shall be evident with HH3-6 PS labelling at positions from 40% to 60%. On the other hand, to date there are no works published showing dyes contribution to DA. For us that indicated inherent unsuitability of dyes labelling method to trace cells contribution to such structures as the DA. In addition, due to the need to wash out dyes residues after injection, embryo survival dropped, so that the embryos rarely developed beyond EC day 2, making assessment of dye contribution to intra-aortic clusters (IAC) impossible.

After we performed PS labelling by grafting, it has become clear why DA labelling with dyes was problematic. As we observed (Figure 20.), cells forming the DA migrate from the bulk of lateral plate mesoderm cells. At every stage of gastrulation, the PS produces the bulk of the lateral plate mesoderm (LPM) cells that migrate laterally and anteriorly, and then limited numbers of LPM cells migrate medially to contribute to the DA. The rest of LPM cells stay at lateral positions and later on contribute to the area pellucida vasculature or lateral body wall. Therefore, limiting the number of labelled PS cells in turn limits the number of labelled DA. It would require further investigation whether LPM cells that contribute to DA are random LPM cells, or these cells are pre-fated to become DA cells. Answering this question would help to label the DA more precisely, avoiding co-labelling of LPM. To sum up, cells that contribute to the DA are intermixed with the rest of LPM cells, and exclusive DA labelling is not possible by labelling the pull of LPM cells. In other words, at present DA labelling is not possible without co-labelling of LPM. For DA sufficient DA labelling, numbers of labelled in PS cells have to be increased. This is possible to achieve by PS grafting.

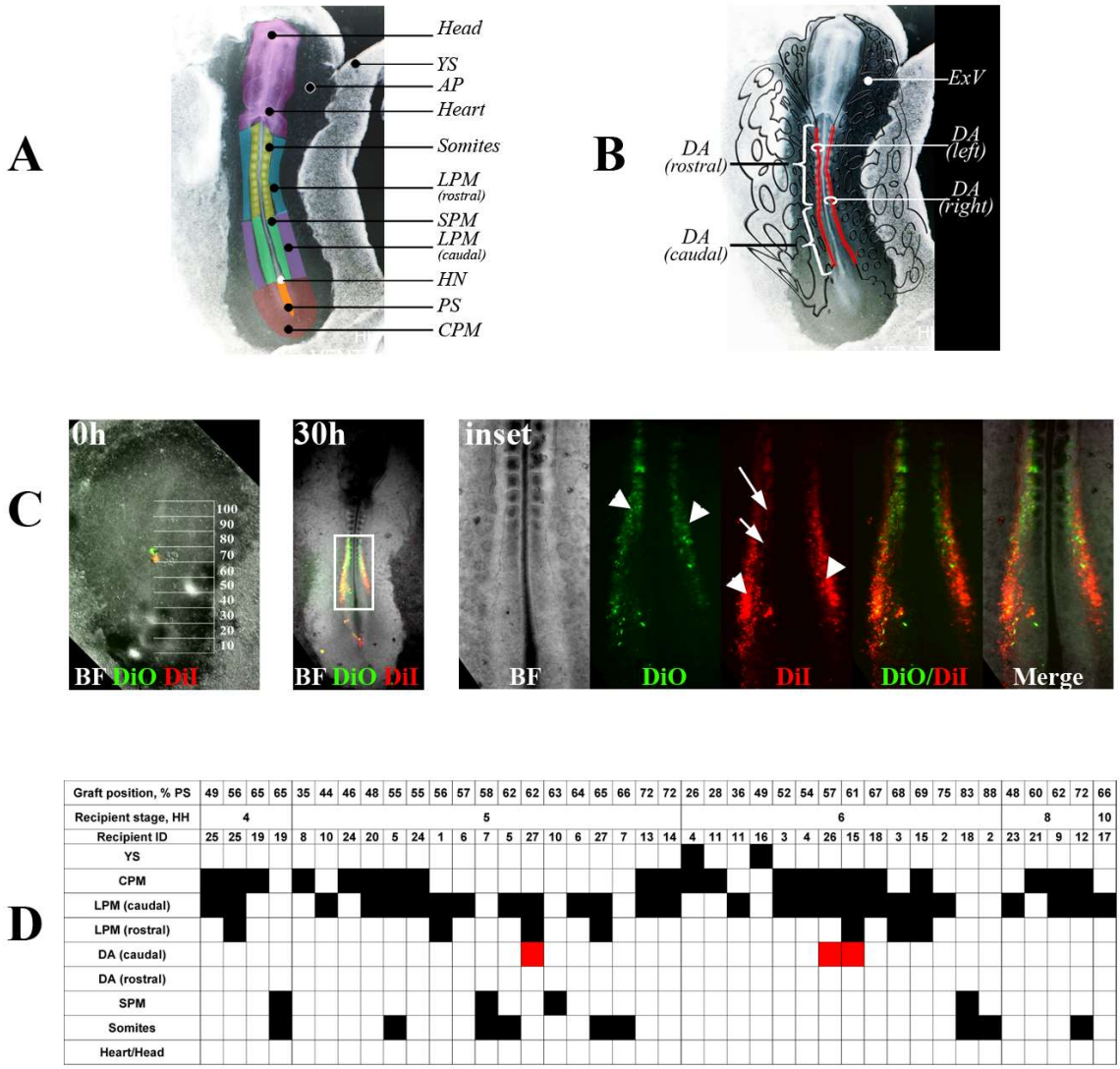

Figure 20. Labelling by lipophilic dyes injection is not efficient method to trace mesodermal progenitors of DA. EC day 2 chick embryo overlaid with the scheme of tissues to which dyes contribution was scored (A); EC day 2 chick embryo overlaid with scheme showing localization of extra-embryonic vasculature (ExV) and dorsal aorta (DA). DA is split in caudal and rostral parts (B); Example of an embryo showing contribution to DA. HH5 chick embryo was injected with DiI at approximately 62% of PS length. In 30h in EC culture, contribution to DA became evident. DiI+ cells formed midline facing DA wall (white arrows). Cells labelled with DiO at approximately 68% of PS length contributed mainly to pre-somitic mesoderm and somites (white arrowheads) (C); Summary of contribution to embryonic tissues shown in (A), revealed by PS labelling at HH4-10 (D).

3.3.5. Tracing dorsal aorta progenitors with primitive streak grafting

3.3.5.1. Primitive streak grafting is an efficient method of dorsal aorta labelling

When the chicken embryo primitive streak (PS) was isotopically grafted with tissues derived from PS of a GFP+ stage matched embryo, clear DA labelling was achieved (Figure 21.). As it was shown with dyes labelling, first GFP+ graft cells migrated to form the lateral plate mesoderm, and then to contribute to the DA or area pellucida vessels. In contrast to dyes labelling, enough cells were labelled with grafting procedure that allowed illuminating the entire dorsal aorta wall.

At "early chick embryo culture" (EC) day one grafted cells migrate anteriorly and laterally contributing to LPM. At EC day 2 GFP+ lateral plate mesoderm (LPM) cells start to migrate towards the chimera's midline to contribute to the DA or laterally – to contribute to area pellucida vessels (Figure 21., A). Though, the majority of cells stay in LPM. Together with enhancement of DA visualization, we increased visualization of the area pellucida vasculature, which is also derived from the same portion of the LPM that contributes to the DA. At EC day 3 the embryo grows and elongates. Because of this, visually the GFP+ region of the DA moves to the anterior. Yet, in fact GFP+ DA position stays unaffected. This can be verified, if DA contribution is reported in relevance to the level of somites, next to which DA contribution is recorded.

Reconstruction of confocal optical sections recorded with EC day 3 whole mount chimeras showed contribution to the DA, which agrees with scoring results obtained under stereomicroscope for these chimeras at EC day 2. Confocal microscopy and cryosections analysis revealed that GFP+ cells also contributed to: dorsal mesentery, peri-neural vascular plexus, somatic and splanchnic lateral plate mesoderm, and vessels of area pellucida (Figure 21. and 3.3.17.).

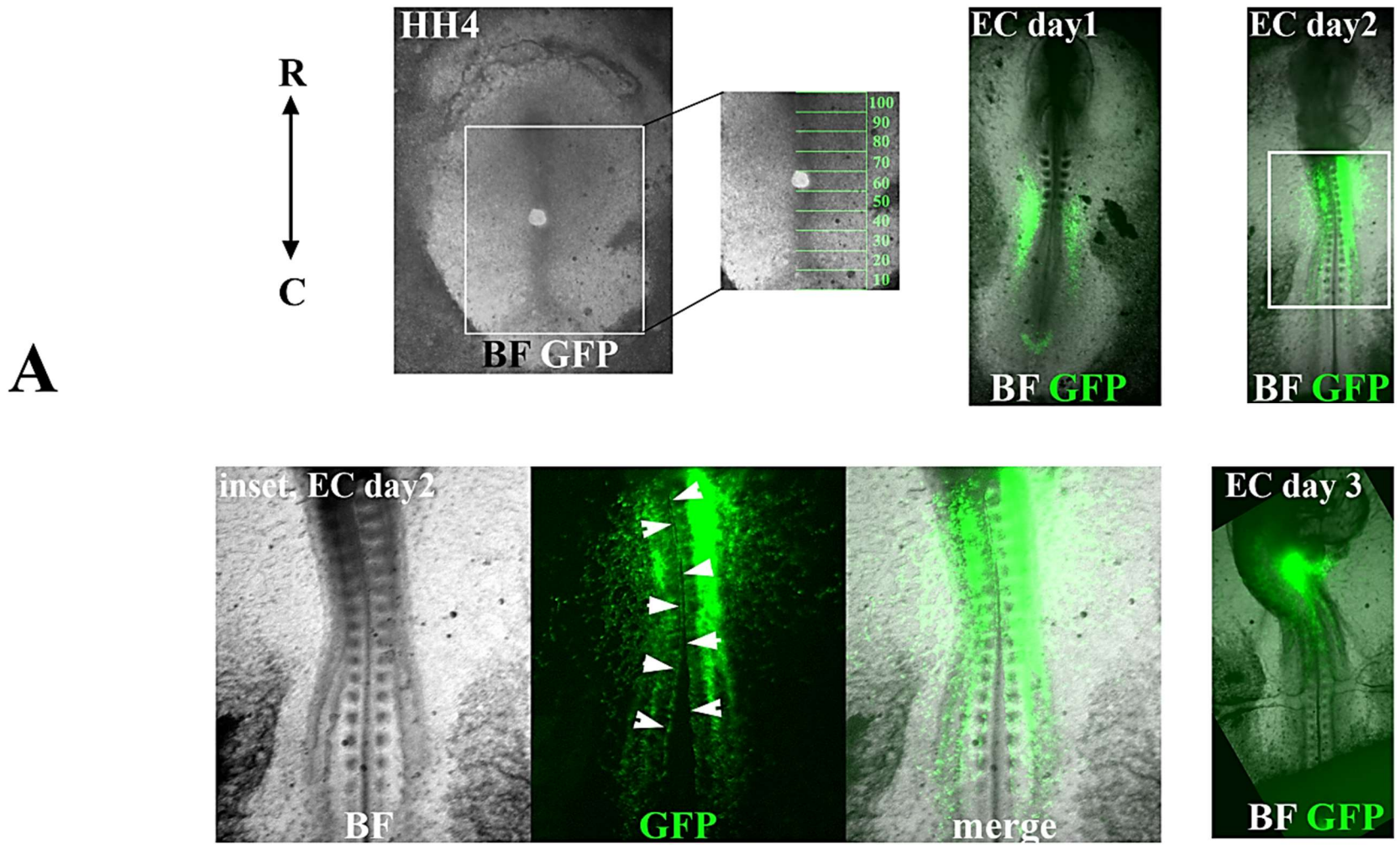

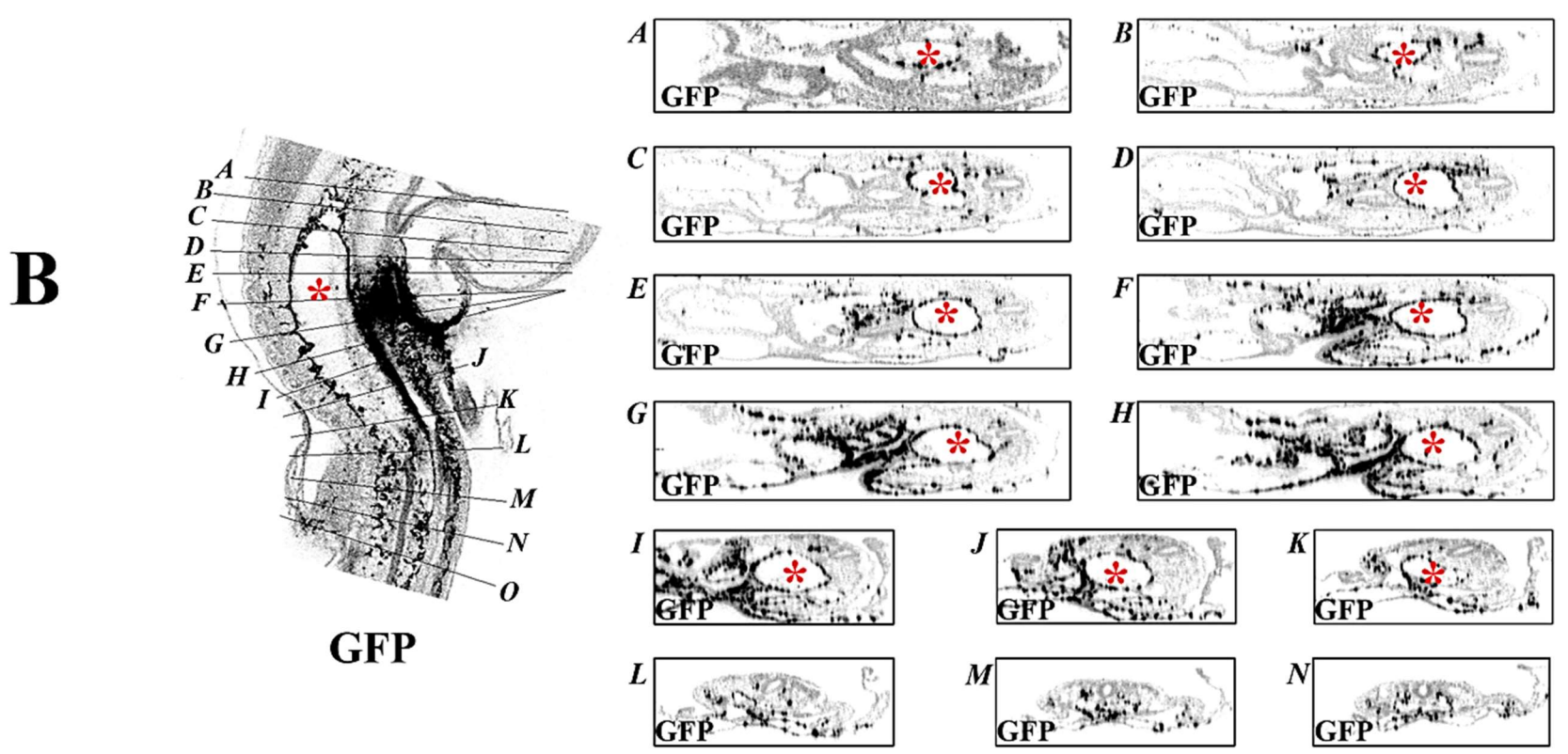

Figure. 21. Primitive streak labelling with GFP+ grafts allows to visualize dorsal aorta. HH4 chick embryo isotopically grafted into approximately 55% of PS length. During EC day1, GFP+ grafts cells migrate laterally and to the anterior, contributing to LPM. At EC day 2, LPM cells contribute to DA and area pellucida vasculature (A); Close up of DA in EC day 2 chick embryo. Contribution to DA wall cells is shown with white arrowheads. At EC day 3, grafts become surrounded by lateral body wall, and scoring contribution to DA becomes impossible. Optical sections reconstruction of the chimera are shown in (A-B). Dorsal aorta is labelled with red star. GFP+ cells are shown in black. GFP+ cells contribute to DA lining (*A-N*), dorsal mesentery (*F-J*), lateral plate mesoderm (*I-K*) and area opaca vasculature (B).

Full 3D visualization of scanned chimeras does not give clear representation due to wide-spread LPM labelling, which obscures the DA. The best visualization results were achieved by optical two plane reconstruction (e.g. XY or YZ or XZ planes). Therefore, for future, we utilized cryosectioning as a way to explore the labelled DA area.

3.3.5.2. In early chick embryo 30-70% region of primitive streak contributes to dorsal aorta

HH3-HH7 chicken embryos were grafted at various positions in the primitive streak (PS) (from 10 to 90% of its length), Appendix A7. As described above, contribution to the DA was scored at EC day 2. From 111 analysed embryos, 35 were excluded due to stage or position mismatch. The rest (76) were analysed for contribution to the following tissues: DA, lateral plate or intermediate plate mesoderm; area pellucida and area opaca vasculature; somites and pre-somitic mesoderm; head and heart region (Figure 22.).

In HH3-4, grafts also intensively labelled extra-embryonic vasculature (area pellucida and yolk sac vasculature). PS region that did not contribute to the yolk sac (60-70%) still contributed to AP vessels (Figure 22.). the Area pellucida gives rise to both extra- and intra-emryembryonic vasculature. In addition, as we will show later, the area pellucida might be implicated in blood cell generation that would complicate interpretation of grafts contribution to haematopoiesis. For our purposes, we had to identify the PS region that does not contribute to pre-aortic haematopoiesis (extra-embryonic haematopoiesis). For instance, 50-60% of HH5 PS region do not contribute significantly to area pellucida vasculature. The only detail to verify would be to check whether this PS region gives rise to IACs.

According to our observations, long stretch of PS (30-70% of its length) contributes to the DA: at HH3-5 – from 30 to 70% of PS length, and at HH 6-8 – from 30 to 60 % of PS length (Figure 22. and Appendix A7). Obtained results are in accordance with previously reported maps of PS contribution to LPM. [Psychoyos and Stern, 1996; Sweetman et al., 2008; Limura et al. 2007; Sawada and Aoyama et al., 1999]. Not reported before, contribution to the mesoderm that gives rise to DA cells continued over the several stages of embryo development, apparently producing the same stretch of DA (Figure 25.). Therefore, we have decided to investigate contribution to rostral and caudal parts of the DA in more detail, and to try to identify the optimal position of PS grafting to achieve IAC labelling.

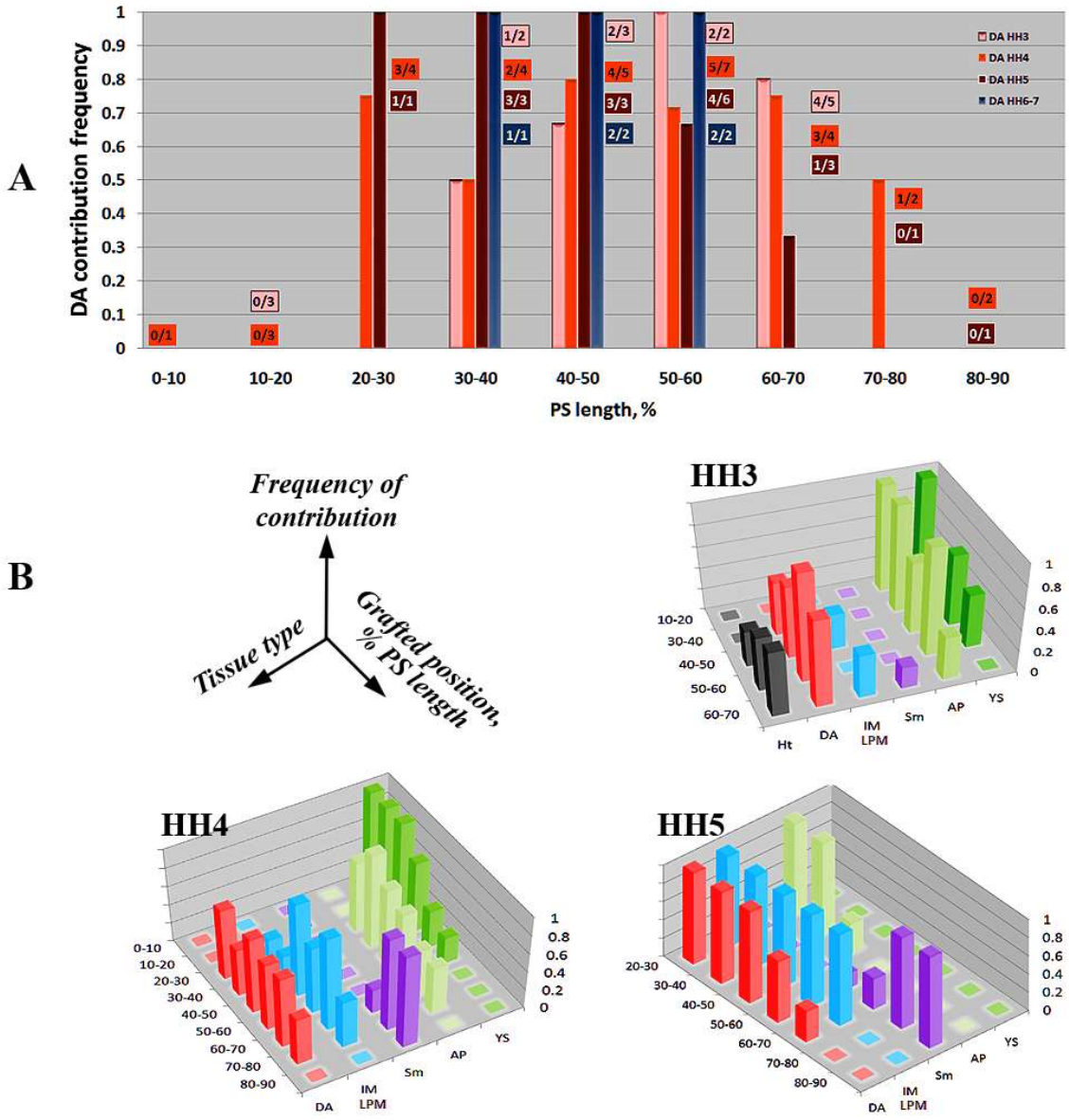

Figure 22. Grafts contribution to DA and adjacent tissues. Mid-primitive streak (30-60% of PS length) contributes to DA over several stages of chick embryo development (A); HH3 and HH4 mid-primitive streak contributes to embryonic and extra-embryonic tissues. Contribution to YS tissues is ceased in HH5 mid-PS, though PS still contributes to area pellucida vasculature (B). 76 observations (Appendix A7) analysed.

3.3.5.3. At different gastrulation stages, mid-primitive streak contributes to overlapping portions of the dorsal aorta

What we found surprising in our results is that the same region of the primitive streak (30-60% of its length) in HH3-6 chick embryo contributes to overlapping portions of the dorsal aorta (DA). Within the same embryonic stage, different regions of primitive streak (PS) also contribute to overlapping portions of the DA; however, anterior mid-streak contributes to rostral DA, and caudal mid-PS – to caudal DA. Additionally, the length and exact position of labelled DA portion varied from chimera to chimera. Therefore, to pool observations and be able to compare chimeras, we had to introduce an additional parameter. As such, we introduced an index of embryo length, which shows where GFP+ cells contribution took place by embryo length. We assigned value "1" to the first somite in the embryo and value "0" to the 20^{th} somite. According to our observations, in 50-60h chick embryos, the omphalomesenteric artery (OMA) connects to the DA approximately at the position of 20^{th} somite, and conveniently indicates the middle of the embryo (Figure 25.). Below OMA-DA junction somites are not formed yet and so, expressing DA contribution in somites number becomes impossible. To approximate length of GFP+ DA caudally to OMA, the caudalmost point of the embryo was assigned value "-1". In this way any point along embryo axis could be expressed in numbers, from -1 to 1 with "0" indicating the OMA-DA junction.

Thirty-four chimeras, in which somites could be clearly counted, were used in analysis of contribution to the DA by embryo length. When grafts were pooled for their corresponding grafting position (20-30; 30-40; 40-50; 50-60; 60-70%) and plotted for their position relative to the embryo length, it has become evident that older grafts contribute to overlap, but shifted caudally portions of the DA (Figure 23.). Within the same embryonic stage, 30-70% PS position contributes to be overlapping, but slightly shifted portions of the DA: more anterior mid-streak regions contributed to more anterior portions of DA (Figure 25.).

Visualized in this indirect way, contribution to DA revealed dense cross-overlapping of LPM contribution to DA – within the same stage and between different embryonic stages of development.

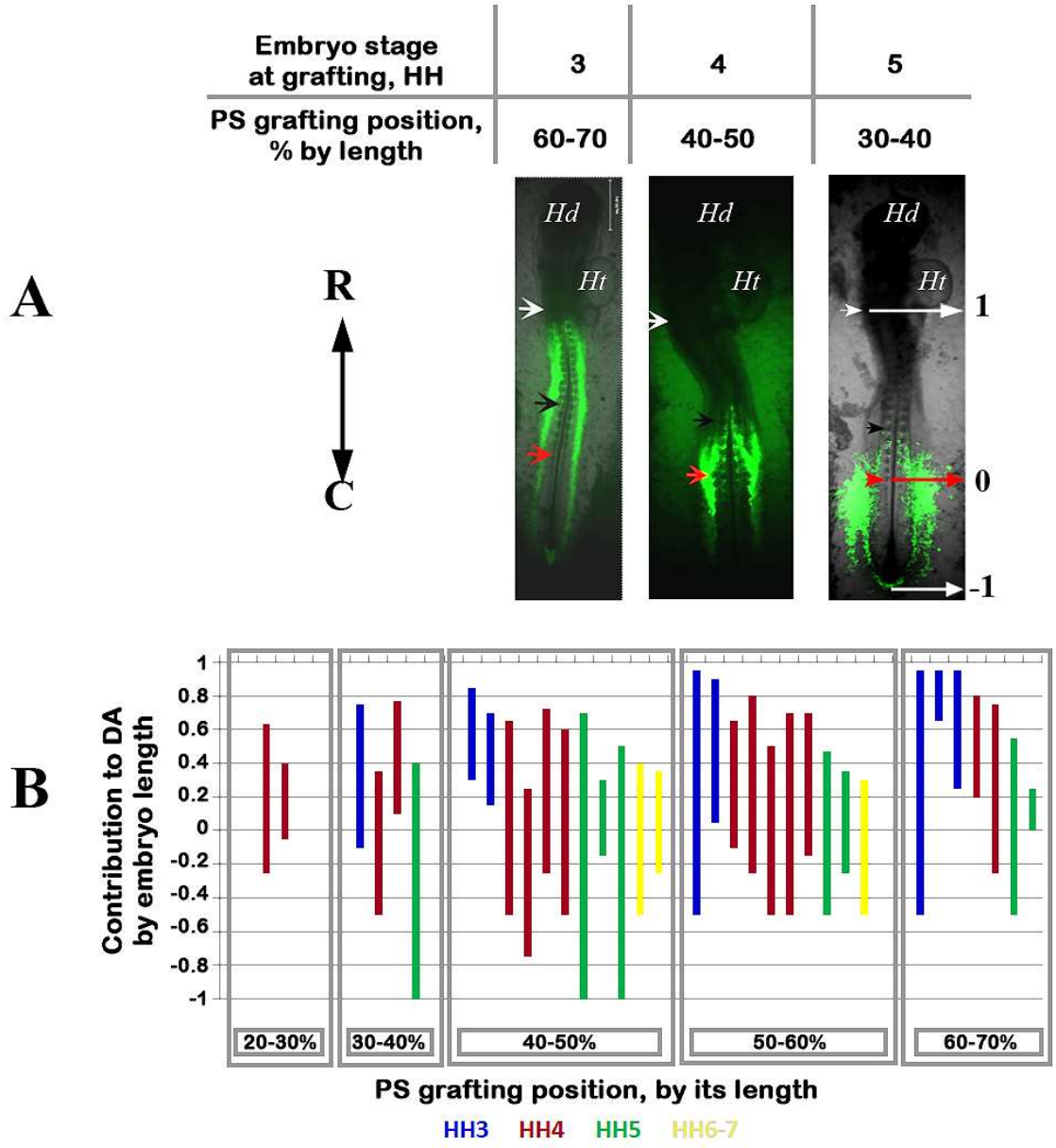

Figure 23. Mid-streak grafts contribution to DA by embryo length. Primitive streak (PS) grafts contribute to overlapping portions of DA. White arrow indicates 1st somite; red arrow indicates 20th somite – position around which OMA connects to DA. Black arrow shows 15th somite – position where first IAC are observed (A); Mid-primitive streak in older embryos contributes to more caudal DA portions. Within the same embryonic stage, more anterior mid-streak contributes to more anterior DA portion. Neighbouring regions in mid-streak give rise to overlapping portions of DA (B).

3.3.5.4. Cells from adjacent regions of PS migrate by different trajectories, but contribute to overlapping portions of DA

To directly verify that the same portion of the dorsal aorta (DA) is built from descendants derived from different regions of the mid-primitive streak, we carried out additional series of multiple grafting experiments. In these experiments chick embryo hosts were isotopically grafted with two or more differentially coloured grafts. In this way, migration of the cells derived from two (or more) primitive streak (PS) regions could be distinguished and traced simultaneously.

Our prior experience with multiple grafts of mid-streak showed that grafts spaced as far away as 10% would contribute to overlapping areas (not shown). Therefore, we had to invent a way to label grafts with different markers. As described above, dye injection does not allow labelling a sufficient number of cells in the PS to be able to label entire portion of the DA. However, cells staining with lipophilic dyes by itself is quite stable (lasts 2-3 days) and allows to mark within the area to which contribution takes place. Therefore, we hypothesized that if we stain grafts externally in DiI, the grafts (a) would provide a sufficient number of cells to trace their contribution to the DA and (b) graft position could be distinguished by DiI presence in the area. Therefore, here we combined PS grafting with GFP+ tissues and GFP+ tissues externally stained with DiI (e.g. by immersion in DiI solution).

Figure 24. shows tripe graft (35-45-55% of PS length) done on HH4 recipient. As it is shown on the figure, migrating cells form a fan-like shape, illuminating migratory routs of PS cells. Yet, already at 13h after grafting, labelled areas are tightly adjacent to each other. Anterior-most PS region (labelled with GFP only) contributes to the upper limit of the lateral plate mesoderm (LPM) and to the corresponding DA portion. Contribution to the DA becomes evident from 30h in EC. DiI labelled area (middle graft) is located in-between of two GFP+

grafts and contributes to the lower portion of the DA at 31 - 42 h of culture. The most caudal GFP+ graft contribute to the area pellucida and yolk sac vasculature from 42 to 70h of culture. Therefore, contribution to lower portions of the DA takes place later than that for more anterior portions of the DA.

Similar results were obtained with HH5 embryo multiple grafting (25-40-50-60% of PS length), see (Figure 25.). Initially well-spaced grafts show typical fan-like migratory routes, but labelled LPM becomes compacted by 16h of embryo culture. By 42h, all labelled areas fuse into one stretch of LPM that does not have any unlabelled gaps within it. This indicates intermixing of mesoderm cells – descendants of adjacent PS regions. Moreover, according to our observations, cells gradually exit the graft position. (Figure 25., 3h – 13h). In this way, labelling the PS at an earlier stage is simultaneously PS labelling at all later stages of the embryo development. We did not investigate whether that would be the same position in shortened PS. This might be an interesting topic for further investigation.

To directly visualize and register LPM cells position before they migrate to contribute to DA and/or extra-embryonic tissues, we carried out timed observations of isotopically grafted (20-70%) HH4 and HH5 chick embryos (Figure 26.-31.). According to our observations, except 20-30% HH4 PS grafts (Figure 26.-9), all 30-70% HH4 PS grafts contributed to the DA. In accordance with our prior observations, HH4 30-50% grafts also contributed to the area pellucida and/or to the yolk sac vasculature. The main difference in migratory routes of LPM cells was their lateral-medial position before these cells initiated secondary lateral or medial migration, leading to their final positions in the DA or yolk sac. It is worth noting here that the bulk of LPM cells stayed in the lateral body wall. As it can be seen from time lapse images, within the same developmental stage anterior-caudal position of labelled LPM cells depends on the graft position in PS: more anterior grafts contribute to the more anterior parts of the DA.

Since we have discovered that adjacent PS regions contribute to overlapping portions of the DA, we looked again at the fraction of embryos excluded from analysis (35 chimeras). We selected embryos grafted within 30-70% with positional mismatch. Maximum mismatch was 15% and the minimum one – 10% of PS length. All these chimeras with a positional graft mismatch contributed to the DA, in agreement with PS grafted position. Therefore, final position of migrating mesodermal cells does not depend on their origin in PS, but on the position where they started their migration from PS to LPM.

To verify this hypothesis, we carried out an additional small scale heterotopic grafting experiment. Since it has become clear that adjacent regions of the PS would produce overlapping portions of DA, we had to distinctly label grafts. For this, we used GFP+ grafts and "wild type" PS grafts stained with DiI. To increase dye penetration into tissues, we reduced size of DiI grafts, and this in turn affected our results. E.g., cells in smaller grafts had to migrate to the border of PS grove, while cells in wider grafts have already covered some distance in the LPM. As a result, (a) small grafts located anteriorly to the wide grafts ended up at the same position as cells from wide grafts; (b) small grafts located caudally to wide grafts ended up directly behind cells from wide grafts in LPM. Therefore, we can conclude that the width of the graft affects contribution to LPM and cells caudal-lateral position in the DA. the Size of the graft also affects the length of the labelled DA section. Yet, this did not affect globally grafts contribution to the DA and /or extraembryonic vasculature.

For instance, on Figure 32. we show results of heterotopic grafting with 35% DiI graft transplanted into 55% PS, and GFP graft from 60% of PS grafted at 45% (Table 7., graft 3). The same as it was described above, the graft was located caudally in the mid-streak (GFP+ graft on Figure 32.) contributed to LPM portion at more lateral position than DiI+ mid-streak graft. Most importantly, grafts derived from 35% of PS (DiI+ graft) did not contribute to extraembryonic vasculature, as it would be expected according to its original position. DiI+

graft contributed to the DA located above OMA, as was predicted by grafting position at 55% of PS length. GFP+ graft which was originally positioned at 60% of PS contributed to the area pellucida vessels, in accordance to its grafted position at 45% of recipient's PS (Figure 32.).

Therefore, we can conclude that the whole mid-streak contributes to the dorsal aorta (DA). Exact cell position in DA is determined by this cells migration route in lateral plate mesoderm (LPM). Not all LPM cells will contribute to the DA. The anterior region of mid-streak contributes cells to anterior part of the DA, and caudal region of mid-streak – to caudal DA. As the embryo develops, the mid-streak contributes to more caudal portions of the DA; yet, those still overlap with DA sections built with prior PS descendants. The caudal mid-streak region (below 45% of total PS length) contributes to the caudal DA and to extraembryonic vasculature.

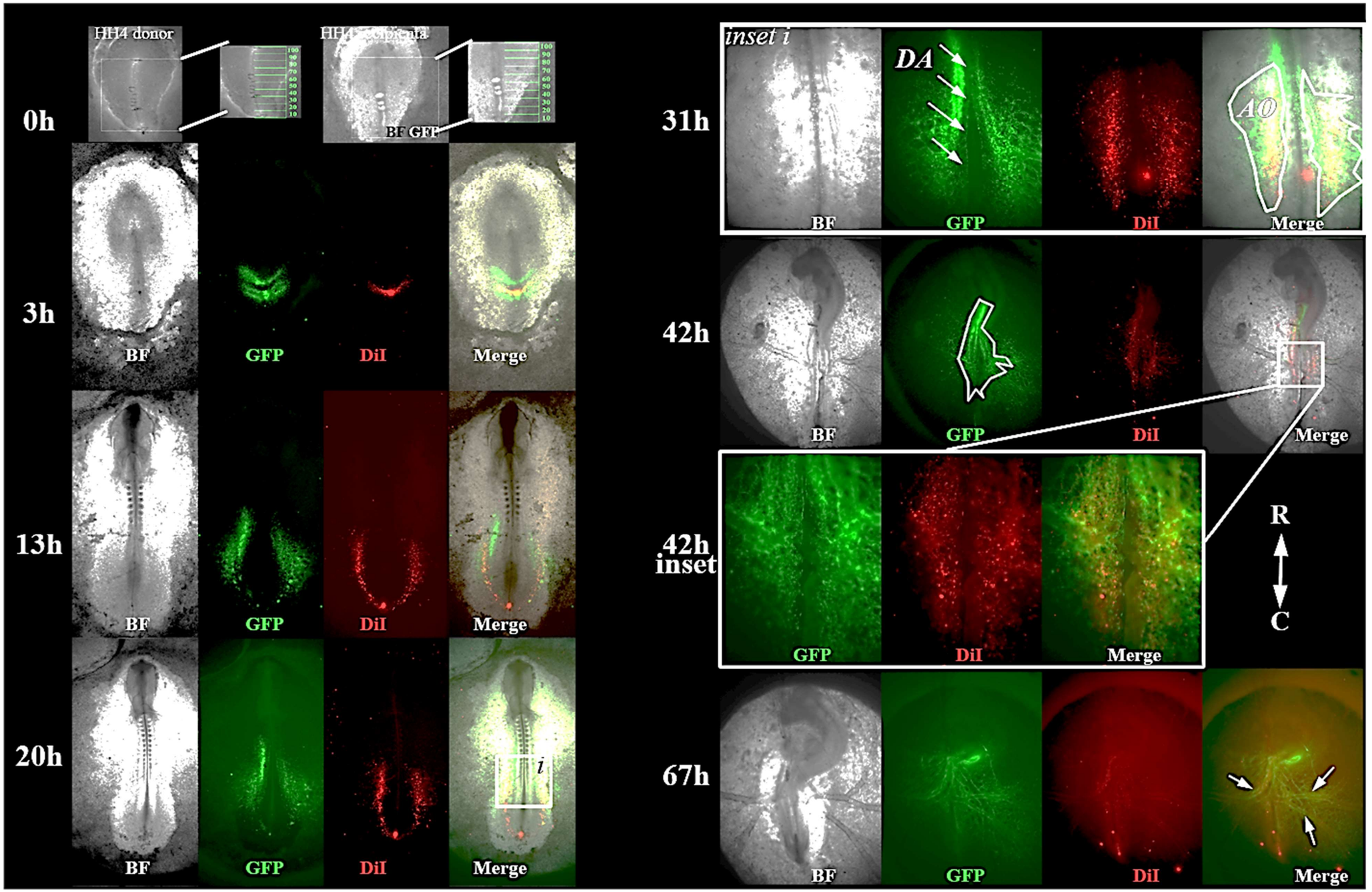

Figure 24. HH4 chick embryo triple graft (35-45-55% of PS length) shows contribution to different portions of DA that substantially overlap. Grafted cells migrate along fan-like trajectories (3-20h). Cells ingressing at more caudal position migrate more laterally than cells ingressing at anterior PS. Labelled LPM areas become closely adjacent (20h). Contribution to rostral DA is evident at 31h of culture (white arrows), while contribution to caudal DA is noticeable at 42 h. Labelled cells (GFP+, DIi+ cells) form one uninterrupted area indicating substantial overlap between descendants of adjacent mid-streak regions (42h). Caudal region of HH4 PS (35-45%) contributes to area pellucida vasculature (42-67h).

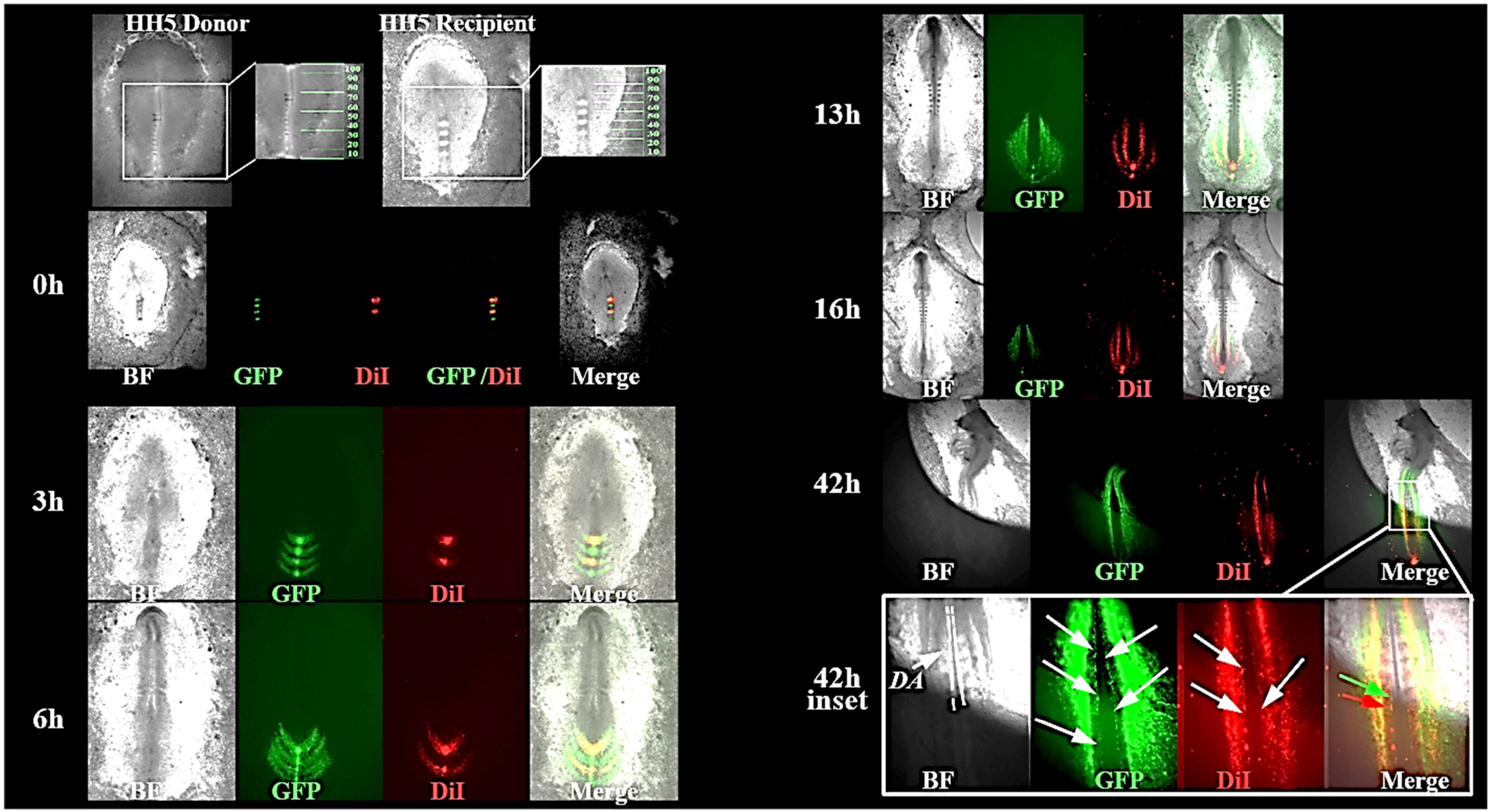

Figure 25. HH5 chick embryo multiple graft (25-40-50-60% of PS length) show contribution to overlapping DA parts. Initially ingressing through mid-streak cells migrate along well separated trajectories (0-13h). By 16h LPM cells align forming one uninterrupted stretch of cells. This stretch of LPM is formed by compacted and so intermixed descendants of neighbouring regions of mid-streak (16h). By 42h a portion of LPM cells migrated towards embryonic midline contributing to DA (write arrows). In this way, DA segments of DA are built from descendants of several mid-PS regions (red and green arrows).

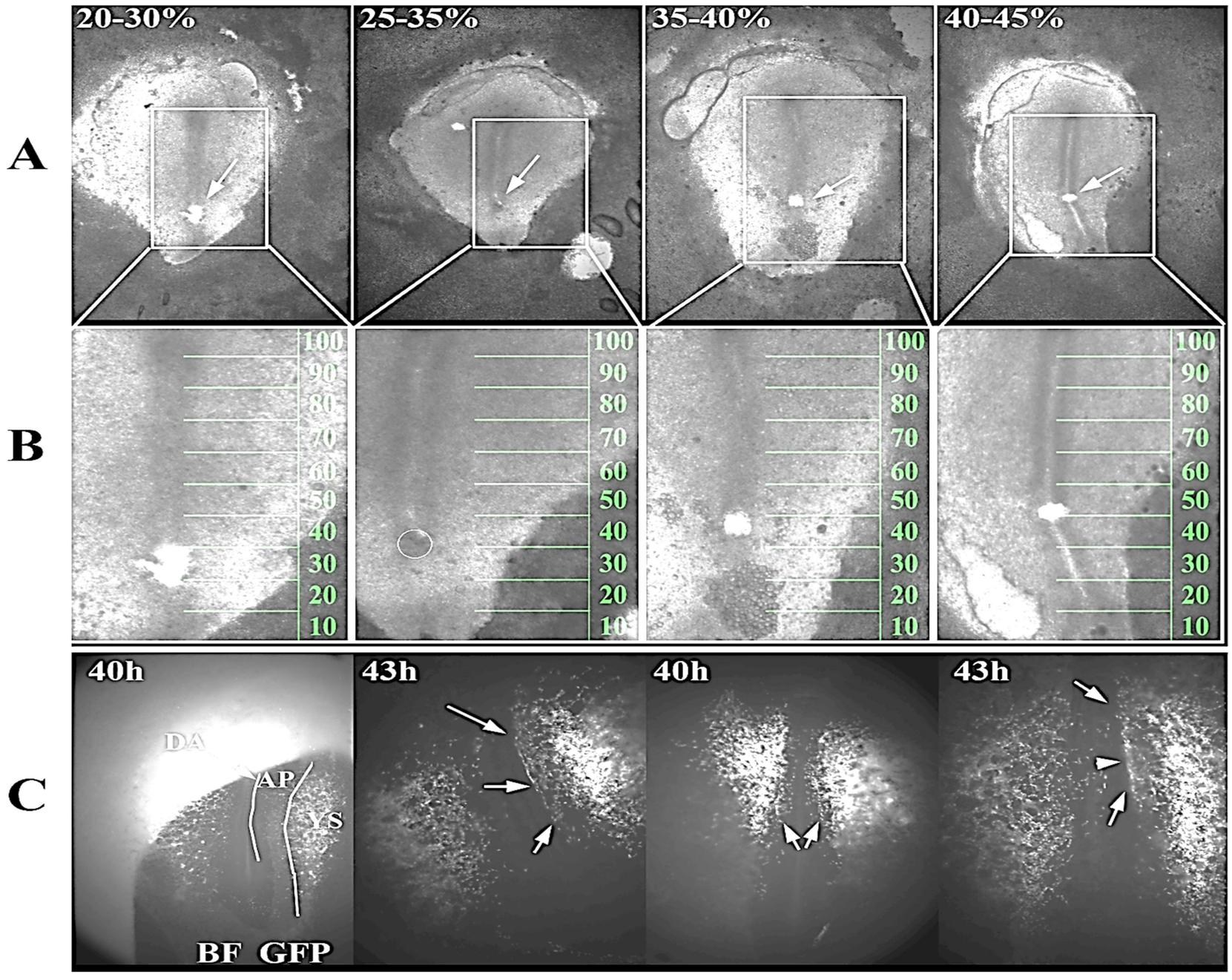

Figure 26. Contribution to extra-embryonic vasculature and DA in chimeras grafted at HH4 20-45% of PS length. Graft position in host embryos (A); PS overlaid with 0-100% scale to show exact graft location (B); GFP+ grafts contribution to extra-and embryonic vasculature, EC day 2. Only in chimera grafted at 20-30% of PS graft did not contribute to DA. In other chimeras, grafted from 25 to 45% of PS length. Grafts contributed to DA (white arrows) and extra-embryonic vasculature (C).

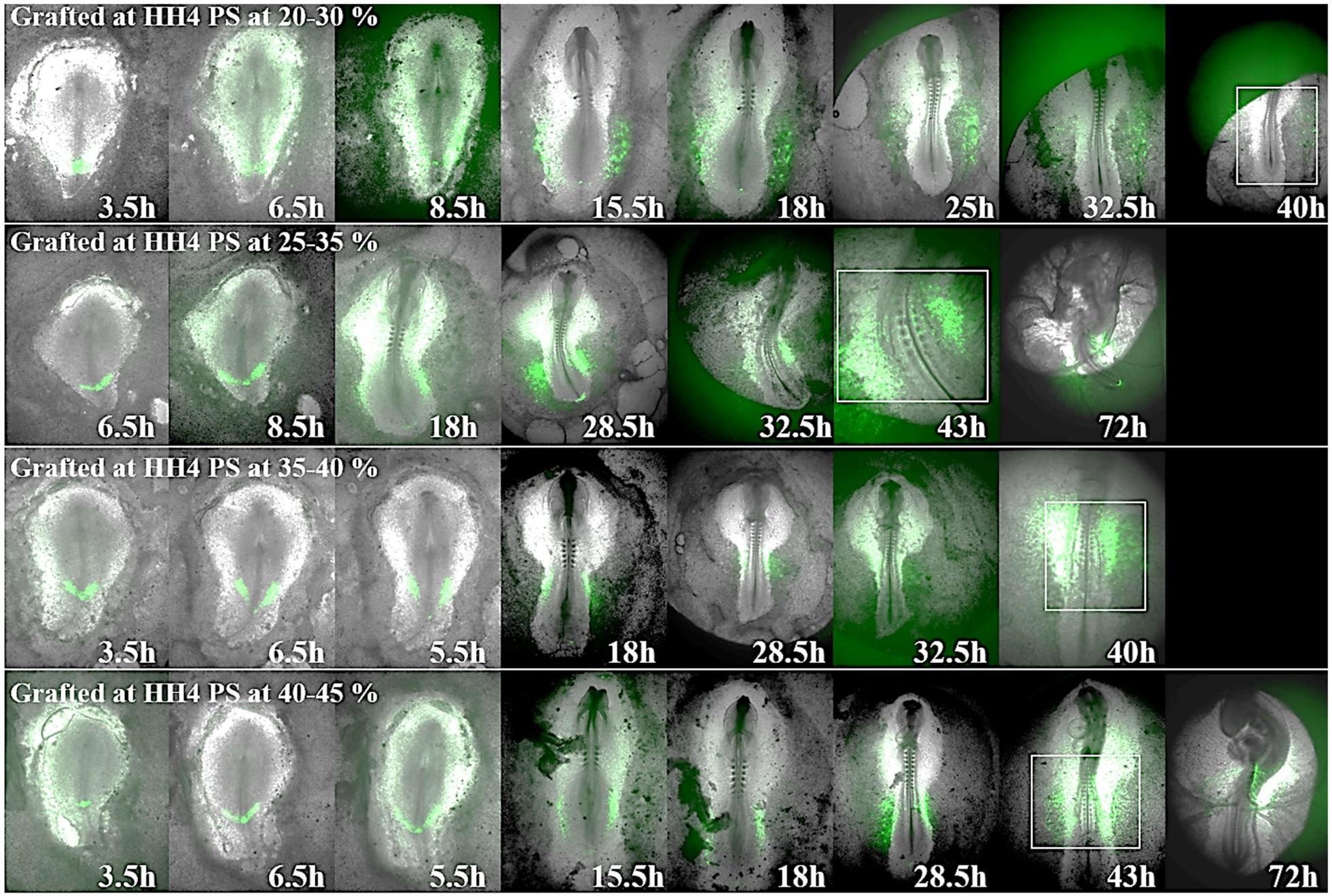

Figure 27. Migration of grafted GFP cells (HH4, positions: 20-45%) to the dorsal aorta. In all but 20-30% grafted chimeras, GFP+ cells first migrate to form LPM (0-18h); The more laterally cells migrate in LPM, broader contribution to extra-embryonic vasculature is observed (15-43h). Close up images of insets are given on Figure 26.

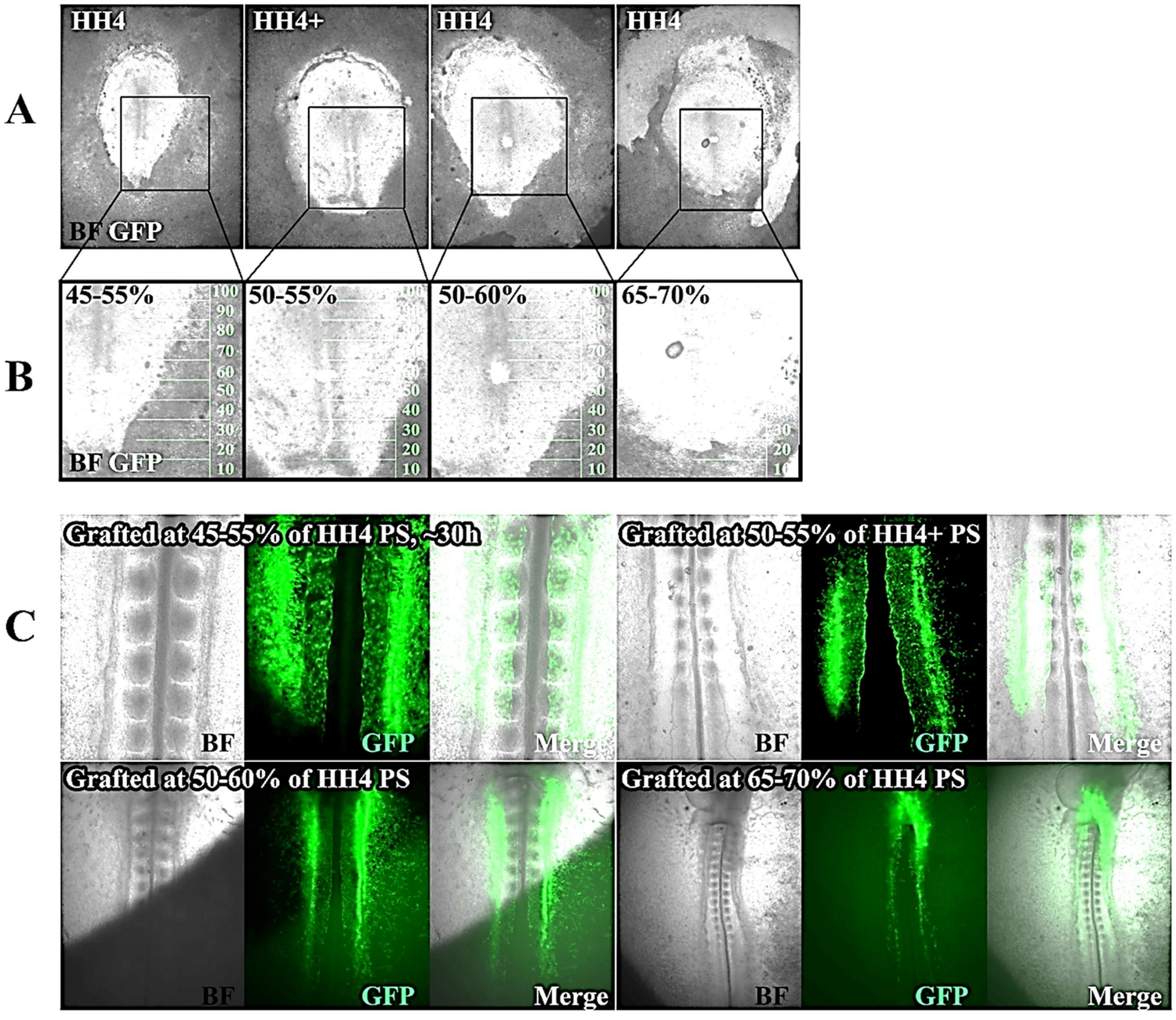

Figure 28. Contribution to DA in HH4 embryos grafted at 45-70% of PS length. Grafts position in the embryo (A); PS overlaid with scale to show exact graft location (B); Insets for Figure 29. Close up of DA area in chimeras at about 30h in EC culture (C).

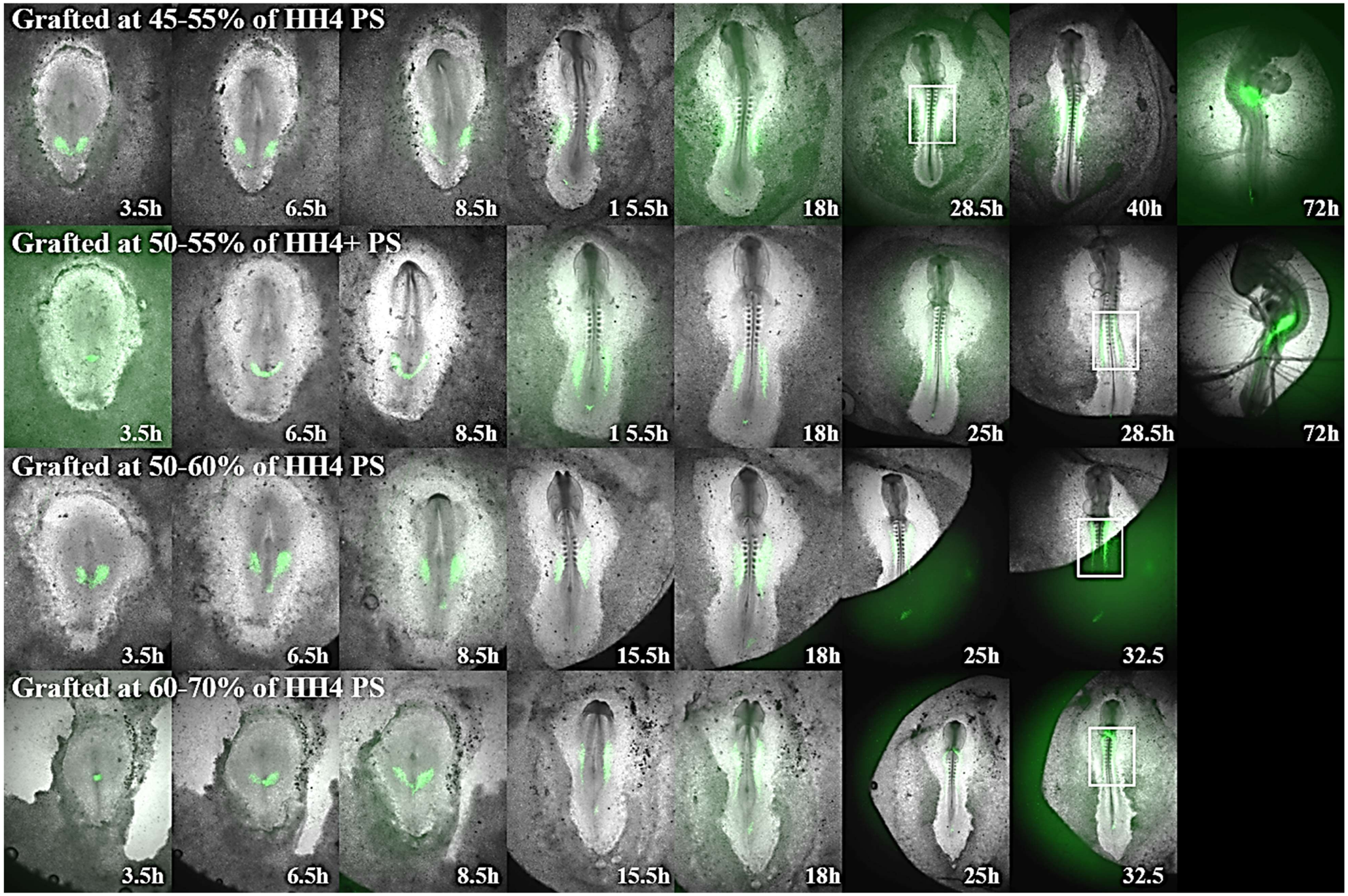

Figure 29. Migration of grafted GFP cells (HH4, positions: 45-70%) to the dorsal aorta. At 0-20h in EC culture grafted cells migrate to form LPM. Final position of LPM in the embryo depends on graft position in PS: more anterior mid-streak grafts contribute to more anterior portions of LPM. In grafts positioned above 50% of PS length, contribution to extraembryonic vasculature is decreased.

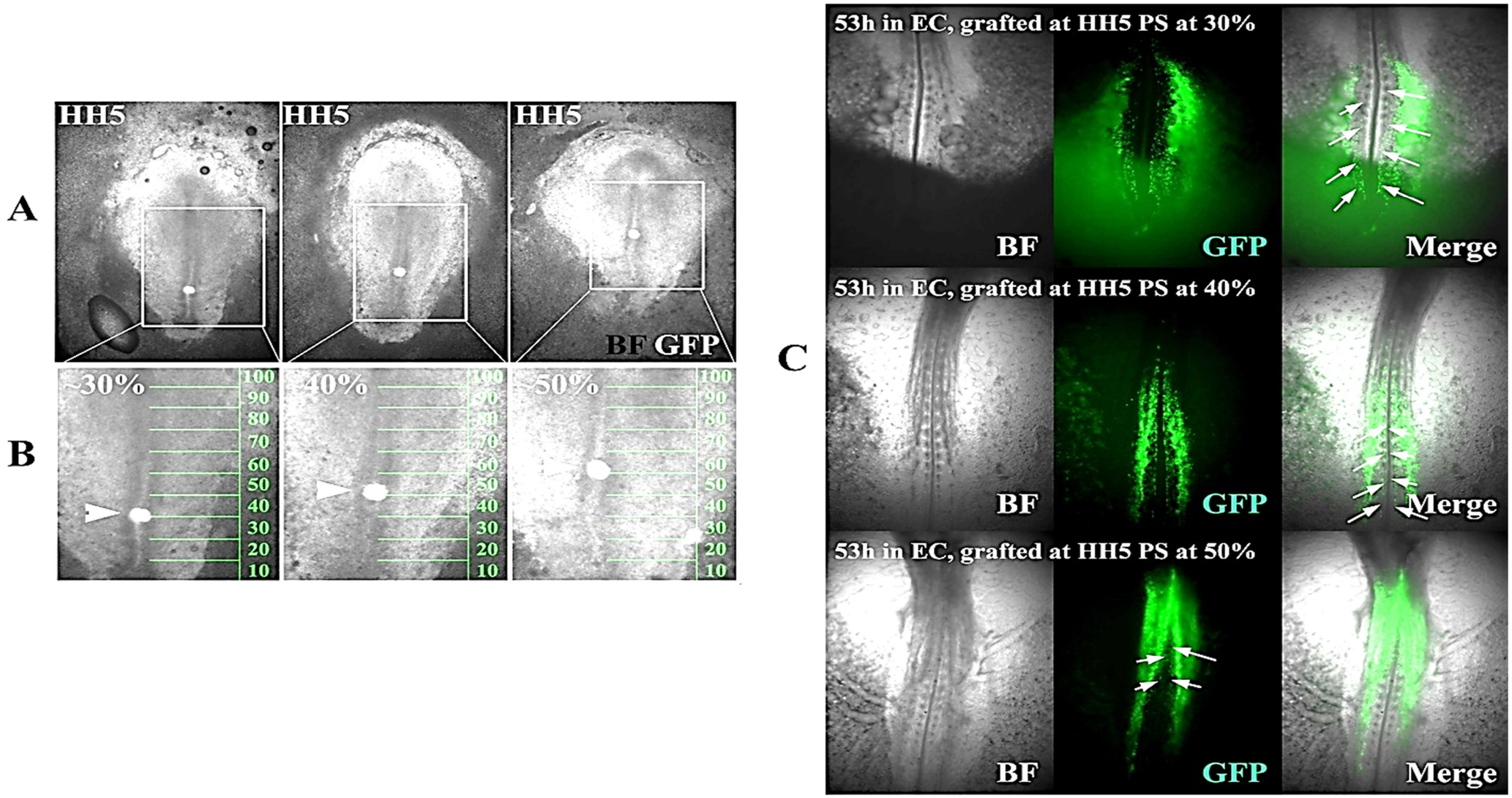

Figure 30. Contribution to DA in embryos grafted at HH5. Graft position in HH5 recipients (A); Exact grafts position shown by on PS overlay with a scale (B); Insets for Figure 31. More caudal mid-streak regions contribute to caudal DA (white arrows, 30% graft) while anterior mid-streak (50-55% graft) contributes to rostral DA (white arrows) (C).

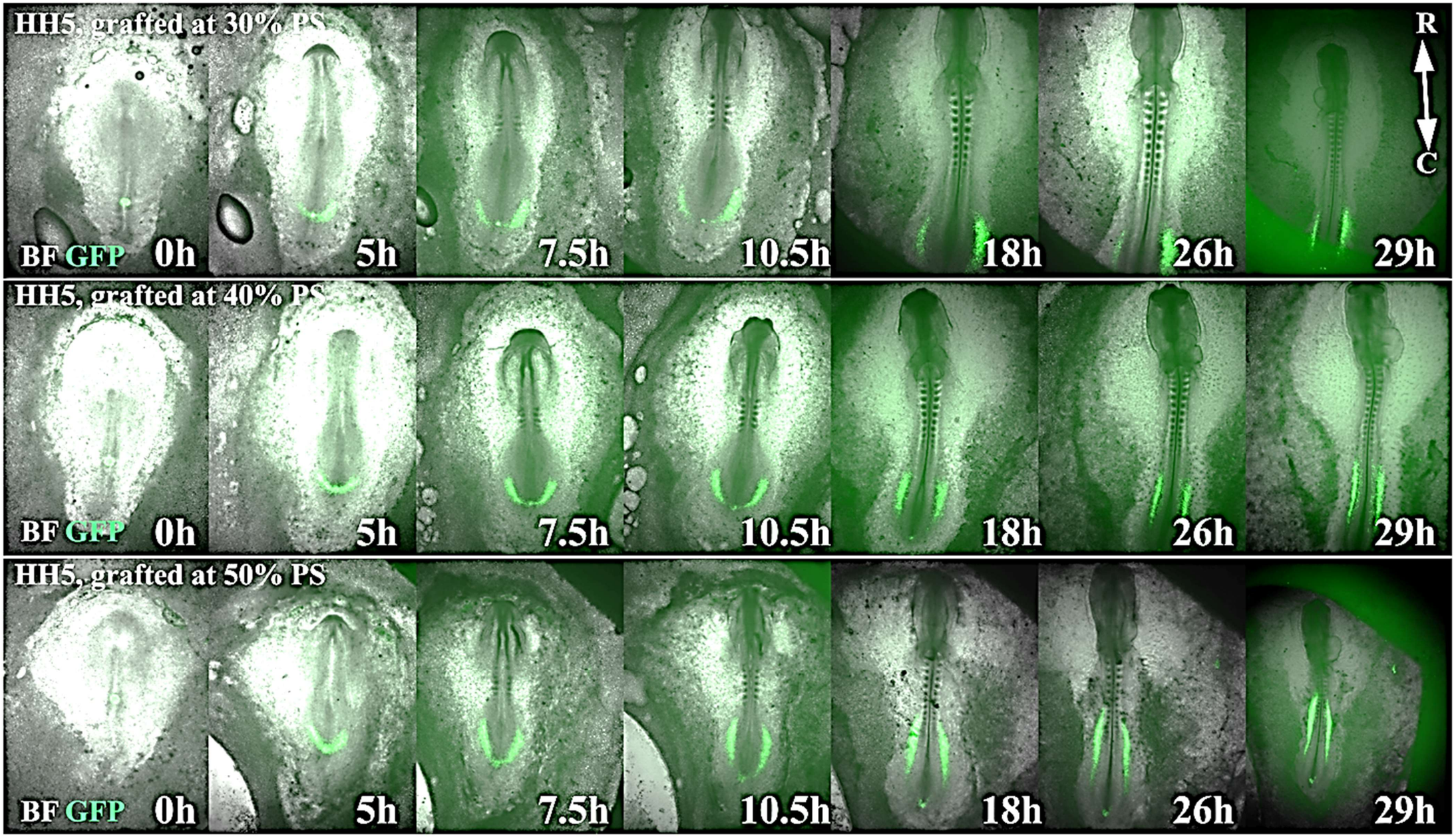

Figure 31. Time-laps of contribution to LPM and DA in chick embryos grafted at HH5. Whole mid-streak (30-50% of full PS length) contributes to LPM. More anterior regions of mid-streak contribute to more anterior portions of LPM. Close-up images of LPM contribution to DA at around 50h of these chimeras EC culture are shown on Figure 30.

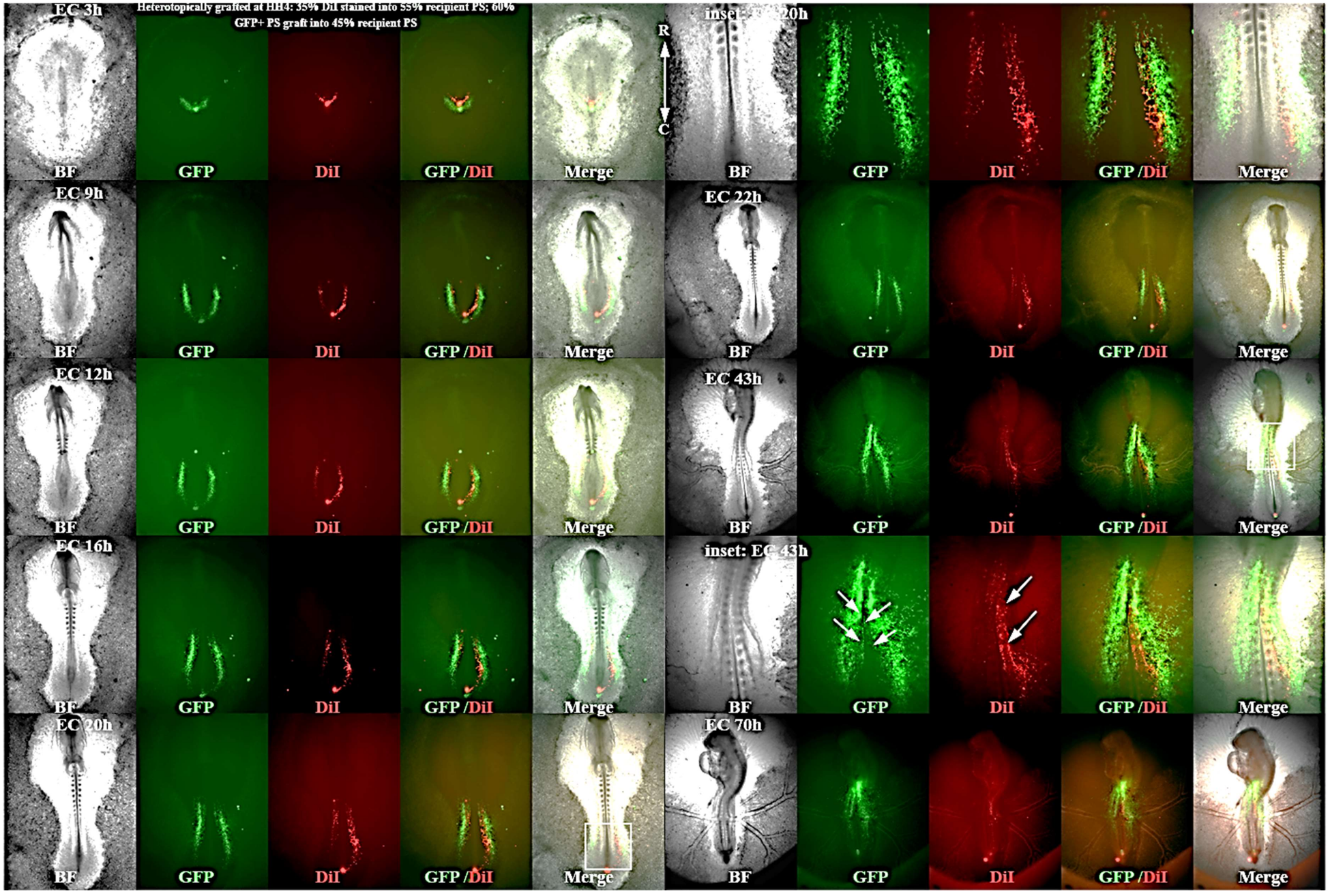

Figure 32. Original cell position in mid-streak does not determine its position in DA. Cell position in DA depends on its migratory trajectory in LPM. Time-laps of HH4 heterotopically grafted chicken embryo development. 35% of PS length wild-type chick embryo tissue stained with DiI and transplanted into 55% PS position in the recipient. Tissue from 60% PS region from GFP+ transplanted into 45% PS position in the recipient. As expected, 45% graft (GFP+) contributes to DA and extraembryonic vasculature, while DiI+ graft does not.

Table 7. Heterotopic grafting within 30-65% of HH4-5 primitive streak

ID	Recipient stage, HH	Original graft position, % PS length	Final graft position, % PS length	Label	Graft iso- or heterotopic	Labelled region	AP vessels labelled?
1	5	35	60	GFP	Yes	Above OMA	no
		55	55	DiI	No	OMA and above	no
2	5	35	65	GFP	Yes	Above OMA	no
		65	55	DiI	Yes	OMA and above	no
3	4	60	45	GFP	Yes	OMA and above	yes
		35	55	DiI	Yes	OMA and above	no

3.3.6. Not only yolk sac produces blood cells in early chick embryo

During chimeras examination at "early chick embryo culture" (EC) day 2 and 3, we noticed that some of the chimeras had fluorescent cells in their blood flow. These cells were fluorescent only in settings for GFP excitation; hence, they were not autofluorescent, but GFP+ cells. Amount of GFP+ cells identified in the blood flow varied between chimeras from rare single cells to the dozens of cells registered per 10 seconds. Frequency of finding chimeras with GFP+ cells in blood flow are given in Table 8. In chimeras grafted at stage HH6 or later, GFP+ cells in blood were identified only in 1 chimera grafted at 70% of PS.

Table 8. Frequencies of finding chimeras with GFP+ cells in blood flow

Recipient stage at grafting	Grafted PS region, % of total PS length	Number of chimeras analysed	Number of chimeras displayed GFP+ cells in blood flow (%)
HH4 -5	<35	14	0 (0)
	35-45	15	1 (6.5)
	45-55	16	4 (25)
	55-70	21	4 (19)
	>70	12	1 (8)

None of the yolk sac (YS) chimeras that survived till the third day in EC on examination had GFP+ blood (Appendix A8). These chimeras had partial GFP+ labelling of YS and had blood circulation but did not have noticeable GFP+ cells contribution to the blood. This is an unexpected result, as the first primitive blood cells arise in the yolk sac. This could be explained if mesoderm progenitors of the first blood cells migrated to the YS prior to the grafting procedure, e.g. before HH4. Indeed, endothelial or Runx1+ cells appear in the area opaca (yolk sac) much earlier than those in the embryo proper [Hirakov and Himura, Jaffredo et al., 2005; geisha.arizona.edu ID ENG.UApct]. However, whether this is the consequence of differentially regulated genes expression in intra- and extraembryonic areas or time restricted cell migration is the question to answer in further investigations.

On examination of sections of chimeras carrying GFP+ cells in blood flow, GFP+Runx1+ cells were identified in the vessels lumen (Figure 35.). Interestingly, embryos that displayed GFP+ cells in blood had contribution to the DA, intermediate mesoderm and to some extent to the vasculature in the area pellucida, but not to the yolk sac. Therefore, here we identified a not earlier appreciated source of early blood cells (or mobile cells that travel with blood flow) that arise not from the yolk sac, but from another embryonic region.

In half of cases GFP+ cells were already identifiable the in blood flow at EC day 2, e.g. before DA fusion and intra-aortic clusters (IAC) appearance. Simultaneously, these cells were still present at EC day 3 (when DA fuse and IAC start to appear). Additional experiments are required to establish if there is a link between IAC and GFP+ cells at day 3 in EC. A possible source of these cells could be area pellucida vessels (AP). At least in some embryos, AP vessels were clearly GFP labelled. According to Sabin, AP also produces blood-islands [Downs 2003].

3.3.7. Dorsal aorta and intra-aortic clusters are mosaic structures formed by descendants of multiple regions of primitive streak

A region of the dorsal aorta (DA) that bears intra-aortic clusters (IAC) contains precursors of definitive HSC. One of the methods to trace IAC's progeny would be to label them and to trace their contribution to the hematopoietic system in an adult chick. According to the current opinion on IAC ontogeny, clusters arise from the DA endothelial lining or from this lining and the cells underlining the DA. Therefore, DA labelling would enable tracing progeny of IAC clusters. In this chapter, we show for the first time that the mesoderm contributing to the DA originates from a wide region of the PS during multiple stages of chick embryo development. Hence, we have encountered a question: whether portions of the mesoderm derived from different parts of the PS have equal ability to produce IAC. To answer this question, chimeras with contribution to the IAC bearing part of DA were sectioned and immunostained for GFP and hematopoietic markers Runx1 and CD45.

Prior reports show that in chicken embryos IAC bearing portion of the DA is located around the 15th somite pair [Drevon et al., 2010; Lassila et al., 1999]. In the chapter above, we show that region of the PS from 45% to 65% of its length contributes to the DA portion spanning from 1st to 20th somite, or the portion of the DA located anterior to the OMA. Hence, the portion of the DA formed by descendants of cells ingressed through the PS at 45-65% of its length shall be IAC progenitors.

To establish whether IAC were formed by PS descendants regardless of the stage when grafting was carried out, in total 8 chimeras were analysed for IAC presence and their phenotype. List of chimeras is given in Table 9.

Table 9. Chimeras examined for the presence of IAC

Chimera ID	*Graft position, % of PS (HH stage)*	*Chimera condition at EC day 3**	*GFP+ DA lining (+/-)*	*GFP+Runx1+ cells in DA lining (+/-)*	*IAC (+/-)*	*GFP+Runx1+ cells in a cluster (+/-)*
1	45 (4)	Good	+	+	+	+**
2	50 (4)	Good	+	+	+	+
3	50 (4)	Poor	+	+	-	-
4	50 (5)	Good	+	+	+	+
5	35 (6)	Good	+	-	+	-
6	45 (6)	Good	+	+	+	+
7	50 (6)	Poor	+	+	-	-

* - "Good" condition - chimera is HH17 or older and presents heartbeat and blood circulation; "Poor" condition – weak heartbeat is present, blood circulation is absent. Chimera did not develop further than HH16; ** - only one GFP+ cell; "+" indicates presence; "-" – absence.

In all examined chimeras, the DA lining was GFP+. The extent to which GFP+ cells contributed to the DA lining varied. The most intensive GFP+ staining was observed in the middle of the area having GFP+ cells contribution. In this position, GFP+ cells were also found in the lateral body wall, dorsal mesentery, peri-neural vascular plexus, somatic and splanchic lateral plate mesoderm (Figure 33.).

Clusters were identified in all chimeras developed in EC day 3 beyond HH17 (Table 9.). IAC clusters containing GFP+ cells were identified in all areas where grafts contributed to the rostral DA. If a graft did not span to the area where the IAC were formed, IAC were still identified, but they did not contain GFP+ cells (e.g. chimera ID5).

In one case (from analysed chimeras), when chimera (ID1) had contribution to area pellucida vasculature, GFP+ blood cells were identified in blood circulation (Figure 34). When sections of this chimera were examined, blood cells were identified as round GFP+Runx1+

cells (Figure 35, B). This chimera had a GFP+ DA lining with a good number of GFP+Runx1+ cells in it. Clusters were mainly represented by Runx1+CD45+ cells. Identified on sections clusters were mainly Runx1+. In one instance, GFP+ cells were at the base of such a cluster (Figure 35., A) and in another case a GFP+ cell was identified inside a budding aortic cluster (Figure 35, D). Identification of mainly GFP- clusters suggests that in this chimera contribution to the DA was mainly not in IAC bearing portion.

Embryos grafted at HH5 and HH6 at 50 and 45% of PS length had contribution of GFP+ cells to the DA lining and to intra-aortic clusters (IAC), (Figure 36. and 37.). IAC were found to contain different numbers of GFP cells: some IAC were entirely GFP positive while others contained just one or two GFP+ cells (Figure 35. D and 37., F). Within clusters, cells also had different expression of hematopoietic markers Runx1 and CD45 (Figure 37. E, F). Dynamics of hematopoietic markers expression within chick embryo IAC is not described and hence, Runx1 and CD45 markers expression migh be upregulated at later developmental stages. For instance, in *in ovo* cultured chicken embryos, cells within one cluster are uniformly Runx1 and CD45 positive (Figure 33.).

As GFP is a permanent marker, occurrence of clusters with a mixture of GFP+ and GFP- cells indicates that IAC are not of a clonal origin. It is also possible that GFP+ cells migrate in and out of a cluster. Entirely GFP+ IAC were observed in chimeras with a complete GFP+ dorsal aorta lining. In chimeras with rare GFP+ cells in the aorta lining, IAC contained rare GFP+ cells. Hence, clusters originated from the mosaic (GFP+GFP-) aortic floor, and correspondingly had a mixture of GFP+GFP- cells. This hypothesis was also supported by our prior observations about DA composition. The DA is a mosaic organ built from descendants of a broad region of the PS arising during several stages of an embryo development. Therefore, complete labelling of all IAC with a single PS graft is hard to achieve. Whether a cluster is a niche for hematopoietic stem cells would require further tracing of GFP+ cells in IAC.

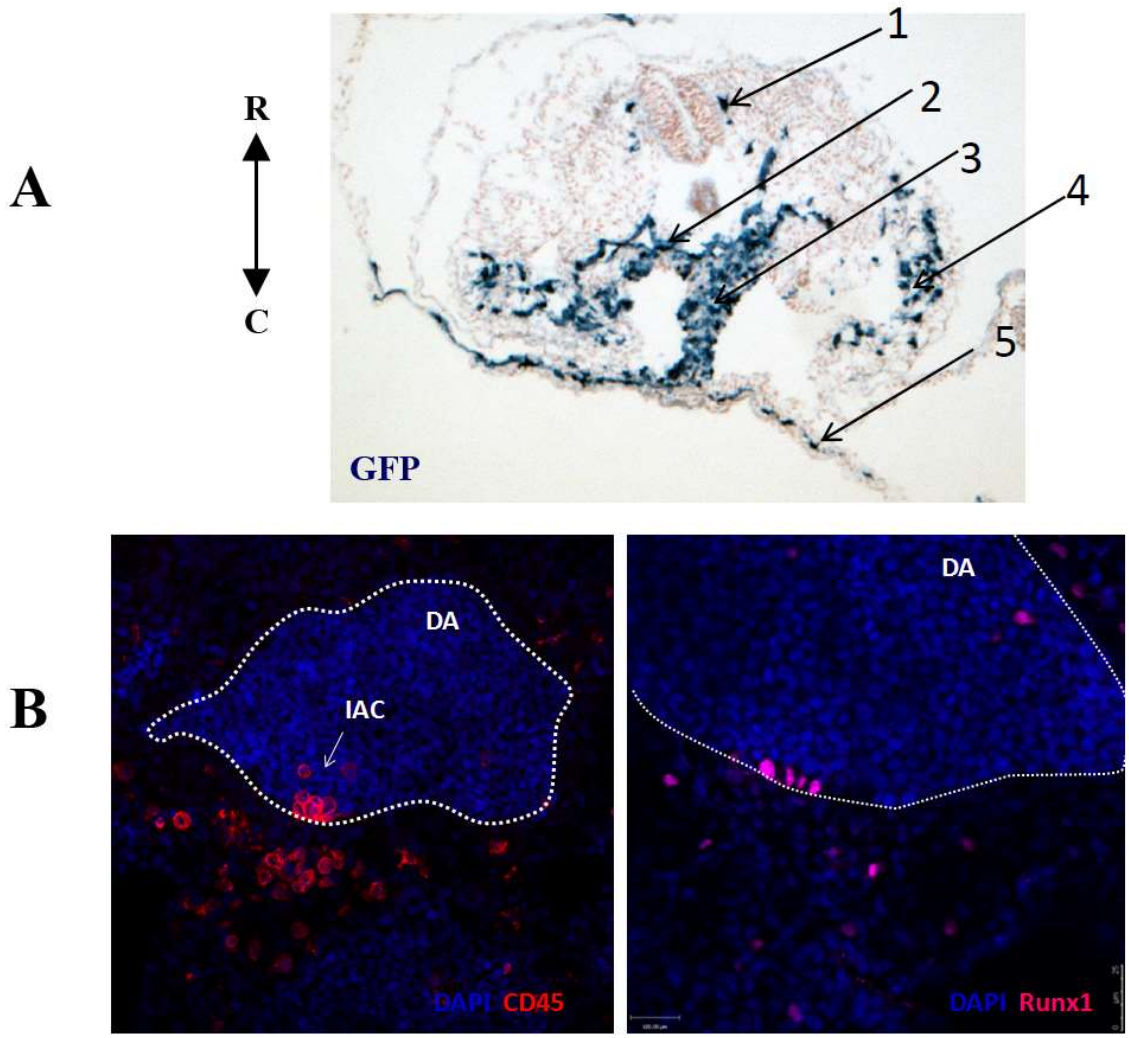

Figure 33. Transverse sections through EC cultured chimera and in ovo cultured ED3 chick embryo. Anti-GFP alkaline peroxidise staining on cross-section through chimera isotopically grafted at mid-streak (45-55%) at HH4) (A); Wild-type *in ovo* cultured ED3 chick embryo cross-sectioned through dorsal aorta showing clusters of cells expressing CD45 and Runx1 (B). Peri-neural vascular plexus (1), DA endothelial lining (2); dorsal mesentery (3), somatic lateral plate mesoderm (4); splanchic lateral plate mesoderm (5).

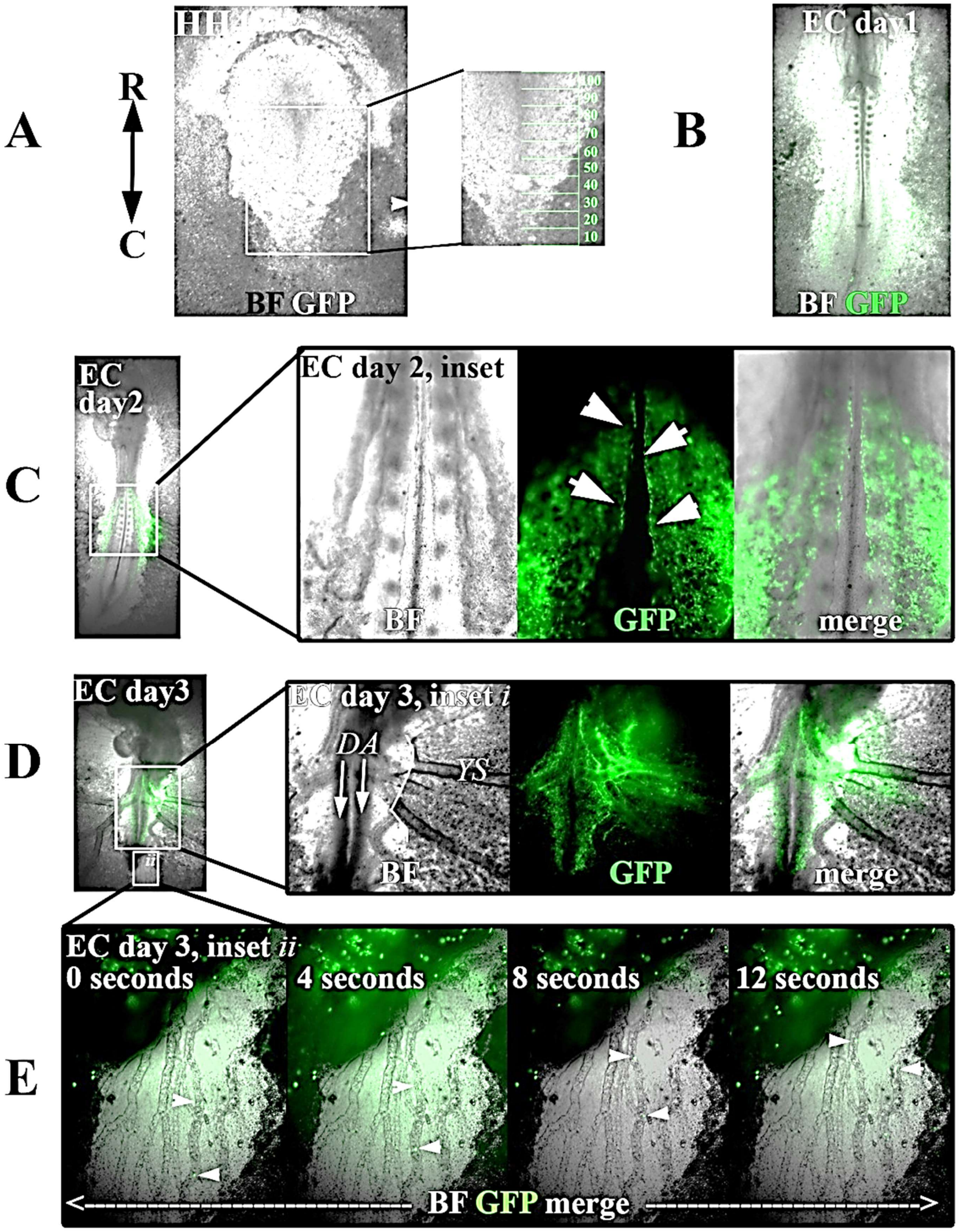

Figure 34. HH4 40-50% region of PS contributes to IAC bearing part of DA, area pellucida vasculature and blood. General view of grafted chimera with inset: PS overlaid with a scale to show exact graft position (A); Contribution of GFP+ cells to LPM during EC day 1 (B); At EC day 2 GFP+ graft cells contributed to DA (white arrows) and area pellucida vessels (C); At EC day 3, graft cells contributed to some vasculature of YS. Rostrally and caudal parts of DA are labelled; area pellucida vasculature is labelled anterior and caudally to OMA-DA junction (D); GFP+ cells are detectable in embryo circulation. White arrowheads show positions of GFP+ cells in area pellucida vessels during 12 s of observation (E). Immunostaining of cryosections of this chimera are given on Figure 35.

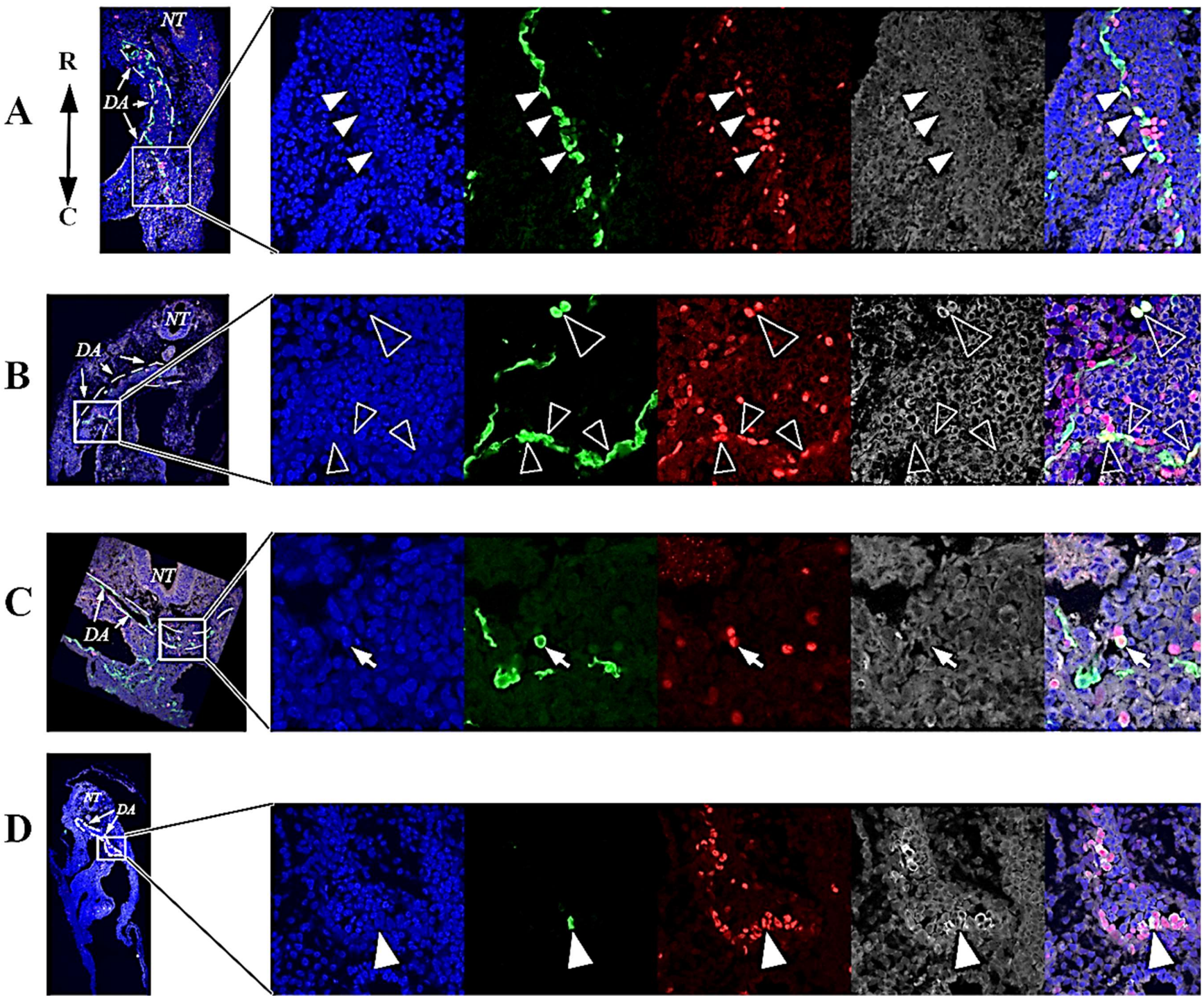

Figure 35. HH4 mid-streak gives rise to DA and early embryonic blood. Immunofluorescence on frozen sections of chimera grafted at 40-50% region of PS. Longitudinal section of chimera shown on Figure 33. GFP+ cells contribute to DA lining. Some GFP+ cells co-express Runx1 (white arrowheads). Runx1+ cluster of cells has GFP+ cells in its base. (A); Another longitudinal section showing contribution to DA lining (small empty arrowheads) and blood cells co-expressing GFP and Runx1 (large empty arrowhead) (B); Sagital cross-section through the chimera showing section through DA with GFP+ cells in blood flow (C); Chimera section through DA, showing Runx1+ cluster of cells with 1 cell expressing GFP (D).

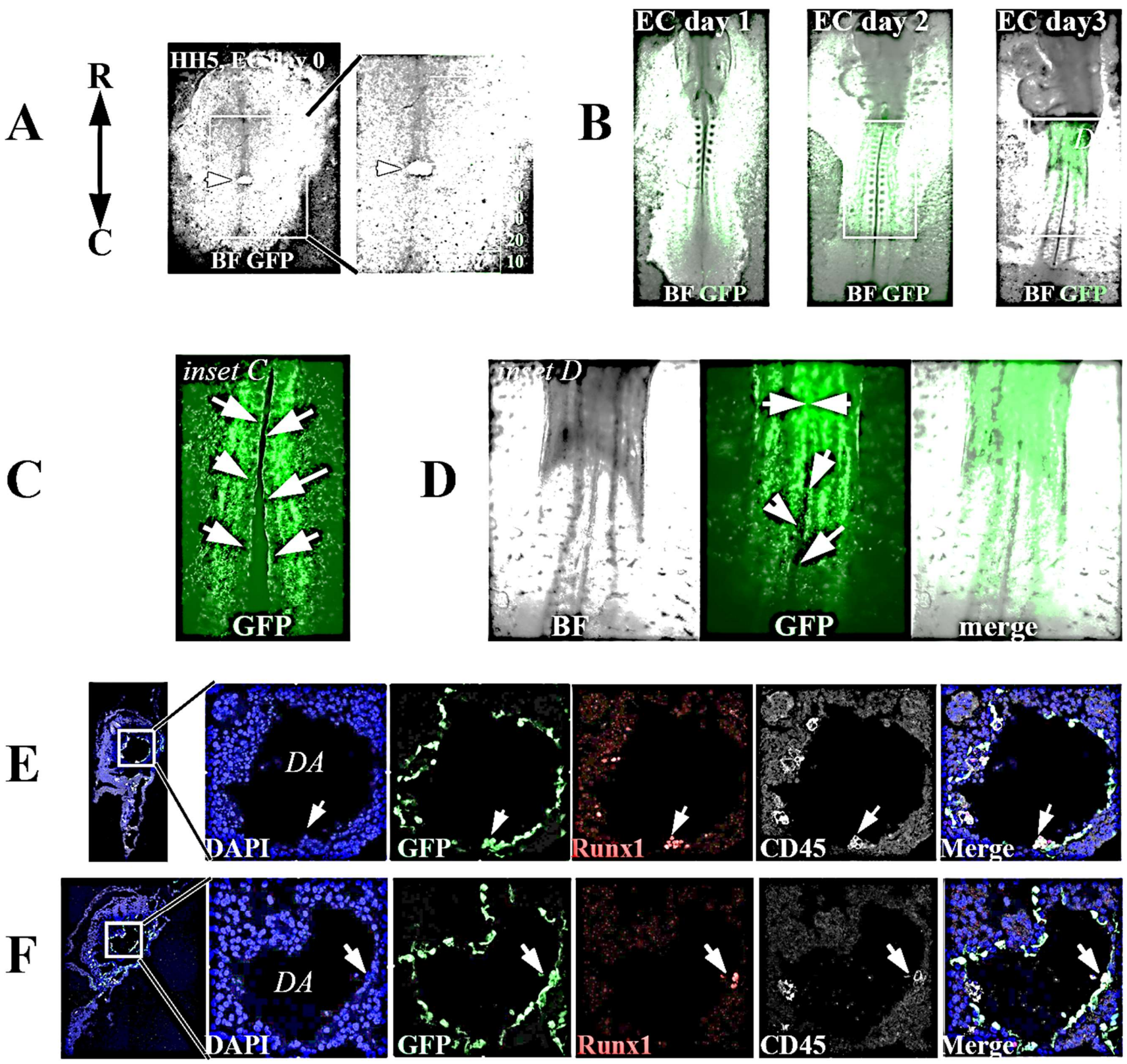

Figure 36. HH5 mid-streak contribution to inta-aortic clusters. HH5 chick embryo grafted at 50% of PS. Inset shows PS overlaid with a scale to show detailed graft (white arrowhead) position (A); GFP+ cells contribution to LPM and lateral body wall at EC day 1-3 (B). Close-up on GFP+ DA (wall is shown with white arrows) in the chimera at EC day 2 (C); Close-up on GFP+ DA (DA wall is shown with white arrows). Aortae fusion is initiated (two pointing to each other white arrows) (D); Chimera cross-section through heart region showing GFP+ DA lining with GFP+ cluster of cells (white arrow). GFP+ cells express Runx1. Some cells in cluster co-express CD45 (E); Chimera cross-section below heart region showing GFP+ DA lining and GFP+ cluster (white arrow) of cells. Some cells in cluster co-express Runx1 and/or CD45 (F).

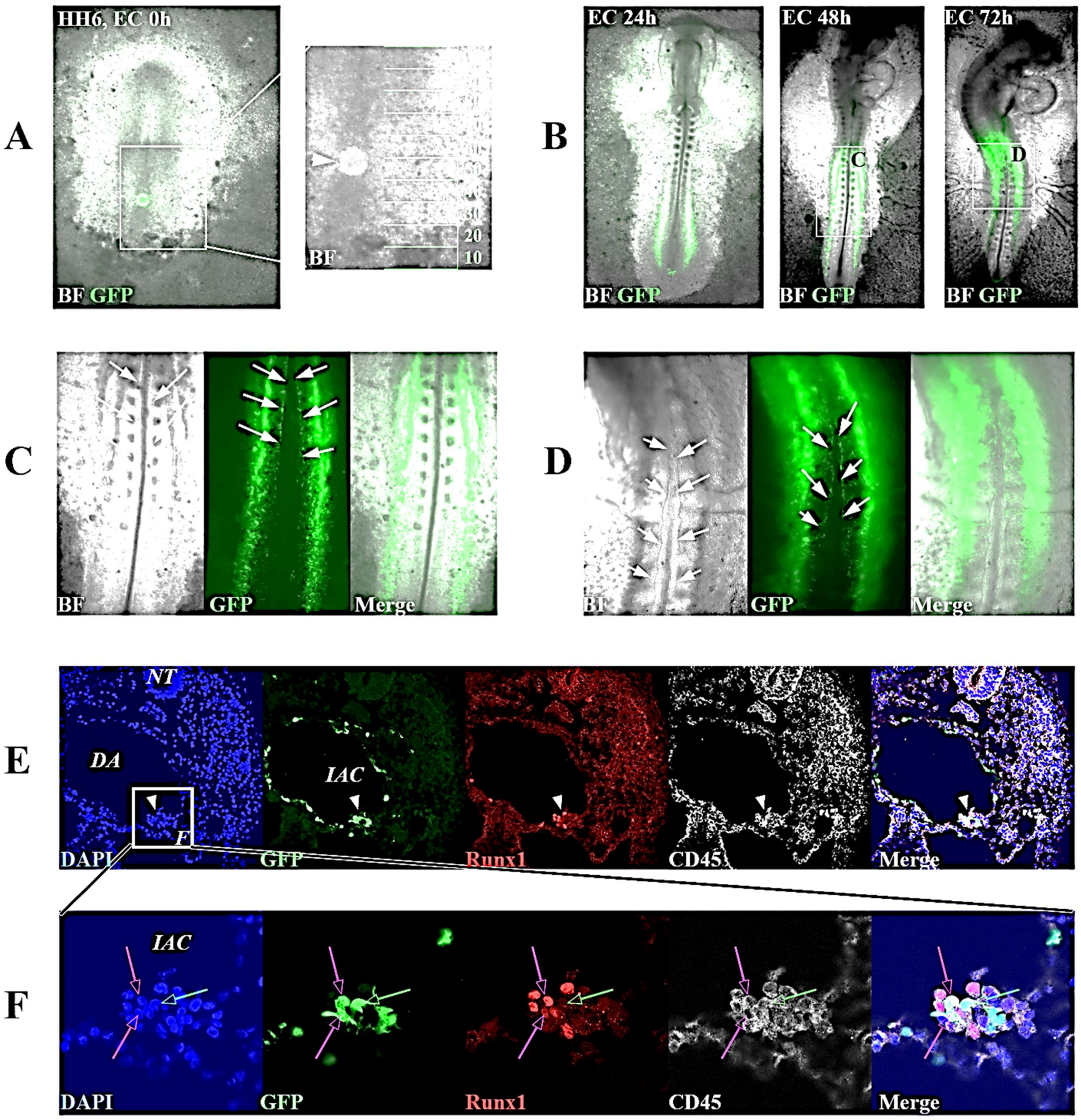

Figure 37. HH6 mid-streak contribution to intra-aortic clusters. HH6 chick embryo grafted at 50% of PS length. Inset: PS overlaid with a scale to show detailed graft (white arrowhead) position (A); Graft cells contribution to LPM at EC day 1-3 (B); Contribution to DA (white arrows pointing to aortae walls) observed at EC day 2 (C); Contribution to DA (white arrows) observed at EC day 3. DA fusion is initiated anterior to shown aortae walls. (D); Chimera cross-section anterior to DA-OMA fusion. DA lining is GFP+. A cluster of cells (white arrowhead) contains GFP+ cells (E). Some GFP+ cells express Runx1 (magenta arrows), other GFP+ cells are Runx1- (green arrow) (F).

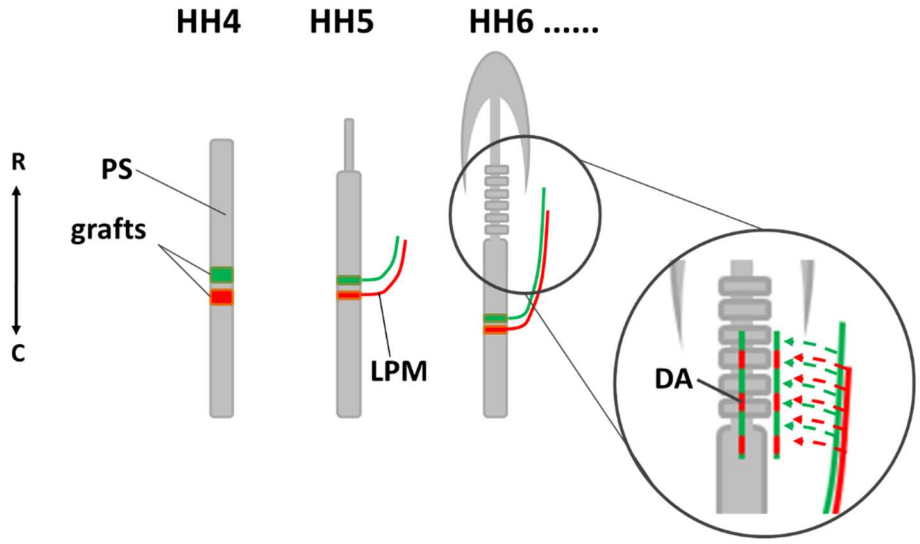

Figure 38. Model of primitive streak contribution to dorsal aorta. Neighboring regions of primitive streak (PS, shown here as grafts of differentr colour) contribute to adjacent stretches of lateral plate mesoderm (LPM). LPM migrate rostrally along chick embryo midline. When LPM cells reach their final position, secondary movement of LPM cells takes place. LPM cells (angioblasts) migrate towards embryo midline where they contribute to the brenches of primordial dorsal aortae. Since stretch of LPM producing DA angioblasts is formed from different PS descendants, DA is formed by descendants of different regions of PS.

3.4. Conclusions

In this chapter we discussed results of tracing progenitors of the dorsal aorta (DA) in chicken embryos from primitive streak stages (PS). In prior works the primitive streak was mapped out in detail, but dorsal aorta mapping was overlooked [Psychoyos and Stern, 1996; Sweetman et al., 2008; Limura et al. 2007; Sawada and Aoyama et al., 1999]. We aimed to establish the area of the primitive streak (PS) that contributes exclusively to the dorsal aorta, but not to extraembryonic tissues (yolk sac). Avoiding labelling of yolk sac tissues is important to eliminate marking of primitive blood cells that are generated in the yolk sac before initiation of blood circulation. Yolk sac cells were previously shown to seed hematopoietic organs in the embryo and might contribute to some obscure pool of HSC in adults [Cumano et al., 1996, Rhodes et al., 2008; Kieusseian et al., 2012; Lassila et al., 1979; 1982].

To this end, primitive streak regions in gastrulating chick embryos (from HH3+ to HH6, stages according to Hamburger and Hamilton) were labelled either with injections of lipophilic dyes or surgically [Hamburger and Hamilton, 1992]. Surgical grafting consisted of substitution of the region of the PS in host embryos with a portion of GFP+ PS tissue derived from the same position in the same stage donor embryo.

According to obtained results, the DA is formed by descendants of a long stretch of the PS: mid-streak (30-60% of full PS length) over the number of stages of chick embryo development (HH3-6). Neighbouring regions of the PS contribute to overlapping portions of the DA. Yet, the anterior mid-streak contributes mainly to the rostral DA portion, while caudal mid-streak – to the caudal DA. Therefore, we can conclude that the dorsal aorta is a mosaic organ formed by several descendants of the primitive streak generated during different stages of chick embryo development. This shall be a result of a compensatory mechanism of embryo protection from injuries. Otherwise, in case of an embryo injury, there would be gaps in the

embryo body plan. In this way, cells derived from adjacent regions of the PS intermix and form one stretch of DA (Appendix A11).

Only rostral part of the DA bears intra-aortic clusters (IAC). All grafts that contributed to the rostral aorta regardless of their original position, gave rise to IAC. Therefore, formation of the IAC is position dependent and cell fate is not determined in the primitive streak. This corellates with prior works showing that the dorsal aorta hemogenic endothelium is formed in response to molecular signalling coming from neighbouring tissues: endoderm and ectoderm [Pardanaud L, Dieterlen-Lièvre F., 1999; Jaffredo et al., 1998; 2005; Bollerot 2005]. According to our data, the most promising position to label DA and IAC to trace their progeny in adult chicks is Hmaburger and Hamilton stage 5 of chick embryo development - 50-60% of primitive streak length.

Intensity of GFP+ DA endothelium labelling varied. Some labelled regions had the whole DA endothelium marked while in other regios, the DA endothelium was not completely labelled. Accoding to our observations, DA formed by rostral and caudal PS grafts were not entirely labelled. In contrast the central portion of the graft was labelled more intensively. This can be explained by a mosaic mode of DA assembly: descendants of adjacent PS regions - overlap. On the other hand, the middle of the graft can be considered as a composition of narrow adjacent grafts. It is important to notice here, that depending on the position in the PS, grafts have different migratory routs. E.g., PS regios situated lower will have wide migration trajectory and hence cover shorter caudal-rostral distance. Nevertheless, in the lateral plate mesoderm, PS descendants line up and then start their movement towards the midline. During this movement PS descendants completely intermix.

Similarly, on examination, not all cells in intra-aortic clusters were GFP+. This is the consequence of the mosaic nature of the DA, but also implies that IAC are not of clonal origin.

If they were, clusters would be formed of GFP+ or GFP- cells only. Hence, the clusters are formed by adjacent endothelial cells that initiated the program of budding into the DA lumen.

Interestingly, up to 25% of grafts did not have GFP+ cells contribution to the yolk sac (YS), but had this contribution to the area pellucida vasculature, generated small number of GFP+ cells in the blood flow. GFP+ cells in blood flow were observed before DA fusion, meaning that they were not aortic HSC or their precursors. This gives rise to the possibility that the YS is not the only source of primitive erythroblasts in the chicken embryo, but also the area pellucida vasculature. What the hematopoietic potential of these GFP+ cells is, do they seed hematopoietic organs, or they migrate towards hemogenic endothelium, requires further investigation.

Recording the position of labelled PS cells in the lateral plate mesoderm (LPM) allows us to establish chick embryo stages, and LPM position for labelling DA at later stages. This is a valuable source of information, as chick embryos grafted at early stages have very limited survival *in ovo*. Grafting at LPM *in ovo* at later stages overcomes this challenge.

CHAPTER 4.

CONCLUSIONS AND FUTURE STUDIES

The first transplantable hematopoietic stem cells (HSC) arise in the aorta-gonad mesonephros region (AGM) during early stages of embryo development [Medvinsky et al., 1996; 2011; Muller et al., 2004; Cumano et al., 1996; 2001; Kieusseian et al., 2012; Eaves et al., 2015; Ivanovs et al., 2014]. To date, it is widely accepted that HSC mature in so-called intra-aortic clusters (IAC), which arise at the aorta floor shortly after primordial aortae fusion [Babovic and Eaves, 2014; Bhatia 2007; Boisset et al., 2010, 2011; Bollerot et al., 2005; de Bruijin et al., 2002; Bertrand et al., 2010]. Yet, it is unclear whether these HSC arise and mature exclusively in the DA, its subluminal space or in IAC, or if HSC precursors migrate into the DA from other parts of the embryo, and what their maturation status is.

To elucidate ontogeny of early HSC precursors (pro-HSC), we mapped potential pro-HSC based on expression of transcription factor Runx1which is critical for HSC maturation. Runx1 expressing cells were mapped before in mouse embryos with established blood circulation and in early haploinsufficient $AML1^{+/LacZ}$ mouse embryos. Runx1 immunostaining on wild type mouse embryos was not reported before [Yokomizo and Dzierzak, 2010; Lam et al., 2010; Liakhovitskaia et al., 2014; Bee et al., 2009; Swiers et al., 2010(b); Cai et al., 2011; Chen et al., 2011].

The yolk sac generates the first wave of Runx1+ hematopoietic cells. To exclude migration of Runx1+ yolk sac cells into embryo proper we performed Runx1+ cells mapping in pre-circulation mouse embryos (E6-E8.5).

Our mapping of Runx1+ cells revealed that in pre-somitic mouse embryos the majority of Runx1+ cells are localized to the yolk sac blood islands and chorionic plate. In the chorionic plate, Runx1+ cells not only line its surface, but also form cell clusters. Additionally, rare Runx1+ cells were found in E7.5 mouse embryo allantois. These cells were marking the point

of amalgamation of extra- and intraembryonic vasculature - the vessel of confluence (VOC). The VOC connects the omphalomesenteric artery (OMA), umbilical artery and dorsal aorta [Zeigler et al., 2006; Daane et al., 2011]. A half of day later in development (headfold stage) Runx1+ cells were often found in clusters positioned in the VOC. We envision that Runx1+ cell clusters are the same clusters found in older embryos (E9-E12) in the omphalomesenteric artery, allantois and in placenta [Rhodes et al., 2008; Gekas et al., 2005; Godin et al., 1995; Palis et al., 1999; Kumaravelu et al., 2003]. Identified clusters could contain pre-HCS. To assess HSC potential of tissues containing prospective HSC, cells were isolated from embryonic day 8 (E8) mouse embryos and, after a culture step, tested in transplantation assays.

In our work, we utilized a powerful pro-HSC maturation system that allowed us to mature E9 pro-HSC to be transplantable into the immunocompetent mouse recipients [Sheridan et al., 2009; Rybtsov et al., 2014, 2016]. Regions containing potential pro-HSC (for example, VOC region, allantois, yolk sac; head and heart) were isolated from embryonic day 8 (E8) mouse embryos, cultured and transplanted into sub-lethally irradiated recipients. From 82 recipients transplanted with E8 derived cells one transplant (head and heart region) repopulated the recipient hematopoietic system at the level of 1.2%. The level of blood chimerism in this mouse dropped to 0.3% after 3.5 months. 19 recipients demonstrated low levels (0.1-0.3%) of blood chimerism with the majority of these grafts (46%) derived from the rostral part of the embryo (head, heart, upper somites). The level of recipients' blood chimerism was low, but above the background level (0.1%) of blood chimersim in mice injected with carrier cells only. Therefore, we propose that we identified a low repopulating multilineage precursors and/or early proHSC. To validate HSC nature of these cells further tests are required, for example serial transplantations in secondary hosts.

If we compare this repopulation activity of E8 derived cells to that of cells derived from 22-26 sp (E9) embryos, it would become evident these cells repopulation activity is similar [Rybtsov et al., 2014]. In contrast, the repopulation capacity of cells derived from caudal parts of slightly older E9 embryos (embryos with more than 26 somite pairs, sp) is comparable to that of definitive embryonic HSC. To explain this, we investigated the events that take place in 21-29 sp mouse embryos.

When we examined early E9 embryos, we found that Runx1 expression patterns essentially are not changed from E8 to early E9 embryos. Intensive Runx1 expression is observed in the area of the vessel of confluence (VOC). In addition, according to our results, Runx1 is specifically expressed in the section of the DA adjacent to the VOC. We also found that the area reported by Rybtsov et al. (2014) to bear the pre-HSC is in fact the site where the paired aortae first fuse. According to our data and prior reports, the aortae fusion takes place immediately before transplantable HSCs cells appear in the embryo [Resse et al., 2004; Garriock et al., 2010; Nagase et al., 2006]. We envision that intimate connection between the DA fusion events and induction of pro-HSCs maturation exists.

Therefore, future studies in the direction of development of pro-HSC maturation systems shall also involve cultures treatment with BMP signalling mediators. For instance, by means of co-culture with Bmp4-expressing (and/or Shh, VEGF) stromal cell lines [Lee at al., 2014; Clements and Traver, 2013; Leung et al., 2013; Lawson et al., 2002].

As it is described above, pro-HSC maturation methods established to date are not efficient for the maturation of early embryonic pro-HSC, and another approach to study HSC ontogeny had to be applied. For example, the labelling of the dorsal aorta (DA) and intra-aortic clusters (IAC) will provide a direct answer on the involvement of the DA in definitive haematopoiesis. As transgenic models to specifically label the DA are not available yet, another

approach would be to label the embryonic DA by grafting with tissues that express a specific marker, for example GFP. Chicken embryo develops *ex utero* and tolerates surgical operations and is an excellent animal model to apply this approach [Stern, 2004]. The first task in developing this approach was to identify cells giving rise to the DA and IAC. We have selected gastrulating chick embryos to identify these cells.

To trace cells giving rise to the DA, regions of the primitive streak (PS) were labelled with lipophilic dyes or GFP+ regions of PS were isotopically grafted into stage matched chick embryo recipients [Psychoyos and Stern, 1996; Hatada and Stern CD, 1994]. Recipients were cultured in "early chick" (EC) embryo culture for 1-3 days, during which cells migration was recorded. On day 3 chimeras were collected and processed for detailed contribution analysis by immuno- and histochemistry.

According to our results, cells giving rise to the DA ingress through the long stretch of PS (35-60%, referred as mid-streak here) during several stages of chick embryo development (HH3-6). Neighbouring regions of mid-streak contribute to overlapping portions of the DA. Cells' position in the mid-streak does not determine their position in the dorsal aorta. Position in the DA is defined by the final cells' position in the lateral plate mesoderm (LPM), which in turn depends on the cells' migratory route. For example, cells situated more caudally in mid-streak migrate by a more lateral trajectory than the cells positioned in the anterior mid-streak. In this way, cells positioned to the anterior mid-streak cover shorter distance in the LPM, while those in the caudal mid-streak cover longer distance. As the time of travel for all cells is the same, cells emigrated from different regions of mid-streak end up at different levels in the LPM. In about 20h after cells left mid-streak, the LPM is compacted and LPM cells now form one uninterrupted stretch of LPM with ordered portions of PS descendants: anterior mid-streak descendants situated to the anterior in LPM, and caudal - to the caudal portion of LPM. After

that, secondary movement of cells takes place. Some LPM cells start migration towards embryonic midline contributing to the DA, while other LPM cells migrate laterally contributing to the area pellucida and yolk sac vasculature. Substantial number of LPM cells stays in place. In turn, this explains the requirement to label a substantial number of cells in the PS to achieve visible labelling of the DA. According to our observations, portions of LPM formed by HH4 PS descendants have higher tendency to contribute to extraembryonic vasculature than mid-streak descendants from older embryos. Similar epiblast migration patterns were recorded by Yang et al., (2002 and 2008).

Mid-streak contributes to LPM and so to the DA over the whole gastrulation period [Garcia-Martinez and Schoenwolf, 1992; Stern, 2004]. Our results show that in older embryos the mid-streak contributes to the DA portions, which are positioned slightly more caudally than the DA portion formed by PS in younger embryos. Yet, DA portions formed by PS descendants from younger and older embryos significantly overlap. Therefore, the DA is a mosaic organ, each section of which is formed by descendants of several PS regions at several stages of embryo development. In HH4-6 embryos, mid-streak below 50% of its length contributes mainly to the DA portion caudally to DA-omphalomesenteric artery (OMA) junction. The mid-streak region above 45% of its length contributes to DA portion above DA-OMA junction. This portion of DA (to the anterior of DA-OMA junction) bears IAC [Drevon et al., 2010; Lassila et al., 1999]. When we examined embryos that had contribution to IAC bearing portion of DA, we have found that regardless of the stage of the grafted embryo all grafts contributed to IAC. An interesting observation is that not all IAC were uniformly GFP+ formations. This could suggest that IAC are not of the clonal origin and/or the cells in the cluster are mobile. On the other hand, to date it is not known whether a cluster is a niche of HSC that carries single HSCs, or a whole cluster is a site of maturation of equally potent HSC. To answer this question, further investigation is required. For example, this could be done with life imaging of IAC in chicken

embryo chimeras with light sheet fluorescence microscopy. Another method would be to trace descendants of GFP+ IAC in adult chicks. This could be achieved either by creating chimeras *in ovo* with consequent chick hatching or with cells suspension transplantations into irradiated chicken embryos or adult chicks [Lassila et al., 1982; Toivanen et al., 1982].

In this work we have developed a method to construct chimeras with labelled DA that bears IAC. Utilization of this method will allow to clarify the role of DA and IAC in definitive haematopoiesis and to answer whether precursors of HSCs arise in DA or in other embryonic areas. We also show that the main embryonic vessel, the dorsal aorta, is a mosaic structure. The same is true for the enigmatic structures, the intra-aortic clusters, which are believed to be the niche for the hematopoietic stem cell. Reported here clusters mosaicity rise the number of questions as for the process of HSC maturation. In particular, are other cells in the clusters serve as the microenvironment for maturing HSC or all cells of the cluster possess the same HSC potential as other cells. Our observations necessitate further cell tracing studies to shed more lights on these questions.

REFERENCES

Adolfsson J, Borge OJ, Bryder D, Theilgaard-Mönch K, Astrand-Grundström I, Sitnicka E, Sasaki Y, Jacobsen SE. Upregulation of Flt3 expression within the bone marrow Lin(-)Sca1(+)c-kit(+) stem cell compartment is accompanied by loss of self-renewal capacity. Immunity. 2001 Oct.15(4):659-69. PubMed PMID: 11672547.

Alexander WS, Roberts AW, Nicola NA, Li R, Metcalf D. Deficiencies in progenitor cells of multiple hematopoietic lineages and defective megakaryocytopoiesis in mice lacking the thrombopoietic receptor c-Mpl. Blood. 1996 Mar 15.8 (6):2162-70. PubMed PMID: 8630375.

Alvarez-Silva M, Belo-Diabangouaya P, Salaün J, Dieterlen-Lièvre F. Mouse placenta is a major hematopoietic organ. Development. 2003 Nov.130(22):5437-44. PubMed PMID: 14507780.

Anderson DM, Lyman SD, Baird A, Wignall JM, Eisenman J, Rauch C, March CJ, Boswell HS, Gimpel SD, Cosman D, et al. Molecular cloning of mast cell growth factor, a hematopoietin that is active in both membrane bound and soluble forms. Cell. 1990 Oct 5.63(1):235-43. PubMed PMID: 1698558.

Anderson DM, Williams DE, Tushinski R, Gimpel S, Eisenman J, Cannizzaro LA, Aronson M, Croce CM, Huebner K, Cosman D, et al. Alternate splicing of mRNAs encoding human mast cell growth factor and localization of the gene to chromosome 12q22-q24. Cell Growth Differ. 1991 Aug.2(8):373-8. PubMed PMID: 1724381.

Arora R, Papaioannou VE. The murine allantois: a model system for the study of blood vessel formation. Blood. 2012 Sep 27.120(13):2562-72. PubMed PMID: 22855605.

Arrighi JF, Hauser C, Chapuis B, Zubler RH, Kindler V. Long-term culture of human CD34(+) progenitors with FLT3-ligand, thrombopoietin, and stem cell factor induces extensive amplification of a CD34(-) CD14(-) and a CD3(-) CD14(+) dendritic cell precursor. Blood. 1999 Apr 1.9 (7):2244-52. PubMed PMID: 10090933.

Babovic S, Eaves CJ. Hierarchical organization of fetal and adult hematopoietic stem cells. Exp Cell Res. 2014 Dec 10.329(2):185-91. PubMed PMID: 25128815.

Batta K, Menegatti S, Garcia-Alegria E, Florkowska M, Lacaud G, Kouskoff V. Concise Review: Recent Advances in the In Vitro Derivation of Blood Cell Populations. Stem Cells Transl Med. 2016 Oct.5(10):1330-1337PubMed PMID: 27388244.

Beachy PA, Hymowitz SG, Lazarus RA, Leahy DJ, Siebold C. Interactions between Hedgehog proteins and their binding partners come into view. Genes Dev. 2010 Sep 15.24(18):2001-12. PubMed PMID: 20844013.

Becker AJ, McCulloch EA, Till JE. Pillars article: Cytological demonstration of the clonal nature of spleen colonies derived from transplanted mouse marrow cells. Nature. 1963. 197:452-454. J Immunol. 2014 Jun 1.192(11):4945-7. PubMed PMID: 24837151.

Beddington RS. An autoradiographic analysis of tissue potency in different regions of the embryonic ectoderm during gastrulation in the mouse. J Embryol Exp Morphol. 1982 Jun.69:265-85. PubMed PMID: 7119671.

Bee T, Ashley EL, Bickley SR, Jarratt A, Li PS, Sloane-Stanley J, Göttgens B, de Bruijn MF. The mouse Runx1 +23 hematopoietic stem cell enhancer confers hematopoietic specificity to both Runx1 promoters. Blood. 2009 May 21.113(21):5121-4. PubMed PMID: 19321859.

Bee T, Liddiard K, Swiers G, Bickley SR, Vink CS, Jarratt A, Hughes JR, Medvinsky A, de Bruijn MF. Alternative Runx1 promoter usage in mouse developmental hematopoiesis. Blood Cells Mol Dis. 2009 Jul-Aug.43(1):35-42. PubMed PMID: 19464215.

Bee T, Swiers G, Muroi S, Pozner A, Nottingham W, Santos AC, Li PS, Taniuchi I, de Bruijn MF. Nonredundant roles for Runx1 alternative promoters reflect their activity at discrete stages of developmental hematopoiesis. Blood. 2010 Apr 15.115(15):3042-50. PubMed PMID: 20139099.

Bell, G.W., Yatskievych, T.A., and Antin, P.B. (2004) GEISHA, a high throughput whole mount in situ hybridization screen in chick embryos. Devel. Dynamics 229: 677-687.

Bellairs, Ruth, and Mark Osmond. 2005. The atlas of chick development. Amsterdam: Elsevier.

Bertrand JY, Chi NC, Santoso B, Teng S, Stainier DY, Traver D. Haematopoietic stem cells derive directly from aortic endothelium during development. Nature. 2010 Mar 4.46 (7285):108-11. PubMed PMID: 20154733.

Bertrand JY, Cisson JL, Stachura DL, Traver D. Notch signaling distinguishes 2 waves of definitive hematopoiesis in the zebrafish embryo. Blood.2010.115(14):2777-2783

Bhatia M. Hematopoietic development from human embryonic stem cells. Hematology Am Soc Hematol Educ Program. 2007:11-6. Review. PubMed PMID: 18024603.

Bleesing JJ, Fleisher TA. Human B cells express a CD45 isoform that is similar to murine B220 and is downregulated with acquisition of the memory B-cell marker CD27. Cytometry B Clin Cytom. 2003 Jan.51(1):1-8. PubMed PMID: 12500291.

Blume-Jensen P, Siegbahn A, Stabel S, Heldin CH, Rönnstrand L. Increased Kit/SCF receptor induced mitogenicity but abolished cell motility after inhibition of protein kinase C. EMBO J. 1993 Nov.12(11):4199-209. PubMed PMID: 7693453.

Boisset JC, Andrieu-Soler C, van Cappellen WA, Clapes T, Robin C. Ex vivo time-lapse confocal imaging of the mouse embryo aorta. Nat Protoc. 2011 Oct 27.6(11):1792-805. PubMed PMID: 22036882.

Boisset JC, van Cappellen W, Andrieu-Soler C, Galjart N, Dzierzak E, Robin C. In vivo imaging of haematopoietic cells emerging from the mouse aortic endothelium. Nature. 2010 Mar 4.464(7285):116-20. PubMed PMID: 20154729.

Bollerot K, Pouget C, Jaffredo T. The embryonic origins of hematopoietic stem cells: a tale of hemangioblast and hemogenic endothelium. APMIS. 2005 Nov-Dec.113(11-12):790-803. PubMed PMID: 16480450.

Bollerot K, Romero S, Dunon D, Jaffredo T. Core binding factor in the early avian embryo: cloning of Cbfbeta and combinatorial expression patterns with Runx1. Gene Expr Patterns. 2005 Dec.6(1):29-39. PubMed PMID: 16033710.

Boyer SW, Schroeder AV, Smith-Berdan S, Forsberg EC. All hematopoietic cells develop from hematopoietic stem cells through Flk2/Flt3-positive progenitor cells. Cell Stem Cell. 2011 Jul 8.9(1):64-73. PubMed PMID: 21726834.

Bray S. A Notch affair. Cell. 1998 May 15.93(4):499-503. PubMed PMID: 9604926.

Bressan M, Mikawa T. Avians as a model system of vascular development. Methods Mol Biol. 2015.1214:225-42. PubMed PMID: 25468608.

Broudy VC. Stem cell factor and hematopoiesis. Blood. 1997 Aug 15.90(4):1345-64. Review. PubMed PMID: 9269751.

Broughton SE, Dhagat U, Hercus TR, Nero TL, Grimbaldeston MA, Bonder CS, Lopez AF, Parker MW. The GM-CSF/IL-3/IL-5 cytokine receptor family: from ligand recognition to initiation of signaling. Immunol Rev. 2012 Nov.250(1):277-302. doi: 10.1111/j.1600-065X.2012.01164.x. Review. PubMed PMID: 23046136.

Broughton SE, Nero TL, Dhagat U, Kan WL, Hercus TR, Tvorogov D, Lopez AF, Parker MW. The βc receptor family - Structural insights and their functional implications. Cytokine. 2015 Aug.74(2):247-58. Review. PubMed PMID: 25982846.

Bryder D, Jacobsen SE. Interleukin-3 supports expansion of long-term multilineage repopulating activity after multiple stem cell divisions in vitro. Blood. 2000 Sep 1.96(5):1748 55. PubMed PMID: 10961873.

Burns CE, Traver D, Mayhall E, Shepard JL, Zon LI. Hematopoietic stem cell fate is established by the Notch-Runx pathway. Genes Dev.2005.19(19):2331-2342.

Busch K, Klapproth K, Barile M, Flossdorf M, Holland-Letz T, Schlenner SM, Reth M, Höfer T, Rodewald HR. Fundamental properties of unperturbed haematopoiesis from stem cells in vivo. Nature. 2015 Feb 26.518(7540):542-6. PubMed PMID: 25686605.

Butko E, Distel M, Pouget C, Weijts B, Kobayashi I, Ng K, Mosimann C, Poulain FE, McPherson A, Ni CW, Stachura DL, Del Cid N, Espín-Palazón R, Lawson ND, Dorsky R, Clements WK, Traver D. Gata2b is a restricted early regulator of hemogenic endothelium in the zebrafish embryo. Development. 2015 Mar 15.142(6):1050-61.

Butko E, Pouget C, Traver D. Complex regulation of HSC emergence by the Notch signaling pathway. Dev Biol. 2016 Jan 1.409(1):129-38. PubMed PMID: 26586199.

Byrd, N., Becker, S., Maye, P., Narasimhaiah, R., St-Jacques, B., Zhang, X., McMahon, J., McMahon, A. and Grabel, L. (2002). Hedgehog is required for murine yolk sac angiogenesis. Development 129, 361-372

Cai X, Gaudet JJ, Mangan JK, Chen MJ, De Obaldia ME, Oo Z, Ernst P, Speck NA. Runx1 loss minimally impacts long-term hematopoietic stem cells. PLoS One. 2011.6(12):e28430. PubMed PMID: 22145044.

Cai Z, de Bruijn M, Ma X, Dortland B, Luteijn T, et al. Haploinsufficiency of AML1 affects the temporal and spatial generation of hematopoietic stem cells in the mouse embryo. Immunity. 2000 Oct.13(4):423-31. PubMed PMID: 11070161.

Camp E, Munsterberg A. Ingression, migration and early differentiation of cardiac progenitors. Front Biosci (Landmark Ed). 2011 Jun 1.16:2416-26. Review. PubMed PMID: 21622186.

Capmany G, Querol S, Cancelas JA, García J. Short-term, serum-free, static culture of cord blood-derived CD34+ cells: effects of FLT3-L and MIP-1alpha on in vitro expansion of hematopoietic progenitor cells. Haematologica. 1999 Aug.84(8):675-82. PubMed PMID: 10457401.

Carlesso N, Cardoso AA. Stem cell regulatory niches and their role in normal and malignant hematopoiesis. Curr Opin Hematol. 2010 Jul.17(4):281-6. PubMed PMID: 20473160.

Celebi B, Mantovani D, Pineault N. Irradiated Mesenchymal Stem Cells improve the ex vivo expansion of Hematopoietic Progenitors by partly mimicking the bone marrow endosteal environment. J Immunol Methods. 2011 Jul 29.370(1-2):93-103. PubMed PMID: 21699899.

Challen GA, Goodell MA. Runx1 isoforms show differential expression patterns during hematopoietic development but have similar functional effects in adult hematopoietic stem cells. Exp Hematol. 2010 May.38(5):403-16. PubMed PMID: 20206228.

Chen J, Streit A. Induction of the inner ear: stepwise specification of otic fate from multipotent progenitors. Hear Res. 2013 Mar.297:3-12. PubMed PMID: 23194992.

Chen MJ, Li Y, De Obaldia ME, Yang Q, Yzaguirre AD, Yamada-Inagawa T, Vink CS, Bhandoola A, Dzierzak E, Speck NA. Erythroid/myeloid progenitors and hematopoietic stem cells originate from distinct populations of endothelial cells. Cell Stem Cell. 2011 Dec 2.9(6):541-52. PubMed PMID: 22136929.

Chen MJ, Yokomizo T, Zeigler BM, Dzierzak E, Speck NA. Runx1 is required for the endothelial to haematopoietic cell transition but not thereafter. Nature. 2009 Feb 12.457(7231):887-91. PubMed PMID: 19129762.

Chen TT, Luque A, Lee S, Anderson SM, Segura T, Iruela-Arispe ML. Anchorage of VEGF to the extracellular matrix conveys differential signaling responses to endothelial cells. J Cell Biol. 2010 Feb 22. 188(4):595-609. PubMed PMID: 20176926.

Christensen JL, Wright DE, Wagers AJ, Weissman IL. Circulation and chemotaxis of fetal hematopoietic stem cells. PLoS Biol. 2004 Mar.2(3):E75. Epub 2004 Mar 16. PubMed PMID: 15024423.

Ciau-Uitz A, Pinheiro P, Gupta R, Enver T, Patient R. Tel1/ETV6 specifies blood stem cells through the agency of VEGF signaling. Dev Cell. 2010 Apr 20.18(4):569-78. PubMed PMID: 20412772.

Cleaver O, Krieg PA. VEGF mediates angioblast migration during development of the dorsal aorta in Xenopus. Development. 1998 Oct.125(19):3905-14. PubMed PMID: 9729498.

Copley MR, Beer PA, Eaves CJ. Hematopoietic stem cell heterogeneity takes center stage. Cell Stem Cell. 2012 Jun 14.10(6):690-7. PubMed PMID: 22704509.

Corbel C, Salaün J, Belo-Diabangouaya P, Dieterlen-Lièvre F. Hematopoietic potential of the pre-fusion allantois. Dev Biol. 2007 Jan 15.301(2):478-88. PubMed PMID: 17010964.

Crisan M, Dzierzak E. The many faces of hematopoietic stem cell heterogeneity. Development. 2016 Dec 15.143(24):4571-4581. Review. PubMed PMID: 27965438.

Crisan M, Solaimani Kartalaei P, Neagu A, Karkanpouna S, Yamada-Inagawa T, Purini C, Vink CS, van der Linden R, van Ijcken W, Chuva de Sousa Lopes SM, Monteiro R, Mummery C, Dzierzak E. BMP and Hedgehog Regulate Distinct AGM Hematopoietic Stem Cells Ex Vivo. Stem Cell Reports. 2016 Mar 8.6(3):383-95. PubMed PMID: 26923823.

Cumano A, Dieterlen-Lievre F, Godin I. Lymphoid potential, probed before circulation in mouse, is restricted to caudal intraembryonic splanchnopleura. Cell. 1996 Sep 20.86(6):907-16. PubMed PMID: 8808626.

Cumano A, Ferraz JC, Klaine M, Di Santo JP, Godin I. Intraembryonic, but not yolk sac hematopoietic precursors, isolated before circulation, provide long-term multilineage reconstitution. Immunity. 2001 Sep.15(3):477-85. PubMed PMID: 11567637.

Custer RP, Bosma GC, Bosma MJ. Severe combined immunodeficiency (SCID) in the mouse. Pathology, reconstitution, neoplasms. Am J Pathol. 1985 Sep.120(3):464-77. PubMed PMID: 2412448. PubMed Central PMCID: PMC1887984.

Daane JM, Enders AC, Downs KM. Mesothelium of the murine allantois exhibits distinct regional properties. J Morphol. 2011 May.272(5):536-56. PubMed PMID: 21284019. NIHMSID: NIHMS262562. PubMed Central PMCID: PMC3078636.

Darnell, D.K., Kaur, S., Stanislaw, S., Davey, S., Konieczka, J.H., Yatskievych, T.A., and Antin, P.B. (2007). GEISHA: An In situ hybridization gene expression resource for the chicken embryo. Cytogenet. Genome Res. 117:30-35.

Davidson AJ, Ernst P, Wang Y, Dekens MP, Kingsley PD, Palis J, Korsmeyer SJ, Daley GQ, Zon LI. cdx4 mutants fail to specify blood progenitors and can be rescued by multiple hox genes. Nature. 2003 Sep 18.425(6955):300-6. PubMed PMID: 13679919.

Davis RL, Turner DL. Vertebrate hairy and Enhancer of split related proteins: transcriptional repressors regulating cellular differentiation and embryonic patterning. Oncogene. 2001 Dec 20.20(58):8342-57. Review. PubMed PMID: 11840327.

de Bruijn M, Dzierzak E. Runx transcription factors in the development and function of the definitive hematopoietic system. Blood. 2017 Apr 13.129(15):2061-2069. doi: 10.1182/blood-2016-12-689109. Epub 2017 Feb 8. Review. PubMed PMID: 28179276.

de Bruijn MF, Ma X, Robin C, Ottersbach K, Sanchez MJ, Dzierzak E. Hematopoietic stem cells localize to the endothelial cell layer in the midgestation mouse aorta. Immunity. 2002 May.16(5):673-83. PubMed PMID: 12049719.

de Bruijn MF, Speck NA, Peeters MC, Dzierzak E. Definitive hematopoietic stem cells first develop within the major arterial regions of the mouse embryo. EMBO J. 2000 Jun 1.19(11):2465-74. PubMed PMID: 10835345. PubMed Central PMCID: PMC212758.

de Haan G, et al. In vitro generation of long-term repopulating hematopoietic stem cells by fibroblast growth factor-1. Developmental cell. 2003. 4:241–251. PubMed ID: 12586067.

De La Garza A, Sinha A, Bowman TV. Concise Review: Hematopoietic Stem Cell Origins: Lessons from Embryogenesis for Improving Regenerative Medicine. Stem Cells Transl Med. 2017 Jan.6(1):60-67. doi: 10.5966/sctm.2016-0110. Epub 2016 Aug 2. PubMed PMID: 28170201.

de Pater E, Kaimakis P, Vink CS, Yokomizo T, Yamada-Inagawa T, van der Linden R, Kartalaei PS, Camper SA, Speck N, Dzierzak E. Gata2 is required for HSC generation and survival. J Exp Med. 2013 Dec 16.210(13):2843-50. doi: 10.1084/jem.20130751. Epub 2013 Dec 2. PubMed PMID: 24297996. PubMed Central PMCID: PMC3865477.

Dentelli P, Del Sorbo L, Rosso A, Molinar A, Garbarino G, Camussi G, Pegoraro L, Brizzi MF. Human IL-3 stimulates endothelial cell motility and promotes in vivo new vessel formation. J Immunol. 1999 Aug 15.163(4):2151-9. PubMed PMID: 10438956.

Dialynas DP, Quan ZS, Wall KA, Pierres A, Quintáns J, Loken MR, Pierres M, Fitch FW. Characterization of the murine T cell surface molecule, designated L3T4, identified by monoclonal antibody GK1.5: similarity of L3T4 to the human Leu-3/T4 molecule. J Immunol. 1983 Nov.131(5):2445-51. PubMed PMID: 6415170.

Dieterlen-Lièvre F, Corbel C, Salaün J. Allantois and placenta as developmental sources of hematopoietic stem cells. Int J Dev Biol. 2010.54(6-7):1079-87. PubMed PMID: 20563985.

Dieterlen-Lièvre F, Jaffredo T. Decoding the hemogenic endothelium in mammals. Cell Stem Cell. 2009 Mar 6.4(3):189-90. PubMed PMID: 19265651.

Dieterlen-Lièvre F, Martin C. Diffuse intraembryonic hemopoiesis in normal and chimeric avian development. Dev Biol. 1981 Nov.88(1):180-91. PubMed PMID: 7286444.

Dieterlen-Lievre F. On the origin of haemopoietic stem cells in the avian embryo: an experimental approach. J Embryol Exp Morphol. 1975 Jun.33(3):607-19. PubMed PMID: 1176862.

Dieterlen-Lièvre F. The quest for hematopoietic stem cells in the embryo An interview with Françoise Dieterlen-Lièvre Interview by Thierry Jaffredo and Charles Durand. Int J Dev Biol. 2010.54(6-7):1075-8. PubMed PMID: 20711985.

DiGiusto D, Chen S, Combs J, Webb S, Namikawa R, Tsukamoto A, Chen BP, Galy AH. Human fetal bone marrow early progenitors for T, B, and myeloid cells are found exclusively in the population expressing high levels of CD34. Blood. 1994 Jul 15.84(2):421-32. PubMed PMID: 7517715.

Ding L, Saunders TL, Enikolopov G, Morrison SJ. Endothelial and perivascular cells maintain haematopoietic stem cells. Nature. 2012 Jan 25.481(7382):457-62. PubMed PMID: 22281595.

Dong HY, Wilkes S, Yang H. CD71 is selectively and ubiquitously expressed at high levels in erythroid precursors of all maturation stages: a comparative immunochemical study with glycophorin A and hemoglobin A. Am. J. Surg. Pathol. 2011 May.35(5):723-32. PubMed PMID: 21415701.

Dorshkind K, Montecino-Rodriguez E. Fetal B-cell lymphopoiesis and the emergence of B-1-cell potential. Nat Rev Immunol. 2007 Mar.7(3):213-9. PubMed PMID: 17318232.

Doulatov S, Vo LT, Chou SS, Kim PG, Arora N, Li H, Hadland BK, Bernstein ID, Collins JJ, Zon LI, Daley GQ. Induction of multipotential hematopoietic progenitors from human pluripotent stem cells via respecification of lineage-restricted precursors. Cell Stem Cell. 2013 Oct 3.13(4):459-70. PubMed PMID: 24094326.

Dowdy CR, Frederick D, Zaidi SK, Colby JL, Lian JB, van Wijnen AJ, Gerstein RM, Stein JL, Stein GS. A germline point mutation in Runx1 uncouples its role in definitive hematopoiesis from differentiation. Exp Hematol. 2013 Nov.41(11):980-991.e1. PubMed PMID: 23823022.

Downs KM, Davies T. Staging of gastrulating mouse embryos by morphological landmarks in the dissecting microscope. Development. 1993 Aug.118(4):1255-66. PubMed PMID: 8269852.

Downs KM, Gifford S, Blahnik M, Gardner RL. Vascularization in the murine allantois occurs by vasculogenesis without accompanying erythropoiesis. Development. 1998 Nov.125(22):4507-20. PubMed PMID: 9778509.

Downs KM, Hellman ER, McHugh J, Barrickman K, Inman KE. Investigation into a role for the primitive streak in development of the murine allantois. Development. 2004 Jan.131(1):37-55. PubMed PMID: 14645124.

Downs KM, Inman KE, Jin DX, Enders AC. The Allantoic Core Domain: new insights into development of the murine allantois and its relation to the primitive streak. Dev Dyn. 2009 Mar.238(3):532-53. PubMed PMID: 19191225.

Downs KM. Florence Sabin and the mechanism of blood vessel lumenization during vasculogenesis. Microcirculation. 2003 Jan.10(1):5-25. PubMed PMID: 12610661.

Driessen RL, Johnston HM, Nilsson SK. Membrane-bound stem cell factor is a key regulator in the initial lodgment of stem cells within the endosteal marrow region. Exp Hematol. 2003 Dec.31(12):1284-91. PubMed PMID: 14662336.

Duarte A, Hirashima M, Benedito R, et al. Dosage sensitive requirement for mouse Dll4 in artery development. Genes Dev.2004.18(20):2474-2478.

Dunn NR, Winnier GE, Hargett LK, Schrick JJ, Fogo AB, Hogan BL. Haploinsufficient phenotypes in Bmp4 heterozygous null mice and modification by mutations in Gli3 and Alx4. Dev Biol. 1997 Aug 15.188(2):235-47. PubMed PMID: 9268572.

Durand C, Robin C, Bollerot K, Baron MH, Ottersbach K, Dzierzak E. Embryonic stromal clones reveal developmental regulators of definitive hematopoietic stem cells. Proc Natl Acad Sci U S A. 2007 Dec 26.104(52):20838-43. Epub 2007 Dec 17. PubMed PMID: 18087045.

Dyer, M. A., Farrington, S. M., Mohn, D., Munday, J. R. and Baron, M. H. (2001). Indian hedgehog activates hematopoiesis and vasculogenesis and can respecify prospective neurectodermal cell fate in the mouse embryo. Development 128, 1717-1730

Dykstra B, Kent D, Bowie M, McCaffrey L, Hamilton M, Lyons K, Lee SJ, Brinkman R, Eaves C. Long-term propagation of distinct hematopoietic differentiation programs in vivo. Cell Stem Cell. 2007 Aug 16.1(2):218-29. PubMed PMID: 18371352.

Dzierzak E. Ontogenic emergence of definitive hematopoietic stem cells. Curr Opin Hematol. 2003 May.10(3):229-34. Review. PubMed PMID: 12690291.

Eaves CJ. Hematopoietic stem cells: concepts, definitions, and the new reality. Blood. 2015 Apr 23.125(17):2605-13. PubMed PMID: 25762175.

Evans CA, Pierce A, Winter SA, Spooncer E, Heyworth CM, Whetton AD. Activation of granulocyte-macrophage colony-stimulating factor and interleukin-3 receptor subunits in a multipotential hematopoietic progenitor cell line leads to differential effects on development. Blood. 1999 Sep 1.94(5):1504-14. PubMed PMID: 10477674.

Eyal-Giladi H, Kochav S. From cleavage to primitive streak formation: a complementary normal table and a new look at the first stages of the development of the chick. I. General morphology. Dev Biol. 1976 Apr.49(2):321-37. PubMed PMID: 944662.

Fahl SP, Crittenden RB, Allman D, Bender TP. c-Myb is required for pro-B cell differentiation. J Immunol. 2009 Nov 1.183(9):5582-92. PubMed PMID: 19843942.

Fibbe WE, Zijlmans JM, Willemze R. Differential short-term and long-term repopulating ability of stem cell subsets in mice. Stem Cells. 1997.1. Pub Med PMID: 9368324.

Fleming TJ, Fleming ML, Malek TR. Selective expression of Ly-6G on myeloid lineage cells in mouse bone marrow. RB6-8C5 mAb to granulocyte-differentiation antigen (Gr-1) detects members of the Ly-6 family. J Immunol. 1993 Sep 1.151(5):2399-408. PubMed PMID: 8360469.

Fraser ST, Baron MH. Embryonic fates for extraembryonic lineages: New perspectives. J Cell Biochem. 2009 Jul 1.107(4):586-91. PubMed PMID: 19415688.

Fraser ST, Ogawa M, Yu RT, Nishikawa S, Yoder MC, et al. Definitive hematopoietic commitment within the embryonic vascular endothelial-cadherin(+) population. Exp Hematol. 2002 Sep.30(9):1070-8. PubMed PMID: 12225799.

Fu JR, Liu WL, Zhou YF, Zhou JF, Sun HY, Luo L, Zhang H, Xu HZ. Expansive effects of aorta-gonad mesonephros-derived stromal cells on hematopoietic stem cells from embryonic stem cells. Chin Med J (Engl). 2005 Dec 5.118(23):1979-86. PubMed PMID: 16336834.

Fujiwara T, Alqadi YW, Okitsu Y, Fukuhara N, Onishi Y, Ishizawa K, Harigae H. Role of transcriptional corepressor ETO2 in erythroid cells. Exp Hematol. 2013 Mar.41(3):303-15.e1. PubMed PMID: 23127762.

Fujiwara Y, Browne CP, Cunniff K, Goff SC, Orkin SH. Arrested development of embryonic red cell precursors in mouse embryos lacking transcription factor GATA-1. Proc Natl Acad Sci U S A. 1996 Oct 29.93(22):12355-8. PubMed PMID: 8901585.

Gabbianelli M, Pelosi E, Montesoro E, Valtieri M, Luchetti L, Samoggia P,Vitelli L, Barberi T, Testa U, Lyman S, et al. Multi-level effects of flt3 ligand on human hematopoiesis: expansion of putative stem cells and proliferation of granulomonocytic progenitors/monocytic precursors. Blood. 1995 Sep 1.86(5):1661-70. PubMed PMID: 7544638.

Gao X, Johnson KD, Chang YI, Boyer ME, Dewey CN, Zhang J, Bresnick EH. Gata2 cis-element is required for hematopoietic stem cell generation in the mammalian embryo. J Exp Med. 2013 Dec 16.21 (13):2833-42. doi: 10.1084/jem.20130733. Epub 2013 Dec 2. PubMed PMID: 24297994. PubMed Central PMCID: PMC3865483.

Garcia-Martinez V, Schoenwolf GC. Positional control of mesoderm movement and fate during avian gastrulation and neurulation. Dev Dyn. 1992 Mar.193(3):249-56. PubMed PMID: 1600243.

Garcia-Porrero JA, Manaia A, Jimeno J, Lasky LL, Dieterlen-Lièvre F, et al. Antigenic profiles of endothelial and hemopoietic lineages in murine intraembryonic hemogenic sites. Dev Comp Immunol. 1998 May-Jun.22(3):303-19. PubMed PMID: 9700460.

Garriock RJ, Czeisler C, Ishii Y, Navetta AM, Mikawa T. An anteroposterior wave of vascular inhibitor downregulation signals aortae fusion along the embryonic midline axis. Development. 2010 Nov.137(21):3697-706. PubMed PMID: 20940228.

Garriock RJ, Mikawa T. Early arterial differentiation and patterning in the avian embryo model. Semin Cell Dev Biol. 2011 Dec.22(9):985-92. PubMed PMID: 22020129.

Gekas C, Dieterlen-Lièvre F, Orkin SH, Mikkola HK. The placenta is a niche for hematopoietic stem cells. Dev Cell. 2005 Mar.8(3):365-75. PubMed PMID: 15737932.

Gering M, Patient R. Hedgehog signaling is required for adult blood stem cell formation in zebrafish embryos. Dev Cell. 2005 Mar.8(3):389-400. PubMed PMID: 15737934.

Godin I, Dieterlen-Lièvre F, Cumano A. Emergence of multipotent hemopoietic cells in the yolk sac and paraaortic splanchnopleura in mouse embryos, beginning at 8.5 days postcoitus. Proc Natl Acad Sci U S A. 1995 Jan 31.92(3):773-7. PubMed PMID: 7846049.

Godin IE, Garcia-Porrero JA, Coutinho A, Dieterlen-Lièvre F, Marcos MA. Para-aortic splanchnopleura from early mouse embryos contains B1a cell progenitors. Nature. 1993 Jul 1.364(6432):67-70. PubMed PMID: 8316299.

Gomes I, Sharma TT, Mahmud N, Kapp JD, Edassery S, Fulton N, Liang J, Hoffman R, Westbrook CA. Highly abundant genes in the transcriptosome of human and baboon CD34 antigen-positive bone marrow cells. Blood. 2001 Jul 1.98(1):93-9. PubMed PMID: 11418467.

Gordon-Keylock S, Sobiesiak M, Rybtsov S, Moore K, Medvinsky A. Mouse extraembryonic arterial vessels harbor precursors capable of maturing into definitive HSCs. Blood. 2013 Oct 3.122(14):2338-45. PubMed PMID: 23863896.

Gori JL, Butler JM, Chan YY, Chandrasekaran D, Poulos MG, Ginsberg M, Nolan DJ, Elemento O, Wood BL, Adair JE, Rafii S, Kiem HP. Vascular niche promotes hematopoietic multipotent

progenitor formation from pluripotent stem cells. J Clin Invest. 2015 Mar 2.125(3):1243-54. PubMed PMID: 25664855.

Guiu J, Shimizu R, D'Altri T, Fraser ST, Hatakeyama J, Bresnick EH, Kageyama R, Dzierzak E, Yamamoto M, Espinosa L, Bigas A. Hes repressors are essential regulators of hematopoietic stem cell development downstream of Notch signaling. J Exp Med. 2013 Jan 14.210(1):71-84. PubMed PMID: 23267012.

Guthridge MA, Stomski FC, Thomas D, Woodcock JM, Bagley CJ, Berndt MC, Lopez AF. Mechanism of activation of the GM-CSF, IL-3, and IL-5 family of receptors. Stem Cells. 1998.16(5):301-13. Review. PubMed PMID: 9766809.

Hadland BK, Huppert SS, Kanungo J, Xue Y, Jiang R, Gridley T, Conlon RA, Cheng AM, Kopan R, Longmore GD. A requirement for Notch1 distinguishes 2 phases of definitive hematopoiesis during development. Blood. 2004 Nov 15.104(10):3097-105. PubMed PMID: 15251982.

Hamburger V, Hamilton HL. A series of normal stages in the development of the chick embryo. 1951. Dev Dyn. 1992 Dec.195(4):231-72. PubMed PMID: 1304821.

Hardy RE, Ikpeazu EV. Bone marrow transplantation: a review. J Natl Med Assoc. 1989 May.81(5):518-23. Review. PubMed PMID: 2664196.

Hashimoto K, Fujimoto T, Shimoda Y, Huang X, Sakamoto H, et al. Distinct hemogenic potential of endothelial cells and CD41+ cells in mouse embryos. Dev Growth Differ. 2007 May.49(4):287-300. PubMed PMID: 17501906.

Hatada Y, Stern CD. A fate map of the epiblast of the early chick embryo. Development. 1994 Oct.120(10):2879-89. PubMed PMID: 7607078.

Heike T, Nakahata T. Ex vivo expansion of hematopoietic stem cells by cytokines. Biochim Biophys Acta. 2002 Nov 11.1592(3):313-21. Review. PubMed PMID: 12421675.

Hirakow R, Hiruma T. Scanning electron microscopic study on the development of primitive blood vessels in chick embryos at the early somite-stage. Anat Embryol (Berl). 1981.163(3):299-306. PubMed PMID: 7340557.

Hirakow R, Hiruma T. TEM-studies on development and canalization of the dorsal aorta in the chick embryo. Anat Embryol (Berl). 1983.166(3):307-15. PubMed PMID: 6869848.

Hiruma T, Hirakow R. Formation of the pharyngeal arch arteries in the chick embryo Observations of corrosion casts by scanning electron microscopy. Anat Embryol (Berl). 1995 May.191(5):415-23. PubMed PMID: 7625612.

Hoffman R, Tong J, Brandt J, Traycoff C, Bruno E, McGuire BW, Gordon MS, McNiece I, Srour EF. The in vitro and in vivo effects of stem cell factor on human hematopoiesis. Stem Cells. 1993 Jul.11 Suppl 2:76-82. Review. PubMed PMID: 7691331.

Hogan BL. Bone morphogenetic proteins: multifunctional regulators of vertebrate development. Genes Dev. 1996 Jul 1.10(13):1580-94. Review. PubMed PMID: 8682290.

Hogan KA, Bautch VL. Blood vessel patterning at the embryonic midline. Curr Top Dev Biol. 2004. 62:55-85. Review. PubMed PMID: 15522739.

Hopman RK, DiPersio JF. Advances in stem cell mobilization. Blood Rev. 2014 Jan.28(1):31-40. PubMed PMID: 24476957.

Hori K, Sen A, Artavanis-Tsakonas S. Notch signaling at a glance. J Cell Sci. 2013 May 15.126(Pt 10):2135-40. PubMed PMID: 23729744.

Huber TL, Zhou Y, Mead PE, Zon LI. Cooperative effects of growth factors involved in the induction of hematopoietic mesoderm. Blood. 1998 Dec 1.92(11):4128-37. PubMed PMID: 9834218.

Ichikawa M, Yoshimi A, Nakagawa M, Nishimoto N, Watanabe-Okochi N, Kurokawa M. A role for RUNX1 in hematopoiesis and myeloid leukemia. Int J Hematol. 2013 Jun.97(6):726-34. PubMed PMID: 23613270.

Ikeya M, Takada S. Wnt-3a is required for somite specification along the anteroposterior axis of the mouse embryo and for regulation of cdx-1 expression. Mech Dev. 2001 May.103(1-2):27-33. PubMed PMID: 11335109.

Inman KE, Downs KM. The murine allantois: emerging paradigms in development of the mammalian umbilical cord and its relation to the fetus. Genesis. 2007 May.45(5):237-58. PubMed PMID: 17440924.

Iso T, Kedes L, Hamamori Y. HES and HERP families: multiple effectors of the Notch signaling pathway. J Cell Physiol. 2003 Mar.194(3):237-55. Review. PubMed PMID: 12548545.

Itoh Y, Ikebuchi K, Hirashima K. Interleukin-3 and granulocyte colony-stimulating factor as survival factors in murine hemopoietic stem cells in vitro. Int J Hematol. 1992 Apr.55(2):139-45. PubMed PMID: 1380844.

Ivanovic Z. Interleukin-3 and ex vivo maintenance of hematopoietic stem cells: facts and controversies. Eur Cytokine Netw. 2004 Jan-Mar.15(1):6-13. Review. PubMed PMID: 15217747.

Ivanovs A, Rybtsov S, Anderson RA, Turner ML, Medvinsky A. Identification of the niche and phenotype of the first human hematopoietic stem cells. Stem Cell Reports. 2014 Apr 8.2(4):449-56. PubMed PMID: 24749070. PubMed Central PMCID: PMC3986508.

Ivanovs A, Rybtsov S, Welch L, Anderson RA, Turner ML, et al. Highly potent human hematopoietic stem cells first emerge in the intraembryonic aorta-gonad-mesonephros region. J Exp Med. 2011 Nov 21.208(12):2417-27. PubMed PMID: 22042975.

Jaffredo T, Gautier R, Brajeul V, Dieterlen-Lièvre F. Tracing the progeny of the aortic hemangioblast in the avian embryo. Dev Biol. 2000 Aug 15.224(2):204-14. PubMed PMID: 10926760.

Jaffredo T, Gautier R, Eichmann A, Dieterlen-Lièvre F. Intraaortic hemopoietic cells are derived from endothelial cells during ontogeny. Development. 1998 Nov.125(22):4575-83. PubMed PMID: 9778515.

Jaffredo T, Nottingham W, Liddiard K, Bollerot K, Pouget C, de Bruijn M. From hemangioblast to hematopoietic stem cell: an endothelial connection? Exp Hematol. 2005 Sep.33(9):1029-40. Review. PubMed PMID: 16140151.

Jaye M, Schlessinger J, Dionne CA. Fibroblast growth factor receptor tyrosine kinases: molecular analysis and signal transduction. Biochim Biophys Acta. 1992 Jun 10.1135(2):185-99. Review. PubMed PMID: 1319744.

Ji J, Vijayaragavan K, Bosse M, Menendez P, Weisel K, et al. OP9 stroma augments survival of hematopoietic precursors and progenitors during hematopoietic differentiation from human embryonic stem cells. Stem Cells. 2008 Oct.26(10):2485-95. PubMed PMID: 18669904.

Johansson BM, Wiles MV. Evidence for involvement of activin A and bone morphogenetic protein 4 in mammalian mesoderm and hematopoietic development. Mol Cell Biol. 1995 Jan.1 (1):141-51. PubMed PMID: 7799920.

Jones EA. The initiation of blood flow and flow induced events in early vascular development. Semin Cell Dev Biol. 2011 Dec.22(9):1028-35. PubMed PMID: 22001248.

Kantor AB, Herzenberg LA. Origin of murine B cell lineages. Annu Rev Immunol. 1993. 11:501-38. Review. PubMed PMID: 8476571. Alvarez-Silva M, Belo-Diabangouaya P, Salaün J, Dieterlen-Lièvre F. Mouse placenta is a major hematopoietic organ. Development. 2003 Nov.130(22):5437-44. PubMed PMID: 14507780.

Kawabata M, Imamura T, Miyazono K. Signal transduction by bone morphogenetic proteins. Cytokine Growth Factor Rev. 1998 Mar.9(1):49-61. Review. PubMed PMID: 9720756.

Kawamoto H, Wada H, Katsura Y. A revised scheme for developmental pathways of hematopoietic cells: the myeloid-based model. Int Immunol. 2010 Feb.22(2):65-70. PubMed PMID: 20053701.

Keller JR, Ortiz M, Ruscetti FW. Steel factor (c-kit ligand) promotes the survival of hematopoietic stem/progenitor cells in the absence of cell division. Blood. 1995 Sep 1.86(5):1757-64. PubMed PMID: 7544641.

Keshet E, Lyman SD, Williams DE, Anderson DM, Jenkins NA, Copeland NG, Parada LF. Embryonic RNA expression patterns of the c-kit receptor and its cognate ligand suggest multiple functional roles in mouse development. EMBO J. 1991Sep.10(9):2425-35. PubMed PMID: 1714375.

Kieusseian A, Brunet de la Grange P, Burlen-Defranoux O, Godin I, Cumano A. Immature hematopoietic stem cells undergo maturation in the fetal liver. Development. 2012 Oct.139(19):3521-30.

Kikushige Y, Yoshimoto G, Miyamoto T, Iino T, Mori Y, Iwasaki H, Niiro H, Takenaka K, Nagafuji K, Harada M, Ishikawa F, Akashi K. Human Flt3 is expressed at the hematopoietic stem cell and the granulocyte/macrophage progenitor stages to maintain cell survival. J Immunol. 2008 Jun 1.180(11):7358-67. PubMed PMID: 18490735.

Kim AD, Melick CH, Clements WK, Stachura DL, Distel M, Panáková D, MacRae C, Mork LA, Crump JG, Traver D. Discrete Notch signaling requirements in the specification of hematopoietic stem cells. EMBO J. 2014 Oct 16.33(20):2363-73. PubMed PMID: 25230933.

Kim PG, Nakano H, Das PP, Chen MJ, Rowe RG, Chou SS, Ross SJ, Sakamoto KM, Zon LI, Schlaeger TM, Orkin SH, Nakano A, Daley GQ. Flow-induced protein kinase A-CREB pathway acts via BMP signaling to promote HSC emergence. J Exp Med. 2015 May 4.212(5):633-48. PubMed PMID: 25870201.

Kim S, Prout M, Ramshaw H, Lopez AF, LeGros G, Min B. Cutting edge: basophils are transiently recruited into the draining lymph nodes during helminth infection via IL-3, but infection-induced Th2 immunity can develop without basophil lymph node recruitment or IL-3. J Immunol. 2010 Feb 1.184(3):1143-7. PubMed PMID: 20038645.

Kimura A, Inose H, Yano F, Fujita K, Ikeda T, Sato S, Iwasaki M, Jinno T, Ae K, Fukumoto S, Takeuchi Y, Itoh H, Imamura T, Kawaguchi H, Chung UI, Martin JF, Iseki S, Shinomiya K, Takeda S. Runx1 and Runx2 cooperate during sternal morphogenesis. Development. 2010 Apr.137(7):1159-67. PubMed PMID: 20181744.

Kina T, Ikuta K, Takayama E, Wada K, Majumdar AS, Weissman IL, Katsura Y. The monoclonal antibody TER-119 recognizes a molecule associated with glycophorin A and specifically marks the late stages of murine erythroid lineage. Br J Haematol. 2000 May.109(2):280-7. PubMed PMID: 10848813.

Kissa K, Herbomel P. Blood stem cells emerge from aortic endothelium by a novel type of cell transition. Nature. 2010 Mar 4.464(7285):112-5. PubMed PMID: 20154732.

Kobayashi A, Senzaki K, Ozaki S, Yoshikawa M, Shiga T. Runx1 promotes neuronal differentiation in dorsal root ganglion. Mol Cell Neurosci. 2012 Jan.49(1):23-31. PubMed PMID: 21906677.

Kobayashi I, Kobayashi-Sun J, Kim AD, Pouget C, Fujita N, Suda T, Traver D. Jam1a-Jam2a interactions regulate haematopoietic stem cell fate through Notch signalling. Nature. 2014 Aug 21.512(7514):319-23. PubMed PMID: 25119047.

Komuro K, Itakura K, Boyse E.A., John M, Ly-5: A new T-lymphocyte antigen system. Immunogenetics. 1974. 1: 452. doi:10.1007/BF01564083.

Kopan R, Ilagan MX. The canonical Notch signaling pathway: unfolding the activation mechanism. Cell. 2009 Apr 17.137(2):216-33. PubMed PMID: 19379690.

Krassowska A, Gordon-Keylock S, Samuel K, Gilchrist D, Dzierzak E, et al. Promotion of haematopoietic activity in embryonic stem cells by the aorta-gonad-mesonephros microenvironment. Exp Cell Res. 2006 Nov 1.312(18):3595-603. PubMed PMID: 16952354.

Krebs LT, Shutter JR, Tanigaki K, Honjo T, Stark KL, Gridley T. Haploinsufficient lethality and formation of arteriovenous malformations in Notch pathway mutants. Genes Dev.2004.18(20):2469-2473.

Krebs LT, Xue Y, Norton CR, Shutter JR, Maguire M, Sundberg JP, Gallahan D, Closson V, Kitajewski J, Callahan R, Smith GH, Stark KL, Gridley T. Notch signaling is essential for vascular morphogenesis in mice. Genes Dev. 2000 Jun 1.14(1):1343-52. PubMed PMID: 10837027.

Krebs LT, Xue Y, Norton CR, Shutter JR, Maguire M, Sundberg JP, Gallahan D, Closson V, Kitajewski J, Callahan R, Smith GH, Stark KL, Gridley T. Notch signaling is essential for v scular morphogenesis in mice. Genes Dev. 2000 Jun 1.14(1):1343-52. PubMed PMID: 10837027.

Kulkeaw K, Mizuochi C, Horio Y, Osumi N, Tsuji K, et al. Application of whole mouse embryo culture system on stem cell research. Stem Cell Rev. 2009 Jun.5(2):175-80. PubMed PMID: 19521805.

Kumano K, Chiba S, Kunisato A, Sata M, Saito T, Nakagami-Yamaguchi E, Yamaguchi T, Masuda S, Shimizu K, Takahashi T, Ogawa S, Hamada Y, Hirai H. Notch1 but not Notch2 is essential for generating hematopoietic stem cells from endothelial cells. Immunity. 2003 May.18(5):699-711. PubMed PMID: 12753746.

Kumaravelu P, Hook L, Morrison AM, Ure J, Zhao S, Zuyev S, Ansell J, Medvinsky A. Quantitative developmental anatomy of definitive haematopoietic stem cells/long-term repopulating units (HSC/RUs): role of the aorta-gonad-mesonephros (AGM) region and the yolk sac in colonisation of the mouse embryonic liver. Development. 2002 Nov.129(21):4891-9. Erratum in: Development. 2003 Jan.130(2):425.. PubMed PMID: 12397098.

Kurokawa M. AML1/Runx1 as a versatile regulator of hematopoiesis: regulation of its function and a role in adult hematopoiesis. Int J Hematol. 2006 Aug.84(2):136-42. Review. PubMed PMID: 16926135.

Lacaud G, Kouskoff V, Trumble A, Schwantz S, Keller G. Haploinsufficiency of Runx1 results in the acceleration of mesodermal development and hemangioblast specification upon in vitro

differentiation of ES cells. Blood. 2004 Feb 1.103(3):886 -9. Epub 2003 Oct 2. PubMed PMID: 14525762.

Lai L, Alaverdi N, Maltais L, Morse HC 3rd. Mouse cell surface antigens: nomenclature and immunophenotyping. J Immunol. 1998 Apr 15.160 (8):3861-8. Review. PubMed PMID: 9558091.

Lam EY, Hall CJ, Crosier PS, Crosier KE, Flores MV. Live imaging of Runx1 expression in the dorsal aorta tracks the emergence of blood progenitors from endothelial cells. Blood. 2010 Aug 12.116(6):909-14. PubMed PMID: 20453160.

Lantz CS, Boesiger J, Song CH, Mach N, Kobayashi T, Mulligan RC, Nawa Y, Dranoff G, Galli SJ. Role for interleukin-3 in mast-cell and basophil development and in immunity to parasites. Nature. 1998 Mar 5.392(6671):90-3. PubMed PMID: 9510253.

LaRue AC, Mironov VA, Argraves WS, Czirók A, Fleming PA, et al. Patterning of embryonic blood vessels. Dev Dyn. 2003 Sep.228(1):21-9. PubMed PMID: 12950076.

Lassila O, Eskola J, Toivanen P. Prebursal stem cells in the intraembryonic mesenchyme of the chick embryo at 7 days of incubation. J Immunol. 1979 Nov.123(5):2091-4. PubMed PMID: 489971.

Lassila O, Martin C, Dieterlen-Lièvre F, Gilmour DG, Eskola J, et al. Migration of prebursal stem cells from the early chicken embryo to the yolk sac. Scand J Immunol. 1982 Sep.16(3):265-8. PubMed PMID: 6959256.

Lawson KA, Meneses JJ, Pedersen RA. Clonal analysis of epiblast fate during germ layer formation in the mouse embryo. Development. 1991 Nov.113(3):891-911. PubMed PMID: 1821858.

Lawson ND, Scheer N, Pham VN, et al. Notch signaling is required for arterial-venous differentiation during embryonic vascular development. Development.2001.128(19):3675-3683

Lawson ND, Vogel AM, Weinstein BM. Sonic hedgehog and vascular endothelial growth factor act upstream of the Notch pathway during arterial endothelial differentiation. Dev Cell. 2002 Jul.3(1):127-36. PubMed PMID: 12110173.

Le Douarin NM, Dieterlen-Lièvre F. How studies on the avian embryo have opened new avenues in the understanding of development: a view about the neural and hematopoietic systems. Dev Growth Differ. 2013 Jan.55(1):1-14. PubMed PMID: 23278669.

Ledbetter JA, Herzenberg LA. Xenogeneic monoclonal antibodies to mouse lymphoid differentiation antigens. Immunol. Rev. 1979. 47:63-90. Review. PubMed PMID: 398327.

Lee Y, Manegold JE, Kim AD, Pouget C, Stachura DL, Clements WK, Traver D. FGF signalling specifies haematopoietic stem cells through its regulation of somitic Notch signalling. Nat Commun. 2014 Nov 27.5:5583. PubMed PMID: 25428693.

Lengerke C, Schmitt S, Bowman TV, Jang IH, Maouche-Chretien L, McKinney-Freeman S, Davidson AJ, Hammerschmidt M, Rentzsch F, Green JB, Zon LI, Daley GQ. BMP and Wnt specify hematopoietic fate by activation of the Cdx-Hox pathway. Cell Stem Cell. 2008 Jan 10.2(1):72-82. PubMed PMID: 18371423.

Lennartsson J, Blume-Jensen P, Hermanson M, Pontén E, Carlberg M, Rönnstrand L. Phosphorylation of Shc by Src family kinases is necessary for stem cell factorreceptor/c-kit mediated activation of the Ras/MAP kinase pathway and c-fos induction. Oncogene. 1999 Sep 30.18(40):5546-53. PubMed PMID: 10523831.

Leung A, Ciau-Uitz A, Pinheiro P, Monteiro R, Zuo J, Vyas P, Patient R, Porcher C. Uncoupling VEGFA functions in arteriogenesis and hematopoietic stem cell specification. Dev Cell. 2013 Jan 28.24(2):144-58. PubMed PMID: 23318133.

Lev S, Blechman JM, Givol D, Yarden Y. Steel factor and c-kit protooncogene: genetic lessons in signal transduction. Crit Rev Oncog. 1994.5(2-3):141-68. Review. PubMed PMID: 7531500.

Levis M, Small D. FLT3: ITDoes matter in leukemia. Leukemia. 2003 Sep.17(9):1738-52. Review. PubMed PMID: 12970773.

Li Z, Lan Y, He W, Chen D, Wang J, et al. Mouse embryonic head as a site for hematopoietic stem cell development. Cell Stem Cell. 2012 Nov 2.11(5):663-75. PubMed PMID: 23122290.

Liakhovitskaia A, Gribi R, Stamateris E, Villain G, Jaffredo T, Wilkie R, Gilchrist D, Yang J, Ure J, Medvinsky A. Restoration of Runx1 expression in the Tie2 cell compartment rescues definitive hematopoietic stem cells and extends life of Runx1 knockout animals until birth. Stem Cells. 2009 Jul.27(7):1616-24. doi: 10.1002/stem.71. PubMed PMID: 19544462.

Liakhovitskaia A, Lana-Elola E, Stamateris E, Rice DP, van 't Hof RJ, Medvinsky A. The essential requirement for Runx1 in the development of the sternum. Dev Biol. 2010 Apr 15.340(2):539-46. Epub 2010 Feb 10. PubMed PMID: 20152828.

Liakhovitskaia A, Rybtsov S, Smith T, Batsivari A, Rybtsova N, Rode C, de Bruijn M, Buchholz F, Gordon-Keylock S, Zhao S, Medvinsky A. Runx1 is required for progression of CD41+ embryonic precursors into HSCs but not prior to this. Development. 2014 Sep.141(17):3319-23. doi: 10.1242/dev.110841. PubMed PMID: 25139854. PubMed Central PMCID: PMC4199125.

Lichanska AM, Hume DA. Origins and functions of phagocytes in the embryo. Exp Hematol. 2000 Jun.28(6):601-11. Review. PubMed PMID: 10880746.

Ling KW, Ottersbach K, van Hamburg JP, Oziemlak A, Tsai FY, Orkin SH, Ploemacher R, Hendriks RW, Dzierzak E. GATA-2 plays two functionally distinct roles during the ontogeny of hematopoietic stem cells. J Exp Med. 2004 Oct 4.200(7):871-82. PubMed PMID: 15466621. PubMed Central PMCID: PMC2213282.

Liu J, Sato C, Cerletti M, Wagers A. Notch signaling in the regulation of stem cell self-renewal and differentiation. Curr Top Dev Biol. 2010.92:367-409. PubMed PMID: 20816402.

Liu L, Papa EF, Dooner MS, Machan JT, Johnson KW, Goldberg LR, Quesenberry PJ, Colvin GA. Homing and long-term engraftment of long- and short-term renewal hematopoietic stem cells. PLoS One. 2012.7(2): e31300. PubMed PMID: 22347459

Lizama CO, Hawkins JS, Schmitt CE, Bos FL, Zape JP, Cautivo KM, Borges Pinto H, Rhyner AM, Yu H, Donohoe ME, Wythe JD, Zovein AC. Repression of arterial genes in hemogenic endothelium is sufficient for haematopoietic fate acquisition. Nat Commun. 2015 Jul 23. 6: 7739. PubMed PMID: 26204127.

Look AT. Oncogenic transcription factors in the human acute leukemias. Science. 1997 Nov 7.278(5340):1059-64. Review. PubMed PMID: 9353180.

Lopez-Sanchez C, Garcia-Martinez V, Schoenwolf GC. Localization of cells of the prospective neural plate, heart and somites within the primitive streak and epiblast of avian embryos at intermediate primitive-streak stages. Cells Tissues Organs. 2001.169(4):334-46. PubMed PMID: 11490112.

Lorenz E, Ccongdon C, Uphoff D. Modification of acute irradiation injury in mice and guinea-pigs by bone marrow injections. Radiology. 1952 Jun.58(6):863-77. PubMed PMID: 14941986.

Lux CT, Yoshimoto M, McGrath K, Conway SJ, Palis J, et al. All primitive and definitive hematopoietic progenitor cells emerging before E10 in the mouse embryo are products of the yolk sac. Blood. 2008 Apr 1.111(7):3435-8. PubMed PMID: 17932251.

Lyman SD, James L, Escobar S, Downey H, de Vries P, Brasel K, Stocking K, Beckmann MP, Copeland NG, Cleveland LS, et al. Identification of soluble and membrane-bound isoforms of the murine flt3 ligand generated by alternative splicing of mRNAs. Oncogene. 1995 Jan 5.10(1):149-57. PubMed PMID: 7824267.

Lyman SD, James L, Johnson L, Brasel K, de Vries P, Escobar SS, Downey H, Splett RR, Beckmann MP, McKenna HJ. Cloning of the human homologue of the murine flt3 ligand: a growth factor for early hematopoietic progenitor cells. Blood. 1994 May 15.83(10):2795-801. PubMed PMID: 8180375.

Lyman SD, James L, Zappone J, Sleath PR, Beckmann MP, Bird T. Characterization of the protein encoded by the flt3 (flk2) receptor-like tyrosine kinase gene. Oncogene. 1993 Apr.8(4):815-22. PubMed PMID: 7681159.

Malda J, Klein TJ, Upton Z. The roles of hypoxia in the in vitro engineering of tissues. Tissue Eng. 2007 Sep.13(9):2153-62. PubMed PMID: 17516855.

MaMorrison SJ, Weissman IL. The long-term repopulating subset of hematopoietic stem cells is deterministic and isolatable by phenotype. Immunity. 1994 Nov.1(8):661-73. PubMed PMID: 7541305.

Mangi MH, Newland AC. Interleukin-3 in hematology and oncology: current state of knowledge and future directions. Cytokines Cell Mol Ther. 1999 Jun.5(2):87-95. Review. PubMed PMID: 10515681.

Manova K, Bachvarova RF. Expression of c-kit encoded at the W locus of mice in developing embryonic germ cells and presumptive melanoblasts. Dev Biol. 1991 Aug.146(2):312-24. PubMed PMID: 1713863.

Marsee DK, Pinkus GS, Yu H. CD71 (transferrin receptor): an effective marker for erythroid precursors in bone marrow biopsy specimens. Am. J. Clin. Pathol. 2010 Sep.134(3):429-35. PubMed PMID: 20716799.

Marshall CJ, Kinnon C, Thrasher AJ. Polarized expression of bone morphogenetic protein-4 in the human aorta-gonad-mesonephros region. Blood. 2000 Aug 15.96(4):1591-3. PubMed PMID: 10942412.

Martin C, Lassila O, Nurmi T, Eskola J, Dieterlen-Liévre F, et al. Intraembryonic origin of lymphoid stem cells in the chicken: studies with sex chromosome and IgG allotype markers in histocompatible yolk sac-embryo chimaeras. Scand J Immunol. 1979.10(4):333-8. PubMed PMID: 316918.

Matsui Y, Zsebo KM, Hogan BL. Embryonic expression of a haematopoietic growth factor encoded by the Sl locus and the ligand for c-kit. Nature. 1990 Oct 18.347(6294):667-9. PubMed PMID: 1699134. promote the survival of hematopoietic progenitor cells in the absence of cell division

Matsunaga T, Hirayama F, Yonemura Y, Murray R, Ogawa M. Negative regulation by interleukin-3 (IL-3) of mouse early B-cell progenitors and stem cells in culture: transduction of the negative signals by betac and betaIL-3 proteins of IL-3 receptor and absence of negative regulation by granulocyte-macrophage colony-stimulating factor. Blood. 1998 Aug 1.92(3):901-7. PubMed PMID: 9680358.

Matsuoka S, Tsuji K, Hisakawa H, Xu Mj, Ebihara Y, et al. Generation of definitive hematopoietic stem cells from murine early yolk sac and paraaortic splanchnopleures by aorta-gonad-mesonephros region-derived stromal cells. Blood. 2001 Jul 1.98(1):6-12. PubMed PMID: 11418454.

Matthews W, Jordan CT, Gavin M, Jenkins NA, Copeland NG, Lemischka IR. A receptor tyrosine kinase cDNA isolated from a population of enriched primitive hematopoietic cells and exhibiting close genetic linkage to c-kit. Proc Natl Acad Sci U S A. 1991(a) Oct 15.88(20):9026-30. PubMed PMID: 1717995

McCulloch EA, Till JE. Perspectives on the properties of stem cells. Nat Med. 2005 Oct.11(10):1026-8. Review. PubMed PMID: 16211027.

McGrath KE, Koniski AD, Malik J, Palis J. Circulation is established in a stepwise pattern in the mammalian embryo. Blood. 2003 Mar 1.101(5):1669-76. PubMed PMID: 12406884.

McGrath KE, Palis J. Hematopoiesis in the yolk sac: more than meets the eye. Exp Hematol. 2005 Sep.33(9):1021-8. Review. PubMed PMID: 16140150.

McGrew MJ, Sherman A, Ellard FM, Lillico SG, Gilhooley HJ, Kingsman AJ, Mitrophanous KA, Sang H. Efficient production of germline transgenic chickens using lentiviral vectors. EMBO Rep. 2004 Jul.5(7):728-33. PubMed PMID: 15192698.

McKenna HJ, Stocking KL, Miller RE, Brasel K, De Smedt T, Maraskovsky E, Maliszewski CR, Lynch DH, Smith J, Pulendran B, Roux ER, Teepe M, Lyman SD, Peschon JJ. Mice lacking flt3 ligand have deficient hematopoiesis affecting hematopoietic progenitor cells, dendritic cells, and natural killer cells. Blood. 2000 Jun 1.95(11):3489-97. PubMed PMID: 10828034.

McKinney-Freeman SL, Naveiras O, Daley GQ. Isolation of hematopoietic stem cells from mouse embryonic stem cells. Curr Protoc Stem Cell Biol. 2008 Feb.Chapter 1:Unit 1F.3. PubMed PMID: 18770632.

Meadows SM, Ratliff LA, Singh MK, Epstein JA, Cleaver O. Resolution of defective dorsal aortae patterning in Sema3E-deficient mice occurs via angiogenic remodeling. Dev Dyn. 2013 May.242(5):580-90. PubMed PMID: 23444297.

Medvinsky A, Dzierzak E. Definitive hematopoiesis is autonomously initiated by the AGM region. Cell. 1996 Sep 20.86(6):897-906. PubMed PMID: 8808625.

Medvinsky A, Rybtsov S, Taoudi S. Embryonic origin of the adult hematopoietic system: advances and questions. Development. 2011 Mar.138(6):1017-31. PubMed PMID: 21343360.

Medvinsky AL, Gan OI, Semenova ML, Samoylina NL. Development of day-8 colony-forming unit-spleen hematopoietic progenitors during early murine embryogenesis: spatial and temporal mapping. Blood. 1996 Jan 15.87(2):557-66. PubMed PMID: 8555477.

Meininger CJ, Yano H, Rottapel R, Bernstein A, Zsebo KM, Zetter BR. The c-kit receptor ligand functions as a mast cell chemoattractant. Blood. 1992 Feb 15.79(4):958-63. PubMed PMID: 1371080.

Melchers F. Murine embryonic B lymphocyte development in the placenta. Nature. 1979 Jan 18.277(5693):219-21. PubMed PMID: 317835.

Mendelson A, Frenette PS. Hematopoietic stem cell niche maintenance during homeostasis and regeneration. Nature medicine. 2014.20(8):833-846. doi:10.1038/nm.3647.

Merad M, Sathe P, Helft J, Miller J, Mortha A. The dendritic cell lineage: ontogeny and function of dendritic cells and their subsets in the steady state and the inflamed setting. Annu Rev Immunol. 2013.31:563-604. PubMed PMID: 23516985.

Metcalf D. On hematopoietic stem cell fate. Immunity. 2007 Jun.26(6):669-73. PubMed PMID: 17582339.

Mikedis MM, Downs KM. STELLA-positive subregions of the primitive streak contribute to posterior tissues of the mouse gastrula. Dev Biol. 2012 Mar 1.363(1):201-18. PubMed PMID: 22019303

Mikkola HK, Fujiwara Y, Schlaeger TM, Traver D, Orkin SH. Expression of CD41 marks the initiation of definitive hematopoiesis in the mouse embryo. Blood. 2003 Jan 15.101(2):508-16. PubMed PMID: 12393529.

Minegishi N, Ohta J, Yamagiwa H, Suzuki N, Kawauchi S, Zhou Y, Takahashi S, Hayashi N, Engel JD, Yamamoto M. The mouse GATA-2 gene is expressed in the para-aortic splanchnopleura and aorta-gonads and mesonephros region. Blood. 1999 Jun 15.93(12):4196-207. PubMed PMID: 10361117.

Mizuochi C, Fraser ST, Biasch K, Horio Y, Kikushige Y, et al. Intra-aortic clusters undergo endothelial to hematopoietic phenotypic transition during early embryogenesis. PLoS One. 2012.7(4):e35763. PubMed PMID: 22558218.

Möhle R, Kanz L. Hematopoietic growth factors for hematopoietic stem cell mobilization and expansion. Semin Hematol. 2007 Jul.44(3):193-202. Review. PubMed PMID: 17631183.

Mombaerts P, Iacomini J, Johnson RS, Herrup K, Tonegawa S, Papaioannou VE. RAG-1-deficient mice have no mature B and T lymphocytes. Cell. 1992 Mar 6.68(5):869-77. PubMed PMID: 1547488.

Moore MA, Owen JJ. Chromosome marker studies on the development of the haemopoietic system in the chick embryo. Nature. 1965 Dec 4.208(5014):956 passim. PubMed PMID: 5868856.

Mukherjee A, Veraksa A, Bauer A, Rosse C, Camonis J, Artavanis-Tsakonas S. Regulation of Notch signalling by non-visual beta-arrestin. Nat Cell Biol. 2005 Dec.7(12):1191-201. PubMed PMID: 16284625.

Müller AM, Huppertz S, Henschler R. Hematopoietic Stem Cells in Regenerative Medicine: Astray or on the Path? Transfus Med Hemother. 2016 Jul.43(4):247-254. Epub 2016 Jul 26. Review. PubMed PMID: 27721700.

Müller AM, Medvinsky A, Strouboulis J, Grosveld F, Dzierzak E. Development of hematopoietic stem cell activity in the mouse embryo. Immunity. 1994 Jul.1(4):291-301. PubMed PMID: 7889417

Muller-Sieburg CE, Sieburg HB, Bernitz JM, Cattarossi G. Stem cell heterogeneity: implications for aging and regenerative medicine. Blood. 2012 Apr 26.119(17):3900-7. PubMed PMID: 22408258.

Münsterberg A, Yue Q. Cardiac progenitor migration and specification: The dual function of Wnts. Cell Adh Migr. 2008 Apr-May.2(2):74-6. Epub 2008 Apr 15. PubMed PMID: 19262099

Muschler GF, Nakamoto C, Griffith LG. Engineering principles of clinical cell-based tissue engineering. J Bone Joint Surg Am. 2004 Jul.86-A(7):1541-58. PubMed PMID: 15252108.

Nagase T, Nagase M, Yoshimura K, Machida M, Yamagishi M. Defects in aortic fusion and craniofacial vasculature in the holoprosencephalic mouse embryo under inhibition of sonic hedgehog signaling. J Craniofac Surg. 2006 Jul.17(4):736-44. PubMed PMID: 16877927.

Nakagawa M, Ichikawa M, Kumano K, Goyama S, Kawazu M, Asai T, Ogawa S, Kurokawa M, Chiba S. AML1/Runx1 rescues Notch1-null mutation-induced deficiency of para-aortic splanchnopleural hematopoiesis. Blood. 2006 Nov 15.108(10):3329-34. PubMed PMID: 16888092.

Nakano H, Liu X, Arshi A, Nakashima Y, van Handel B, et al. Haemogenic endocardium contributes to transient definitive haematopoiesis. Nat Commun. 2013.4:1564. PubMed PMID: 23463007.

Nakazawa F, Nagai H, Shin M, Sheng G. Negative regulation of primitive haematopoiesis by the FGF signalling pathway. Blood. 2006. 108:3335–3343.10.1182/blood-2006-05-021386. PubMed ID: 16888091.

Nguyen PD, Hollway GE, Sonntag C, Miles LB, Hall TE, Berger S, Fernandez KJ, Gurevich DB, Cole NJ, Alaei S, Ramialison M, Sutherland RL, Polo JM, Lieschke GJ, Currie PD. Haematopoietic

stem cell induction by somite-derived endothelial cells controlled by meox1. Nature. 2014 Aug 21.512(7514):314-8. doi: 10.1038/nature13678. Epub 2014 Aug 13. PubMed PMID: 25119043.

Nishikawa M, Tahara T, Hinohara A, Miyajima A, Nakahata T, Shimosaka A. Role of the microenvironment of the embryonic aorta-gonad-mesonephros region in hematopoiesis. Ann N Y Acad Sci. 2001 Jun.938:109-16. Review. PubMed PMID: 11458497.

Nishikawa SI, Nishikawa S, Kawamoto H, Yoshida H, Kizumoto M, et al. In vitro generation of lymphohematopoietic cells from endothelial cells purified from murine embryos. Immunity. 1998 Jun.8(6):761-9. PubMed PMID: 9655490.

Noda S, Horiguchi K, Ichikawa H, Miyoshi H. Repopulating activity of ex vivo-expanded murine hematopoietic stem cells resides in the CD48-c-Kit+Sca-1+lineage marker- cell population. Stem Cells. 2008 Mar.26(3):646-55. PubMed PMID: 18079432.

Nohe A, Keating E, Knaus P, Petersen NO. Signal transduction of bone morphogenetic protein receptors. Cell Signal. 2004 Mar.16(3):291-9. Review. PubMed PMID: 14687659.

North T, Gu TL, Stacy T, Wang Q, Howard L, et al. Cbfa2 is required for the formation of intra-aortic hematopoietic clusters. Development. 1999 Jun.126(11):2563-75. PubMed PMID: 10226014.

Nottingham WT, Jarratt A, Burgess M, Speck CL, Cheng JF, Prabhakar S, Rubin EM, Li PS, Sloane-Stanley J, Kong-A-San J, de Bruijn MF. Runx1-mediated hematopoietic stem-cell emergence is controlled by a Gata/Ets/SCL-regulated enhancer. Blood. 2007 Dec 15.110(13):4188-97. PubMed PMID: 17823307.

Oberlin E, Tavian M, Blazsek I, Péault B. Blood-forming potential of vascular endothelium in the human embryo. Development. 2002 Sep.129(17):4147-57. PubMed PMID: 12163416.

Ohishi K, Katayama N, Shiku H, Varnum-Finney B, Bernstein ID. Notch signalling in hematopoiesis. Semin Cell Dev Biol. 2003 Apr.14(2):143-50. Review. PubMed PMID: 12651098.

Okada S, Nakauchi H, Nagayoshi K, Nishikawa S, Nishikawa S, Miura Y, Suda T. Enrichment and characterization of murine hematopoietic stem cells that express c-kit molecule. Blood. 1991 Oct 1.78(7):1706-12. PubMed PMID: 1717068.

Okuda T, van Deursen J, Hiebert SW, Grosveld G, Downing JR. AML1, the target of multiple chromosomal translocations in human leukemia, is essential for normal fetal liver hematopoiesis. Cell. 1996 Jan 26.84(2):321-30. PubMed PMID: 8565077.

Ooi VE, Sanders EJ, Bellairs R. The contribution of the primitive streak to the somites in the avian embryo. J Embryol Exp Morphol. 1986 Mar.92:193-206. PubMed PMID: 3723062.

Oostendorp RA, Harvey KN, Kusadasi N, de Bruijn MF, Saris C, Ploemacher RE, Medvinsky AL, Dzierzak EA. Stromal cell lines from mouse aorta-gonads-mesonephros subregions are potent supporters of hematopoietic stem cell activity. Blood. 2002 Feb 15.99(4):1183-9. PubMed PMID: 11830464.

Osorio KM, Lilja KC, Tumbar T. Runx1 modulates adult hair follicle stem cell emergence and maintenance from distinct embryonic skin compartments. J Cell Biol. 2011 Apr 4.193(1):235-50. PubMed PMID: 21464233.

Ottersbach K, Dzierzak E. The murine placenta contains hematopoietic stem cells within the vascular labyrinth region. Dev Cell. 2005 Mar.8(3):377-87. PubMed PMID: 15737933.

Oubari F, Amirizade N, Mohammadpour H, Nakhlestani M, Zarif MN. The Important Role of FLT3-L in Ex Vivo Expansion of Hematopoietic Stem Cells following Co-Culture with Mesenchymal Stem Cells. Cell J. 2015 Summer.17(2):201-10. Epub 2015 Jul 11. PubMed PMID: 26199899.

Palis J, Robertson S, Kennedy M, Wall C, Keller G. Development of erythroid and myeloid progenitors in the yolk sac and embryo proper of the mouse. Development. 1999 Nov.126(22):5073-84. PubMed PMID: 10529424.

Pandolfi PP, Roth ME, Karis A, Leonard MW, Dzierzak E, et al. Targeted disruption of the GATA3 gene causes severe abnormalities in the nervous system and in fetal liver haematopoiesis. Nat Genet. 1995 Sep.11(1):40-4. PubMed PMID: 7550312.

Pannett, Charles A. et al. The Cultivation of tissues in saline embryonic juice. The Lancet , Volume 203 , Issue 5243 , 381 – 384.

Parameswaran M, Tam PP. Regionalisation of cell fate and morphogenetic movement of the mesoderm during mouse gastrulation. Dev Genet. 1995.17(1):16-28. PubMed PMID: 7554492.

Pardanaud L, Dieterlen-Lièvre F. Manipulation of the angiopoietic/hemangiopoietic commitment in the avian embryo. Development. 1999 Feb.126(4):617-27. PubMed PMID: 9895310.

Pardanaud L, Luton D, Prigent M, Bourcheix LM, Catala M, et al. Two distinct endothelial lineages in ontogeny, one of them related to hemopoiesis. Development. 1996 May.122(5):1363-71. PubMed PMID: 8625825.

Passegué E, Wagers AJ, Giuriato S, Anderson WC, Weissman IL. Global analysis of proliferation and cell cycle gene expression in the regulation of hematopoietic stem and progenitor cell fates. J Exp Med. 2005 Dec 5.202(11):1599-611. PubMed PMID: 16330818.

Peault B, Tavian M. Hematopoietic stem cell emergence in the human embryo and fetus. Ann N Y Acad Sci. 2003 May.996:132-40. PubMed PMID: 12799291.

Peeters M, Ottersbach K, Bollerot K, Orelio C, de Bruijn M, Wijgerde M, Dzierzak E. Ventral embryonic tissues and Hedgehog proteins induce early AGM hematopoietic stem cell development. Development. 2009 Aug.136(15):2613-21. PubMed PMID: 19570846.

Pepinsky RB, Rayhorn P, Day ES, Dergay A, Williams KP, Galdes A, Taylor FR, Boriack-Sjodin PA, Garber EA. Mapping sonic hedgehog-receptor interactions by steric interference. J Biol Chem. 2000 Apr 14.275(15):10995-1001. PubMed PMID: 10753901.

Pereira C, Clarke E, Damen J. Hematopoietic colony-forming cell assays. Methods Mol Biol. 2007. 407:177-208. PubMed PMID: 18453257.

Pick M, Azzola L, Mossman A, Stanley EG, Elefanty AG. Differentiation of human embryonic stem cells in serum-free medium reveals distinct roles for bone morphogenetic protein 4, vascular endothelial growth factor, stem cell factor, and fibroblast growth factor 2 in hematopoiesis. Stem Cells. 2007 Sep.25(9):2206-14. Epub 2007 Jun 7. PubMed PMID: 17556598.

Pietras EM, Warr MR, Passegué E. Cell cycle regulation in hematopoietic stem cells. J Cell Biol. 2011 Nov 28.195(5):709-20. PubMed PMID: 22123859.

Pilon N, Oh K, Sylvestre JR, Bouchard N, Savory J, Lohnes D. Cdx4 is a direct target of the canonical Wnt pathway. Dev Biol. 2006 Jan 1.289(1):55-63. Epub 2005 Nov 23. PubMed PMID: 16309666.

Pimanda JE, Donaldson IJ, de Bruijn MF, Kinston S, Knezevic K, Huckle L, Piltz S, Landry JR, Green AR, Tannahill D, Göttgens B. The SCL transcriptional network and BMP signaling pathway interact to regulate RUNX1 activity. Proc Natl Acad Sci U S A. 2007 Jan 16.104(3):840-5. Epub 2007 Jan 9. PubMed PMID: 17213321.

Polli M, Dakic A, Light A, Wu L, Tarlinton DM, et al. The development of functional B lymphocytes in conditional PU1 knock-out mice. Blood. 2005 Sep 15.106(6):2083-90. PubMed PMID: 15933053.

Pouget C, Gautier R, Teillet MA, Jaffredo T. Somite-derived cells replace ventral aortic hemangioblasts and provide aortic smooth muscle cells of the trunk. Development. 2006 Mar.133(6):1013-22. PubMed PMID: 16467362.

Pouget C, Pottin K, Jaffredo T. Sclerotomal origin of vascular smooth muscle cells and pericytes in the embryo. Developmental biology. 2008. 315:437–447.10.1016/j.ydbio.2007.12.045. PubMed ID: 18255054.

Pozner A, Lotem J, Xiao C, Goldenberg D, Brenner O, Negreanu V, Levanon D, Groner Y. Developmentally regulated promoter-switch transcriptionally controls Runx1 function during embryonic hematopoiesis. BMC Dev Biol. 2007 Jul 12.7:84. PubMed PMID: 17626615.

Prinos P, Joseph S, Oh K, Meyer BI, Gruss P, Lohnes D. Multiple pathways governing Cdx1 expression during murine development. Dev Biol. 2001 Nov 15.239(2):257-69. PubMed PMID: 11784033.

Psychoyos D, Stern CD. Fates and migratory routes of primitive streak cells in the chick embryo. Development. 1996 May.122(5):1523-34. PubMed PMID: 8625839.

Pui JC, Allman D, Xu L, DeRocco S, Karnell FG, Bakkour S, Lee JY, Kadesch T, Hardy RR, Aster JC, Pear WS. Notch1 expression in early lymphopoiesis influences B versus T lineage determination. Immunity. 1999 Sep.11(3):299-308. PubMed PMID: 10514008.

Qiu L, Meagher R, Welhausen S, Heye M, Brown R, Herzig RH. Ex vivo expansion of CD34+ umbilical cord blood cells in a defined serum-free medium (QBSF-60) with early effect cytokines. J Hematother Stem Cell Res. 1999 Dec.8(6):609-18. PubMed PMID: 10645768.

Querol S, Capmany G, Cancelas JA, García J. Expansion of cord blood progenitor cells. Bone Marrow Transplant. 1998 Jun.21 Suppl 3:S77-80. PubMed PMID: 9712502.

Radtke F, Wilson A, Stark G, Bauer M, van Meerwijk J, MacDonald HR, Aguet M. Deficient T cell fate specification in mice with an induced inactivation of Notch1. Immunity. 1999 May.10(5):547-58. PubMed PMID: 10367900. Immunity. 1999 May.10(5):547-58.

Ramsfjell V, Bryder D, Björgvinsdóttir H, Kornfält S, Nilsson L, Borge OJ, Jacobsen SE. Distinct requirements for optimal growth and In vitro expansion of human CD34(+ CD38(-) bone marrow long-term culture-initiating cells (LTC-IC), extended LTC-IC, and murine in vivo long-term reconstituting stem cells. Blood. 1999 Dec 15.94(12):4093-102. PubMed PMID: 10590054.

Ran D, Shia WJ, Lo MC, Fan JB, Knorr DA, Ferrell PI, Ye Z, Yan M, Cheng L, Kaufman DS, Zhang DE. RUNX1a enhances hematopoietic lineage commitment from human embryonic stem cells and inducible pluripotent stem cells. Blood. 2013 Apr 11.121(15):2882-90. PubMed PMID: 23372166.

Reese DE, Hall CE, Mikawa T. Negative regulation of midline vascular development by the notochord. Dev Cell. 2004 May.6(5):699-708. PubMed PMID: 15130494.

Rhee JM, Iannaccone PM. Mapping mouse hemangioblast maturation from headfold stages. Dev Biol. 2012 May 1.365(1):1-13. PubMed PMID: 22426104

Rhodes KE, Gekas C, Wang Y, Lux CT, Francis CS, et al. The emergence of hematopoietic stem cells is initiated in the placental vasculature in the absence of circulation. Cell Stem Cell. 2008 Mar 6.2(3):252-63. PubMed PMID: 18371450

Richard C, Drevon C, Canto PY, Villain G, Bollérot K, et al. Endothelio-mesenchymal interaction controls Runx1 expression and modulates the notch pathway to initiate aortic hematopoiesis. Dev Cell. 2013 Mar 25.24(6):600-11. PubMed PMID: 23537631

Robert-Moreno A, Espinosa L, Sanchez MJ, de la Pompa JL, Bigas A. The notch pathway positively regulates programmed cell death during erythroid differentiation. Leukemia.2007. 21(7):1496-1503.

Robert-Moreno A, Guiu J, Ruiz-Herguido C, López ME, Inglés-Esteve J, Riera L, Tipping A, Enver T, Dzierzak E, Gridley T, Espinosa L, Bigas A. Impaired embryonic haematopoiesis yet normal arterial development in the absence of the Notch ligand Jagged1. EMBO J. 2008 Jul 9.27(13):1886-95. PubMed PMID: 18528438.

Rodrigues NP, Janzen V, Forkert R, Dombkowski DM, Boyd AS, Orkin SH, Enver T, Vyas P, Scadden DT. Haploinsufficiency of GATA-2 perturbs adult hematopoietic stem-cell homeostasis. Blood. 2005 Jul 15.106(2):477-84. Epub 2005 Apr 5. PubMed PMID: 15811962.

Rohatgi R, Milenkovic L, Scott MP. Patched1 regulates hedgehog signaling at the primary cilium. Science. 2007 Jul 20.317(5836):372-6. PubMed PMID: 17641202.

Rolink A, ten Boekel E, Melchers F, Fearon DT, Krop I, Andersson J. A subpopulation of B220+ cells in murine bone marrow does not express CD19 and contains natural killer cell progenitors. J Exp Med. 1996 Jan 1.183(1):187-94. PubMed PMID: 8551222.

Rönnstrand L. Signal transduction via the stem cell factor receptor/c-Kit. Cell Mol Life Sci. 2004 Oct.61(19-20):2535-48. Review. PubMed PMID: 15526160.

Rosnet O, Marchetto S, deLapeyriere O, Birnbaum D. Murine Flt3, a gene encoding a novel tyrosine kinase receptor of the PDGFR/CSF1R family. Oncogene. 1991 Sep.6(9):1641-50. PubMed PMID: 1656368.

Rowe RG, Mandelbaum J, Zon LI, Daley GQ. Engineering Hematopoietic Stem Cells: Lessons from Development. Cell Stem Cell. 2016 Jun 2.18(6):707-20. PubMed PMID: 27257760.

Rowlinson JM, Gering M. Hey 2 acts upstream of Notch in hematopoietic stem cell specification in zebrafish embryos. Blood. 2010. 116:2046–2056.10.1182/blood-2009-11-252635. PubMed ID: 20511544.

Rybtsov S, Batsivari A, Bilotkach K, Paruzina D, Senserrich J, et al. Tracing the origin of the HSC hierarchy reveals an SCF-dependent, IL-3-independent CD43(-) embryonic precursor. Stem Cell Reports. 2014 Sep 9.3(3):489-501. PubMed PMID: 25241746.

Rybtsov S, Ivanovs A, Zhao S, Medvinsky A. Concealed expansion of immature precursors underpins acute burst of adult HSC activity in foetal liver. Development. 2016 Apr 15.143(8):1284-9. PubMed PMID: 27095492.

Rybtsov S, Sobiesiak M, Taoudi S, Souilhol C, Senserrich J, et al. Hierarchical organization and early hematopoietic specification of the developing HSC lineage in the AGM region. J Exp Med. 2011 Jun 6.208(6):1305-15. PubMed PMID: 21624936.

Sabin FR. Preliminary note on the differentiation of angioblasts and the method by which they produce blood-vessels, blood-plasma and red blood-cells as seen in the living chick 1917. J Hematother Stem Cell Res. 2002 Feb.11(1):5-7. PubMed PMID: 11846999.

Samokhvalov A, Gribi R, Stamateris E, Villain G, Jaffredo T, Wilkie R, Gilchrist D, Yang J, Ure J, Medvinsky A. Restoration of Runx1 expression in the Tie2 cell compartment rescues definitive hematopoietic stem cells and extends life of Runx1 knockout animals until birth. Stem Cells. 2009 Jul.2 (7):1616-24. PubMed PMID: 19544462.

Samokhvalov IM, Samokhvalova NI, Nishikawa S. Cell tracing shows the contribution of the yolk sac to adult haematopoiesis. Nature. 2007 Apr 26.446(7139):1056-61. Epub 2007 Mar 21. PubMed PMID: 17377529.

Samokhvalov IM, Thomson AM, Lalancette C, Liakhovitskaia A, Ure J, et al. Multifunctional reversible knockout/reporter system enabling fully functional reconstitution of the AML1/Runx1 locus and rescue of hematopoiesis. Genesis. 2006 Mar.44(3):115-21. PubMed PMID: 16496309.

Samokhvalov IM. Deconvoluting the ontogeny of hematopoietic stem cells. Cell Mol Life Sci. 2014 Mar.71(6):957-78. PubMed PMID: 23708646.

Saravanaperumal SA, Pediconi D, Renieri C, La Terza A. Skipping of exons by premature termination of transcription and alternative splicing within intron-5 of the sheep SCF gene: a novel splice variant. PLoS One. 2012.7(6):e38657PubMed PMID: 22719917.

Sato Y, Poynter G, Huss D, Filla MB, Czirok A, et al. Dynamic analysis of vascular morphogenesis using transgenic quail embryos. PLoS One. 2010 Sep 14.5(9):e12674. PubMed PMID: 20856866.

Sato Y. Dorsal aorta formation: separate origins, lateral-to-medial migration, and remodeling. Dev Growth Differ. 2013 Jan.55(1):113-29. PubMed PMID: 23294360.

Sauvageau G, Humphries RK. Medicine. The blood stem cell Holy Grail? Science. 2010 Sep 10.329(5997):1291-2. PubMed PMID: 20829472.

Sauvageau G, Iscove NN, Humphries RK. In vitro and in vivo expansion of hematopoietic stem cells. Oncogene. 2004 Sep 20.23(43):7223-32. Review. PubMed PMID: 15378082.

Sawada K, Aoyama H. Fate maps of the primitive streak in chick and quail embryo: ingression timing of progenitor cells of each rostro-caudal axial level of somites. Int J Dev Biol. 1999 Nov.43(8):809-15. PubMed PMID: 10707904.

Scheid, M.P. and Triglia, D. Further description of theLy-5 system Immunogenetics. 1979. 9: 423. doi:10.1007/BF01570435.

Schoenwolf GC, Garcia-Martinez V, Dias MS. Mesoderm movement and fate duringavian gastrulation and neurulation. Dev Dyn. 1992 Mar.193(3):235-48. PubMed PMID:1600242.

Schoenwolf GC, Garcia-Martinez V, Dias MS. Mesoderm movement and fate during avian gastrulation and neurulation. Dev Dyn. 1992 Mar.193(3):235-48. PubMed PMID: 1600242.

Schwaber JL, Brunck ME, Lévesque JP, Nielsen LK. Filling the void: allogeneic myeloid cells for transplantation. Curr Opin Hematol. 2016 Jan.23(1):72-7. PubMed PMID: 26554894.

Scott F. Gilbert. Developmental Biology, Seventh Edition, 2003, Sinauer Associates, Inc., Sunderland, MA, ISBN 0-87893-258-5.

Seita J, Weissman IL. Hematopoietic stem cell: self-renewal versus differentiation. Wiley Interdiscip Rev Syst Biol Med. 2010 Nov-Dec.2(6):640-53. doi: 10.1002/wsbm.86. Review. PubMed PMID: 20890962.

Selleck MA, Stern CD. Fate mapping and cell lineage analysis of Hensen's node in the chick embryo. Development. 1991 Jun.112(2):615-26. PubMed PMID: 1794328.

Shah AJ, Smogorzewska EM, Hannum C, Crooks GM. Flt3 ligand induces proliferation of quiescent human bone marrow CD34+CD38- cells and maintains progenitor cells in vitro. Blood. 1996 May 1.87(9):3563-70. PubMed PMID: 8611678.

Shergill B, Meloty-Kapella L, Musse AA, Weinmaster G, Botvinick E. Optical tweezers studies on Notch: single-molecule interaction strength is independent of ligand endocytosis. Dev Cell. 2012 Jun 12.22(6):1313-20. PubMed PMID: 22658935.

Sheridan JM, Taoudi S, Medvinsky A, Blackburn CC. A novel method for the generation of reaggregated organotypic cultures that permits juxtaposition of defined cell populations. Genesis. 2009 May.47(5):346-51. PubMed PMID: 19370754.

Shivdasani RA, Fujiwara Y, McDevitt MA, Orkin SH. A lineage-selective knockout establishes the critical role of transcription factor GATA-1 in megakaryocyte growth and platelet development. EMBO J. 1997 Jul 1.16(13):3965-73. PubMed PMID: 9233806. PubMed Central PMCID: PMC1170020.

Shivdasani RA, Mayer EL, Orkin SH. Absence of blood formation in mice lacking the T-cell leukaemia oncoprotein tal-1/SCL. Nature. 1995 Feb 2.373(6513):432-4. PubMed PMID: 7830794.

Siminovitch L, McCulloch E.A., Till J.E. The distribution of colony forming-forming cells among spleen colonies. J Cell Comp Physiol. 1963 Dec. 62:327-36. PubMed PMID: 14086156.

Sitnicka E, Bryder D, Theilgaard-Mönch K, Buza-Vidas N, Adolfsson J, Jacobsen SE. Key role of flt3 ligand in regulation of the common lymphoid progenitor but not in maintenance of the hematopoietic stem cell pool. Immunity. 2002 Oct.17(4):463-72. PubMed PMID: 12387740.

Snoeck HW. Aging of the hematopoietic system. Curr Opin Hematol. 2013 Jul.20(4):355-61. PubMed PMID: 23739721.

Solar GP, Kerr WG, Zeigler FC, Hess D, Donahue C, de Sauvage FJ, Eaton DL. Role of c-mpl in early hematopoiesis. Blood. 1998 Jul 1.92(1):4-10. PubMed PMID: 9639492.

Souilhol C, Gonneau C, Lendinez JG, Batsivari A, Rybtsov S, et al. Inductive interactions mediated by interplay of asymmetric signalling underlie development of adult haematopoietic stem cells. Nat Commun. 2016 Mar 8.7:10784. PubMed PMID: 26952187

Souilhol C, Lendinez JG, Rybtsov S, Murphy F, Wilson H, Hills D, Batsivari A, Binagui-Casas A, McGarvey AC, MacDonald HR, Kageyama R, Siebel C, Zhao S, Medvinsky A. Developing HSCs become Notch independent by the end of maturation in the AGM region. Blood. 2016B Sep 22.128(12):1567-77.

Spangrude GJ, Heimfeld S, Weissman IL. Purification and characterization of mouse hematopoietic stem cells. Science. 1988 Jul 1.241(4861):58-62. Erratum in: Science 1989 Jun 2.244(4908):1030. PubMed PMID: 2898810.

Speck NA, Gilliland DG. Core-binding factors in haematopoiesis and leukaemia. Nat Rev Cancer. 2002 Jul.2(7):502-13. Review. PubMed PMID: 12094236.

Sroczynska P, Lancrin C, Kouskoff V, Lacaud G. The differential activities of Runx1 promoters define milestones during embryonic hematopoiesis. Blood. 2009 Dec 17.114(26):5279-89. PubMed PMID: 19858498.

Stanley ER. Lineage commitment: cytokines instruct, at last! Cell Stem Cell. 2009 Sep 4.5(3):234-6. PubMed PMID: 19733531.

Stern CD. The chick embryo--past, present and future as a model system in developmental biology. Mech Dev. 2004 Sep.121(9):1011-3. PubMed PMID: 15358007.

Stewart M, Thiel M, Hogg N. Leukocyte integrins. Curr. Opin. Cell Biol. 1995 Oct.7(5):690-6. Review. PubMed PMID: 8573344.

Stier S, Cheng T, Dombkowski D, Carlesso N, Scadden DT. Notch1 activation increases hematopoietic stem cell self-renewal in vivo and favors lymphoid over myeloid lineage outcome. Blood. 2002 Apr 1.99(7):2369-78. PubMed PMID: 11895769.

Strilić B, Kucera T, Eglinger J, Hughes MR, McNagny KM, et al. The molecular basis of vascular lumen formation in the developing mouse aorta. Dev Cell. 2009 Oct.17(4):505-15. PubMed PMID: 19853564.

Sugiyama D, Ogawa M, Nakao K, Osumi N, Nishikawa S, et al. B cell potential can be obtained from pre-circulatory yolk sac, but with low frequency. Dev Biol. 2007 Jan 1.301(1):53-61. PubMed PMID: 17092496.

Sun W, Downing JR. Haploinsufficiency of AML1 results in a decrease in the number of LTR-HSCs while simultaneously inducing an increase in more mature progenitors. Blood. 2004 Dec 1.104(12):3565-72. PubMed PMID: 15297309.

Suzuki N, Yamazaki S, Yamaguchi T, Okabe M, Masaki H, Takaki S, Otsu M, Nakauchi H. Generation of engraftable hematopoietic stem cells from induced pluripotent stem cells by way of teratoma formation. Mol Ther. 2013 Jul.21(7):1424-31. doi: 10.1038/mt.2013.71. Epub 2013 May 14. PubMed PMID: 23670574. PubMed Central PMCID: PMC3705943.

Sweetman D, Wagstaff L, Cooper O, Weijer C, Münsterberg A. The migration of paraxial and lateral plate mesoderm cells emerging from the late primitive streak is controlled by different Wnt signals. BMC Dev Biol. 2008 Jun 9.8:63.

Swiers G, de Bruijn M, Speck NA. Hematopoietic stem cell emergence in the conceptus and the role of Runx1. Int J Dev Biol. 2010b.54(6-7):1151-63. PubMed PMID: 20711992.

Szilvassy SJ, Humphries RK, Lansdorp PM, Eaves AC, Eaves CJ. Quantitative assay for totipotent reconstituting hematopoietic stem cells by a competitive repopulation strategy. Proc Natl Acad Sci USA 1990. 87: 8736–8740.

Takakura N, Watanabe T, Suenobu S, Yamada Y, Noda T, et al. A role for hematopoietic stem cells in promoting angiogenesis. Cell. 2000 Jul 21.102(2):199-209. PubMed PMID: 10943840.

Takase Y, Tadokoro R, Takahashi Y. Low cost labeling with highlighter ink efficiently visualizes developing blood vessels in avian and mouse embryos. Dev Growth Differ. 2013 Dec.55(9):792-801. doi: 10.1111/dgd.12106. Epub 2013 Dec 1. PubMed PMID: 24289211.

Tam PP, Beddington RS. The formation of mesodermal tissues in the mouse embryo during gastrulation and early organogenesis. Development. 1987 Jan.99(1):109-26. PubMed PMID: 3652985.

Tanaka Y, Joshi A, Wilson NK, Kinston S, Nishikawa S, et al. The transcriptional programme controlled by Runx1 during early embryonic blood development. Dev Biol. 2012 Jun 15.366(2):404-19. PubMed PMID: 22554697. c-kit/SCF signalling for HSC maturation in AGM –

Tang Y, Bai H, Urs S, Wang Z, Liaw L. Notch1 activation in embryonic VE-cadherin populations selectively blocks hematopoietic stem cell generation and fetal liver hematopoiesis. Transgenic Res. 2013 Apr.22(2):403-10. PubMed PMID: 22851140.

Taoudi S, Medvinsky A. Functional identification of the hematopoietic stem cell niche in the ventral domain of the embryonic dorsal aorta. Proc Natl Acad Sci U S A. 2007 May 29.104(22):9399-403. PubMed PMID: 17517650.

Tavian M, Coulombel L, Luton D, Clemente HS, Dieterlen-Lièvre F, Péault B. Aorta-associated CD34+ hematopoietic cells in the early human embryo. Blood. 1996 Jan 1.87(1):67-72. PubMed PMID: 8547678.

Tavian M, Hallais MF, Péault B. Emergence of intraembryonic hematopoietic precursors in the pre-liver human embryo. Development. 1999 Feb.126(4):793-803. PubMed PMID: 9895326.

Tavian M, Péault B. Embryonic development of the human hematopoietic system. Int J Dev Biol. 2005.49(2-3):243-50. Review. PubMed PMID: 15906238.

Testa U, Riccioni R, Militi S, Coccia E, Stellacci E, Samoggia P, Latagliata R, Mariani G, Rossini A, Battistini A, Lo-Coco F, Peschle C. Elevated expression of IL-3Ralpha in acute myelogenous leukemia is associated with enhanced blast proliferation, increased cellularity, and poor prognosis. Blood. 2002 Oct 15.100(8):2980-8. PubMed PMID: 12351411.

Thomas ED, Buckner CD, Rudolph RH, Fefer A, Storb R, Neiman PE, Bryant JI, Chard RL, Clift RA, Epstein RB, Fialkow PJ, Funk DD, Giblett ER, Lerner KG, Reynolds FA, Slichter S. Allogeneic marrow grafting for hematologic malignancy using HL-A matched donor-recipient sibling pairs. Blood. 1971 Sep.38(3):267-87. PubMed PMID: 4399859.

Thomas ED, LeBlond R, Graham T, Storb R: Marrow infusions in dogs given midlethal or lethal irradiation. Radiat Res 1970.41:113–124.

Till J.E., McCulloch E.A., A direct measurement of the radiation sensitivity of normal mouse bone marrow cells. Radiat Res. 1961 Feb.14:213-22. PubMed PMID:13776896.

Toivanen P, Lassila O, Eskola J, Martin C, Dieterlen-Lievre F, et al. Migration of erythropoietic and prebursal stem cells from the early chicken embryo to the yolk sac. Adv Exp Med Biol. 1982.149:11-7. PubMed PMID: 7148560.

Tsai FY, Keller G, Kuo FC, Weiss M, Chen J, Rosenblatt M, Alt FW, Orkin SH. An early haematopoietic defect in mice lacking the transcription factor GATA-2. Nature. 1994 Sep 15.371(6494):221-6. PubMed PMID: 8078582.

Tsai FY, Orkin SH. Transcription factor GATA-2 is required for proliferation/survival of early hematopoietic cells and mast cell formation, but not for erythroid and myeloid terminal differentiation. Blood. 1997 May 15.89(10):3636-43. PubMed PMID: 9160668.

Tsapogas P, Swee LK, Nusser A, Nuber N, Kreuzaler M, Capoferri G, Rolink H, Ceredig R, Rolink A. In vivo evidence for an instructive role of fms-like tyrosine kinase-3 (FLT3) ligand in hematopoietic development. Haematologica. 2014 Apr.99(4):638-46. PubMed PMID: 24463214.

Tun T, Hamaguchi Y, Matsunami N, Furukawa T, Honjo T, Kawaichi M. Recognition sequence of a highly conserved DNA binding protein RBP-J kappa. Nucleic Acids Res. 1994 Mar 25.22(6):965-71. PubMed PMID: 8152928.

Tung JW, Mrazek MD, Yang Y, Herzenberg LA, Herzenberg LA. Phenotypically distinct B cell development pathways map to the three B cell lineages in the mouse. Proc Natl Acad Sci U S A. 2006 Apr 18.103(16):6293-8. Epub 2006 Apr 10. PubMed PMID: 16606838. PubMed Central PMCID: PMC1458871.

Turpen JB, Knudson CM, Hoefen PS. The early ontogeny of hematopoietic cells studied by grafting cytogenetically labeled tissue anlagen: localization of a prospective stem cell compartment. Dev Biol. 1981 Jul 15.85(1):99-112. PubMed PMID: 6972885.

Udan RS, Piazza VG, Hsu CW, Hadjantonakis AK, Dickinson ME. Quantitative imaging of cell dynamics in mouse embryos using light-sheet microscopy. Development. 2014 Nov.141(22):4406-14. PubMed PMID: 25344073.

Urso P, Congdon CC. The effect of the amount of isologous bone marrow injected on the recovery of hematopoietic organs, survival and body weight after lethal irradiation injury in mice. Blood. 1957 Mar.12(3):251-60. PubMed PMID: 13403988.

Varnum-Finney B, Xu L, Brashem-Stein C, Nourigat C, Flowers D, Bakkour S, Pear WS, Bernstein ID. Pluripotent, cytokine-dependent, hematopoietic stem cells are immortalized by constitutive Notch1 signaling. Nat Med. 2000 Nov.6(11):1278-81. PubMed PMID: 11062542.

Vereide DT, Vickerman V, Swanson SA, Chu LF, McIntosh BE, Thomson JA. An expandable, inducible hemangioblast state regulated by fibroblast growth factor. Stem Cell Reports. 2014 Dec 9.3(6):1043-57. doi: 10.1016/j.stemcr.2014.10.003. Epub 2014 Nov 13. PubMed PMID: 25458896. PubMed Central PMCID: PMC4264065.

Vicari AP, Zlotnik A. Mouse NK1.1+ T cells: a new family of T cells. Immunol Today. 1996 Feb.17(2):71-6. Review. PubMed PMID: 8808053.

Vodyanik MA, Bork JA, Thomson JA, Slukvin II. Human embryonic stem cell-derived CD34+ cells: efficient production in the coculture with OP9 stromal cells and analysis of lymphohematopoietic potential. Blood. 2005 Jan 15.105(2):617-26. PubMed PMID: 15374881.

Volkmer E, Drosse I, Otto S, Stangelmayer A, Stengele M, et al. Hypoxia in static and dynamic 3D culture systems for tissue engineering of bone. Tissue Eng Part A. 2008 Aug.14(8):1331-40. PubMed PMID: 18601588.

Walker L, Carlson A, Tan-Pertel HT, Weinmaster G, Gasson J. The notch receptor and its ligands are selectively expressed during hematopoietic development in the mouse. Stem Cells. 2001.19(6):543-52. PubMed PMID: 11713346.

Walls JR, Coultas L, Rossant J, Henkelman RM. Three-dimensional analysis of vascular development in the mouse embryo. PLoS One. 2008 Aug 6.3(8):e2853. PubMed PMID: 18682734.

Walmsley M, Cleaver D, Patient R. Fibroblast growth factor controls the timing of Scl, Lmo2, and Runx1 expression during embryonic blood development. Blood. 2008. 111:1157–1166.10.1182/blood-2007-03-081323. PubMed ID: 17942750.

Wang L, Wang J, Li Z, Liu Y, Jiang M, Li Y, Cao D, Zhao M, Wang F, Luo F. Silencing stem cell factor attenuates stemness and inhibits migration of cancer stem cells derived from Lewis lung carcinoma cells. Tumour Biol. 2016 Jun.37(6):7213-27. PubMed PMID: 26666817.

Wang Q, Stacy T, Binder M, Marin-Padilla M, Sharpe AH, Speck NA. Disruption of the Cbfa2 gene causes necrosis and hemorrhaging in the central nervous system and blocks definitive hematopoiesis. Proc Natl Acad Sci U S A. 1996 Apr 16.93(8):3444-9. PubMed PMID: 8622955.

Wang Y, Yates F, Naveiras O, Ernst P, Daley GQ. Embryonic stem cell-derived hematopoietic stem cells. Proc Natl Acad Sci U S A. 2005 Dec 27.102(52):19081-6. PubMed PMID: 16357205.

Wasteson P, Johansson BR, Jukkola T, Breuer S, Akyürek LM, Partanen J, Lindahl P. Developmental origin of smooth muscle cells in the descending aorta in mice. Development. 2008 May.135(10):1823-32. doi: 10.1242/dev.020958. Epub 2008 Apr 16. PubMed PMID: 18417617.

Watowich SS, Liu Y-J. Mechanisms regulating dendritic cell specification and development. Immunological reviews. 2010.238(1):76-92.

Weisel KC, Gao Y, Shieh JH, Moore MA. Stromal cell lines from the aorta-gonado-mesonephros region are potent supporters of murine and human hematopoiesis. Exp Hematol. 2006 Nov.34(11):1505-16. PubMed PMID: 17046570.

Weissman IL. Clonal origins of the hematopoietic system: the single most elegant experiment. J Immunol. 2015 Jun 1.192(11):4943-4. doi: 10.4049/jimmunol.1400902. PubMed PMID: 24837150.

Whetton AD, Bazill GW, Dexter TM. Stimulation of hexose uptake by haemopoietic cell growth factor occurs in WEHI-3B myelomonocytic leukaemia cells: a possible mechanism for loss of growth control. J Cell Physiol. 1985 Apr.123(1):73-8. PubMed PMID: 3882726.

Wiegreffe C, Christ B, Huang R, Scaal M. Remodelling of aortic smooth muscle during avian embryonic development. Developmental dynamics: an official publication of the American Association of Anatomists. 2009. 238:624–631.10.1002/dvdy.21888. PubMed ID: 19235723.

Wiegreffe C, Christ B, Huang R, Scaal M. Sclerotomal origin of smooth muscle cells in the wall of the avian dorsal aorta. Developmental dynamics : an official publication of the American Association of Anatomists. 2007. 236:2578–2585.10.1002/dvdy.21279. PubMed ID: 17685486.

Wilkinson RN, Pouget C, Gering M, Russell AJ, Davies SG, Kimelman D, Patient R. Hedgehog and Bmp polarize hematopoietic stem cell emergence in the zebrafish dorsal aorta. Dev Cell. 2009 Jun.16(6):909-16. PubMed PMID: 19531361.

Wilson A, Laurenti E, Oser G, van der Wath RC, Blanco-Bose W, Jaworski M, Offner S, Dunant CF, Eshkind L, Bockamp E, Lió P, Macdonald HR, Trumpp A. Hematopoietic stem cells reversibly switch from dormancy to self-renewal during homeostasis and repair. Cell. 2008 Dec 12.135(6):1118-29. PubMed PMID: 19062086.

Wilson V, Beddington RS. Cell fate and morphogenetic movement in the late mouse primitive streak. Mech Dev. 1996 Mar.55(1):79-89. PubMed PMID: 8734501.

Withington S, Beddington R, Cooke J. Foregut endoderm is required at head process stages for anteriormost neural patterning in chick. Development. 2001 Feb.128(3):309-20. PubMed PMID: 11152630.

Wolf NS, Trentin JJ. Hemopoietic colony studies. V. Effect of hemopoietic organ stroma on differentiation of pluripotent stem cells. J Exp Med. 1968 Jan 1.127(1):205-14. PubMed PMID: 5635040.

Wood HB, May G, Healy L, Enver T, Morriss-Kay GM. CD34 expression patterns during early mouse development are related to modes of blood vessel formation and reveal additional sites of hematopoiesis. Blood. 1997 Sep 15.90(6):2300-11. PubMed PMID: 9310481.

Xu A, Haines N, Dlugosz M, Rana NA, Takeuchi H, Haltiwanger RS, Irvine KD. In vitro reconstitution of the modulation of Drosophila Notch-ligand binding by Fringe. J Biol Chem. 2007 Nov 30.282(48):35153-62. Epub 2007 Oct 8. PubMed PMID: 17923477.

Yamamoto S, Charng WL, Bellen HJ. Endocytosis and intracellular trafficking of Notch and its ligands. Curr Top Dev Biol. 2010.92:165-200. doi: 10.1016/S0070-2153(10)92005-X. Review. PubMed PMID: 20816395.

Yanai T, Sugimoto K, Takashita E, Aihara Y, Tsurumaki Y, Tsuji T, Mori KJ. Separate control of the survival, the self-renewal and the differentiation of hemopoietic stem cells. Cell Struct Funct. 1995 Apr.20(2):117-24. PubMed PMID: 7641293.

Yang X, Chrisman H, Weijer CJ. PDGF signalling controls the migration of mesoderm cells during chick gastrulation by regulating N-cadherin expression. Development. 2008 Nov.135(21):3521-30.

Yang X, Dormann D, Münsterberg AE, Weijer CJ. Cell movement patterns during gastrulation in the chick are controlled by positive and negative chemotaxis mediated by FGF4 and FGF8. Dev Cell. 2002 Sep.3(3):425-37. PubMed PMID: 12361604.

Yoder MC, Hiatt K, Dutt P, Mukherjee P, Bodine DM, Orlic D. Characterization of definitive lymphohematopoietic stem cells in the day 9 murine yolk sac. Immunity. 1997 Sep.7(3):335-44. PubMed PMID: 9324354.

Yoder MC, Hiatt K, Mukherjee P. In vivo repopulating hematopoietic stem cells are present in the murine yolk sac at day 9.0 postcoitus. Proc Natl Acad Sci U S A. 1997 Jun 24.94(13):6776-80. PubMed PMID: 9192641

Yoder MC, Hiatt K, Mukherjee P. In vivo repopulating hematopoietic stem cells are present in the murine yolk sac at day 9.0 postcoitus. Proc Natl Acad Sci U S A. 1997 Jun 24.94(13):6776-80. PubMed PMID: 9192641. PubMed Central PMCID: PMC21234.

Yokomizo T, Dzierzak E. Three-dimensional cartography of hematopoietic clusters in the vasculature of whole mouse embryos. Development. 2010 Nov.137(21):3651-61. PubMed PMID: 20876651.

Yokomizo T, Ng CE, Osato M, Dzierzak E. Three-dimensional imaging of whole midgestation murine embryos shows an intravascular localization for all hematopoietic clusters. Blood. 2011 Jun 9.117(23):6132-4. PubMed PMID: 21505195.

Yonemura Y, Ku H, Hirayama F, Souza LM, Ogawa M. Interleukin 3 or interleukin 1 abrogates the reconstituting ability of hematopoietic stem cells. Proc Natl Acad Sci U S A. 1996 Apr 30.93(9):4040-4. PubMed PMID: 8633013.

Yoshimoto M, Montecino-Rodriguez E, Ferkowicz MJ, Porayette P, Shelley WC, et al. Embryonic day 9 yolk sac and intra-embryonic hemogenic endothelium independently generate a B-1 and marginal zone progenitor lacking B-2 potential. Proc Natl Acad Sci U S A. 2011 Jan 25.108(4):1468-73. PubMed PMID: 21209332.

Yoshimoto M, Porayette P, Glosson NL, Conway SJ, Carlesso N, et al. Autonomous murine T-cell progenitor production in the extra-embryonic yolk sac before HSC emergence. Blood. 2012 Jun 14.119(24):5706-14. PubMed PMID: 22431573.

Yoshino T, Murai H, Saito D. Hedgehog-BMP signalling establishes dorsoventral patterning in lateral plate mesoderm to trigger gonadogenesis in chicken embryos. Nat Commun. 2016 Aug 25.7:12561. doi: 10.1038/ncomms12561. PubMed PMID: 27558761. PubMed Central PMCID: PMC5007334.

Yu M, Luo J, Yang W, Wang Y, Mizuki M, Kanakura Y, Besmer P, Neel BG, Gu H. The scaffolding adapter Gab2, via Shp-2, regulates kit-evoked mast cell proliferation by activating the Rac/JNK pathway. J Biol Chem. 2006 Sep 29.281(39):28615-26. PubMed PMID: 16873377.

Yue Q, Wagstaff L, Yang X, Weijer C, Münsterberg A. Wnt3a-mediated chemorepulsion controls movement patterns of cardiac progenitors and requires RhoA function. Development. 2008 Mar.135(6):1029-37.

Zagami CJ, Stifani S. Molecular characterization of the mouse superior lateral parabrachial nucleus through expression of the transcription factor Runx1. PLoS One. 2010 Nov 11.5(11):e13944. PubMed PMID: 21085653.

Zandstra PW, Conneally E, Petzer AL, Piret JM, Eaves CJ. Cytokine manipulation of primitive human hematopoietic cell self-renewal. Proc Natl Acad Sci U S A. 1997 Apr 29.94(9):4698-703. PubMed PMID: 9114054.

Zeigler BM, Sugiyama D, Chen M, Guo Y, Downs KM, et al. The allantois and chorion, when isolated before circulation or chorio-allantoic fusion, have hematopoietic potential. Development. 2006 Nov.133(21):4183-92. PubMed PMID: 17038514.

Zhang CC, Lodish HF. Cytokines regulating hematopoietic stem cell function. Curr Opin Hematol. 2008 Jul.15(4):307-11. PubMed PMID: 18536567.

Zhu J, Emerson SG. Hematopoietic cytokines, transcription factors and lineage commitment. Oncogene. 2002 May 13.2 (21):3295-313. Review. PubMed PMID: 12032771.

Zovein AC, Hofmann JJ, Lynch M, French WJ, Turlo KA, Yang Y, Becker MS, Zanetta L, Dejana E, Gasson JC, Tallquist MD, Iruela-Arispe ML. Fate tracing reveals the endothelial origin of hematopoietic stem cells. Cell Stem Cell. 2008 Dec 4.3(6):62 -36. PubMed PMID: 19041779.

Zovein AC, Turlo KA, Ponec RM, Lynch MR, Chen KC, et al. Vascular remodelling of the vitelline artery initiates extravascular emergence of hematopoietic clusters. Blood. 2010 Nov 4.116(18):3435-44. PubMed PMID: 20699440.

APPENDICES

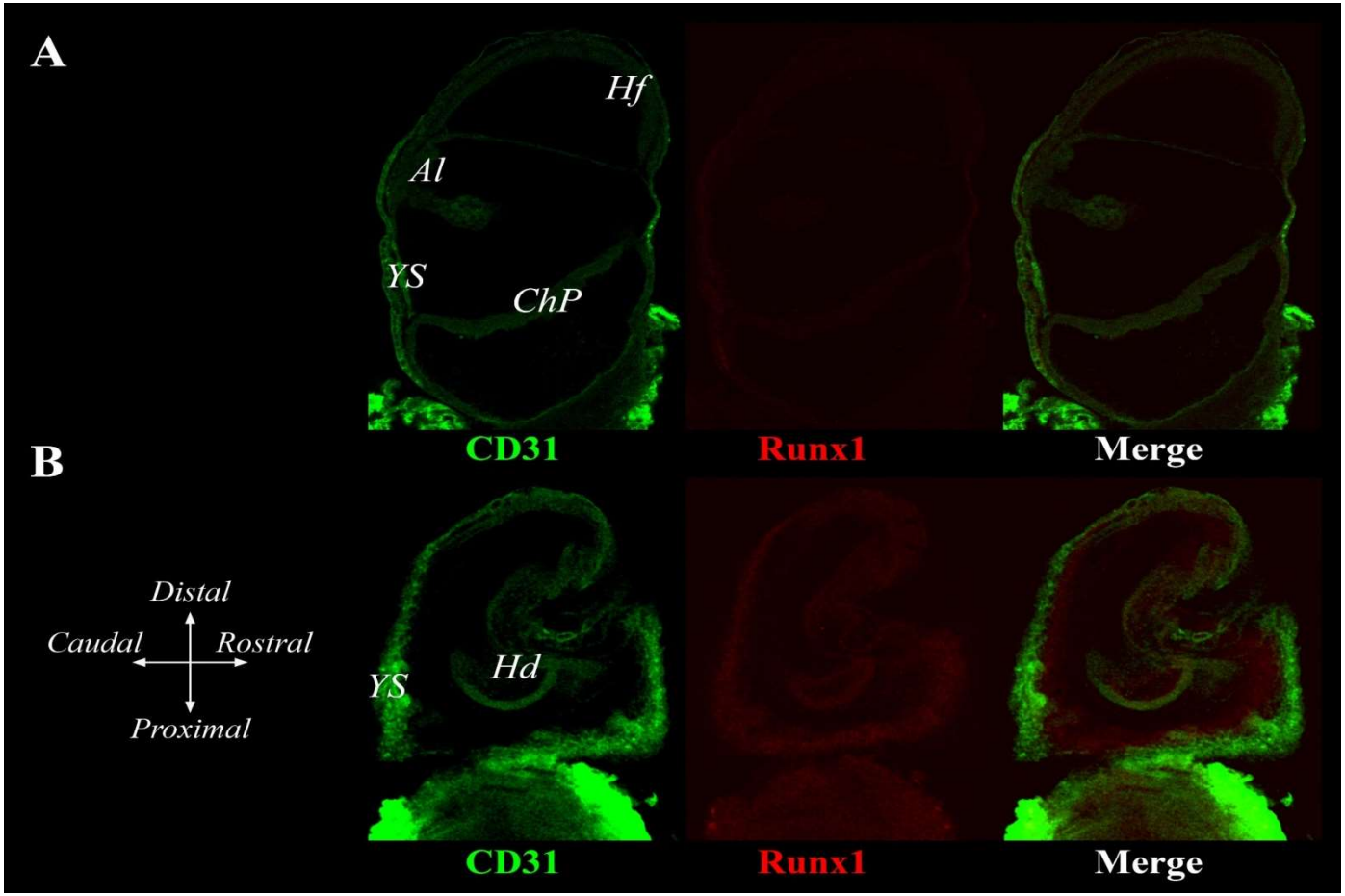

Appendix A1. Primary Runx1 antibody control on Runx1 KO mouse embryos. Anti-Runx1/anti-CD31 staining on AML1$^{LacZ/LacZ}$ pre-somitic mouse embryo. Typical Runx1+ staining is absent on yolk sac (A); the same on 5 sp mouse embryo. Yolk sac (YS); allantois (AL); chorionic plate (ChP); headfold (Hf).

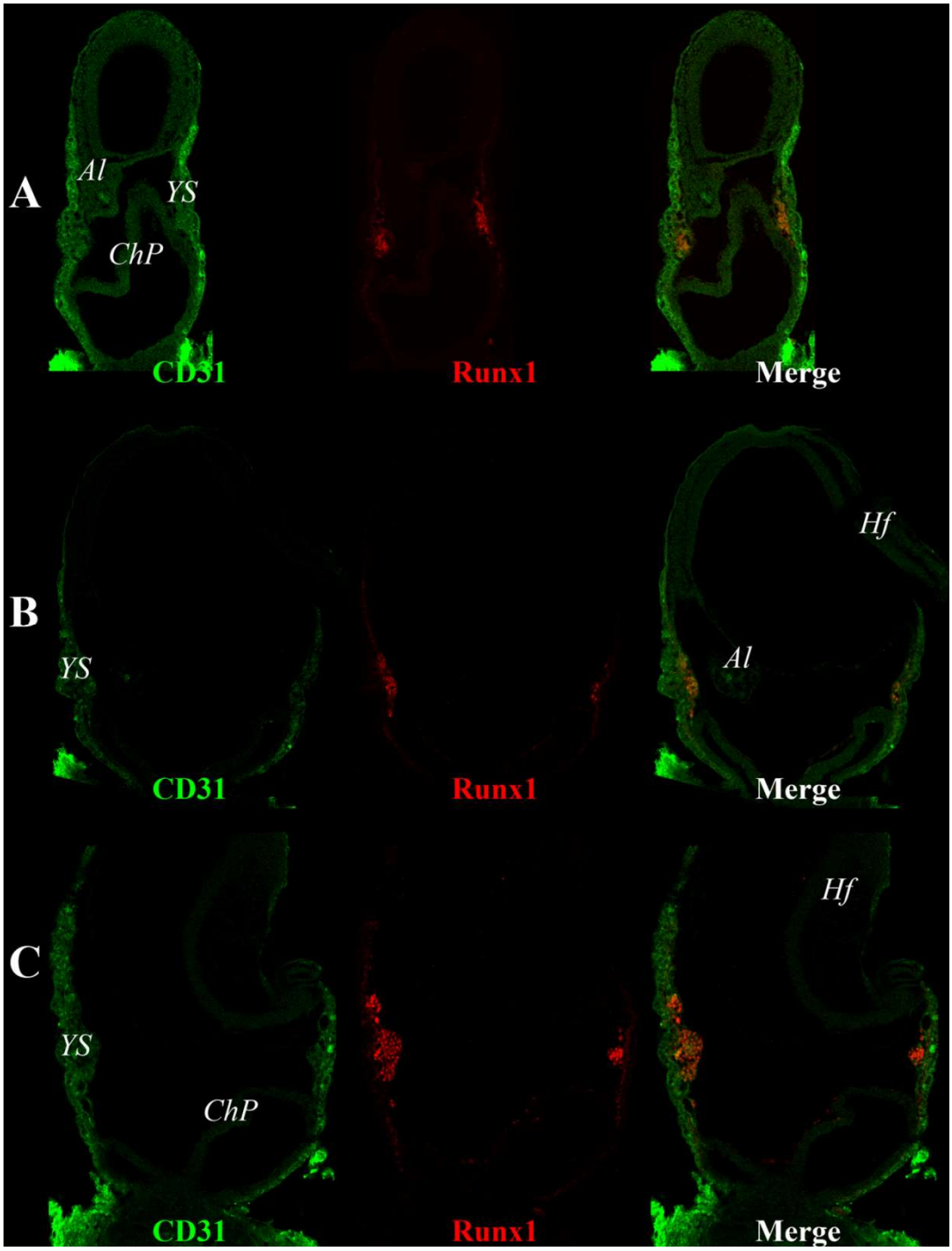

Appendix A2. Immuno-fluorescent staining for Runx1 on E8 AML$^{+/LacZ}$ mouse embryos. Neural plate mouse embryo showing typical pattern for Runx1 staining (in YS); Headfold stage mouse embryo showing Runx1 staining in YS and chorionic plate (B); 5 sp mouse embryo showing Runx1 staining in YS and ChP. Yolk sac (YS); allantois (Al); Chorionic plate (ChP); head-fold (Hf).

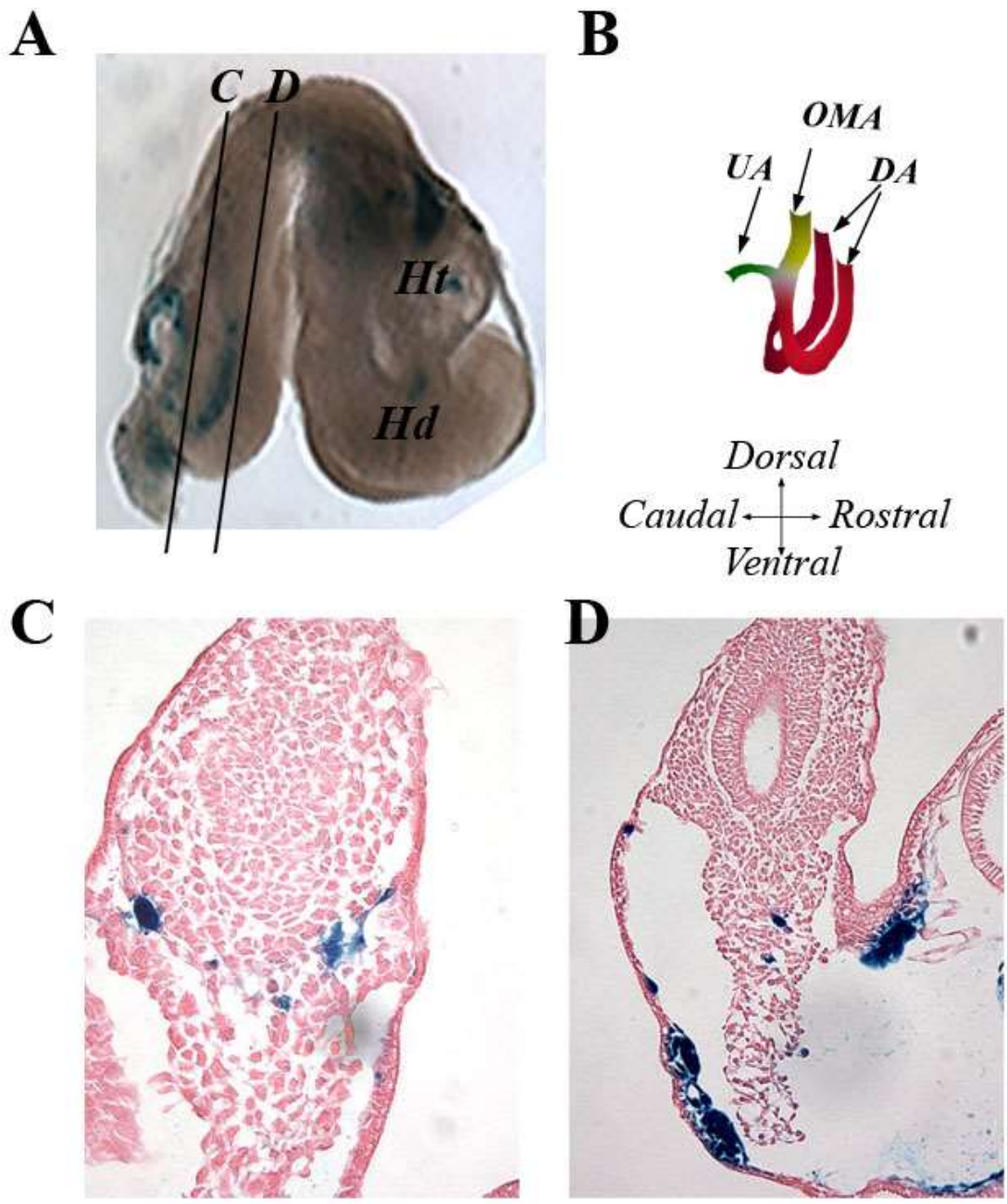

Appendix A3. Beta-galactosidase staining on E8 Runx1$^{+/LacZ}$ embryos. Whole mount anti-beta-galactosidase stained 5 sp mouse embryo (A); Scheme of connection of extra-and intra-embryonic vessels (B); Clusters of Runx1+ cells in nascent DA. Section C shown in A (C); Runx1+ cells in allantois and yolk sac in section D shown on A, (D). Umbilical artery (UA); omphaloemsenteric artery (OMA); dorsal aorta (DA).

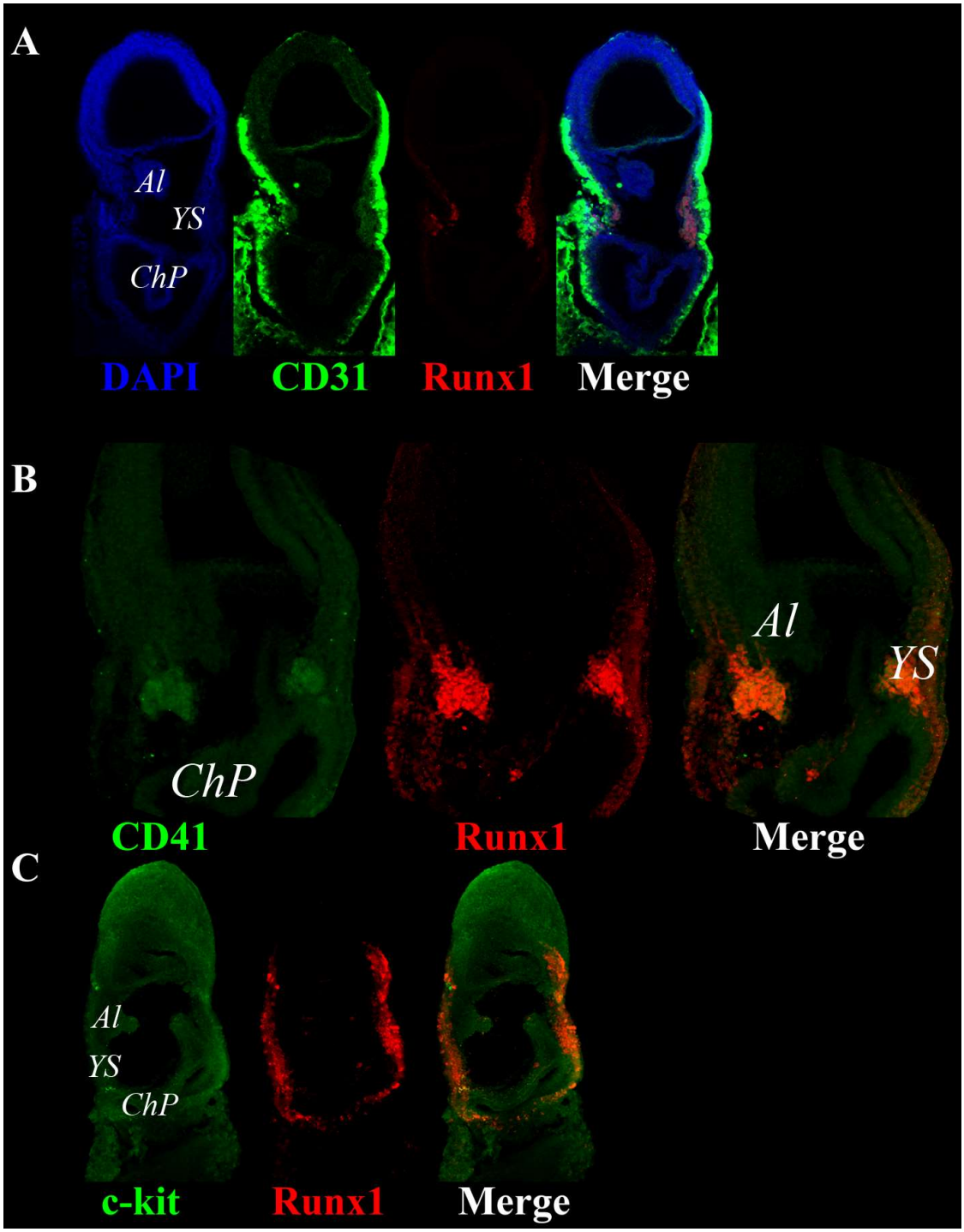

Appendix A4. Neural plate stage mouse embryos exhibiting no CD31, CD41 or c-kit staining outside of the yolk sac.

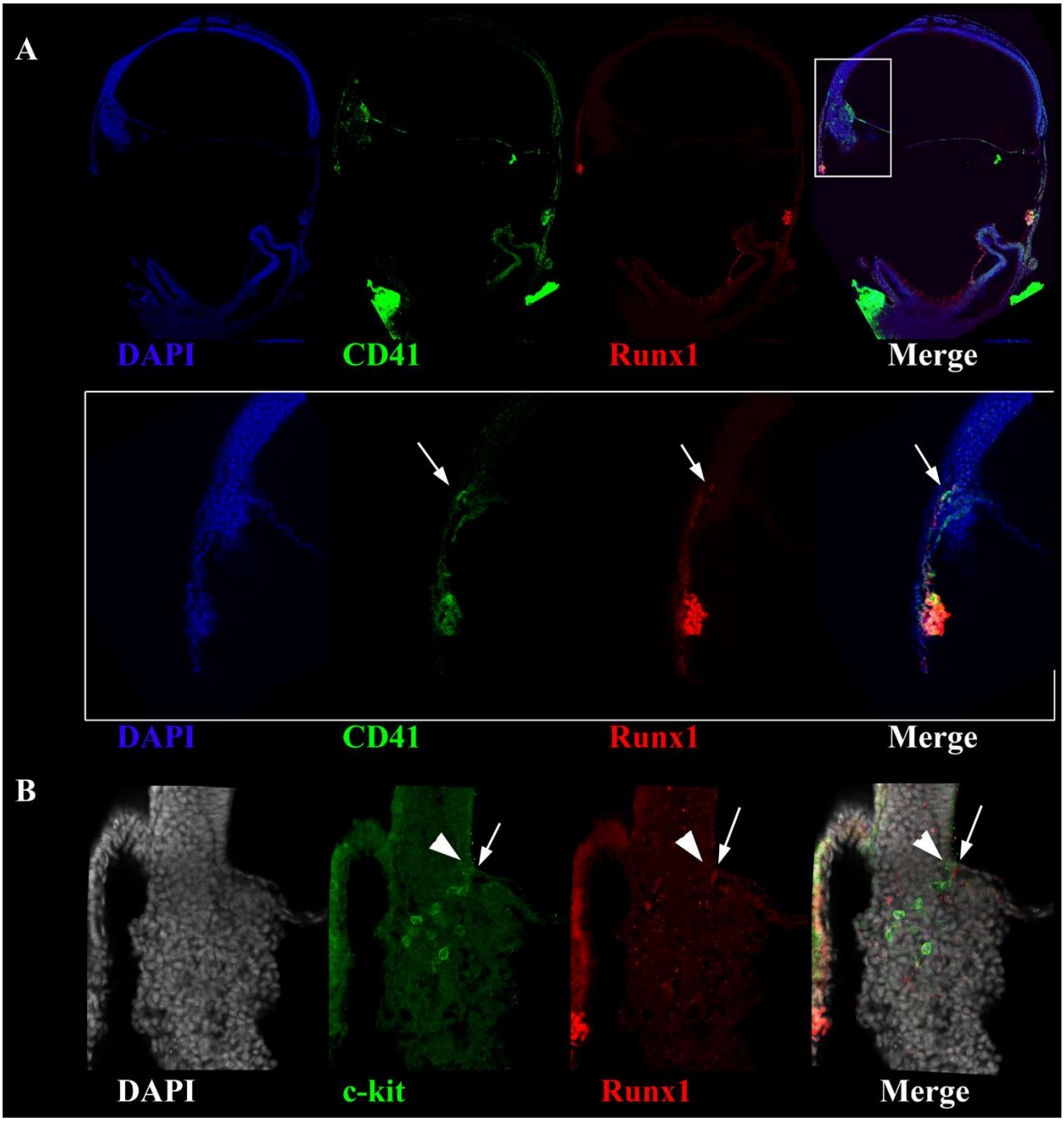

Appendix A5. HF stage mouse embryos, Runx1+ and CD41+ (or c-kit+) cells are present at the base of allantois.

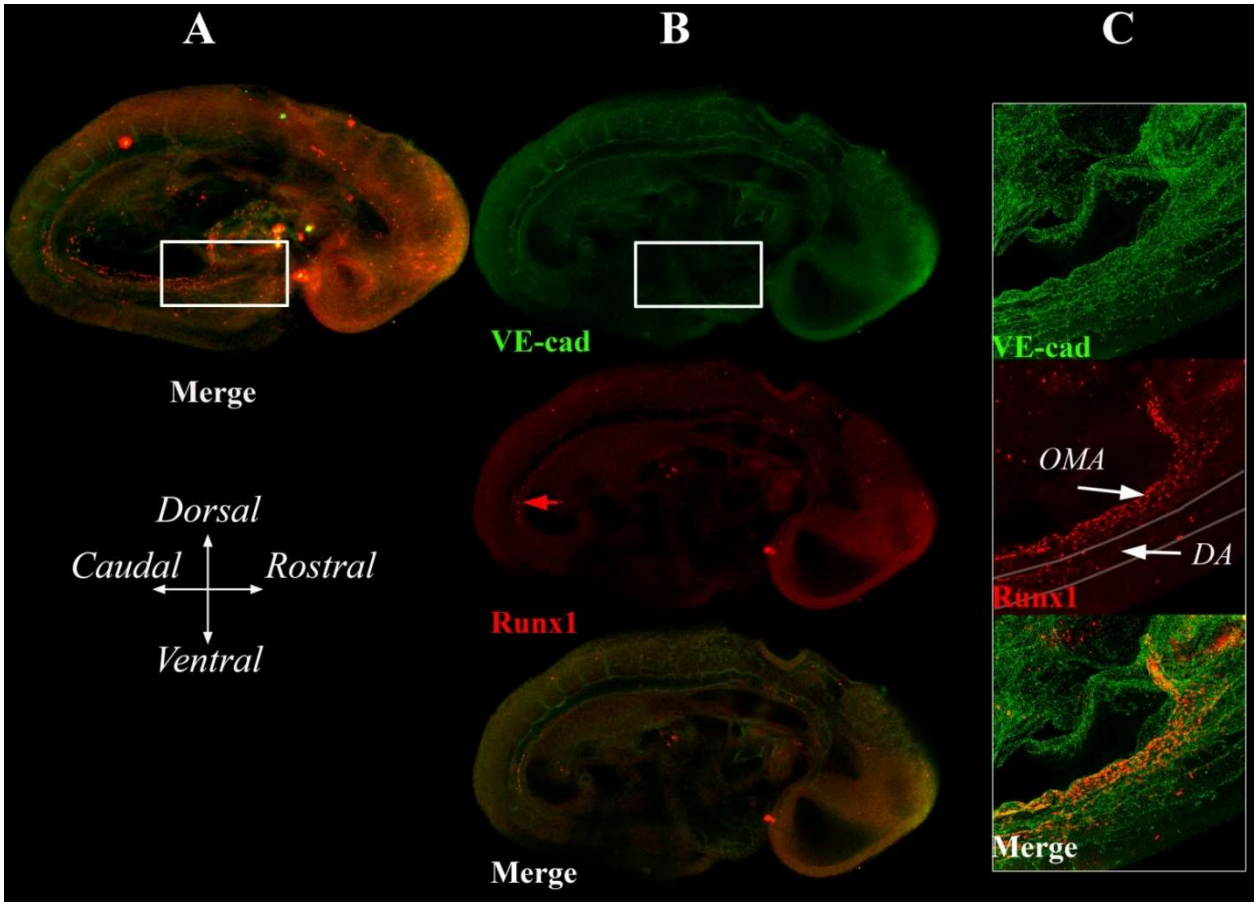

Appendix A6. Runx1 expression in caudal region of DA in 26 sp mouse embryo

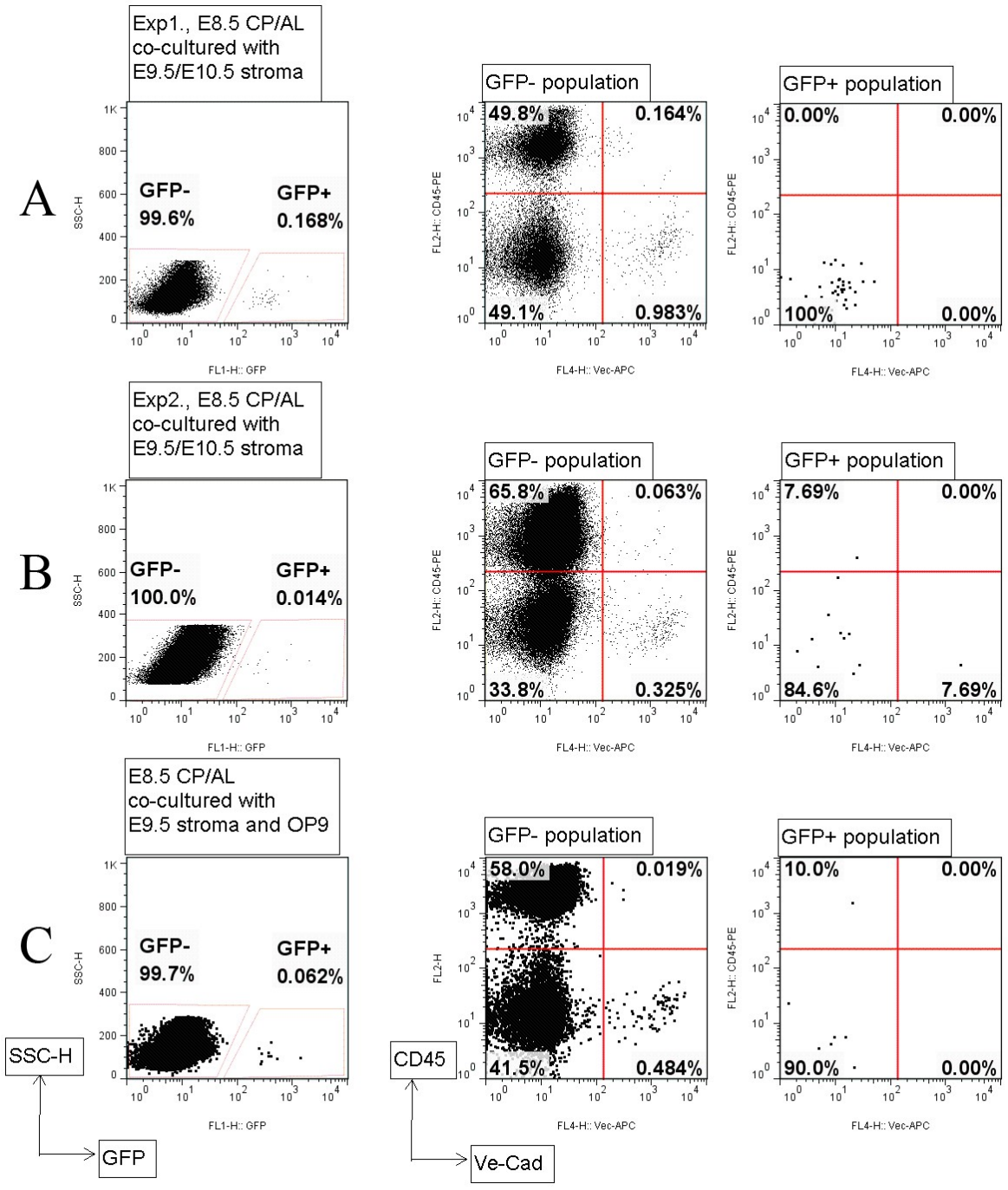

Appendix A7. Flow cytometric analysis of co-aggregates prepared from E8.5 caudal tissues of stromal cells. Markers used: hematopoietic CD45, endothelial Ve_cad and GFP for E8.5 isolated cells. CP/AL – E8.5 mouse embryis caudal parts and allantoid. Culture duration: E8/E9 co-aggregates – 2 days; E8/E9/E10 or OP9 co-aggregates – 7 days.

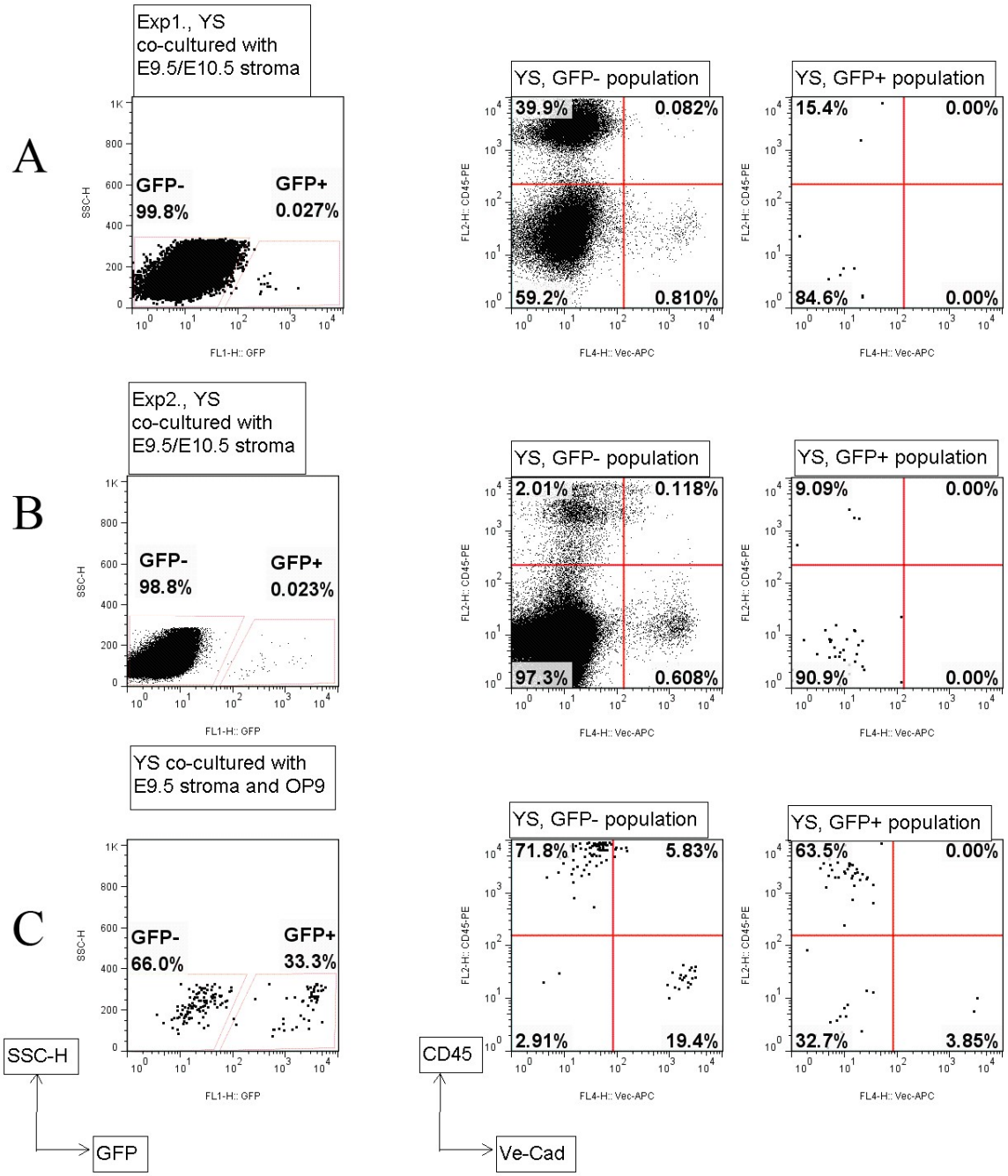

A8. Flow cytometric analysis of E8.5 yolk sac tissues from co-aggregate culture using surface expression markers for hematopoietic (CD45) and endothelial (Ve_Cad) markers. GFP+ E8.5 yolk sac (YS) co-cultured for two days with E9.5 stroma cells and consequent seven-day co-aggregate culture with E10.5 stroma cells (A). Repeated experiment as in A, (B). GFP+ E8.5 YS co-cultured for two days with E9.5 stroma cells and consequent seven-day co-aggregate culture with OP9 cell line (C)

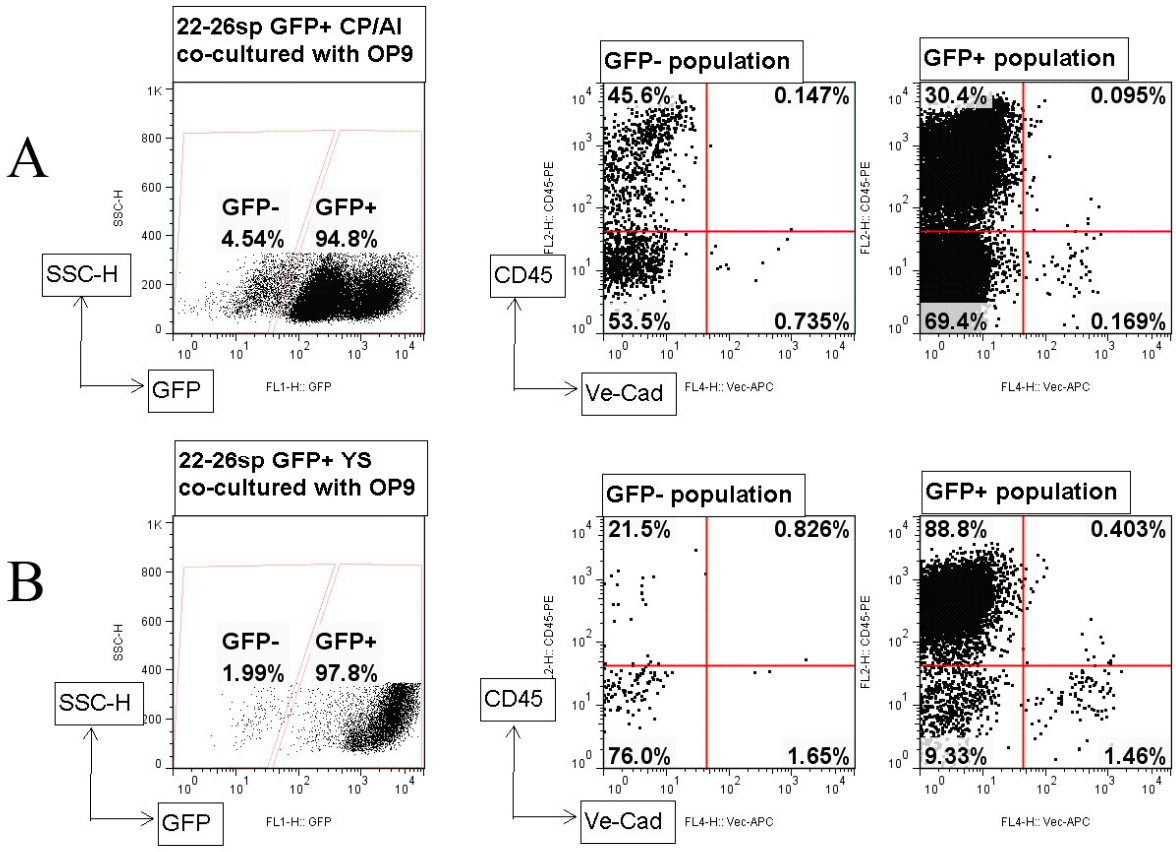

A9. Flow cytometric analysis of E9 tissues from co-aggregate culture using surface expression markers for hematopoietic (CD45) and endothelial (Ve_Cad) markers. GFP+ E9 (22-26sp) caudal part and allantois (CP/AL) co-cultured for seven days with OP9 stromal cell line (A). GFP+ E9 (22-26sp) yolk sac (YS) co-cultured for seven days with OP9 stromal cell line (B)

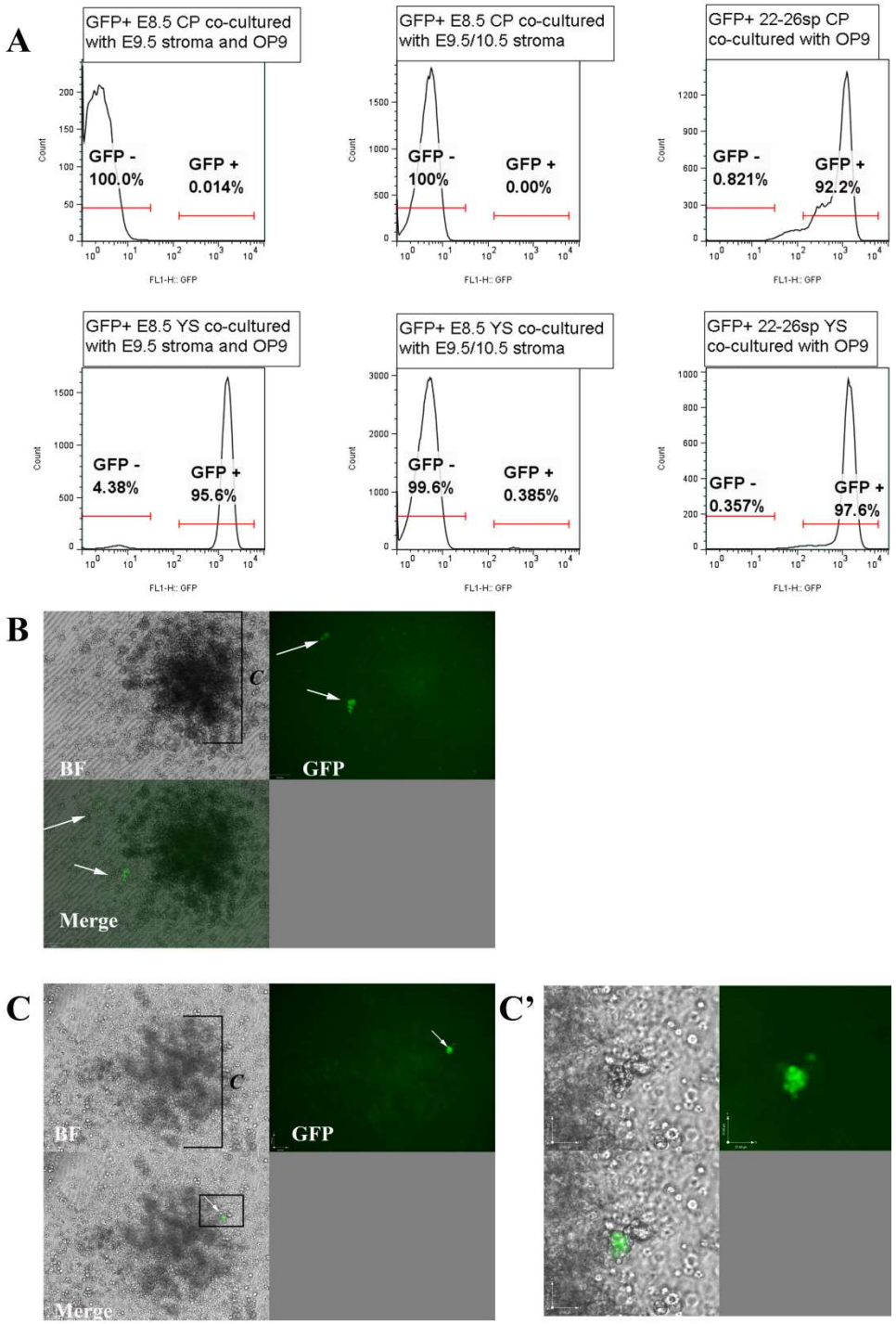

A10. Hematopoietic potential assessment of cultured E8 and E9 cells in methylcellulose media. After E8 or E9 cells co-aggregate culture, cell suspension was plated into methylcellulose. Cells were recovered from methylcellulose and analysed by flow cytometry (A). In seven days in methylcellulose no GFP+ hematopoietic colonies (cut off level - 4-6 cells colony) were found (B-C). Only clumps of GFP+ cells were observed in YS sample (C').

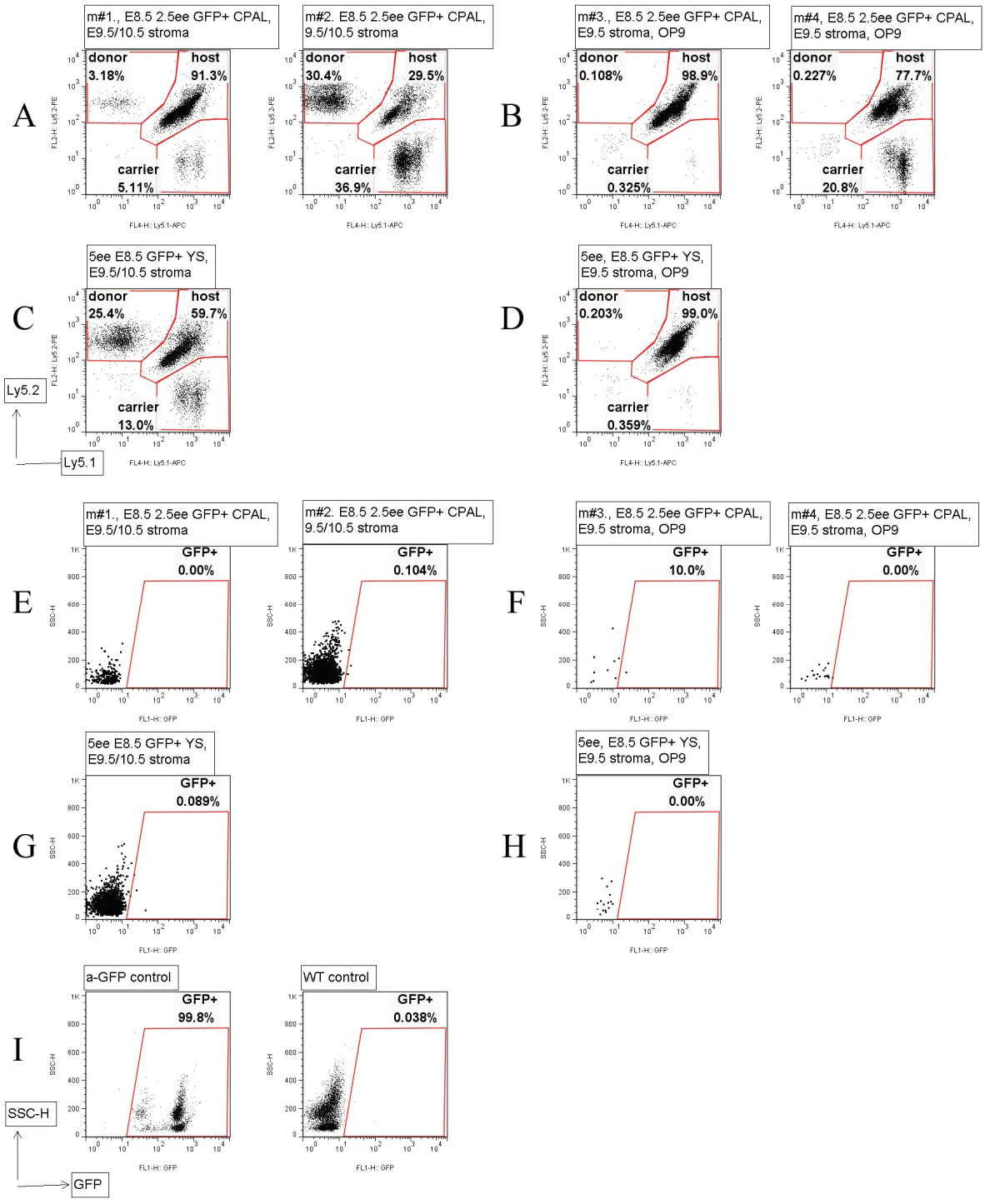

A11. Flow cytometric blood chimerism assessment six weeks after transplantation. Blood chimerism in mice injected with cells derived from GFP+ E8 caudal parts and allantois (CP/AL), co-cultured with E9 and E10 fresh stroma cells(A). Blood chimersim in mice transplanted with cells derived from GFP+ E8 yolk sac (YS) co-cultured with E9 stroma and OP9 line(B). The same as in (A) for yolk sac tissues (C). The same as in (B) for yolk sac tissues (D). GFP+ content of donor cell population for (A), (E). GFP+ content of donor cell population in (B), (F). GFP+ population in donor cells for (C), (G). GFP+ cell content for donor population in (D), (H). Control samples (I).

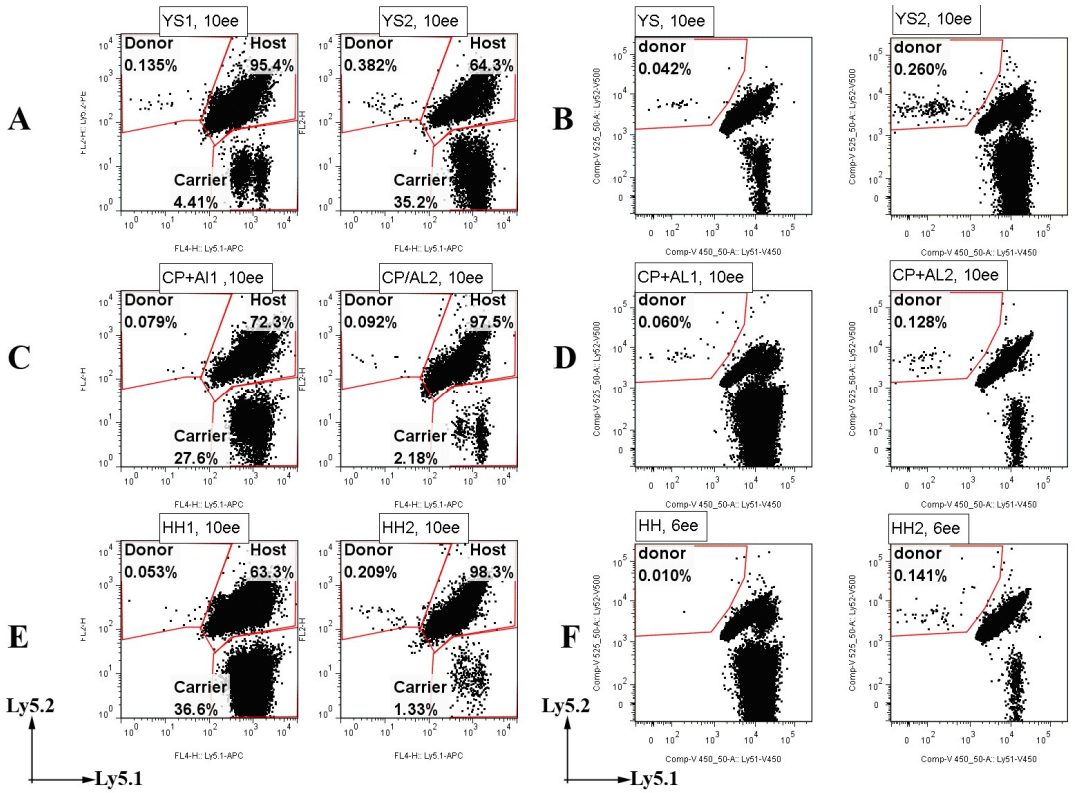

A12. Blood chimerism in mice transplanted with cells derived from E8 (3-8sp) tissues cultured as explants with consequent co-aggregation with OP9 stromal cell line. Blood chimerism six weeks after transplantation (A, C, E). Blood chimerism 3.5 months after transplantation (B, D, F). Yolk sac tissues (YS), caudal part and allantois tissues (CP+AL), head and heart tissues (HH).

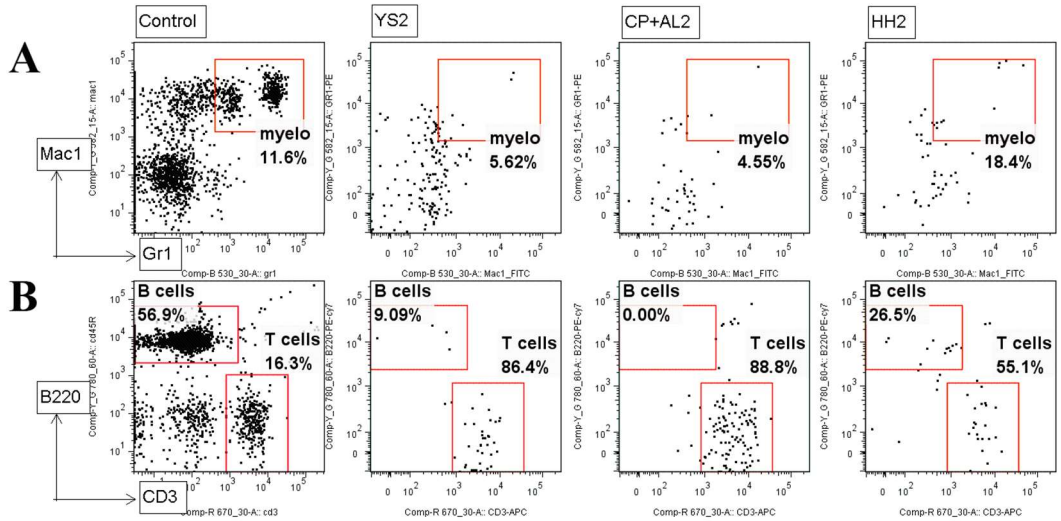

A13. Multilineage blood repopulation in mice engrafted at level higher than 0.1% (from A12). Myeloid lineage repopulation (A); Lymphoid lineage repopulation (B).

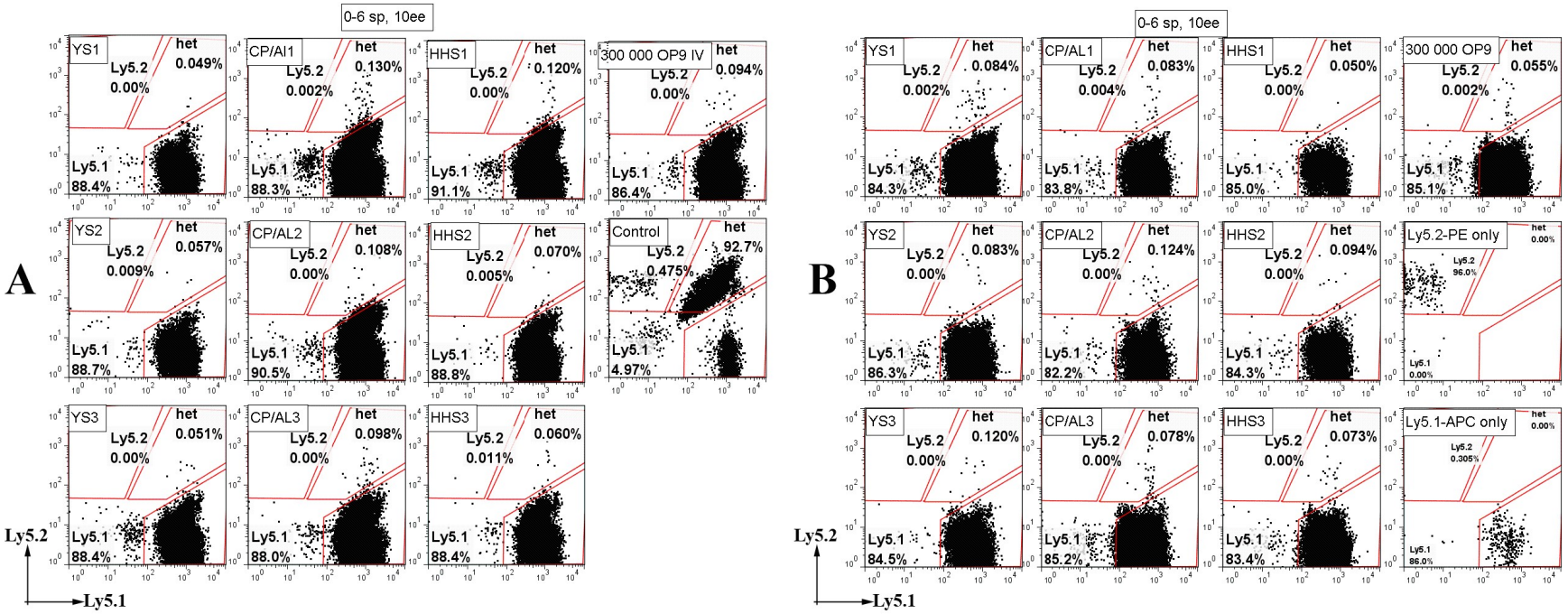

A14. Blood chimerism in mice transplanted with cells suspensions derived from cultured E8 tissues: as explants on air-liquid interface and subsequently in co-aggregates with OP9 cell line. Blood chimerism six weeks after transplantation (A). Blood chimerism after 3.5 months after transplantation (B).

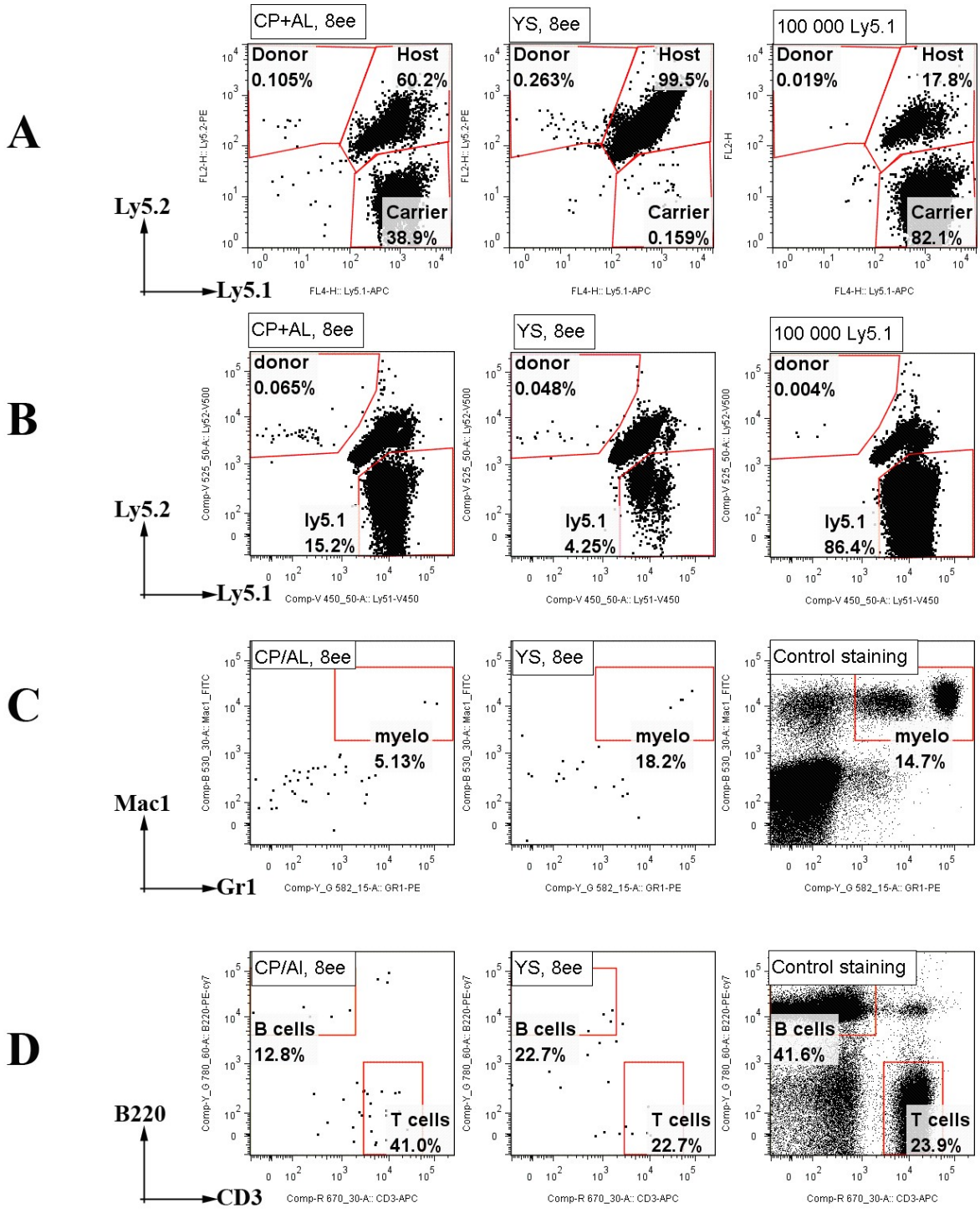

A15. Blood chimerism in mice transplanted with cells derived from E8.5 air-liquid interface explants. Blood chimerism (donor – Ly5.2 homo) six weeks after injection (A). Blood chimerism 3.5 months after injection (B). Multilineage analysis of donor cell population for myeloid (C) and lymphoid lineage contribution (D).

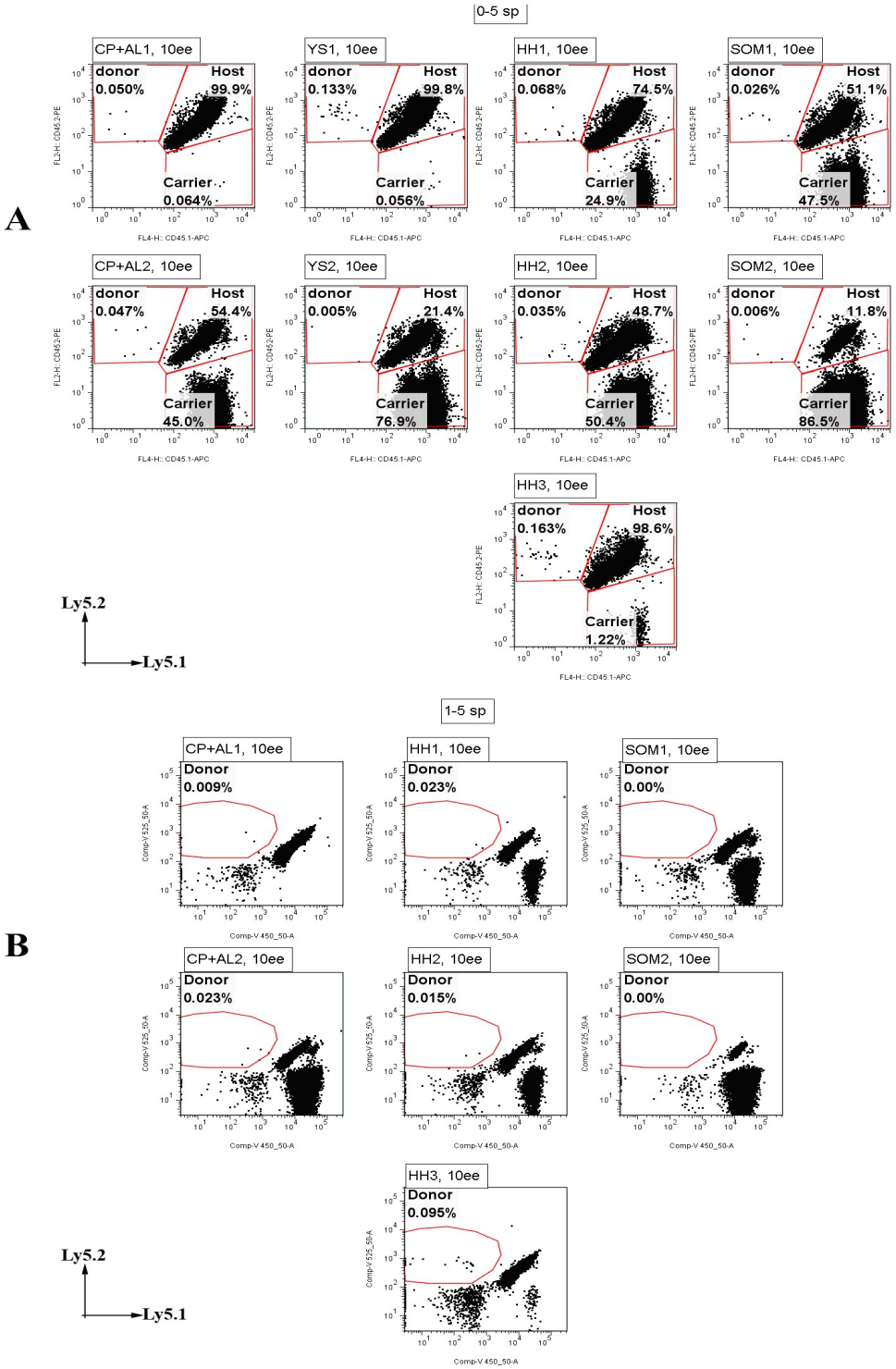

A16. Blood chimerism in mice transplanted with cell suspensions derived from embryonic (0-5sp) tissues cultured as submerged explants for four days. Short term repopulation (A). Long term repopulation (B).

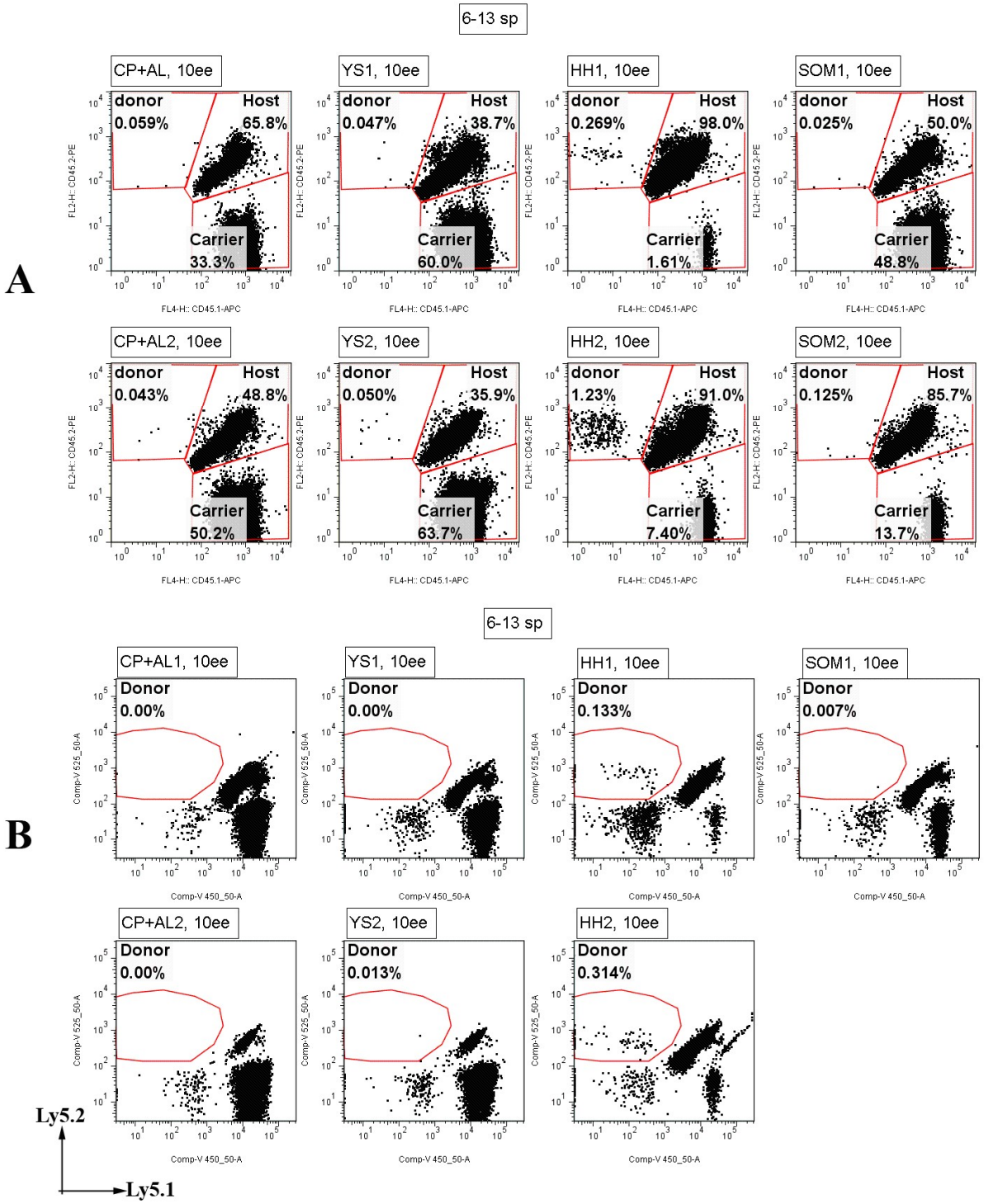

A17. Blood chimerism in mice transplanted with cell suspensions derived from embryonic (6-13sp) tissues cultured as submerged explants for four days. Short term repopulation (A). Long term repopulation (B).

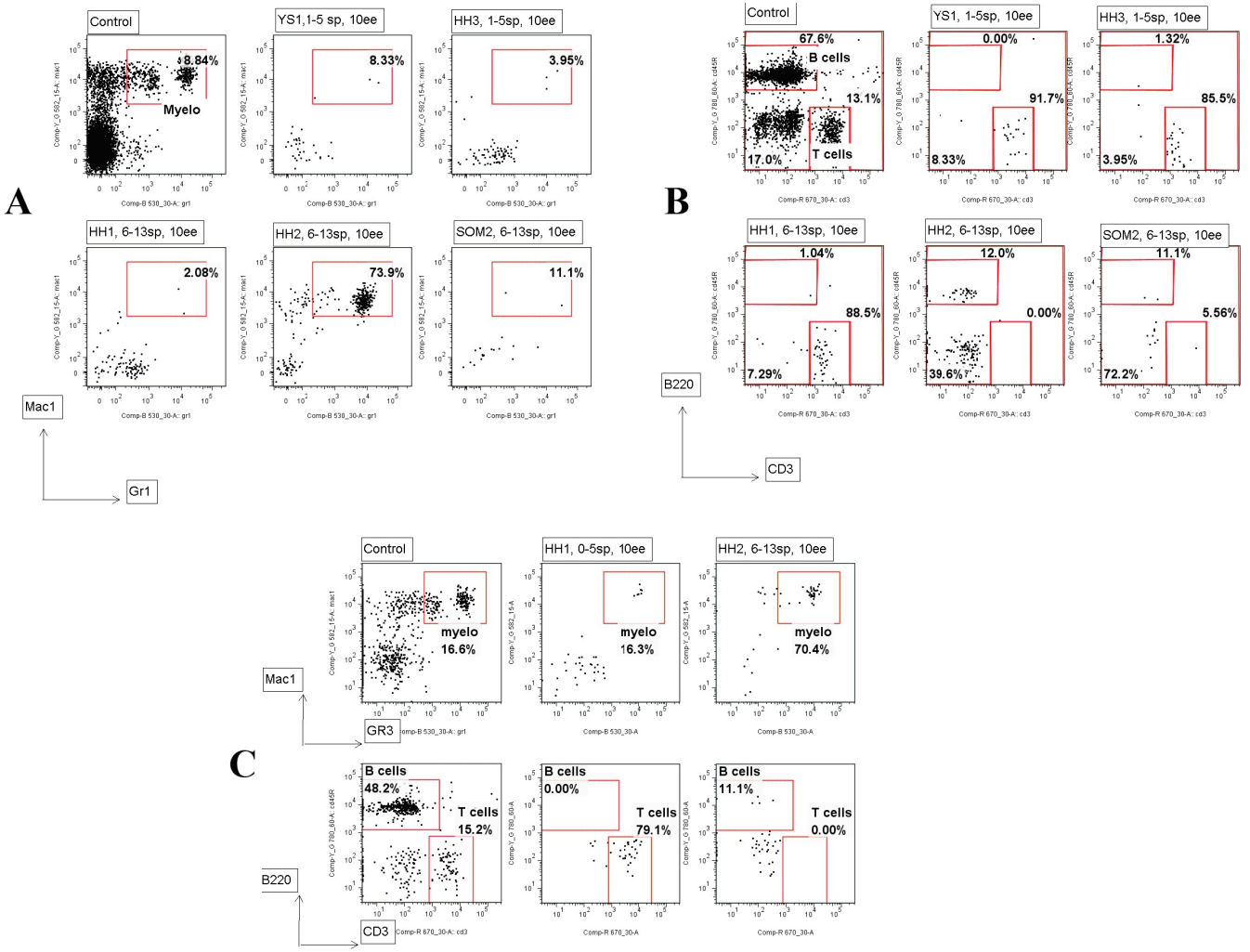

A18. Multilineage repopulation in mice from Figure 3.2.12-13 with level of blood chimerism higher than 0.1%. Myeloid engraftment six weeks after transplantation (A); Lymphocytes engraftment six weeks after transplantation (B); Myeloid and lymphoid engraftments 3.5 months after transplantation (C).

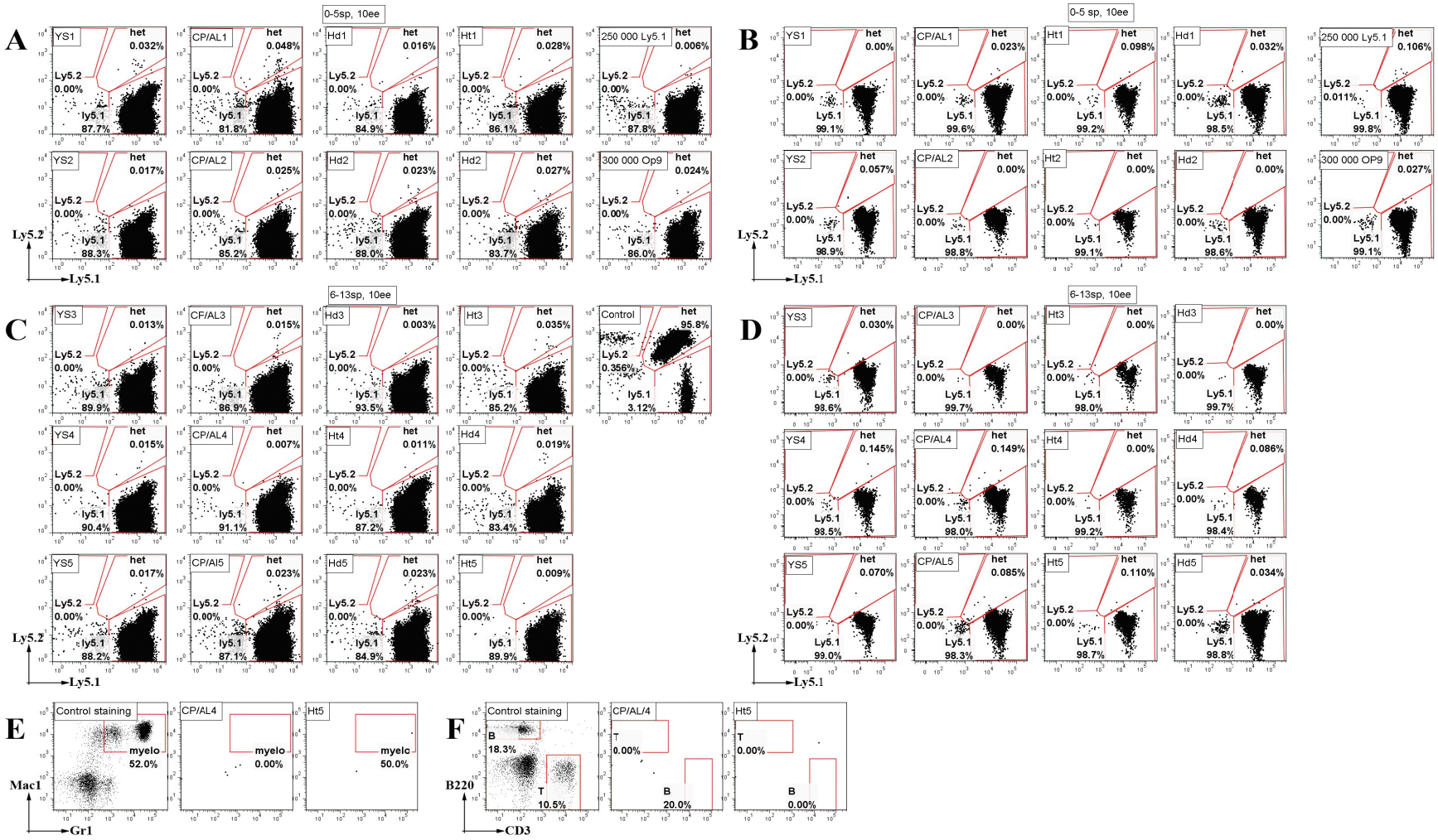

Appendix A19. Blood chimerism in mice transplanted with cell suspensions derived from embryonic (0-13sp) tissues cultured as submerged explants for four days. Short term repopulation (A, C). Long term repopulation (B, D). Flow cytometric analysis on donor cells population with blood chimerism level higher than 0.1% with markers for myeloid (Mac1, Gr1) and lymphoid (B220, CD3) lineage (C).

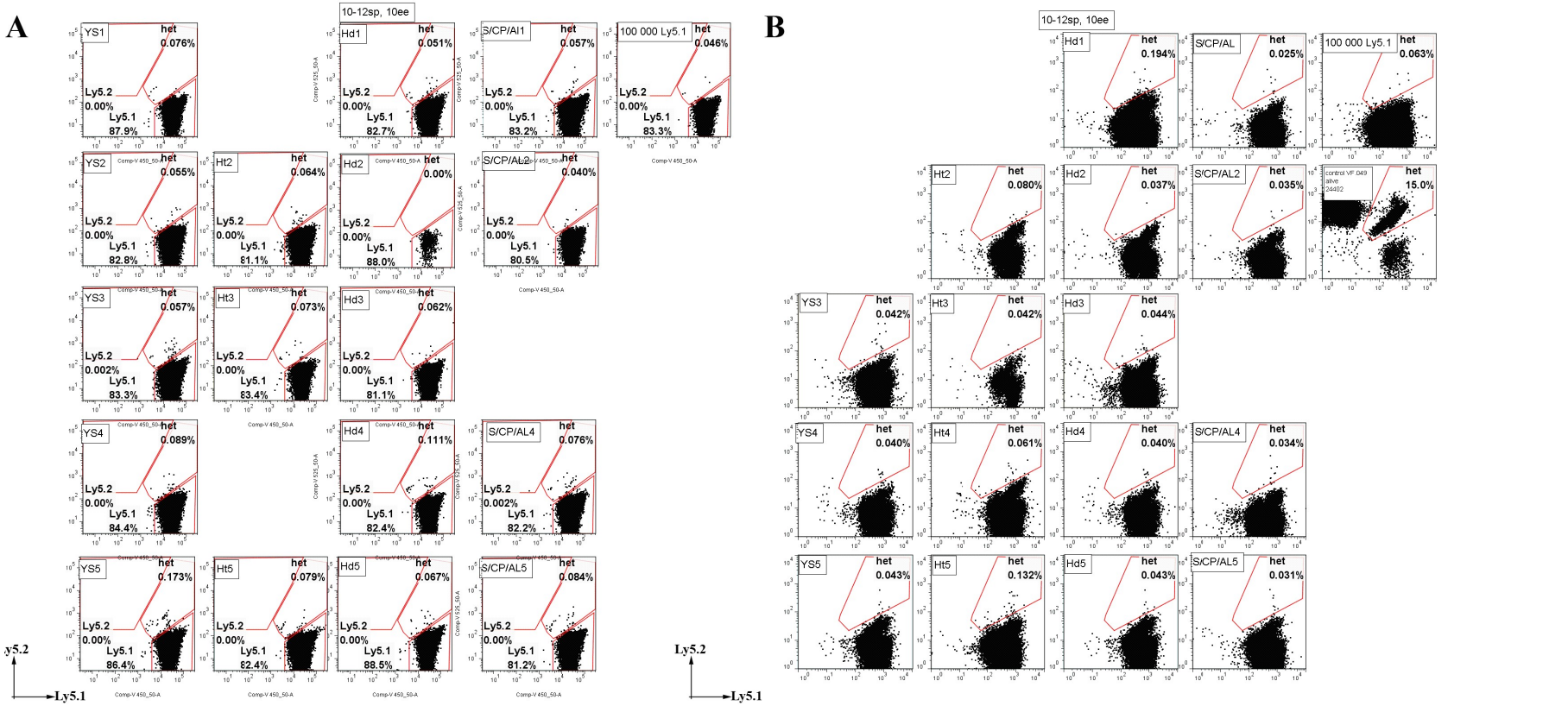

A19. Blood chimerism in mice transplanted with cell suspensions derived from embryonic (0-13sp) tissues cultured as submerged explants for four days. Short term repopulation (A). Long term repopulation (B). Flow cytometric analysis on donor cells population with blood chimerism level higher than 0.1% with markers for myeloid (Mac1, Gr1) and lymphoid (B220, CD3) lineage (C).

Table A20. Results of transplantation of cells from E8 mouse tissues cultured as explants on air-liquid interface with subsequent co-aggregation with OP9

	Yolk sac	**Caudal part and Allantois**	**Head, heart and somites**
# of injected mice	5	5	5
# STR repopulated (blood chimerism, %)	2 (0.134, 0.365*)	2 (0.108, 0.13)	2 (0.12, 0.21*)
# LTR repopulated (blood chimerism, %)	1 (0.26*)	2 (0.124, 0.128*)	1 (0.14*)
Multilineage repopulation for LTR			
Myeloid cells, % donor popul.	5.62	4.55	18.4
B cells, % donor popul.	9.09	0	26.5
T cells, % donor popul.	86.4	88.8	55.1

* - multilineage analysis was done for these samples; STR – short term repopulation; LTR – long term repopulation.

Table A21. Results of transplantation of cells from E8 mouse tissues cultured as explants

	Yolk sac	**Caudal part and allantois**
# of injected mice	1	1
# STR repopulated (blood chimerism, %)	1 (0.263)	1 (0.105)
# LTR repopulated (blood chimerism, %)	0	0
Multilineage repopulation for STR		
Myeloid cells, % donor population	5.13	18.2
B cells, % donor population	12.8	27.7
T cells, % donor population	41	22.7

Table A22. Transplantations results done with cells derived from E8 mouse tissues cultured as explants in submerged culture

	Yolk sac	**Caudal part and Allantois**	**Head and/or heart**	**Somites**
# of injected mice	8	8	14	4
# STR repopulated (blood chimerism, %)	2 (0.13*, 0.17)	0	4 (0.163*, 0.269*, 1.23*, 0.11)	1 (0.125)
# LTR repopulated (blood chimerism, %)	1 (0.145)	1 (0.149)	5 (0.13*, 0.31*, 0.11*, 0.194, 0.132)	0
Multilineage repopulation for STR				
Myeloid cells, % donor population	8.33	x	3.95/2.08/73.9	x
B cells, % donor population	0	x	1.32/1.04/12	x
T cells, % donor population	91.7	x	85.5/88.5/0	x
Multilineage repopulation for STR				
Myeloid cells, % donor population	x	x	18.3/70.4	x
B cells, % donor population	x	x	0/11.1	x
T cells, % donor population	x	x	79.1/0	x

* - multilineage repopulation is given for this sample; x – no data

Table A23. Frequency of grafts contribution to early chick embryo tissues

Embryo Stage, HH	Number of embryos analyzed	Grafting position, % PS length	Frequency of contribution (contributed/grafted at given position)						
			Tissues						
			DA	LPM/IM	APV	Somites	AOV	Ht	Hd
3	16	10-20	0/3	0/3	3/3	0/3	3/3	0/3	0/3
		30-40	1/2	0/2	2/2	0/2	1/2	0/2	0/2
		40-50	2/3	1/3	2/3	0/3	2/3	1/3	0/3
		50-60	2/2	0/2	2/2	0/2	1/2	1/2	0/2
		60-70	4/5	2/5	2/5	1/5	0/5	3/5	0/5
		90-100	0/1	0/1	0/1	0/1	0/1	0/1	1/1
4	32	0-10	0/1	0/1	0/1	0/1	1/1	0/1	0/1
		10-20	0/3	0/3	0/3	0/3	3/3	0/3	0/3
		20-30	3/4	1/4	3/4	0/4	4/4	0/4	0/4
		30-40	2/4	1/4	4/4	0/4	3/4	0/4	0/4
		40-50	4/5	5/5	4/5	0/5	2/5	0/5	0/5
		50-60	5/7	5/7	5/7	0/7	2/7	0/7	0/7
		60-70	3/4	4/4	2/4	1/4	0/4	0/4	0/4
		70-80	1/2	1/2	1/2	2/2	0/2	0/2	0/2
		80-90	0/2	0/2	0/2	2/2	0/2	0/2	0/2
5	18	20-30	1/1	1/1	1/1	0/1	0/1	0/1	0/1
		30-40	3/3	3/3	3/3	0/3	0/3	0/3	0/3
		40-50	3/3	3/3	1/3	0/3	0/3	0/3	0/3
		50-60	4/6	6/6	0/6	1/6	0/6	0/6	0/6
		60-70	1/3	3/3	0/3	1/3	0/3	0/3	0/3
		70-80	0/1	0/1	0/1	1/1	0/1	0/1	0/1
		80-90	0/1	0/1	0/1	1/1	0/1	0/1	0/1
6-8	7	30-40	1/1	1/1	1/1	0/1	1/1	0/1	0/1
		40-50	2/2	2/2	0/2	0/2	0/2	0/2	0/2
		50-60	2/3	2/3	0/3	1/3	0/3	0/3	0/3
		60-70	0/1	0/1	0/1	1/1	0/1	0/1	0/1

DA – dorsal aorta; LPM – lateral plate mesoderm; IM – intermediate mesoderm; APV – area pellucida vessels; AOV – area opaca vessels (area vasculosa or yolk sac); Ht – heart; Hd – head.

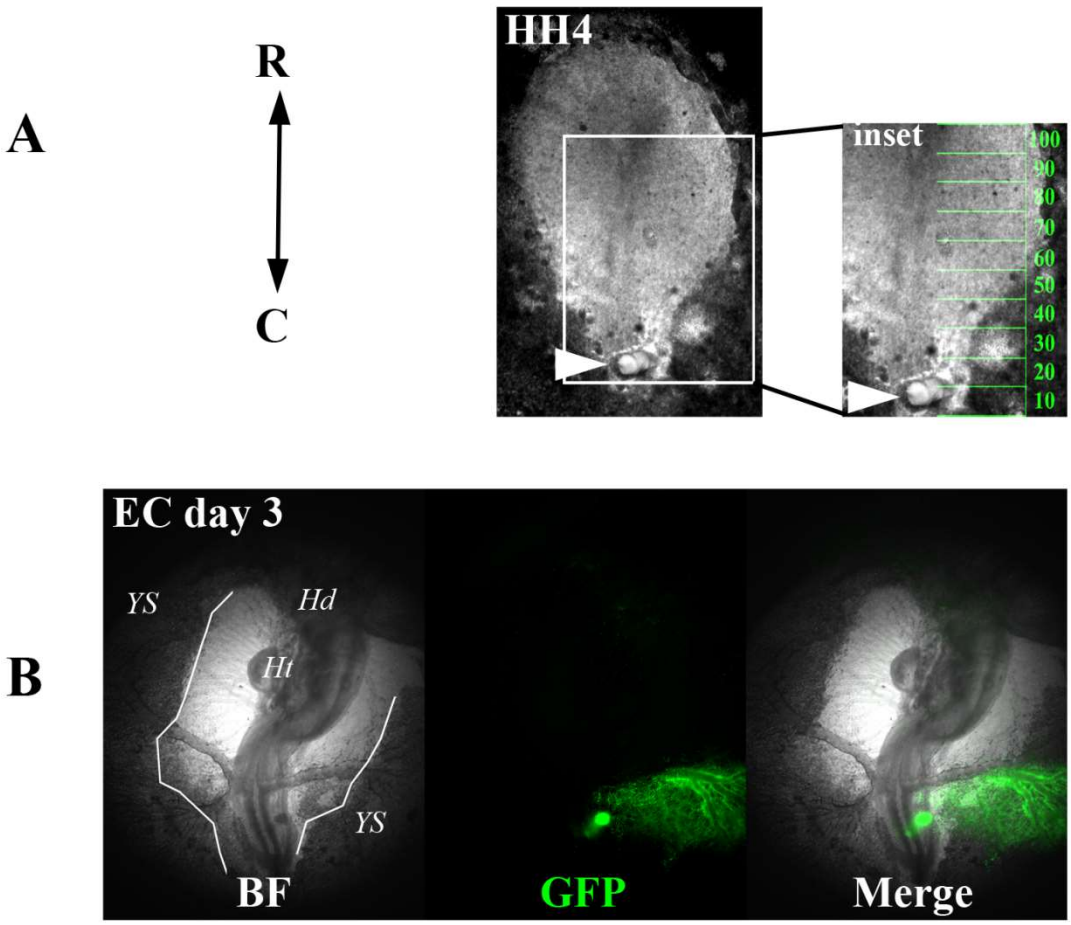

Appendix A8. Example of chick embryo with contribution to yolk sac.

A25. Beta-galactosidase staining buffer recipes

Buffer A:

- 10%FCS;
- PBS (tissue culture grade, without Mg, Ca ions);
- 2 mM MgCl2;
- 5 mM EGTA.

Buffer B:

- 0.1M PBS (pH 7.3);
- 2mM MgCl2;
- 5mM EGTA;
- 0.2% glutaraldehyde.

Buffer C:

- 0.1M PBS (pH 7.3);
- 2 mM MgCl2;
- 0.1% Na desoxyholate;
- 0.02% NP40;
- 0.5 mg/mL BSA.

Buffer D:

- 5 mM K3Fe(CN)6;
- 5 mM K4Fe(CN)6x3H2O;
- 0.24 mg/mL Spermidine;
- 0.25 mM NaCl;
- 1mg/mL X-Gal (add before incubation).

Store Buffer D at 4 oC. Protect from light.

Appendix A26. Pannett and Compton saline stock for early chick culture.

Stock solution A:

- 121 g NaCl;
- 15.5 g KCl;
- 10.42 g CaCl2*2H2O (or 7.7 gCaCl2);
- 12.7 g MgCl2*6H2O.

Dilute in 1 L of water. Solution A was autoclaved prior to storage.

Stock solution B:

- 2.365 g Na2HPO4*2H2O (or 1.886 g Na2HPO4);
- 0.188g NaH2PO4*2H2O (or 0.166 g NaH2PO4*H2O).

Add distilled water to 1 L. The resulting solution was autoclaved prior to storage.

Both solutions were stored at 21 ^{o}C for 2 months. After opening, solutions were stored at 4 ^{o}C. Pannet-Compton saline working solution was prepared by mixing 40 ml of saline A, 900 ml of distilled water and 60 ml of saline B.

Appendix A27 List of antibodies used for blood chimerism assessment

Antibodies set A:

Fc block (anti-CD16/32, clone 93, Abcam, 1:200;

anti-mouse CD45.1-APC, clone A20, Abcam, 1:100;

anti-mouse CD45.2-PE, clone 104, Abcam, 1:100.

Antibodies set B:

Fc block (anti-CD16/32, clone 93, Abcam), 1:200;

anti-mouse CD45.1-V450, clone A20, BD Horizon 1:100;

anti-mouse CD45.2-V500, clone 104, Biolegend, 1:100;

anti-mouse CD11b-PE (Mac-1), clone M1/70, eBioscience; 1:600;

anti-mouse GR-1 (Ly6C)-FITC, clone RB6-8C5, BD Pharmingen, 1:600;

anti mouse CD3e-APC, clone 145-2C11, eBioscience, 1:100;

anti mouse CD45R/220- PE-Cy7, BD Pharmingen, 1:200.